



Cunningham, Richard (2020) *Subtype specific metabolic vulnerabilities in pancreatic cancer*. PhD thesis.

<https://theses.gla.ac.uk/80267/>

Copyright and moral rights for this work are retained by the author

A copy can be downloaded for personal non-commercial research or study, without prior permission or charge

This work cannot be reproduced or quoted extensively from without first obtaining permission in writing from the author

The content must not be changed in any way or sold commercially in any format or medium without the formal permission of the author

When referring to this work, full bibliographic details including the author, title, awarding institution and date of the thesis must be given

Enlighten: Theses

<https://theses.gla.ac.uk/>
research-enlighten@glasgow.ac.uk

Subtype Specific Metabolic Vulnerabilities in Pancreatic Cancer



University
of Glasgow

Pancreatic
Cancer
UK

Richard Cunningham

BA (Mod), MSc

Submitted to the University of Glasgow in fulfilment of the
requirements for the Degree of the Doctor of Philosophy

*Institute of Cancer Sciences
College of Medical, Veterinary and Life Sciences
University of Glasgow*

October 2019

Abstract

Pancreatic cancer has historically been characterised by its poor prognosis, with very little increase in 5-year expectancy relative to other, comparable cancer-types. This clinical observation is largely due to existing difficulties in identifying therapeutics effective in managing metastasised disease, a task compounded by the heterogeneity associated with pancreatic cancers. Concentrated efforts have been made in recent times to mitigate this issue, with the emergence of a range of subtyping strategies allowing for the stratification of patients. This categorisation of patients into workable groups thus serves to limit the degree of heterogeneity found within subgroups, with hypothetical, and otherwise unobservable, vulnerabilities shared between subtypes. This thesis aims to explore these potential therapeutically exploitable vulnerabilities by describing the extensive characterisation of pancreatic cancer subtypes via a diverse collection of patient derived cell-lines. This characterisation was achieved by profiling of the transcriptome via RNA-seq analyses, the proteome via mass-spectrometric approaches, and activation status of metabolic processes associated with oncogenesis in pancreatic cancer via functional assays. This work therefore facilitates the identification of vulnerabilities by utilising the profiles of subtypes generated in this manner and devising therapeutic strategies effective in treating the disease by interrogating dysregulated pathways.

Within PDCLs, two pancreatic cancer subtypes were first identified which aligned with those described in patients: the squamous and classical subtypes. Preliminary profiling efforts highlighted a dysregulation of genes involved in metabolism across these subtypes *in vitro*, with active glycolysis associated with the aggressive squamous subtype and fatty acid biosynthesis and metabolism upregulated in the classical subtype. Further proteomic characterisation then validated this observation, providing further evidence for the existence of distinct metabolic profiles associated with these subgroups. Follow-up experimentation which

focused on metabolic outputs then generated metabolic profiles for each subtype, with *in vitro* phenotypes reflecting findings at the transcriptome and proteome level and demonstrating enhanced glycolysis and fatty acid oxidation in the squamous and classical subtypes respectively.

Subsequent attempts to target arms within those subtype-associated metabolic pathways yielded mixed results. Inhibiting glycolysis via targeting of ALDOA successfully mediated a selective response in cell-lines associated with the squamous subtype, while classical cell-lines required a combination therapy to suppress metabolic flexibility to induce sensitivity to inhibition of fatty acid synthesis via targeting of FASN.

An adjacent and complementary arm of research involved collaborative high-throughput drug repurposing screens to identify additional targets for follow-up. This involved an initial screen of ~600 compounds in 8 PDCLs. Results generated as part of this screening approach highlighted the potency of statins in effecting a significant response selectively in squamous cell-lines. Research probing the mechanism by which statins induce this selective inhibition suggested that differences in degradation of the statin target HMGCR and cholesterol homeostasis may confer resistance to cell-lines classified as squamous, with findings demonstrating the potential of dietary components found in commonly ingested foodstuffs to mitigate the effects of statins in the otherwise sensitive, squamous subtype.

This thesis therefore identified a range of therapeutic strategies effective in mediating sensitivity in *in vitro* pancreatic subtypes, with mechanisms of actions determined for each strategy. Results have demonstrated that pancreatic cancer cells exhibit differential sensitivities to metabolic inhibition, with subtype classification found to act as a predictor of sensitivity. As these *in vitro* subtypes recapitulate stratifications described in patients, these therapeutic strategies are of clinical relevance in the treatment of pancreatic cancer.

Table of Contents

| | |
|---|-----------|
| Abstract | 3 |
| Table of Contents | 5 |
| List of Tables | 9 |
| List of Figures | 10 |
| Acknowledgements | 13 |
| Authors Declaration..... | 14 |
| Abbreviations | 15 |
| Chapter 1 Introduction..... | 17 |
| 1.1 Introduction..... | 18 |
| 1.2 General characteristics of pancreatic cancer | 18 |
| 1.2.1 <i>Anatomy and development of the pancreas</i> | 18 |
| 1.2.2 <i>Tumour initiation</i> | 20 |
| 1.2.3 <i>Epidemiology and aetiology</i> | 21 |
| 1.3 Molecular characteristics of pancreatic cancer | 21 |
| 1.3.1 <i>Common driver mutations</i> | 21 |
| 1.3.2 <i>Genomic instability and mutation burden</i> | 23 |
| 1.3.3 <i>Dysregulation of gene expression</i> | 23 |
| 1.3.4 <i>Epigenetic perturbations in pancreatic cancer</i> | 23 |
| 1.4 A need for defined subtypes in pancreatic cancer..... | 24 |
| 1.4.1 <i>Different approaches to defining subtypes</i> | 25 |
| 1.4.2 <i>A multi-omics characterisation of pancreatic cancer subtypes</i> | 26 |
| 1.5 Metabolism in cancer cells..... | 27 |
| 1.5.1 <i>Cancer cells and glucose</i> | 29 |
| 1.5.2 <i>Lipid and fatty acid biosynthesis in cancer</i> | 32 |
| 1.5.3 <i>The mevalonate pathway and cholesterol synthesis in cancer</i> | 33 |
| 1.5.4 <i>Fatty acid oxidation in cancer</i> | 34 |
| 1.5.5 <i>Autophagy in cancer</i> | 36 |
| 1.5.6 <i>Metabolic perturbations as a result of pancreatic cancer drivers</i> | 36 |
| 1.6 Thesis aims and objectives | 38 |
| Chapter 2 Materials and Methods | 40 |
| 2.1 General reagents..... | 41 |
| 2.2 Cell culture methods | 45 |

| | | |
|------------------|--|-----------|
| 2.2.1 | <i>Cell-lines</i> | 45 |
| 2.2.2 | <i>Culture maintenance</i> | 46 |
| 2.2.3 | <i>Splitting cells</i> | 47 |
| 2.2.4 | <i>Freezing/thawing cells</i> | 48 |
| 2.3 | Protein handling methods | 49 |
| 2.3.1 | <i>Cell lysate preparation</i> | 49 |
| 2.3.2 | <i>Quantifying lysate protein concentration</i> | 49 |
| 2.3.3 | <i>Sodium Dodecyl Sulfate-Polyacrylamide Gel Electrophoresis (SDS-PAGE)</i> | 50 |
| 2.3.4 | <i>Western blotting</i> | 50 |
| 2.4 | RNA handling methods | 51 |
| 2.4.1 | <i>RNA isolation from PDCLs</i> | 51 |
| 2.4.2 | <i>cDNA synthesis</i> | 51 |
| 2.4.3 | <i>qPCR assays</i> | 51 |
| 2.4.4 | <i>siRNA transfections</i> | 51 |
| 2.4.5 | <i>RNA-seq</i> | 52 |
| 2.5 | Drug treatments | 52 |
| 2.5.1 | <i>Generating dose-response curves</i> | 52 |
| 2.6 | Metabolic assays | 53 |
| 2.6.1 | <i>Extracellular metabolic flux assays</i> | 53 |
| 2.6.2 | <i>Glycolytic stress test</i> | 54 |
| 2.6.3 | <i>FAO assay</i> | 54 |
| 2.6.4 | <i>Mito Fuel Flex Test</i> | 55 |
| 2.6.5 | <i>Lactate production and glucose consumption assays</i> | 55 |
| 2.6.6 | <i>Generating delipidated serum for metabolic studies</i> | 56 |
| 2.6.7 | <i>Stable isotope tracer metabolomics</i> | 56 |
| 2.7 | Immunofluorescence and confocal microscopy | 56 |
| 2.7.1 | <i>Preparing cells for staining</i> | 56 |
| 2.7.2 | <i>Staining cells for imaging</i> | 57 |
| 2.7.3 | <i>Image acquisition</i> | 57 |
| 2.8 | Data analysis | 58 |
| 2.8.1 | <i>General statistical analysis</i> | 58 |
| 2.8.2 | <i>Drug screening analysis</i> | 58 |
| 2.8.3 | <i>Immunofluorescence image analysis</i> | 58 |
| Chapter 3 | <i>Defining Candidate Metabolic Vulnerabilities</i> | 59 |
| 3.1 | Introduction | 60 |
| 3.2 | Transcriptomic profiling of PDCLs reveals subtype-specific metabolic dysregulation | 61 |
| 3.2.1 | <i>Analysis of PDCL transcriptomes identifies in vitro subtypes</i> | 61 |
| 3.2.2 | <i>Subtype-associated metabolic signatures within PDCL transcriptomes</i> | 66 |
| 3.3 | Proteomic profiling validates and expands on transcriptomic analysis | 70 |

| | | |
|------------------|---|------------|
| 3.4 | Metabolic characterisation reveals distinct metabolic phenotypic differences between subtypes | 72 |
| 3.4.1 | <i>Determining optimal conditions for bioenergetics assays</i> | 73 |
| 3.4.2 | <i>Rates of glycolysis differ between subtypes in PDCLs</i> | 74 |
| 3.4.3 | <i>Functional metabolic outputs validate subtype aligned-glycolytic phenotypes</i> | 76 |
| 3.4.4 | <i>Rates of Fatty Acid Oxidation co-segregate with PDCL subtypes</i> | 80 |
| 3.4.5 | <i>Metabolic flexibility is associated with classical PDCLs</i> | 83 |
| 3.5 | <i>KRAS and mitochondrial gene mutation status do not account for subtype-associated metabolic dysregulation</i> | 86 |
| 3.1 | Association of KRAS amino acid substitution and subtype specification | 87 |
| 3.2 | Discussion | 89 |
| Chapter 4 | <i>Targeting Subtype-associated Metabolic Processes</i> | 92 |
| 4.1 | Introduction | 93 |
| 4.2 | Inhibiting squamous-associated glycolysis limits viability in PDCLs | 94 |
| 4.2.1 | <i>Identifying ALDOA as a potential target for inhibition of glycolysis in squamous subtype</i> | 94 |
| 4.2.2 | <i>Inhibiting glycolysis via TDZD-8 treatment is effective in squamous PDCLs</i> | 96 |
| 4.1 | Inhibition of fatty acid metabolism in classical subtype reveals metabolic flexibility | 99 |
| 4.1.1 | <i>Inhibiting general oxidative phosphorylation in classical cells limits viability</i> | 99 |
| 4.1.2 | <i>Inhibiting fatty acid biosynthesis in classical PDCLs induces increased glycolysis</i> | 104 |
| 4.2 | Modulating metabolic flexibility in classical subtype PDAC | 108 |
| 4.2.1 | <i>JQ1 treatment enhances subtype-associated metabolism in PDCLs</i> | 108 |
| 4.2.1 | <i>JQ1's effect on metabolism is mediated by increased lipogenesis and associated stress response</i> | 111 |
| 4.2.2 | <i>JQ1 treatment enhances sensitivity to inhibitors of lipogenesis, highlighting potential as a combination treatment</i> | 118 |
| 4.1 | Discussion | 118 |
| Chapter 5 | <i>High-Throughput Drug Screening Reveals potential of Statins in PC Treatment</i> | 122 |
| 5.1 | Introduction | 123 |
| 5.2 | Identifying candidate metabolic targets via high-throughput screening | 124 |
| 5.2.1 | <i>Optimising PDCLs for High-Throughput Screening</i> | 124 |
| 5.2.1.1 | Selecting PDCLs for screening | 124 |
| 5.2.1.2 | DMSO and Staurosporine Concentration | 126 |
| 5.2.2 | <i>High-Throughput Screening of PDCLs</i> | 127 |
| 5.2.2.1 | Primary Screening | 127 |
| 5.2.3 | <i>Analysis of Results from In-house Screening</i> | 128 |
| 5.2.4 | <i>Validating statins as major hit from screening</i> | 130 |
| 5.3 | Cholesterol synthesis and HMGCR degradation potentially contribute to statin resistance in classical PDCLs | 132 |

| | | |
|-------------------------|---|------------|
| 5.3.1 | <i>Quantifying anabolic processes reveals differences in cholesterol biosynthesis between subtypes</i> | 132 |
| 5.3.2 | <i>HMGCR degradation is found to be dysregulated between subtypes</i> | 134 |
| 5.3.3 | <i>Proteasomal inhibition partially inhibits HMGCR cleavage in vitro</i> | 135 |
| 5.3.4 | <i>Mevalonate induces negligible levels of cleavage of HMGCR in vitro</i> | 137 |
| 5.4 | Cholesterol localisation and lipid raft formation are indicators of statin sensitivity..... | 140 |
| 5.4.1 | <i>Caveolin-1, a regulator of cholesterol homeostasis, is found selectively in squamous PDCLs</i> | 140 |
| 5.4.2 | <i>Cholesterol localisation differs between subtypes in vitro</i> | 142 |
| 5.4.3 | <i>Lipid rafts are enriched in select squamous PDCLs, while CAV1 appears to colocalise with cholesterol</i> | 144 |
| 5.5 | Interrogating downstream arms of mevalonate pathway implicates GGPP and cholesterol in mediating sensitivity to statins | 146 |
| 5.5.1 | <i>Mevalonate pathway intermediates and cancer initiation and progression</i> | 146 |
| 5.5.1 | <i>Dietary metabolites within mevalonate pathway induce pitavastatin resistance in squamous PDCLs</i> | 147 |
| 5.6 | Statin sensitivity is enhanced by concomitant EGFR inhibition | 149 |
| 5.6.1 | <i>Pitavastatin inhibits Akt activation in squamous PDCLs</i> | 150 |
| 5.6.2 | <i>Combinatorial gefitinib treatment induces cell-death at low pitavastatin concentration in squamous PDCLs</i> | 151 |
| 5.7 | Potential <i>in vivo</i> testing of statin efficacy | 152 |
| 5.8 | Discussion..... | 155 |
| Chapter 6 | <i>Concluding Remarks</i> | 159 |
| 6.1 | Summary of project findings | 160 |
| 6.2 | Conclusions and future work | 161 |
| References | | 166 |

List of Tables

| | |
|---|-----|
| Table 1.1 PDAC drivers are associated with metabolic reprogramming..... | 38 |
| Table 2.1 Table listing materials used throughout project. | 41 |
| Table 2.2 PDCLs and general characteristics. | 45 |
| Table 2.3 Media formulations for tissue culture. | 48 |
| Table 2.4 Seahorse media formulations. | 53 |
| Table 3.1 Cell-line optimisations determined for bioenergetic stress tests on Seahorse platform. 74 | |
| Table 3.2 There is no apparent association between KRAS mutation copy number, mitochondrial mutations and PDCL subtype. | 87 |
| Table 3.3 Within PDCLs, mutations in <i>KRAS</i> do not show association between codon specificity or residue change and subtype. | 88 |
| Table 5.1 Selecting PDCLs for inclusion in screening project..... | 125 |
| Table 5.2 Identifying subtype-selective, metabolically active compounds..... | 129 |

List of Figures

| | |
|---|-----|
| Figure 1.1 Temporal expression of genes necessary for pancreatic differentiation..... | 19 |
| Figure 1.2 Gene programmes constituting pancreatic cancer subtypes reveal metabolic dysregulation. | 28 |
| Figure 1.3 Overview of metabolic pathways dysregulated in cancers. | 31 |
| Figure 2.1 Principle components analysis highlighting PDCL subtyping. | 46 |
| Figure 3.1 RNA-seq reveals two distinct subtypes in PDCLs. | 63 |
| Figure 3.2 Genes associated with pancreatic identity are downregulated in squamous PDCLs. | 65 |
| Figure 3.3 Metabolic genes are dysregulated between subtypes..... | 67 |
| Figure 3.4 Impact of metabolic isoform ratio on subtype and outcome. | 69 |
| Figure 3.5 Expression of metabolic genes correlates strongly to protein abundances in PDCLs..... | 71 |
| Figure 3.6 Classical subtype PDCLs are defined by the presence of metabolic networks of proteins. | 72 |
| Figure 3.7 Conducting glycolytic stress tests in PDCLs..... | 75 |
| Figure 3.8 Distinct glycolytic signatures define PDCL subtypes. | 78 |
| Figure 3.9 Validating PDCL metabolic signature. | 79 |
| Figure 3.10 Measuring rates of fatty acid oxidation in PDCLs..... | 80 |
| Figure 3.11 Rates of FAO differ across PDCL subtypes. | 82 |
| Figure 3.12 Classical PDCLs display greater metabolic flexibility than squamous. | 85 |
| Figure 3.13 Two concurrent approaches taken to identify novel therapeutics. | 91 |
| Figure 4.1 ALDOA identified as possible target via siRNA-mediated KD..... | 95 |
| Figure 4.2 ALDOA inhibition selectively reduces rates of glycolysis in Squamous PDCLs. | 96 |
| Figure 4.3 Determining optimal conditions for TDZD-8 treatment..... | 97 |
| Figure 4.4 Squamous PDCLs are selectively sensitive to ALDOA inhibition. | 98 |
| Figure 4.5 Inhibition of glycolysis by TDZD-8 is sustained at extended time-points. | 100 |
| Figure 4.6 AMPK is activated in classical PDCLs..... | 101 |

| | |
|--|-----|
| Figure 4.7 Classical cell-lines exhibit increased sensitivity to compound C. | 102 |
| Figure 4.8 AMPK inhibition decreases rates of stress-induced oxidative phosphorylation in classical PDCLs. | 103 |
| Figure 4.9 AMPK inhibition decreases glycolysis in classical PDCLs. | 104 |
| Figure 4.10 FASN inhibition reduces rates of triglyceride/lipid droplet production in classical PDCLs. | 106 |
| Figure 4.11 GSK2194069-mediated FASN inhibition leads to increase in glycolysis in classical PDCLs. | 107 |
| Figure 4.12 JQ1 treatment differentially affects glycolysis across subtypes. | 110 |
| Figure 4.13 JQ1 selectively activates mitochondrial stress in classical PDCLs. | 112 |
| Figure 4.14 JQ1 reduces overall levels of mitochondrial respiration in classical PDCL, while increasing FAO rates. | 113 |
| Figure 4.15 JQ1 treatment increases transcription of genes involved in lipogenesis. | 114 |
| Figure 4.16 JQ1 treatment leads to increased levels of proteins involved in lipogenesis. | 116 |
| Figure 4.17 JQ1 increases rates of lipid biosynthesis across both PDCL subtypes. | 117 |
| Figure 4.18 JQ1 treatment suppresses induced metabolic plasticity in classical PDCL and increases sensitivity to FASN inhibition. | 119 |
| Figure 5.1 Workflow of high-throughput screening with Beatson Screening Facility. | 126 |
| Figure 5.2 Pitavastatin selectively inhibits squamous subtype PDCLs. | 131 |
| Figure 5.3 Inhibition of HMGCR activity induces apoptosis in squamous PDCLs. | 132 |
| Figure 5.4 Rates of cholesterol biosynthesis differ between subtypes. | 133 |
| Figure 5.5 HMGCR is potentially selectively cleaved in classical PDCLs. | 136 |
| Figure 5.6 Treatment with protease inhibitor ALLN moderately inhibits HMGCR cleavage <i>in vitro</i> | 138 |
| Figure 5.7 Mevalonate exposure induces some HMGCR cleavage <i>in vitro</i> | 139 |
| Figure 5.8 CAV1 protein and mRNA is upregulated in the statin-sensitive, squamous subtype. | 141 |
| Figure 5.9 Optimising filipin III concentrations in cholesterol visualisation reveals differential localisation between subtypes. | 143 |
| Figure 5.10 Lipid rafts and CAV1 are visible only in squamous cell-lines, while pitavastatin has a minor effect on lipid raft formation. | 145 |

| | |
|---|-----|
| Figure 5.11 Supplementing various metabolites in the mevalonate pathway rescues pitavastatin-induced apoptosis in vitro. | 148 |
| Figure 5.12 Inhibition or loss of HMGCR leads to inactivation of AKT in sensitive PDCLs. | 151 |
| Figure 5.13 Pitavastatin and erlotinib synergise at low concentrations in squamous PDCLs..... | 153 |
| Figure 5.14 Cell-lines derived from mouse models of pancreatic cancer exhibit differential sensitivity to pitavastatin treatment..... | 154 |
| Figure 5.15 Subtype-specific markers of pitavastatin sensitivity persist in mice models of pancreatic cancer. | 155 |

Acknowledgements

I would first like to thank Professor Andrew Biankin for providing me the opportunity to undertake a PhD within his group. The time spent within his lab, and the experiences over the years have been indispensable for my personal and professional development. Thank you for providing the support and feedback necessary to see the project through to the end, and for your guidance through the thesis writing stage. Thank you to Holly Brunton for her tireless efforts assisting in the development of this thesis, as well as her and Bryan Serrels' input and supervision throughout the years, and for providing the direction required for personal growth as a scientist.

I also appreciate all the time and effort afforded to me by every member of GPOL, past and present, including Giusy Caligiuri, Selma Rebus, Eirini-Maria Lampraki, Stephan Dreyer, Maja Bailey, Kim Moran-Jones, Marc Jones, Derek Wright, Rosanna Upstill-Goddard, Peter Bailey and David Chang, as well as Amanda Ewing for all her assistance in organising so much over the years.

Additionally, I'd like to mention the kind help provided to me from Pablo Baquero while establishing a protocol for metabolic assays, as well as the continued assistance from Vignir Helgason and his group throughout the duration of the project. I am grateful too for the help provided by the Beatson Screening Facility and Karen Pickering in establishing protocols for drug-screening, and to Grace McGregor from Jurre and Andy Finch from the University of Edinburgh for assisting me with metabolomic assays. My time here was funded by Pancreatic Cancer UK, and I would like to extend my sincere thanks to all those in the organisation, those involved in fundraising, and all donators.

Finally, I'd like to thank all my family for all the support throughout the years, and for Amani, who motivated me through her own strength.

Authors Declaration

I declare that, except where explicit reference is made to the contribution of others, this dissertation is the result of my own work and has not been submitted for any other degree at the University of Glasgow or any other institution.

Printed Name: Richard Cunningham

Signature: _____

Abbreviations

| | |
|----------------|--|
| ADEX | Abnormally Differentiated Endocrine eXocrine |
| ALDOA | Aldolase A |
| AMPK | AMP-activated Protein Kinase |
| BET | Bromodomain and extra terminal domain |
| CT-B | Cholera toxin subunit B |
| DDR | DNA-damage response |
| DMSO | Dimethyl sulfoxide |
| ECAR | Extracellular Acidification Rate |
| EGF | Epidermal growth factor |
| EGFR | Epidermal growth factor receptor |
| EMT | Epithelial-mesenchymal transition |
| ER | Endoplasmic reticulum |
| FAO | Fatty Acid Oxidation |
| FASN | Fatty Acid Synthase |
| FBS | Fetal bovine serum |
| FDG-PET | Fluorodeoxyglucose-positron emission tomography |
| FPP | Farnesyl pyrophosphate |
| GEMM | Genetically engineered mouse model |
| GGPP | Geranylgeranyl pyrophosphate |
| GO | Gene Ontology |
| GP | Gene programme |
| HMGR | β -Hydroxy β -methylglutaryl-CoA Reductase |
| HNF1A | Hepatocyte nuclear factor 1A |
| HNF4A | Hepatocyte nuclear factor 4A |
| KD | Knockdown |
| KPC | LSL-KrasG12D/+; LSL-Trp53R172H/+; Pdx1-Cre |
| LDH | Lactate dehydrogenase |
| LFQ | Label-free quantification |

| | |
|-----------------|--|
| LogCPM | Log counts per million |
| ME | Module eigengene |
| MODY | Maturity-Onset Diabetes of the Young |
| mRNA | Messenger RNA |
| MTS | (3-(4,5-dimethylthiazol-2-yl)-5-(3-carboxymethoxyphenyl)-2-(4-sulfophenyl)-2H-tetrazolium) |
| OCR | Oxygen consumption rate |
| OXPHOS | Oxidative phosphorylation |
| PanIN | Pancreatic intraepithelial neoplasm |
| PCR | Polymerase Chain Reaction |
| PBS | Phosphate Buffered Saline |
| PDAC | Pancreatic ductal adenocarcinoma |
| PDCL | Patient derived cell-line |
| PDX | Patient derived xenograft |
| SDS-PAGE | Sodium Dodecyl Sulfate Polyacrylamide Gel Electrophoresis |
| siRNA | Small interfering RNA |
| SNP | Single nucleotide polymorphism |
| TBS-T | Tris buffered saline/0.1% TWEEN® 20 |
| ZIP | Zero interaction potency |

Chapter 1 *Introduction*

1.1 Introduction

Pancreatic ductal adenocarcinoma (PDAC) is a highly aggressive disease notoriously resistant to treatment, with a 5-year survival rate of less than 8% for patients diagnosed with the disease (Siegel, Miller and Jemal, 2017). Currently, the only means of curing the disease is surgical resection, a measure available only to ~20% of patients, and even then, a patient can expect just a 25% chance of surviving five years after surgery (Gillen *et al.*, 2010). Over the past two decades, the standard of care treatment given to non-resectable PDAC patients has been Gemcitabine (Burris *et al.*, 1997), with FOLFIRINOX (Conroy *et al.*, 2011) and gemcitabine with nab-paclitaxel (Von Hoff *et al.*, 2013) emerging more recently as alternatives. Though they represent the most effective therapeutics currently available to clinicians, the median survival for metastatic patients receiving these regimens of chemotherapy falls short of a year (Kamisawa *et al.*, 2016). This highlights a clear need for novel therapeutic avenues that may be effective in treating the majority of patients.

1.2 General characteristics of pancreatic cancer

1.2.1 Anatomy and development of the pancreas

The pancreas consists of a combination of interspersed exocrine and endocrine tissue, and as an organ, acts as a secretory gland to regulate metabolism. Its primary functions are to provide enzymes to the duodenum necessary for digestion, as well as to generate regulatory hormones to enter the circulatory system, controlling systemic metabolism; these two functions are carried out by the exocrine and endocrine lineages respectively. The exocrine system is made up of acinar and duct cells, while the endocrine component is comprised of a combination of cell-types, α -, β - and δ -cells, which constitute the islets of Langerhans. In the context of pancreatic cancer, it is important to consider the molecular mechanisms that regulate pancreatic formation and cell differentiation

(Figure 1.1) in order to understand the pathological rewiring that leads to oncogenic transformation.

In mice, both *PDX1* and *GATA6* are necessary for the development of pancreatic tissue (Ahlgren, Jonsson and Edlund, 1996; Decker *et al.*, 2006), with *PDX1* expression driving the early development of cells of all lineages within the pancreas (Wilding and Gannon, no date; Hale *et al.*, 2005). Beyond formation of the pancreas, *PDX1* is associated with insulin-producing β -cells, which are instrumental in carrying out the endocrine function of the pancreas: regulating metabolism. The collective expression of Forkhead Box A family of transcription factors, *FOXA1*, *FOXA2* and *FOXA3*, is also associated with the developing pancreas (Monaghan *et al.*, 1993).

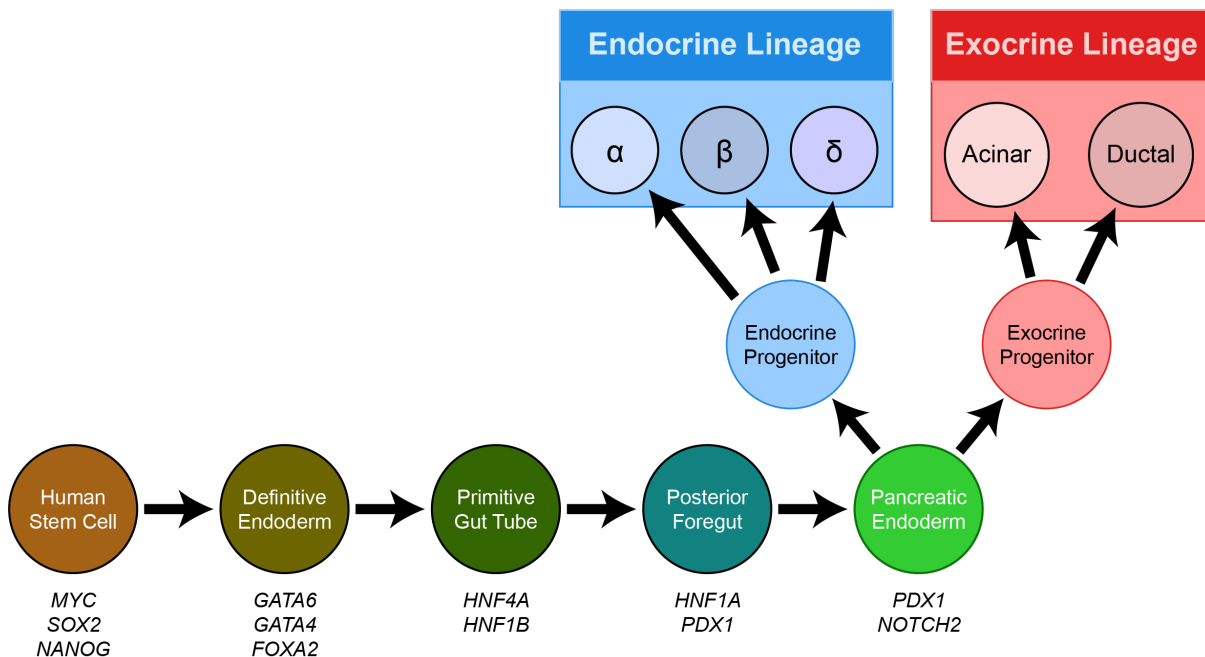


Figure 1.1 | Temporal expression of genes necessary for pancreatic differentiation. Schematic displaying different stages of development (circles) leading to terminal differentiation of pancreatic tissue of both endocrine (blue) and exocrine (red) lineages, along with genes that regulate function/differentiation. Adapted from (Beer and Gloyn, 2016) and (Hruban *et al.*, 2006).

Mutations within the Hepatocyte Nuclear Factor (HNF) family of transcription factors have long been associated with maturity-onset diabetes of the young (MODY), implicating their involvement in the maturation and function of β -cells (Fajans, Bell and Polonsky, 2001). A range of genomic and chromatin-immunoprecipitation (ChIP) assays have validated this observation, and reinforced the role of HNF1A, HNF1B and HNF4 in pancreatic formation (Shih *et al.*, 2001; Odom *et al.*, 2004; Edghill *et al.*, 2006).

1.2.2 Tumour initiation

The long-standing model of cancer formation holds that pancreatic precursor lesions, such as pancreatic intraepithelial neoplasms (PanINs) or intraductal papillary mucinous neoplasms (IPMNs), acquire mutations associated with oncogenesis over time. In this fashion, it is a gradual, multi-step process leading to progression to invasive carcinoma (Moskaluk, Hruban and Kern, 1997; Basturk *et al.*, 2015), the most common of which likely occurs in ductal tissue giving rise to PDAC, accounting for 85% of all pancreatic malignancies (Alexakis *et al.*, 2004).

There remain issues with this model to this day however, with current research suggesting that oncogenesis can initiate within a tight time-frame, with simultaneous mutations potentially occurring concomitantly (Notta *et al.*, 2016). If this is indeed the case, with progression occurring rapidly in a significant population of patients, there is then an even greater need for therapeutics effective in the management of advanced disease alongside the development of methods to assist in early diagnosis. Even the tissue of origin is a point of contention in PDAC, with evidence suggesting the transformative potential of cells of various lineage (Kleeff *et al.*, 2007; Yonezawa *et al.*, 2008). As such, much remains to be done to increase our understanding of pancreatic cancer oncogenesis, particularly to facilitate and advance the range of clinical interventions available to treat the disease.

1.2.3 Epidemiology and aetiology

PDAC tends to occur in older populations, with the majority of cases found in patients over 60 years of age (Raimondi *et al.*, 2007). A number of factors are thought to contribute to the occurrence of PDAC beyond age, with smoking found to contribute to incidence most from a range of various factors (Vrieling *et al.*, 2010; Bosetti *et al.*, 2012). Body mass index is another contributor (Aune *et al.*, 2012), along with, although to a lesser extent, diet (Li *et al.*, 2007). A family history of pancreatic cancer, along with germ-line mutations in genes that have long been associated with cancer susceptibility, are also found to increase the chances of developing pancreatic cancer (Lal *et al.*, 2000; Jacobs *et al.*, 2010). Despite these various risk factors that associate with PDAC, there are currently very few indicators to confidently identify high risk individuals for PDAC screening efforts, compounding early diagnosis of the disease and again, highlighting the necessity for late-stage treatments.

1.3 Molecular characteristics of pancreatic cancer

1.3.1 Common driver mutations

Although a high degree of heterogeneity exists within pancreatic cancer, as seen in the high number of low prevalence mutations identified, mutations in *KRAS* are present in ~90% of PDAC cases (Biankin *et al.*, 2012; Witkiewicz *et al.*, 2015). *KRAS* is a membrane-bound GTPase, a member of the Ras superfamily of small GTPases that, when active, regulate a variety of pathways associated with oncogenesis, including survival and cell cycle progression (Vigil *et al.*, 2010). In PDAC, 98% of *KRAS* mutations occur at the 12th glycine residue, leading to a constitutively active form of *KRAS*.

In mouse models, maintenance of PDAC is dependent on continuous expression of activated *KRAS* (Collins *et al.*, 2012). *KRAS* has proven to be a largely undruggable

target up to now (Gysin *et al.*, 2011), though some experimental, clinically relevant methods have shown promise in treating pancreatic cancer in a preclinical setting, including the use of exosomes loaded with small interfering RNA (siRNA) designed to target mutant KRAS (Kamerkar *et al.*, 2017). In addition to this, some small inhibitory molecules have been developed against KRAS^{G12C} (Ostrem *et al.*, 2013), however this specific mutation is present only in a very small percentage (3%) of PDAC patients (Cox *et al.*, 2014), meaning these compounds will likely be clinically viable in other cancer-types and not pancreatic cancer. Should drug discovery research efforts lead to the development of a KRAS inhibitor effective in the context of pancreatic cancer, there is evidence from knockdown/knockout assays that subsets of cancer cell populations may prove refractory to KRAS inhibition (Singh *et al.*, 2009; Muzumdar *et al.*, 2017), with additional studies showing the potential of acquired resistance to KRAS inhibition as a possible mitigator of clinical efficacy (Collins *et al.*, 2012). These observations indicate that pathways downstream of *KRAS* mutation may provide more promising drug targets than the gene product itself.

Beyond *KRAS* alterations, mutations are found at high frequency in *CDKN2A*, *TP53*, and *SMAD4* (Jones *et al.*, 2008). PDAC is additionally characterised by an abundance of low prevalence mutations (Waddell, Pajic, A.-M. Patch, *et al.*, 2015), with experimental evidence highlighting the range of genes capable of driving pancreatic cancer initiation upon mutation (Mann *et al.*, 2012). Despite a clear diversity in driver genes, the majority of mutations tend to occur in a number of canonical pathways central to cancer development (Jones *et al.*, 2008). These studies therefore indicate that approaches to identifying therapeutics effective in treatment of PDAC be focused on targeting these pathways in general, rather than one specific genetic target, while these common driver mutations are also found to activate pathways commonly associated with the development of pancreatic cancer. These include the PI3K/Akt pathway (Ng SSW *et al.*, 2000; Perugini *et al.*, 2000; Bondar *et al.*, 2002) and the oncogene *c-Myc* (Asano *et al.*, 2004; Hessmann *et al.*, 2016).

1.3.2 Genomic instability and mutation burden

Previous research has investigated the degree of genomic instability found in PDAC, with results highlighting the presence of disrupting structural variants in previously mentioned driver genes (Waddell, Pajic, A.-M. Patch, *et al.*, 2015). Additionally, a subset of 14% of pancreatic cancer patients exhibit highly unstable genomes, with a further 36% displaying scattered chromosomal rearrangements. Those patients with a high degree of chromosomal instability also score highly for a point-mutational signature associated with *BRCA1* and *BRCA2* mutation (Alexandrov *et al.*, 2013). Additionally, concurrent mutations in *KRAS* and *TP53* in mice models drive genomic instability in the context of PDAC (Hingorani *et al.*, 2005), providing evidence for a single event leading to wide-spread alterations of the genome.

1.3.3 Dysregulation of gene expression

While cancer signatures based on mutations and genetic alterations have informed the development of therapeutics effective in the treatment of various cancer-types in the past (Lynch *et al.*, 2004; Druker *et al.*, 2006), analyses into gene expression and regulation are likely to provide more in-depth insights into the arms of targetable pathways that will be susceptible to inhibition. With the wide-spread availability of next-generation sequencing platforms, a number of large-scale studies have been conducted utilising RNA-seq to compare the transcriptomes of tumour and paired benign tissue (Mao *et al.*, 2017), which has revealed similar dysregulation within pathways observed to exhibit increased rates of mutations (Jones *et al.*, 2008).

1.3.4 Epigenetic perturbations in pancreatic cancer

Epigenetics is a term that describes genetic regulation beyond the genome, initially defined in the context of developmental biology (Margueron, Trojer and Reinberg, 2005; Holliday, 2006). Though cancer is inherently a genetic disease, with mutations driving oncogenic progression, the prevalence of gene

dysregulation in cancers attests to the contribution of epigenetic factors. Over the past couple of decades, the extent to which various cancer-types are driven by epigenetic perturbations has been extensively interrogated (Nebbio *et al.*, 2018), highlighting the involvement of histone modification (Martinez-Garcia *et al.*, 2011; McCabe *et al.*, 2012; Zhao *et al.*, 2016) and DNA methylation (Cai *et al.*, 2017; Hao *et al.*, 2017) events in multiple cancers.

Heterogenous epigenomic landscapes have been observed within pancreatic cancer, with distinct chromatin states found to predict prognosis in patients (Lomberk *et al.*, 2018), while sweeping changes in chromatin structure have been described in pancreatic cancer metastases (McDonald *et al.*, 2017). These observations, coupled with the finding that cells across multiple cancer types undergo epigenetic changes underpinning drug tolerance (Sharma *et al.*, 2010), highlight the potential of therapeutically targeting epigenetic players in pancreatic cancer. To this end, there have been a number of novel inhibitors tested in the context of pancreatic cancer targeted towards a variety of classes of epigenetic enzymes (Hessmann *et al.*, 2016). This includes proteins that regulate histone acetylation, including histone acetyltransferases (Ono, Basson and Ito, 2016) and histone deacetylases (Lee *et al.*, 2017; Booth *et al.*, 2019), histone methylation, such as polycomb proteins (Avan *et al.*, 2012), and the reading of epigenetic marks, such as the bromodomain and extra terminal domain (BET) family (Mazur *et al.*, 2015; Sherman *et al.*, 2017).

1.4 A need for defined subtypes in pancreatic cancer

Preclinical research efforts to identify new treatments are compounded by the previously described genomic diversity that exists within pancreatic cancer. By their design, classical clinical trials generally fail to appropriately address heterogeneity as patients are, by necessity, grouped together in large numbers. For this reason, drugs that may have potential in treating smaller subsets of actionable groups of patients may be overlooked, with exceptional responders

being dismissed as outliers rather than meaningful results. This highlights a need to break down pancreatic cancers into subtypes, each with unique sets of characteristics including differential sensitivities. Previous research efforts have succeeded in identifying effective therapeutic strategies in the treatment of other cancer-types in this manner (Slamon *et al.*, 2001; Davies *et al.*, 2002; Druker *et al.*, 2006; Chapman *et al.*, 2011).

1.4.1 Different approaches to defining subtypes

In order to address this diversity and develop methods allowing for the stratification of patients, various studies have attempted to define subtypes within pancreatic cancer. These research efforts have employed a range of approaches, including attempts that recognised the need for subtypes in pancreatic cancer, and considered physical properties/tissue of origin as pertinent characteristics for classification (Cubilla and Fitzgerald, 1979). Additional examples are the previously described subtyping study that looked at variability in genomic instability (Waddell, Pajic, A.-M. Patch, *et al.*, 2015). Several successful attempts have also involved microarray assays, applied directly to multiple sources of tumour tissue (Collisson *et al.*, 2011), and cells from metastatic sites and the surrounding microenvironment (Moffitt *et al.*, 2015).

With the advent of next-generation sequencing, transcriptome-based subtyping methodologies can be extended beyond microarrays, overcoming the limitation of quantifying expression within a pre-specified collection of genes. A recent research project characterised subtypes within PDAC via publicly available transcriptome databases within an entirely metabolic context. This study defined subtypes according to expression patterns of genes involved in glycolysis (Follia *et al.*, 2019). Beyond the transcriptome, subtyping efforts have probed chromatin accessibility and DNA methylation profiles to describe the existence of epigenetic subtypes (Lomberk *et al.*, 2018).

1.4.2 A multi-omics characterisation of pancreatic cancer subtypes

This project will focus on a subtype classification system that employs a multi-omics approach, taking into account the transcriptome, genome and epigenome to analyse a cohort of 457 patients, resulting in a descriptor of four distinct subtypes within PDAC (Bailey *et al.*, 2016). These subtypes have recently been characterised taking into account previously mentioned subtyping efforts (Collisson *et al.*, 2019) and are presented correspondingly as follows: the squamous subtype, characterised by poor prognosis and an upregulation of genes associated with “squamous-like” cancers (Hoadley *et al.*, 2014); the pure classical progenitor subtype, associated with an upregulation of transcription factors involved in endoderm cell-fate determination; exocrine-like, a subtype defined by increased expression of transcriptional networks involved in later stage pancreas development, of both endocrine and exocrine lineages; and the immunogenic progenitor subtype, which shares a transcriptomic profile similar to the pure classical progenitor subtype, but with an additional upregulation of genes suggestive of immune infiltration. Based on their transcriptomic profiles, patients can be classed as belonging to one of the four subtypes (Figure 1.2).

Enrichment analysis to characterise gene programmes (GPs) that define these subtypes facilitates the identification of pathways that may be involved in the initiation, progression or maintenance of tumours belonging to each subtype. When applied to GPs, enrichment analysis reveals the association of a diverse range of pathways with each of the four subtypes. One recurring observation is the enrichment of different pathways involving metabolism, particularly with GPs associated with squamous and pure classical progenitor subtypes (Figure 1.2). Gene programme 1 (GP1), the largest of the gene-sets whose collective expression is associated with both the pure classical progenitor and immunogenic progenitor subtypes, shows a marked enrichment for a broad range of pathways, many of which are associated with the biosynthesis and catabolism of various lipid metabolites. In contrast to this, the squamous subtype exhibits an upregulation of four separate gene programs, each defined by an enrichment for a distinct set of

pathways covering a diverse range of cellular functions. GP2 is the primary program enriched for genes associated with the “squamous-like” cancers and is also the most significantly associated with a worse prognosis, accounting for the poor clinical performance observed in the squamous subtype. Gene members of a range of pathways involving metabolism are enriched within this gene programme, including hypoxia which has long been associated with glycolytic activation (Semenza *et al.*, 1994), as well as canonical glycolysis and glycolytic process pathways.

More recent projects carrying out similar multi-omics analyses have validated and refined these findings, resulting in the description of two clearly distinct subtypes of pancreatic cancer (Cancer Genome Atlas Research Network., 2017). These two subtypes, squamous/basal-like and progenitor/classical, are reflective of the previously discussed attempts to define pancreatic cancer subtypes.

1.5 Metabolism in cancer cells

Metabolism is the process by which cells break down nutrients and generate energy to fuel biological functions. Metabolism in the context of cancer has been studied more and more extensively in recent years, with clear potential recognised in the identification of therapeutic targets that can be exploited after metabolic transformation in tumour cells. Such metabolic inhibitors would have the advantage of selectively killing cancer tissue, having no detrimental effect on normal cells, thus limiting deleterious side-effects associated with systemic chemotherapy (Vander Heiden, 2011).

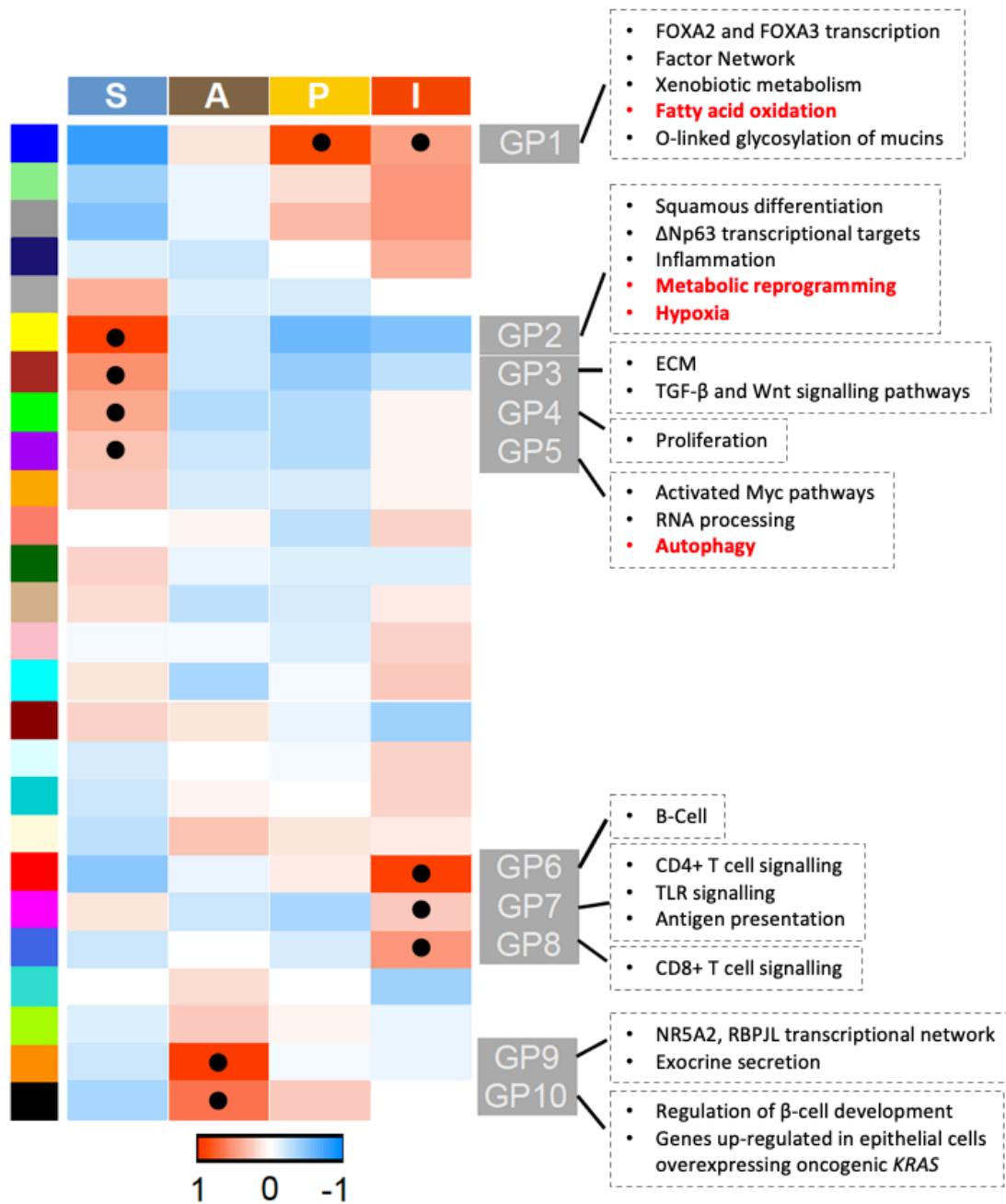


Figure 1.2| Gene programmes constituting pancreatic cancer subtypes reveal metabolic dysregulation. Heatmap showing the collective expression of GPs that define the four subtypes, with black circles denoting GPs that correlate best to specific subtypes. Pathways significantly enriched in those correlated GPs are shown to the right, with those pathways related to metabolic function highlighted in red. Adapted from (Bailey *et al.*, 2016). As can be seen, several metabolic pathways are found to be enriched in programmes associated with the squamous and pure classical progenitor subtypes.

1.5.1 Cancer cells and glucose

One hallmark of transformation is the reliance of cancer cells on glycolysis as a primary source of energy production. This metabolic process, which involves breaking down glucose into pyruvate and then subsequently lactate (or ethanol in unicellular organisms, through the process of fermentation), was originally associated with cells grown in conditions of hypoxia. It is a mechanism less efficient at generating ATP from glucose than oxidative phosphorylation (OXPHOS), the primary means of energy production in most cells and which is reliant upon the tricarboxylic acid (TCA) cycle in mitochondria. Hypoxic cells are dependent on glycolysis as oxidative phosphorylation requires oxygen, as well as NADH and FADH₂ generated via the TCA cycle, to fuel the electron transport chain (ETC) that generates ATP (Figure 1.3).

Aerobic glycolysis, or glycolysis conducted in normoxia, has also been associated with cell-types that exhibit rapid-proliferation. This includes single-cell organisms characterised by rapid growth (Bryant, Voller and Smith, 1964; Rolland, Winderickx and Thevelein, 2002), proliferating fibroblasts (Munyon and Merchant, 1959), stem cells, both induced and embryonic (Folmes *et al.*, 2011), and transformed cells (Warburg, 1956), with cancer-associated aerobic glycolysis frequently termed as the “Warburg Effect” after Otto Warburg, the researcher credited with its discovery. While the reasons that a cell in an oxygen-limiting environment would utilise glycolysis as an energy source are apparent, the advantage of aerobic glycolysis is not immediately obvious, with the observed association between proliferation and glycolysis suggestive of a rapid production of cellular energy to fuel biosynthetic demands made possible by glycolysis. Alternative theories suggest that it may be due to metabolic reprogramming as a result of intermittent exposure to hypoxic conditions associated with the tumour micro-environment (Gatenby and Gillies, 2004).

Since its inception, much work has both reinforced and been influenced by Warburg's theory, with one commonly-used and historically successful diagnostic tool in many cancer-types, FDG-PET, having been developed to detect the Warburg Effect in patients (Adams *et al.*, 1998; Burt *et al.*, 2001; van Tinteren *et al.*, 2002). This test functions via imaging of the radiotracer fluorodeoxyglucose (FDG), a fluorinated glucose analogue that is readily taken up by glycolytic tumour cells and can be detected via positron emission tomography (PET) imaging (Adams *et al.*, 1998). Despite this, research throughout the years has cast doubt as to the veracity of the theory (Weinhouse, 1956), and one meta-analysis demonstrated that higher glycolytic ATP production is not a consistent characteristic of cancer cells on the whole relative to normal tissue (Zu and Guppy, 2004). However, these results highlight a metabolic heterogeneity found within cancer-associated cellular metabolism and suggests that a sub-category of cancer cells likely exhibit the highly glycolytic phenotype described by Warburg. This may also, in part, explain the inconsistency in the success rates of FDG-PET, with some population of cancer-cells utilising glucose to fuel the TCA cycle, and potentially harnessing metabolic intermediates generated in this manner to support anabolic pathways (Lunt and Vander Heiden, 2011).

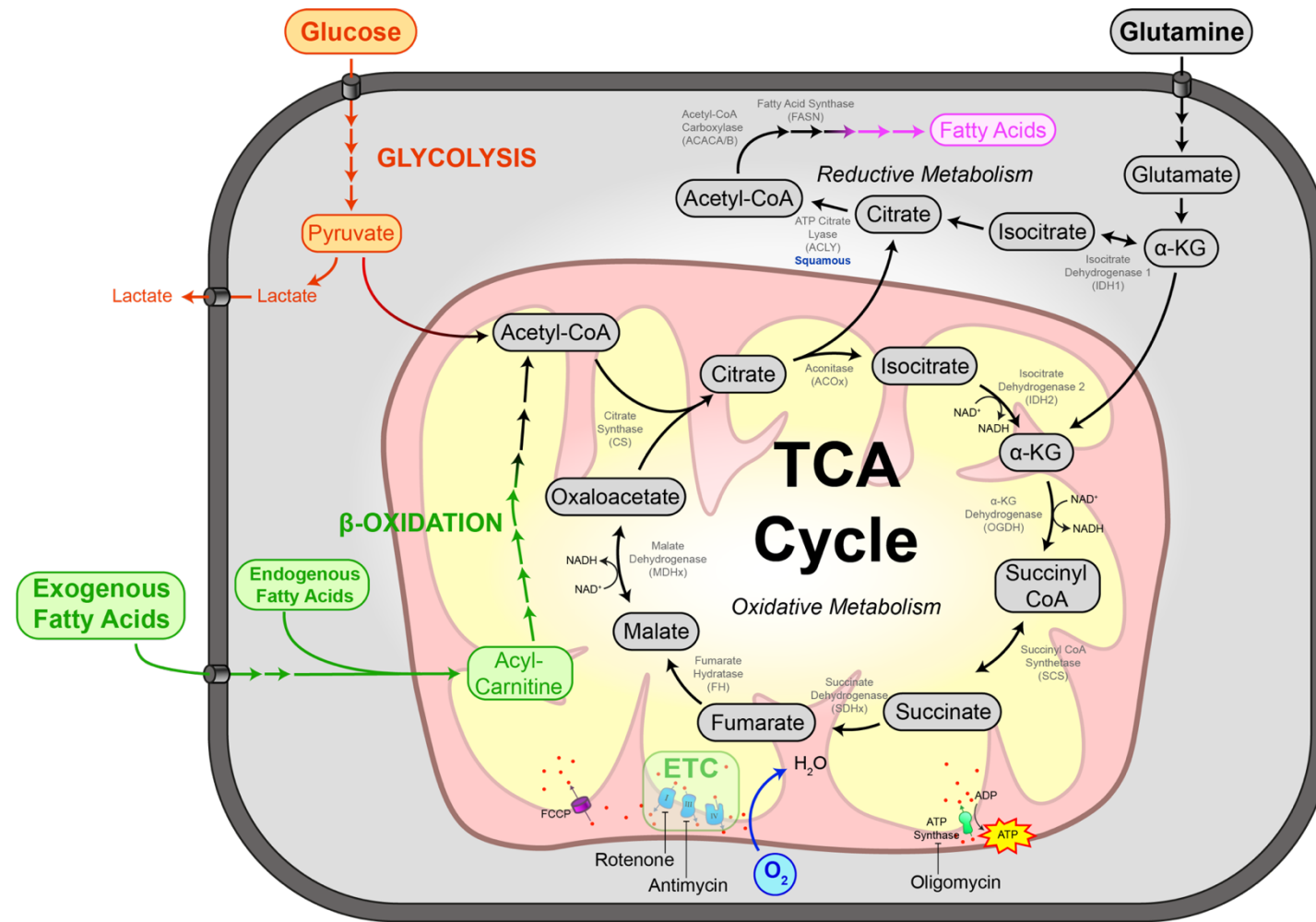


Figure 1.3 | Overview of metabolic pathways dysregulated in cancers. Schematic outlining the various processes and metabolites that contribute to cancer progression. The glycolysis pathway is shown in red, with pyruvate converted to lactate in conditions of aerobic glycolysis and shuttled into mitochondria to fuel the TCA Cycle in most, non-cancerous cell-types. FAO is shown in green, with the end-product of β-oxidation (acetyl-CoA) also acting as a fuel source for the TCA cycle. NADH generated via this cycle acts as an electron carrier, driving the electron transport chain, and allowing the controlled transfer of protons (red circles) from the mitochondrial matrix (yellow) to the intermembrane space (pink). This interaction allows the maintenance of the proton gradient across the inner mitochondrial membrane, and the controlled generation of ATP via ATP synthase.

1.5.2 Lipid and fatty acid biosynthesis in cancer

Lipogenesis is initiated utilising cytoplasmic pools of acetyl-CoA, which are predominantly produced by the breakdown of citrate by ATP citrate lyase (ACLY) within the cytoplasm. This citrate supply originates from within the TCA cycle, and its export from mitochondria is facilitated by the citrate transport protein (SLC25A1). Acetyl-CoA can then be converted to malonyl-CoA by the family of acetyl-CoA carboxylase family, consisting of an alpha and beta subunit (ACACA or ACC1 and ACACB or ACC2). The subsequent step in fatty acid synthesis (FAS) is mediated by fatty acid synthase (FASN), an enzyme integral for fatty acid/cholesterol biosynthesis, which acts to generate palmitate and saturated fatty acids from both acetyl-CoA and malonyl-CoA. This conversion is mediated by multiple reactions, all of which are catalysed by FASN, resulting in elongation cycles iteratively leading to the generation of 16-carbon palmitate (Lomakin, Xiong and Steitz, 2007). FASN has long been associated with cancer, with inhibition associated with an inhibition of growth in tumour cells (Kuhajda *et al.*, 1994). As such, FASN has been considered as a possible target for anti-cancer therapeutics (Menendez and Lupu, 2007).

In cancer cells, lipid biosynthesis is generally primed for the production of membranes and signalling molecules which are required for rapid proliferation (Currie *et al.*, 2013). Cell membranes are primarily composed of phospholipids, and the generation of phosphatidylcholine, the primary phospholipid constituent of membranes, has been shown to promote oncogenesis *in vivo* (Gallego-Ortega *et al.*, 2009), highlighting the link between transformation and lipid synthesis.

Where fatty acid precursors are not synthesised into phospholipids, triacylglycerols (TAGs) are formed instead. These act as stores of cellular energy, and are maintained in the form of lipid droplets (Walther and Farese, 2009). Various families of enzymes are involved in TAG generation, including lipins (Csaki and Reue, 2010). The family of lysophosphatidylcholine acyltransferases (LPCATs) have been shown to localise to lipid droplets, and are thought to assist in LD formation

by providing phosphatidylcholine (Moessinger *et al.*, 2011). Phosphatidylcholine is integral for LD structure, as it is the most abundant component in the polar lipid monolayer encompassing the neutral lipids and TAGs at the core (Bartz *et al.*, 2007).

Transformation induced by *KRAS* mutation, present in the majority of pancreatic cancer, has been linked to a decrease in *de novo* lipid synthesis (Kamphorst *et al.*, 2013). Cells having been affected by such transformation are observed to scavenge exogenous lipids to compensate for the lack of endogenously produced fatty acids, in order to fuel the anabolic pathways rapidly proliferating cells are dependent on.

1.5.3 The mevalonate pathway and cholesterol synthesis in cancer

Beyond conversion to malonyl-CoA, acetyl-CoA may be converted to acetoacetyl-CoA. This step is a necessary precursor for the mevalonate pathway, which is responsible for the generation of cholesterol, alongside a variety of sterol intermediates. The mevalonate pathway is initiated by the conversion of acetoacetyl-CoA to HMG-CoA and subsequently, to mevalonate, a metabolite which has been found to promote tumour progression in a xenograft mouse model utilising MDA-MB-435 (Duncan, El-Sohemy and Archer, 2004), a cell-line most likely of melanoma origin (Prasad and Gopalan, 2015). This discovery points to the involvement of downstream components of the mevalonate pathway on cancer development, the most well-characterised of which being cholesterol.

Cholesterol has been shown to be instrumental in regulating a number of signalling pathways, with a variety of signalling receptors found to be recruited to lipid rafts (Mollinedo and Gajate, 2015), cholesterol-rich membrane microdomains (Brown and London, 1998, 2000). A number of these signalling receptors associated with lipid rafts are known to be involved in pancreatic cancer development, including insulin-like growth factor I receptor (IGF-IR), which is dependent upon lipid rafts for downstream signalling (Huo *et al.*, 2003). IGF-I, the ligand of IGF-IR, has long been known to be overexpressed in PDAC (Bergmann *et al.*, 1995), while

therapeutic inhibition of IGF-IR has been shown to inhibit PC growth in *in vivo* models (Moser *et al.*, 2008), thus demonstrating the indirect involvement of lipid rafts in pancreatic cancer. This relationship is reinforced by the observation that markers involved in lipid raft formation are found to upregulated in a range of cancer-types, particularly breast and colon cancers (Staubach and Hanisch, 2011).

Upstream of sterol synthesis, there are a number of alternative metabolites within the mevalonate pathway associated with cancer development and progression. This includes farnesyl pyrophosphate (FPP) and geranylgeranyl pyrophosphate (GGPP), two metabolites required for the transfer of farnesyl and geranylgeranyl moieties, constituting a post-translational modification known as prenylation. This modification is of particular relevance in PDAC as KRAS has long been known to be farnesylated (Hancock *et al.*, 1989), while inhibition of KRAS prenylation has been shown to prevent tumour growth both *in vitro* and *in vivo* models of PC (Zimmermann *et al.*, 2013; Jansen *et al.*, 2017). Beyond KRAS, the Rho family of GTPases are also known to be prenylated (Clarke, 1992), while RhoA, a member of this family of small GTPases, has been shown to regulate the activity of YAP (Yu *et al.*, 2012). This is of importance as YAP is inactivated by the tumour suppressor Hippo signalling pathway, a pathway known to be repressed in PDAC (Zhang *et al.*, 2014; Wang *et al.*, 2020). These findings collectively highlight the mevalonate pathway's involvement in driving cancer progression in general, with evidence that targeting the mevalonate pathway can disrupt the localisation and function of a range of GTPases (Ali *et al.*, 2010), clearly demonstrating its relevance to PDAC.

1.5.4 Fatty acid oxidation in cancer

Fatty acid oxidations (FAO) is the process by which cells break down reserves of fatty acids, generating NADH and FADH₂ to fuel the ETC. The initial stage of the process is β -oxidation, which occurs primarily within mitochondria and less commonly in peroxisomes. This process involves the recurrent break-down of fatty acids (FAs) to generate stores of acetyl-CoA, which can subsequently be utilised as fuel for the TCA cycle. Long chain FAs, which serve as a common substrate for β -

oxidation, must be shuttled into mitochondria via the carnitine shuttle before they can be broken down (Fritz and Yue, 1963).

Under conditions of metabolic stress, reflected by high AMP/ATP and ADP/ATP ratios, AMP-activated protein kinase (AMPK) modulates a number of signalling pathways that regulate cellular metabolic function. In this manner, AMPK acts as a key regulator of the balance between lipogenesis and FAO, increasing transcription of carnitine transporters, which drive FAO by facilitating the transfer of palmitate across mitochondrial membranes, in colorectal cell-lines and cardiac myocytes (Zaugg *et al.*, 2011; Pflieger, He and Abdellatif, 2015), while directly phosphorylating and inhibiting the acetyl-CoA carboxylase (ACAC) family of enzymes. These enzymes, as described previously in chapter 1.5.2, are necessary for the production of malonyl-CoA, which is essential for fatty acid biosynthesis (Hardie and Pan, 2002). This balance between FA catabolism and anabolism is then influenced by the metabolite malonyl-CoA, which is capable of both driving FAS and inhibiting FAO. The differential compartmentalisation of malonyl-CoA production, as determined by localisation of ACACA and ACACB, decides which pathway is effected, with cytosolic malonyl-CoA produced by ACACA activating lipogenesis, while mitochondrial malonyl-CoA produced by ACACB inhibits FAO in various experimental models (Abu-Elheiga *et al.*, 2000, 2001; Hardie and Pan, 2002). The observation that FAS and FAO are regulated by distinct enzymes challenges the historic assumption that the two pathways are mutually exclusive to one another (Jeon, Chandel and Hay, 2012; Carracedo, Cantley and Pandolfi, 2013).

Beyond the balance between lipogenesis and FAO, AMPK has also been found to regulate lipolysis, the process by which hydrolysis of TAGs induces the liberation of FAs, which can be utilised via FAO to generate cellular energy. In the past, conflicting results demonstrated that AMPK could both promote and inhibit lipolysis in adipocytes (Yin, Mu and Birnbaum, 2003; Daval *et al.*, 2005). However, more recent research has highlighted the complex interplay of this regulatory cycle, with AMPK activation associated with upregulated lipolysis (Gauthier *et al.*,

2008), hypothesised to act to offset the high energy consumption resultant from increased re-esterification of free FAs to TAGs (Ceddia, 2013).

1.5.5 Autophagy in cancer

Beyond regulation of the balance between FAS and FAO, AMPK also activates autophagy, the process by which cellular components such as organelles and cytoplasmic constituents are degraded, allowing for the recycling of energy and molecules required for biosynthesis. The initiation of autophagy facilitates homeostasis and the mitigation mitochondrial stress, which in the context of cancer, promotes cell survival by preventing DNA damage (Karantza-Wadsworth *et al.*, 2007) and necrosis/inflammation (Degenhardt *et al.*, 2006). As these processes are associated with tumorigenesis, the protective role of autophagy is thought to be tumour suppressive, an observation further validated by the enhanced initiation of tumour formation in autophagy-deficient mice (Yue *et al.*, 2003; Takahashi *et al.*, 2007). Despite this, autophagy inhibition has been shown to inhibit tumour growth in PDAC mouse-models (Yang *et al.*, 2011), highlighting the complex interplay between autophagy driven tumour survival and suppression.

1.5.6 Metabolic perturbations as a result of pancreatic cancer drivers

Historic experiments performed in mice showed that transfection of *ras* oncogenes induced an increase in glucose uptake and expression of glucose transporters in rat fibroblasts (Racker, Resnick and Feldman, 1985; Flier *et al.*, 1987). As further validation of the involvement of KRAS in driving glycolysis, previous research has shown that tumours initiated via inducible mutant *KRAS* expression in *in vivo* models regress upon loss of *KRAS* expression, leading to a reduction in glucose uptake and glycolysis (Ying *et al.*, 2012). Building on these findings, work involving a similar inducible model assessing *KRAS* oncogene withdrawal also showed tumour regression, with those cells that survive withdrawal exhibiting decreased glycolysis, as observed in (Ying *et al.*, 2012), as well as enhanced OXPHOS, which

was found to be necessary for the survival of these cells (Viale *et al.*, 2014). In addition to inducing activation of glycolysis in PDAC, oncogenic *KRAS* has also been shown to drive non-canonical glutamine dependency (Son *et al.*, 2013) and lipid uptake (Kamphorst *et al.*, 2013) in *in vitro* models of pancreatic cancer, while signalling pathways downstream of mutant *KRAS*, such as mTOR (Kong *et al.*, 2016; Zeitouni *et al.*, 2016), also mediate metabolic dysregulation (Laplante and Sabatini, 2009).

c-Myc, commonly activated in pancreatic cancer (Asano *et al.*, 2004; Hessmann *et al.*, 2016) and associated with the squamous, GP5 in PDAC patients (Figure 1.2), has been shown to act as a driver of a variety of metabolic pathways. For example, evidence proves that c-Myc mediates a switching from oxidative to glycolytic phenotypes in pancreatic cancer cell-lines (Sancho *et al.*, 2015), an observation supported by past research demonstrating the ability of c-Myc to induce expression of lactate dehydrogenase (Shim *et al.*, 1997) required for aerobic glycolysis. Conversely, c-Myc has also been shown to induce transcription of a number of genes involved in mitochondrial biogenesis in a range of cell-lines (Li *et al.*, 2005; Kim, Lee and Iyer, 2008) and can mediate glutamine addiction in glioma cell-lines (Wise *et al.*, 2008), indicating its ability to drive metabolic processes involving OXPHOS. In addition to this, interplay between mutant *KRAS* and c-Myc effects changes within cellular metabolism, with *KRAS*^{G12D} induced glycolysis shown to be dependent on c-Myc (Ying *et al.*, 2012). These studies highlight the complex contribution of c-Myc to metabolic reprogramming in oncogenesis, as well as its ability to drive both glycolysis and OXPHOS (Dang, Le and Gao, 2009).

Conversely, the hepatocyte nuclear factors (HNFs) are associated with pancreatic development, as described in chapter 1.2.1, and have been found to act as tumour suppressors in pancreatic cancer (Hoskins *et al.*, 2014; Luo *et al.*, 2015), while HNF loss is associated with the aggressive squamous subtype in PDAC subtypes (Bailey *et al.*, 2016). In the context of metabolism, this family of transcription factors have been linked to lipid homeostasis (Hayhurst *et al.*, 2001) and are found to induce expression of genes involved in lipid biosynthesis (Odom *et al.*, 2004).

Table 1.1 | PDAC drivers are associated with metabolic reprogramming. Table showing perturbations commonly associated with PDAC oncogenesis and their demonstrated impacts on metabolism. A variety of molecular drivers of pancreatic cancer have been implicated in modulating metabolism, including *KRAS* mutation, which occurs in ~90% of PC. These are found affect a number of metabolic processes associated with cancer, including glycolysis, OXPHOS and lipogenesis.

| Gene | Perturbation in PDAC | Effect on Metabolism | Reference |
|--------------|----------------------|---|---|
| KRAS | Mutation | <ul style="list-style-type: none"> Enhances glycolysis Inhibits OXPHOS | (Ying <i>et al.</i> , 2012) (Viale <i>et al.</i> , 2014) |
| c-Myc | Activation | <ul style="list-style-type: none"> Enhances glycolysis Associated with OXPHOS | (Sancho <i>et al.</i> , 2015) (Li <i>et al.</i> , 2005; Wise <i>et al.</i> , 2008) |
| HNFs | Tumour Suppressor | Enhances lipogenesis | (Odom <i>et al.</i> , 2004) |

Collectively, these findings highlight the close association between drivers of pancreatic cancer formation and metabolic reprogramming (Table 1.1). This therefore highlights the integral part metabolism likely plays in PC development.

1.6 Thesis aims and objectives

Taking these collective findings into account, it was decided to focus on metabolic perturbations in those clearly defined subtypes of PDAC, with the end goal of selecting therapeutic interventions with clinical potential for subpopulations of patients. In order to enhance the possibility of identifying novel and effective therapeutic interventions, this thesis describes a multi-step approach which included the following specific aims:

- Characterise and validate subtype-associated metabolism in a clinically relevant model of PDAC.
- Identify therapeutics with potential to inhibit metabolic pathways found to associate with subtypes.

- Perform simultaneous, high-throughput drug repurposing screening to identify metabolism modulating therapeutics that effect a subtype-selective response.

These efforts validated observations of metabolic dysregulation observed within patient subtype groups, confirming the upregulation of glycolysis associated with the aggressive, squamous subtype and FAO with the pure classical progenitor subtype in *in vitro* models of PDAC. Attempts to target these metabolic processes were met with success, with squamous PDCLs determined to exhibit sensitivity to inhibition of glycolysis. In contrast to this, PDCLs classified as pure classical progenitor were found to be resistant to attempts to target stores of FAs, with metabolic flexibility identified as the potential mechanism by which PDCLs effect this mechanism of escape.

Chapter 2 Materials and Methods

Materials and Methods

2.1 General reagents

Reagents used throughout the project are listed in table 2.1.

Table 2.1 | Table listing materials used throughout project.

| General Use | | |
|--|-----------------------|-------------|
| Product | Supplier | Cat # |
| AffinityScript cDNA Synthesis Kit | Agilent | 200436 |
| Bovine Serum Albumin (BSA) | Fisher Bioreagents | BP9702 |
| CellTiter 96® Aqueous Non-Radioactive Cell Proliferation Assay (MTS) | Promega | G5430 |
| Cholera Toxin Subunit B (Recombinant), Alexa Fluor™ 594 Conjugate | Thermo Scientific | C34777 |
| Dimethyl sulfoxide (DMSO) | Sigma-Aldrich | D4540 |
| Filipin III | Sigma-Aldrich | F4767 |
| Formaldehyde | Fisher Bioreagents | F/1501/PB17 |
| Fumed Silica | Sigma-Aldrich | S5130-100G |
| 2X Laemmli Sample Buffer | Bio-Rad | 1610737 |
| 4-20% Mini-PROTEAN® TGX™ gel, 10-well, 50 µL | Bio-Rad | 4561094 |
| 4-20% Mini-PROTEAN® TGX™ gel, 12-well, 20 µL | Bio-Rad | 4561095 |
| Mini-PROTEAN® Tetra Cell system | Bio-Rad | 1658004edu |
| Phosphate Buffered Saline (PBS) | Sigma-Aldrich | P4417 |
| Pierce™ BCA Protein Assay Kit | Thermo Scientific | 23227 |

| | | |
|--|--------------------|------------|
| Pierce™ ECL Western Blotting Substrate | Thermo Scientific | 32106 |
| Precision Plus Protein™ Dual Xtra Prestained Protein Standards | Bio-Rad | 1610377 |
| RIPA Buffer | Sigma-Aldrich | R0278 |
| RnaseZap™ RNase Decontamination Solution | Invitrogen | AM9780 |
| RNeasy Mini Kit | Qiagen | 74106 |
| Seahorse XF Palmitate-BSA FAO Substrate | Agilent | 102720-100 |
| SYBR™ Select Master Mix | Applied Biosystems | 4472908 |
| Trans-Blot® Turbo™ Midi Nitrocellulose Transfer Packs | Bio-Rad | 1704159 |
| Trizma® Base | Sigma-Aldrich | T1503 |
| 10X Tris/Glycine/SDS (TGS) | Bio-Rad | 1610732 |
| TWEEN® 20 | Sigma-Aldrich | P7949 |
| Triton X-100 | Sigma-Aldrich | T8787 |
| VECTASHIELD Antifade Mounting Medium | Vector Labs | H-1000 |
| VECTASHILED with DAPI | Vector Labs | H-1200 |
| Tissue Culture | | |
| ¹³ C ₆ -D-Glucose | Sigma-Aldrich | 389374 |
| ¹³ C ₅ -L-Glutamine | Sigma-Aldrich | 605166 |
| 60 mm TC-treated Culture Dish | VWR | 734-1699 |
| 6-well plates, TC treated | VWR | 734-1599 |
| 96-well plates, TC treated | VWR | 734-1794 |
| Apo-Transferrin | Sigma-Aldrich | T1147 |
| D-(+)-Glucose Solution | Sigma-Aldrich | G8644 |
| DMEM | Gibco | 41965039 |
| DMEM/F12 | Gibco | 11320-033 |
| DMEM, no glucose, no glutamine, no phenol red | Gibco | A1443001 |
| Dulbecco's PBS | Gibco | 14190094 |

| | | |
|--|---------------|-------------|
| EGF Recombinant Human Protein | Gibco | PHG0311L |
| Fetal Bovine Serum (FBS) | Gibco | 10270106 |
| Ham's F12 Nutrient Mixture | Gibco | 21765-029 |
| HEPES Buffer Solution | Gibco | 15630-049 |
| Hydrocortisone | Sigma-Aldrich | H0888 |
| IMDM | Gibco | 21980-065 |
| Insulin, Human Recombinant | Gibco | 12585014 |
| KSFM | Gibco | 17005042 |
| L-Glutamine | Gibco | 25030024 |
| Medium M199 | Gibco | 31150-022 |
| MEM Vitamins | Gibco | 11120037 |
| Mevalonic acid 5-phosphate, lithium salt hydrate | Sigma-Aldrich | 79849 |
| MycoAlert™ Mycoplasma Detection Kit | Lonza | LT07-318 |
| O-phosphorylethanolamine | Sigma-Aldrich | P0503 |
| RPMI 1640 Medium | Gibco | 21875034 |
| 3,3',5-Triiodo-L-thyronine | Sigma-Aldrich | T6397 |
| 0.5% Trypsin (10X) | Gibco | 15400054 |
| Versene | Gibco | 15040033 |
| siRNA | | |
| ON-TARGETplus Non-targeting Pool/siRNA #1 | Dharmacon | D-001810 |
| ON-TARGETplus HMGCR individual siRNA | Dharmacon | J-009811-08 |
| ON-TARGETplus HNF4A SMARTpool siRNA | Dharmacon | L-003406-00 |
| Primers/qPCR | | |
| Hs_GAPDH_1_SG QuantiTect Primer | Qiagen | QT00079247 |
| Hs_HMGCR_1_SG QuantiTect Primer | Qiagen | QT00004081 |
| Drugs | | |
| 2-Deoxy-D-Glucose | Sigma-Aldrich | D8375 |
| Antimycin | Sigma-Aldrich | A8674 |
| Carbonyl Cyanide 3-chlorophenylhydrazone | Sigma-Aldrich | C2759 |
| Etomoxir | Sigma-Aldrich | E1905 |

| FDA Approved Drug Library | Selleckchem | L1300 | |
|------------------------------|------------------------|-----------------|-----------------|
| L-Carnitine | Sigma-Aldrich | C0283 | |
| Oligomycin | Sigma-Aldrich | O4876 | |
| Rotenone | Sigma-Aldrich | R8875 | |
| Antibodies | | | |
| Target Protein | Species/Isotype | Supplier | Cat # |
| ACLY | Rabbit IgG | NEB | 13390 |
| Akt (pan) | Rabbit IgG | NEB | 4691 |
| B-Actin | Mouse IgG2b | NEB | 3700 |
| pan-Akt | Rabbit IgG | NEB | 4691 |
| AMPK α | Rabbit IgG | NEB | 5831 |
| Phospho-AMPK α (T172) | Rabbit IgG | NEB | 2531 |
| CAV1 | Rabbit IgG | NEB | 3238 |
| Cleaved Caspase-3 (D175) | Rabbit IgG | NEB | 9661 |
| Cleaved PARP (D214) | Rabbit IgG | NEB | 5625 |
| FASN | | | |
| GAPDH | Mouse IgG1 | NEB | 97166 |
| HMGCR | Rabbit IgG | Abcam | ab174830 |
| P62-I κ k | Mouse IgG1 | BD Biosciences | 610832 |
| Peroxidase Anti-mouse IgG | Donkey IgG | Stratech | 715-035-150-JIR |
| Peroxidase Anti-rabbit IgG | Donkey IgG | Stratech | 711-035-152-JIR |

2.2 Cell culture methods

All methods involving the handling of cell tissue requiring aseptic technique were performed under sterile conditions in class II biological safety cabinets. 70% ethanol was used to sterilise all work surfaces and equipment before use.

2.2.1 Cell-lines

Patient derived cell-lines used throughout the project are characterised briefly in Table 2.2. Principle components analysis of gene expression in PDCLs highlights grouping of cell-lines into subtypes (Figure 2.1).

Table 2.2 | PDCLs and general characteristics. Table showing names of all PDCLs included in project, along with corresponding subtype classification and source of cell-line.

| Name | Subtype | Source | Reference |
|------------|------------|--------------------------------|--------------------------------|
| TKCC-02 | Squamous | The Kinghorn Cancer Centre | (Hardie <i>et al.</i> , 2017) |
| TKCC-02-LO | Squamous | The Kinghorn Cancer Centre | (Hardie <i>et al.</i> , 2017) |
| TKCC-10 | Squamous | The Kinghorn Cancer Centre | (Hardie <i>et al.</i> , 2017) |
| TKCC-18 | Squamous | The Kinghorn Cancer Centre | (Hardie <i>et al.</i> , 2017) |
| TKCC-19 | Squamous | The Kinghorn Cancer Centre | (Hardie <i>et al.</i> , 2017) |
| TKCC-26 | Squamous | The Kinghorn Cancer Centre | (Hardie <i>et al.</i> , 2017) |
| Mayo-4636 | Classical | The Mayo Clinic, Rochester | (Pal <i>et al.</i> , 2014) |
| Mayo-5289 | Classical | The Mayo Clinic, Rochester | (Pal <i>et al.</i> , 2014) |
| TKCC-22 | Classical | The Kinghorn Cancer Centre | (Hardie <i>et al.</i> , 2017) |
| PaCaDD137 | Classical | Technische Universität Dresden | (Rückert <i>et al.</i> , 2012) |
| TKCC-17 | Borderline | The Kinghorn Cancer Centre | (Hardie <i>et al.</i> , 2017) |
| TKCC-09 | Undefined | The Kinghorn Cancer Centre | (Hardie <i>et al.</i> , 2017) |

Cell-lines established from KPC mouse models, originating from c57Bl/6 mice, were generously donated from the Owen Sansom, Beatson Institute.

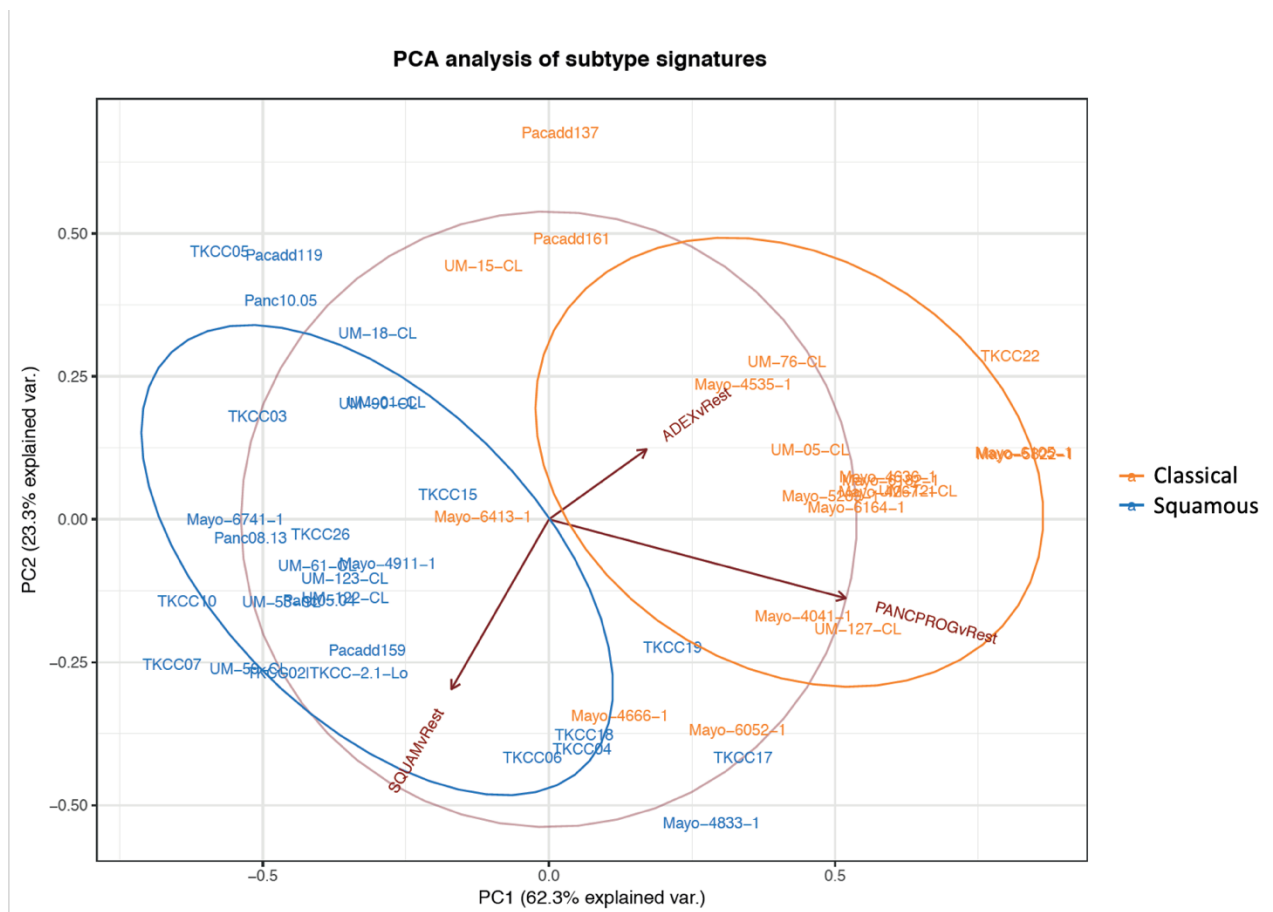


Figure 2.1 | Principle components analysis highlighting PDCL subtyping. PCA plot of gene expression within PDCLs showing principle component 1 (x-axis) plotted against principle component 2 (y-axis). Cells are coloured according to subtype. Arrows show directionality of gene-sets consisting of genes found to be differentially expressed between PDCL subtypes.

Data provided by Peter Bailey (unpublished)

2.2.2 Culture maintenance

TKCC-02-LO, TKCC-09, TKCC-10, TKCC-17 and TKCC-26-LO PDCLs were cultured in a 1:1 mixture of Medium M199 (Gibco) and Ham's F12 nutrient mixture (Gibco) supplemented with 15 mM HEPES Buffer solution (Gibco), 2 mM L-Glutamine (Gibco), 20 ng/mL EGF (Gibco), 40 ng/mL Hydrocortisone (Sigma-Aldrich), 5 µg/mL apo-Transferrin (Sigma-Aldrich), 0.2 IU/mL Insulin (Gibco), 0.06% Glucose Solution (Sigma-Aldrich), 7.5% FBS (Gibco), 0.5 pg/mL Triiodothyronine (Sigma-Aldrich), 1X

MEM vitamins (Gibco) and 2 µg/mL O-phosphoryl ethanolamine (Sigma-Aldrich), referred to as M199/F12 medium. TKCC-18, TKCC-19 and TKCC-22-LO were cultured in IMDM (Gibco) supplemented with 20% FBS, 20 ng/mL EGF, 2.5 µg/mL apo-Transferrin, 0.2 IU/mL Insulin and 0.5X MEM Vitamins, referred to as IMDM Rich medium. Mayo-4636 and Mayo-5289 were cultured in DMEM/F12 (Gibco) supplemented with 10% FBS and 15 mM HEPES Buffer solution, referred to as Mayo medium. TKCC-02 was cultured in RPMI 1640 (Gibco) supplemented with 10% FBS and 20 ng/ml EGF. PaCaDD137 was cultured in DMEM (Gibco) supplemented with 27% KSFM (Gibco) and 10% FBS (Table 2.3). All cell-lines were incubated at 37°C and TKCC-02-LO, TKCC-22-LO and TKCC-26-LO were grown in hypoxia (5% O₂) while TKCC-10, Mayo-4636 and Mayo-5289 was grown in normoxia (20% O₂). Cells were routinely cultured in T75 flasks, with 10 mL appropriate medium. All cells were subject to routine checks for mycoplasma using a MycoAlert™ Mycoplasma Detection Kit (Lonza), with tests conducted by the WWCRC Reagent Services.

2.2.3 Splitting cells

Cells were split at or nearing confluence by aspirating spent medium and adding 10 mL DPBS (Gibco) supplemented with 0.1 mM Versene (Gibco). Cells were incubated at 37°C for 10 minutes in order to detach loosely attached cells, which were then transferred to a 15 mL Falcon tube. In order to dislodge those more strongly adhered cells, 3 mL Trypsin (Gibco) was then added to flasks and incubated at 37°C for no more than 15 minutes, or until total detachment of cells. Detached cells were pooled in Falcon tubes and centrifuged at 1,000 RPM for 5 minutes, with cell pellets subsequently resuspended in fresh, pre-warmed media to be put into new flasks or used for experiments. Cells were then counted using a Nexcelom Cellometer 2000 cell counter.

Table 2.3 | Media formulations for tissue culture. Table showing the complete make-up of all media types used throughout the project upon addition of all base media and supplements. Unless specified otherwise, concentrations are provided in mM.

| | M199/F12 | IMDM Rich | Mayo | RPMI | PaCaDD | | M199/F12 | IMDM Rich | Mayo | RPMI | PaCaDD |
|--|----------|-----------|--------|--------|--------|--|-----------|-----------|----------|---------|---------|
| Amino Acids | | | | | | Inorganic Salts | | | | | |
| Glycine | 0.3353 | 0.3149 | 0.2213 | 0.1200 | 0.2128 | Calcium Chloride (CaCl ₂ -2H ₂ O) | 0.9164 | 1.1727 | 0.0000 | 0.0000 | 0.9554 |
| L-Alanine | 0.1666 | 0.2211 | 0.0442 | 0.0000 | 0.0000 | Calcium Chloride (CaCl ₂) (anhyd.) | 0.0000 | 0.0000 | 0.9296 | 0.0000 | 0.0000 |
| L-Arginine hydrochloride | 0.5825 | 0.3134 | 0.6187 | 1.0237 | 0.2118 | Calcium nitrate (Ca(NO ₃) ₂ 4H ₂ O) | 0.0000 | 0.0000 | 0.0000 | 0.3813 | 0.0000 |
| L-Asparagine | 0.0000 | 0.0000 | 0.0000 | 0.3409 | 0.0000 | Cupric sulfate (CuSO ₄ -5H ₂ O) | 0.0000 | 0.0000 | 0.0000 | 0.0000 | 0.0000 |
| L-Asparagine-H ₂ O | 0.0437 | 0.1490 | 0.0443 | 0.0000 | 0.0000 | Ferric nitrate | 0.0008 | 0.0000 | 0.0001 | 0.0000 | 0.0001 |
| L-Aspartic acid | 0.1424 | 0.1775 | 0.0443 | 0.1353 | 0.0000 | Ferric sulfate (FeSO ₄ -7H ₂ O) | 0.0013 | 0.0000 | 0.0013 | 0.0000 | 0.0000 |
| L-Cysteine hydrochloride-H ₂ O | 0.0875 | 0.0000 | 0.0883 | 0.0000 | 0.0000 | Magnesium Chloride (anhydrous) | 0.0000 | 0.0000 | 0.2668 | 0.0000 | 0.0000 |
| L-Cystine | 0.0000 | 0.2296 | 0.0000 | 0.1875 | 0.0000 | Magnesium Chloride (MgCl ₂ -6H ₂ O) | 0.2629 | 0.0000 | 0.0000 | 0.0000 | 0.0000 |
| L-Cystine 2HCl | 0.0474 | 0.0000 | 0.0885 | 0.0000 | 0.1071 | Magnesium Sulfate (MgSO ₄) (anhyd.) | 0.0000 | 0.0000 | 0.3602 | 0.0000 | 0.0000 |
| L-Glutamic Acid | 0.2425 | 0.4016 | 0.0443 | 0.1224 | 0.0000 | Magnesium Sulfate (MgSO ₄ -2H ₂ O) | 0.0000 | 0.8945 | 0.0000 | 0.0000 | 0.0000 |
| L-Glutamine | 2.7386 | 3.1485 | 2.2125 | 1.8493 | 2.1134 | Magnesium Sulfate (MgSO ₄ -7H ₂ O) | 0.3556 | 0.0000 | 0.0000 | 0.3658 | 0.4325 |
| L-Histidine | 0.0000 | 0.0000 | 0.0000 | 0.0871 | 0.0000 | Potassium Chloride (KCl) | 3.6365 | 3.4634 | 3.6792 | 4.7999 | 2.8373 |
| L-Histidine hydrochloride-H ₂ O | 0.0893 | 0.1574 | 0.1327 | 0.0000 | 0.1064 | Potassium Nitrate (KNO ₃) | 0.0000 | 0.0006 | 0.0000 | 0.0000 | 0.0000 |
| L-Hydroxyproline | 0.0334 | 0.0000 | 0.0000 | 0.1374 | 0.0000 | Sodium Bicarbonate (NaHCO ₃) | 17.5779 | 28.3368 | 25.6861 | 21.4281 | 23.4333 |
| L-Isoleucine | 0.1469 | 0.6309 | 0.3680 | 0.3435 | 0.4264 | Sodium Chloride (NaCl) | 110.0464 | 61.8742 | 106.7417 | 93.1016 | 58.7034 |
| L-Leucine | 0.2441 | 0.6309 | 0.3989 | 0.3435 | 0.4264 | Sodium Phosphate dibasic (Na ₂ HPO ₄) anhydrous | 0.4374 | 0.0000 | 0.4426 | 5.0703 | 0.0000 |
| L-Lysine hydrochloride | 0.2545 | 0.6280 | 0.4413 | 0.1967 | 0.4244 | Sodium Phosphate monobasic (NaH ₂ PO ₄ -2H ₂ O) | 0.4430 | 0.7114 | 0.0000 | 0.0000 | 0.4871 |
| L-Methionine | 0.0572 | 0.1585 | 0.1024 | 0.0906 | 0.1071 | Sodium Phosphate monobasic (NaH ₂ PO ₄ -H ₂ O) | 0.0000 | 0.0000 | 0.4008 | 0.0000 | 0.0000 |
| L-Phenylalanine | 0.0795 | 0.3149 | 0.1903 | 0.0818 | 0.2128 | Sodium Selenite (Na ₂ SeO ₃ -5H ₂ O) | 0.0000 | 0.0001 | 0.0000 | 0.0000 | 0.0000 |
| L-Proline | 0.2833 | 0.2738 | 0.1328 | 0.1565 | 0.0000 | Zinc sulfate (ZnSO ₄ -7H ₂ O) | 0.0013 | 0.0000 | 0.0013 | 0.0000 | 0.0000 |
| L-Serine | 0.1479 | 0.3149 | 0.2213 | 0.2571 | 0.2128 | Other Components | | | | | |
| L-Threonine | 0.1540 | 0.6284 | 0.3975 | 0.1513 | 0.4247 | 2-deoxy-D-ribose | 0.0016 | 0.0000 | 0.0000 | 0.0000 | 0.0000 |
| L-Tyrosine | 0.0130 | 0.0000 | 0.0000 | 0.0994 | 0.2116 | Adenine sulfate | 0.0108 | 0.0000 | 0.0000 | 0.0000 | 0.0000 |
| L-Tyrosine disodium salt | 0.0000 | 0.3638 | 0.0000 | 0.0000 | 0.0000 | Adenosine 5'-phosphate | 0.0003 | 0.0000 | 0.0000 | 0.0000 | 0.0000 |
| L-Tryptophan | 0.0258 | 0.0617 | 0.0391 | 0.0221 | 0.0417 | Adenosine 5'-triphosphate | 0.0007 | 0.0000 | 0.0000 | 0.0000 | 0.0000 |
| L-Tyrosine disodium salt dihydrate | 0.0972 | 0.0000 | 0.1892 | 0.0000 | 0.0000 | Cholesterol | 0.0002 | 0.0000 | 0.0000 | 0.0000 | 0.0000 |
| L-Valine | 0.1372 | 0.6324 | 0.3998 | 0.1538 | 0.4274 | D-Glucose (Dextrose) | 10.1411 | 19.6783 | 15.4924 | 9.9998 | 13.3000 |
| Vitamins | | | | | | Glutathione (reduced) | 0.0001 | 0.0000 | 0.0000 | 0.0029 | 0.0000 |
| Ascorbic Acid | 0.0001 | 0.0000 | 0.0000 | 0.0000 | 0.0000 | Guanine hydrochloride | 0.0007 | 0.0000 | 0.0000 | 0.0000 | 0.0000 |
| Biotin | 0.0000 | 0.0000 | 0.0000 | 0.0007 | 0.0000 | HEPES | 15.0125 | 19.7048 | 15.0000 | 0.0000 | 0.0000 |
| Choline chloride | 0.0524 | 0.0261 | 0.0568 | 0.0193 | 0.0152 | Hypoxanthine | 0.0138 | 0.0000 | 0.0000 | 0.0000 | 0.0000 |
| D-Calcium pantothenate | 0.0026 | 0.0077 | 0.0042 | 0.0005 | 0.0045 | Hypoxanthine Na | 0.0000 | 0.0000 | 0.0133 | 0.0000 | 0.0000 |
| Folic Acid | 0.0036 | 0.0083 | 0.0053 | 0.0020 | 0.0048 | Linoleic Acid | 0.0001 | 0.0000 | 0.0001 | 0.0000 | 0.0000 |
| Menadione (Vitamin K3) | 0.0000 | 0.0000 | 0.0000 | 0.0000 | 0.0000 | Lipoic Acid | 0.0004 | 0.0000 | 0.0005 | 0.0000 | 0.0000 |
| Niacinamide | 0.0084 | 0.0299 | 0.0147 | 0.0074 | 0.0174 | Phenol Red | 0.0246 | 0.0314 | 0.0190 | 0.0120 | 0.0212 |
| Nicotinic acid (Niacin) | 0.0001 | 0.0000 | 0.0000 | 0.0000 | 0.0000 | Putrescine 2HCl | 0.0004 | 0.0000 | 0.0004 | 0.0000 | 0.0000 |
| Para-Aminobenzoic Acid | 0.0002 | 0.0000 | 0.0000 | 0.0066 | 0.0000 | Ribose | 0.0015 | 0.0000 | 0.0000 | 0.0000 | 0.0000 |
| Pyridoxal hydrochloride | 0.0050 | 0.0179 | 0.0000 | 0.0000 | 0.0000 | Sodium acetate-3H ₂ O | 0.2669 | 0.0000 | 0.0000 | 0.0000 | 0.0000 |
| Pyridoxine hydrochloride | 0.0002 | 0.0000 | 0.0086 | 0.0044 | 0.0103 | Sodium Pyruvate | 0.4374 | 0.7871 | 0.4425 | 0.0000 | 0.0000 |
| Riboflavin | 0.0003 | 0.0010 | 0.0005 | 0.0005 | 0.0006 | Thymidine | 0.0013 | 0.0000 | 0.0013 | 0.0000 | 0.0000 |
| Thiamine hydrochloride | 0.0034 | 0.0108 | 0.0057 | 0.0027 | 0.0063 | Thymine | 0.0010 | 0.0000 | 0.0000 | 0.0000 | 0.0000 |
| Vitamin A (acetate) | 0.0001 | 0.0000 | 0.0000 | 0.0000 | 0.0000 | Uracil | 0.0012 | 0.0000 | 0.0000 | 0.0000 | 0.0000 |
| Vitamin B12 | 0.0005 | 0.0000 | 0.0004 | 0.0000 | 0.0000 | Xanthine | 0.0009 | 0.0000 | 0.0000 | 0.0000 | 0.0000 |
| Vitamin D2 (Calciferol) | 0.0001 | 0.0000 | 0.0000 | 0.0000 | 0.0000 | Additional Supplements | | | | | |
| alpha Tocopherol phos. Na salt | 0.0000 | 0.0000 | 0.0000 | 0.0000 | 0.0000 | FBS | 7.50% | 10% | 5% | 5% | 10% |
| i-Inositol | 0.0550 | 0.0371 | 0.0620 | 0.1750 | 0.0213 | Keratinocyte SFM (formulation not specified) | 0 | 0 | 0 | 0 | 27% |
| | | | | | | apo-Transferrin | 5 µg/mL | 2.5 µg/mL | 0 | 0 | 0 |
| | | | | | | Insulin | 0.2 IU/mL | 0.2 IU/mL | 0 | 0 | 0 |
| | | | | | | EGF | 20 ng/mL | 20 ng/mL | 0 | 0 | 0 |
| | | | | | | Hydrocortisone | 40 ng/mL | 0 | 0 | 0 | 0 |
| | | | | | | O-Phosphoryl ethanolamine | 2 µg/mL | 0 | 0 | 0 | 0 |
| | | | | | | Triiodothyronine | 0.5 pg/mL | 0 | 0 | 0 | 0 |

2.2.4 Freezing/thawing cells

To store in liquid nitrogen at -196 °C, cells were split as previously described. Cell pellets were resuspended in FBS supplemented with 10% DMSO (Sigma-Aldrich) to prevent ice crystal formation and stored overnight in a -80 °C freezer. To thaw, cells were incubated in a water bath at 37 °C for one minute before transfer into a

flask containing the appropriate, pre-warmed medium. Cells were incubated overnight to allow for adherence before replacing media containing DMSO.

2.3 Protein handling methods

2.3.1 Cell lysate preparation

Cells were seeded at an appropriate density on a 6-well plate or 60 mm dish (VWR) and incubated overnight at minimum to allow for adherence, with incubation periods extend where required for experimental protocol. When ready for harvesting, spent medium was aspirated and cells were washed once with PBS (Sigma-Aldrich). After washing, cells were scraped on ice in PBS, then centrifuged at 13,300 RPM for 3 minutes at 4°C. The cell pellet was washed in PBS before resuspending 1:5 in cold RIPA buffer (Sigma-Aldrich), and this cell suspension was left on ice for 30 minutes to allow for complete lysis. In order to remove any remaining cell debris, lysates were centrifuged as before, and the resulting pellet was discarded.

2.3.2 Quantifying lysate protein concentration

Lysates were incubated on ice for a minimum of 30 minutes before quantification with a Pierce™ BCA Protein Assay kit (Thermo Scientific) according to the Bicinchoninic Acid assay (Smith *et al.*, 1985). The assay was conducted according to manufacturer's specifications, with known concentrations of albumin used to create a standard-curve. Absorbance values corresponding to each tested sample were subsequently read at 562 nm using a Tecan Infinite 200 plate-reader and converted to protein concentration (µg/mL) using standard-curves.

2.3.3 Sodium Dodecyl Sulfate-Polyacrylamide Gel Electrophoresis (SDS-PAGE)

Electrophoresis was carried out using 20-40 µg of total protein from each cell lysate, diluted 1:1 in 2X Laemmli Buffer (Bio-Rad). Samples were heated at 95 °C for 10 minutes before loading onto precast 4-20% Mini-PROTEAN® TGX™ gels (Bio-Rad). Electrophoresis was run in a Mini-PROTEAN® Tetra Cell system (Bio-Rad) at a constant voltage of 120V for ~1.5 hours in 10X TGS running buffer (Bio-Rad). 10 µL Precision Plus Protein™ Dual Xtra standards (Bio-Rad) was run alongside samples to provide a scale for protein size.

2.3.4 Western blotting

Separated proteins were then transferred from the gel to a nitrocellulose membrane using a Trans-Blot® Turbo™ Midi Nitrocellulose Transfer Pack (Bio-Rad) run on the Trans-Blot® Turbo™ transfer system. After transfer, the membrane was blocked in 5% milk in TBS-T (150 mM NaCl, 20 mM Tris, 0.1% TWEEN® 20) for 1 hour. Membranes were washed twice with TBS-T for 15 minutes before incubation with primary antibodies, diluted according to manufacturer's specifications, for one hour in TBS-T supplemented with 2% BSA (Fisher Bioreagents). The membranes were washed as before and then incubated for an hour with secondary antibodies specific to the primary antibody isotype, conjugated to Horseradish Peroxidase (HRP). Finally, Pierce™ Enhanced Chemiluminescence (ECL) Western Blotting Substrate (Thermo Scientific) was used to produce a visible signal from HRP, which was subsequently imaged using the ChemiDoc MP system (Bio-Rad). Image Lab software was used to process all generated images, as well as for the identification and quantification of bands.

2.4 RNA handling methods

2.4.1 RNA isolation from PDCLs

Cells were seeded at an appropriate density on a 6-well plate and allowed to adhere overnight. RNA was harvested from plates and purified using an RNeasy Mini Kit (Qiagen) according to manufacturer's specification. The workspace used for harvesting was pre-treated with RnaseZap™ (Invitrogen) in order to prevent contamination with RNase. Purified RNA was quantified via NanoDrop™ 2000 spectrophotometer and kept frozen at -80 °C until needed.

2.4.2 cDNA synthesis

In order to generate cDNA necessary to perform quantitative PCR (qPCR), 1 µg of RNA isolated as described previously was subjected to reverse transcription. This was achieved via an AffinityScript cDNA synthesis kit (Qiagen), with the reaction carried out according to all manufacturer's instructions. Any cDNA created in this manner was diluted 1:3 in RNase-free water and frozen at -20 °C until required for qPCR.

2.4.3 qPCR assays

qPCR assays were carried out using 2X SYBR™ Select master mix (Applied Biosystems) and 10X QuantiTect primers (Qiagen), all according to manufacturer's directions. Assays were performed on a QuantStudio 7 Flex Real-Time PCR System, with data processed and analysed using R statistical software.

2.4.4 siRNA transfections

Cells were transfected using RNAiMAX (13778-075, Invitrogen), a Lipofectamine-based transfection reagent. Transfections were carried out with 10 nM appropriate

siRNA, with non-targeting siRNAs (Dharmacon), single or pooled, depending on experimental set-up, as a control.

2.4.5 RNA-seq

Sequencing was carried out on the Illumina HiSeq 2000/2500, generating paired-end reads. These reads were then aligned to the GRCh37 reference genome via STAR (Dobin *et al.*, 2013), with count data subsequently obtained using the *featureCounts* function of the “Rsubread” package (Liao, Smyth and Shi, 2014). Count data were subsequently normalised across samples and log transformed using the DESeq2 package (Love, Huber and Anders, 2014), generating log counts per million (LogCPM) values.

2.5 Drug treatments

2.5.1 Generating dose-response curves.

Drugs were dissolved in appropriate solvent as instructed by manufacturers, where possible, creating 10mM working stocks. Cells were split, plated in a 96-well format and left in incubation for 24 hours to attach. After this attachment period, cells were dosed in 6 replicates with drug concentrations according to a 1:3 serial dilution. Additional wells containing the appropriate maximum percentage DMSO and 0.007% Triton-X100 (T8787, Sigma-Aldrich) were used as drug vehicle controls and 100% kill controls respectively. Viability was measured using an MTS assay kit (G5430, Promega), which acts to provide a quantification of viability via lactate dehydrogenase (LDH) mediated conversion of tetrazolium salt to formazan (Mosmann, 1983). GraphPad Prism version 7 was used to generate and analyse dose-response curves, with error bars shown across three replicates for each cell-line tested.

2.6 Metabolic assays

2.6.1 Extracellular metabolic flux assays

Measurements of extracellular acidification rate (ECAR) and oxygen consumption rate (OCR) were obtained utilizing the Seahorse Xfe96 Analyser (Seahorse Biosciences) as previously described (Wu *et al.*, 2006; Pike Winer and Wu, 2014). In brief, cells were seeded in their respective, fully supplemented medium at a range of densities optimized for each PDCL. 45 minutes prior to starting the assay, cells were equilibrated in basal media with minimal supplementation at 37°C in a non-CO₂ incubator. During the assay, indicated compounds were injected into wells at 18-minute intervals. All results were normalized to total cellular protein content per well by RIPA extraction followed quantification with BCA protein assay kit (ThermoFisher Scientific, #23227) in a 96-well format, with absorbance measured using a Tecan Infinite 200 plate-reader.

Table 2.4 | Seahorse media formulations. Composition of media types used to culture cell-lines during extracellular flux assays. Red shading indicates addition of a supplement, while orange indicates addition conditional upon cell-line requirements.

| | Glycolysis | FAO Assay | |
|--------------------------|------------|-----------|-----|
| | Stres Test | Sub-Limit | FAO |
| SH DMEM | | | |
| KHB | | | |
| GlutaMAX (2 mM) | | | |
| L-Glutamine | | | |
| HEPES | | | |
| Glucose (0.5 mM) | | | |
| FBS (1%) | | | |
| Carnitine | | | |
| MEM-Vitamin | | | |
| Apo-Transferrin | | | |
| EGF | | | |
| Tri-iodotyronine | | | |
| O-phosphorylethanolamine | | | |
| Insulin | | | |
| Hydrocortisone | | | |

2.6.2 Glycolytic stress test

This extracellular flux assay, performed on the Seahorse platform, was initiated in the absence of glucose, with 10 mM glucose, a PDCL-dependent concentration of oligomycin and 50 mM 2-DG sequentially added to generate a profile of glycolysis under various conditions, as described previously (Pike *et al.*, 2011; Pike Winer and Wu, 2014). TKCC-10 and TKCC-22-LO both required 1 μ M while TKCC-02-LO, TKCC-26-LO, Mayo-4636 and Mayo-5289 all required 2.5 μ M oligomycin to achieve a maximal shift in ECAR.

2.6.3 FAO assay

This assay functions as an extension to the Mitochondrial Stress Test described by Seahorse Biosciences. 4-hours prior to beginning this assay, cells were cultured in substrate limited media supplemented with L-carnitine in order to stimulate consumption of endogenous fatty acid (FA) reserves. FAO was then subsequently quantified as a measurement of OCR upon treatment of subsets of cells with either 40 μ M FAO inhibitor Etomoxir or the FA palmitate, purchased as Seahorse XF Palmitate-BSA FAO Substrate, as described previously (Pike *et al.*, 2011; Pike Winer and Wu, 2014). Initial OCR readings of the assay represent basal levels of respiration in the PDCLs, with sequential additions of PDCL-dependent concentrations of oligomycin, 1.6 μ M CCP and a 1 μ M combination of Antimycin and Rotenone providing a profile of OCR under different metabolic conditions. PDCLs were cultured in serum-free Krebs-Henseleit buffer supplemented with all necessary cell-line specific supplements excluding glutamine during the course of OCR recording.

2.6.4 Mito Fuel Flex Test

The Mito Fuel Flex Test assay is designed to quantify the dependency, capacity and flexibility of cells to utilise three the major contributors to oxidative phosphorylation, glucose, glutamine and fatty acids. This is achieved by measuring changes in OCR upon treatment of cells with inhibitors of the metabolic arms corresponding to those three metabolites: UK5099, which inhibits the import of pyruvate into the mitochondria, halting glucose-driven OXPHOS; BPTES, an inhibitor of glutamine hydrolysis; and etomoxir, which inhibits CPT1A transfer of long-chain FAs into mitochondria.

2.6.5 Lactate production and glucose consumption assays

The L-Lactate content of culture media was measured using the colorimetric-based L-Lactate Assay Kit (Abcam, #ab56331) according to manufacturer's specifications. 3×10^4 cells were plated in their respective, fully supplemented medium and 24 hours after seeding, this medium was replaced. Cells were cultured for a further 48 hours before medium was taken for analysis and samples were subsequently deproteinated via PCA/KOH. Lactate levels in spent media were quantified by harnessing NADH generated from the conversion of lactate to pyruvate in order to reduce WST. This reaction yields formazan, which can be quantified spectrophotometrically, allowing a direct measurement of lactate levels. Each test was performed in duplicate, with output adjusted to background lactate levels in medium and normalised to total cell count.

Glucose consumption was quantified via the colorimetric-based Glucose Uptake Assay Kit (Abcam, #ab136955) as per the manufacturer's protocol. The assay functions by exposing cells to 2-DG, a glucose analogue that is taken up alongside glucose, but cannot be broken down beyond the initial step of glycolysis. This leads to accumulation of 2-DG-6-phosphate in cells proportionate to rate of glucose uptake, which can be oxidised to form NADPH. The resultant NADPH is then utilised as a reducing agent to convert glutathione disulphide to glutathione,

which can then be reacted with DTNB to produce a quantifiable colorimetric output. Each test was performed in triplicate and normalized to cellular protein content.

2.6.6 Generating delipidated serum for metabolic studies

Serum was delipidated with fumed silica (Sigma-Aldrich) according to manufacturer's specifications. Briefly, 1 g of fumed silica was added to 50 mL FBS and left rotating overnight at 4°C. The resultant mixture was centrifuged at 2000 g for 15 minutes, and the supernatant filtered through. This method has been determined to most effectively deplete cholesterol, triglycerides and lipoproteins from serum as compared to other, commonly used approaches (Agnese, Spierto and Hannon, 1983), while preserving protein content (Ferraz *et al.*, 2004).

2.6.7 Stable isotope tracer metabolomics

Cells were cultured in DMEM with no glucose, glutamine or phenol red, supplemented with all appropriate additives, replacing glucose and glutamine with isotopically labelled equivalents consisting of ^{13}C . After 72 hours, cells were washed in PBS and collected in chilled 90% methanol. Cholesterol was then extracted after saponification with KOH in hexane. MSTFA was added to silylate samples, allowing for analysis via gas chromatography-mass spectrometry (GC-MS).

2.7 Immunofluorescence and confocal microscopy

2.7.1 Preparing cells for staining

In preparation for microscopy work, cells were grown on coverslips, sterilised via autoclaving, placed in 6-well plates. Cells were incubated overnight to allow for adherence before harvesting for imaging or experimental treatment followed by harvesting. To prepare cells for staining, wells containing coverslips were washed

with PBS and fixed at room temperature with 4% formaldehyde in PBS for 10 minutes. Formaldehyde was then removed, and cells were washed before being permeabilised for 3 minutes in 0.2% Triton X-100 (Sigma-Aldrich) in PBS. Where cells were stained for cholesterol imaging, permeabilization and staining steps were carried out concomitantly as described in the following section.

2.7.2 Staining cells for imaging

Cells were washed x3 with PBS between each described step and all plates were kept from direct light for the duration of staining upon addition of any fluorophore. Firstly, if staining for cholesterol, 100 μ L of 50 μ g/mL Filipin III (Sigma-Aldrich) in PBS was added to each coverslip and incubated at room temperature for 30 minutes. Next, if performing immunofluorescence, primary antibodies were diluted according to manufacturer's specifications in 2% BSA in PBS and added to coverslips. After one-hour incubation at room temperature, coverslips were washed with PBS before the addition of secondary antibody for another hour incubation. Finally, if neutral lipid staining was carried out, 1 μ g/mL BODIPY 493/503 was added to coverslips and incubated at room temperature for 30 minutes. Coverslips were then washed in PBS and mounted on slides in VECTASHIELD, with or without DAPI depending on whether nuclear staining was required.

2.7.3 Image acquisition

All images were captured using a Zeiss LSM 780 confocal microscope system, with preliminary processing carried out using ZEN Black software. Immunofluorescence experiments were carried out with a minimum of 4 positions analysed for each condition, with imaging conducted at either 20X or 40X magnification. Z-stacks were acquired at each position, with sufficient depth to capture the entirety of all cells. Image sequences were then output as TIFFs for downstream analysis.

2.8 Data analysis

2.8.1 General statistical analysis

All statistical processing was carried out in R, while subsequent figure generation was performed using GraphPad Prism. Linear regression was performed using the least squares method of line fitting and was executed using the *lm* function of the “stats” package, which functions via QR decomposition (Goodall, 1993).

2.8.2 Drug screening analysis

Drug target data were obtained from the DrugBank database (Wishart *et al.*, 2018), downloaded in the XML format. Clinical trials data were obtained from the Aggregate Analysis of ClinicalTrials.gov (AACT) database (Clinical Trials Transformation Initiative), downloaded in pipe-delimited format and processed in R.

2.8.3 Immunofluorescence image analysis

Images generated via confocal imaging were further processed using FIJI (Schindelin *et al.*, 2012), allowing for the re-arranging of channels and the generation of maximum intensity Z-projections from a sequence of images representing a Z-stack. Feature detection and quantification was subsequently performed on Z-projections using CellProfiler (Carpenter *et al.*, 2006) utilising the various functions to identify and enhance various features such as nuclei, lipid droplets, cleaved PARP and cleaved Caspase-3. Where necessary, additional processing allowed for the expansion of features and assessment of overlap of objects.

Chapter 3 *Defining Candidate Metabolic Vulnerabilities*

Defining Candidate Metabolic Vulnerabilities

3.1 Introduction

In order to identify therapeutics potentially effective in treating pancreatic cancer, studies concentrated on characterising subtypes previously found to exist within patients (Bailey *et al.*, 2016). To this end, a diverse collection of patient derived cell-lines (PDCLs) generated directly from tumour tissue was used as a potential model for subtype-specific therapeutic development for pancreatic cancer. To first validate their application to this end, extensive transcriptomic profiling of PDCLs via RNA-seq was performed. To act as further verification of the robustness of the approach and model, subtyping of cell-lines was performed independently of the patient from which they were derived.

Though the central dogma of genetics holds that translation of proteins is dependent on transcription of RNA, the relationship between mRNA and protein abundances are not directly proportionate, largely in part due to regulation at the post-transcriptional level (Lai, 2002; Thomson *et al.*, 2006). Though previous evidence shows that gene expression in pancreatic tissue is closely correlated with protein abundance, more so than in a number of other tissue-types (Kosti *et al.*, 2016), proteomic characterisation was performed to confirm clinical relevance of dysregulation observed at the transcriptome level.

Simultaneous characterisation of both transcriptomes and proteomes within PDCLs enabled the interrogation of both datasets to quantify dysregulation of pathways associated with oncogenesis and subtype differentiation in PDAC (Jones *et al.*, 2008; Bailey *et al.*, 2016). This approach was intended to further reinforce the validity of the PDCL model, while allowing focus to be directed to pathways which represent potential for subtype-specific vulnerabilities.

In line with recent research that ties metabolic perturbations to pancreatic cancer development and progression (Ying *et al.*, 2012; Kamphorst *et al.*, 2013; Son *et al.*, 2013), PDCLs were additionally subject to a range of assays assessing metabolic outputs. Specifically, rates at which cells utilised both glucose and fatty acids as energy sources were interrogated, which were then compared to findings at the transcriptomic and proteomic level. These analyses collectively revealed differential metabolic profiles that exist between subtypes, with subsequent research efforts aimed at identifying vulnerabilities within these metabolic arms.

3.2 Transcriptomic profiling of PDCLs reveals subtype-specific metabolic dysregulation

3.2.1 Analysis of PDCL transcriptomes identifies *in vitro* subtypes

In order to determine potential subtypes in PDCLs, RNA-seq was performed on a set of 48 novel, patient derived cell-lines (PDCLs), provided by the Australian Pancreatic Cancer Genome Initiative (for details on origin, see Table 2.2). This provided a comprehensive profile of PDCL transcriptomes, with subsequent hierarchical clustering of RNA-seq data revealing the existence of two broad subtype groups (Figure 3.1a) (Peter Bailey, unpublished data). These two subtypes were classified as squamous and classical. As was seen within bulk tumour and described in chapter 1.2.1, the PDCL squamous subtype was characterised by the loss in expression of a number of genes associated with pancreatic identity determination, including *PDX1* and *HNFs* (Figure 3.2). Clustering did reveal the existence of three PDCLs that could be classed as exocrine-like, which displayed expression of genes associated with terminally differentiated pancreatic epithelia such as *CPA1*, *INS* and *GCG*. Beyond those perturbations, these exocrine-like PDCLs showed similar transcriptional patterns as 17 PDCLs determined to belong to the pure classical progenitor subtype, and as such, these subtypes were grouped and referred to as classical, representative of the classical-pancreatic subgroup described in patients (Collisson *et al.*, 2019).

Weighted Gene Co-expression Network Analysis (WGCNA) was then performed on transcriptome data to identify co-ordinately regulated gene programmes across the subtypes (Langfelder and Horvath, 2008), as previously conducted in bulk tumour data (Bailey *et al.*, 2016). This analysis was conducted independently of that performed in patient samples, similarly generating gene networks assigned colour identifiers to facilitate the plotting of data. By comparing the composition and connectivity patterns of gene programmes between PDCL and patient data, it was possible to quantify conservation between tumour and cell-line gene networks, as previously described in literature (Langfelder *et al.*, 2011). One major observation from this assessment of conservation was the recapitulation of a majority of gene programmes identified in bulk tumours, in particular those associated with the squamous and pancreatic progenitor subtypes, and those found in PDCLs. This can be seen in the high Z_{summary} measures obtained for gene programmes 1-5, which constitute all GPs that define squamous and pancreatic progenitor subtypes. Conservation scores are all greater than 10 in these GPs (Figure 3.1b), suggesting a preservation across these modules. Additionally, gene networks within cell-lines that share a high degree of similarity to subtype-associated bulk tumour GPs are associated with subtype specification in cell-lines. This is seen in the module eigengene (ME) values, or values of expression that typify the collective expression of gene networks (Langfelder and Horvath, 2007), in those conserved modules. When plotting ME values of PDCL modules in cell-lines, cell-lines are shown to cluster according to subtype (Figure 3.1c). An example of this can be seen within the turquoise GP in PDCLs, which has significant overlap with GP1, the GP most associated with the pancreatic progenitor subtype in patients. The ME values of this module are consistently higher across cell-lines grouped as classical. These observations collectively point to the existence of patterns which define patient subtypes in an *in vitro* context, thus highlighting the potential of cell-lines as a model of patient subtypes.

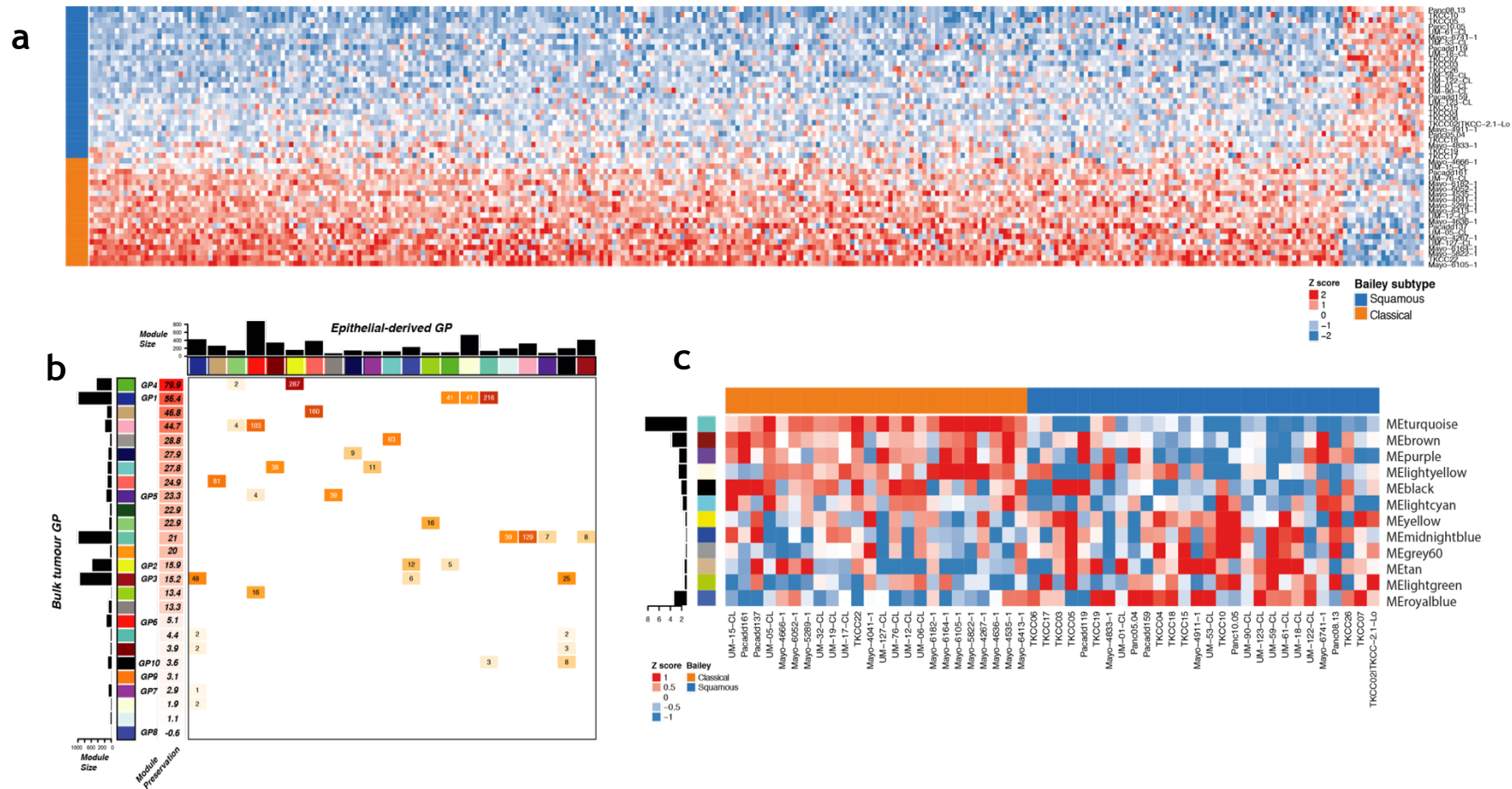


Figure 3.1 | RNA-seq reveals two distinct subtypes in PDCLs. **a** Heatmap displaying hierarchical, unsupervised clustering of PDCL RNA-seq data. This analysis yields a clear, binary subtyping (squamous blue, classical orange). **b** Plot highlighting conservation between GPs previously described in patient tumour (y-axis, colour identifiers and GP numbers shown) and GPs identified in PDCLs (x-axis). Preservation scoring was achieved by computing $Z_{summary}$ statistics (Langfelder *et al.*, 2011) for bulk tumour GPs and shown along the y-axis (module preservation), with scores of >10 indicating preservation across modules, 2-10 suggesting weak preservation and scores <2 indicating no preservation. **c** Module eigengene values of PDCL modules for each cell-line, with subtyping shown along top. A number of modules are seen to associate with each of the two subtypes. Data provided by Peter Bailey (unpublished).

The mirroring of subtypes observed is a positive indicator of sample purity and suggests there was little to no stromal contamination of cancer epithelia while generating PDCLs. Though there may be strength in modelling interactions between stroma and tumour tissue, particularly as evidence shows cross-talk between the dense stroma associated with PDAC and tumour promotes cancer progression (Hwang *et al.*, 2008), monocultures were studied to reduce complexity, thus facilitating the primary goal of identifying therapeutics that selectively target tumour cells. The immunogenic subtype, which is defined by gene programmes suggestive of significant immune infiltration, was not identified within PDCLs. This observation is expected as the immune component is naturally absent in monoculture systems derived from tumour epithelia. Reinforcing this, it was found that 74% (86 out of 116) of genes determined to be differentially up-regulated in the immunogenic subtype in patient transcriptomes, as determined via Voom package (Law *et al.*, 2014), were not found to be expressed in any PDCL. In comparison, when looking at each of the gene-sets significantly up-regulated in the three other subtypes, <10% were not found to be expressed within PDCLs. Interestingly though, gene programmes were found that were enriched for genes involved in immune regulation, likely resulting from cell autonomous signalling pathways previously described as being associated with the squamous subtype (Bailey *et al.*, 2016).

In summary, by comparing the co-ordinately regulated gene modules that exist in both patient and PDCL transcriptomes, the potential in harnessing PDCLs as a model of clinically relevant pancreatic cancer subtypes is evident. This then justified subsequent interrogation of the transcriptomes and proteomes of the two subtypes in PDCLs to search for therapeutic vulnerabilities. RNA-seq data were obtained and processed by Peter Bailey and Rosanna Upstill-Goddard.

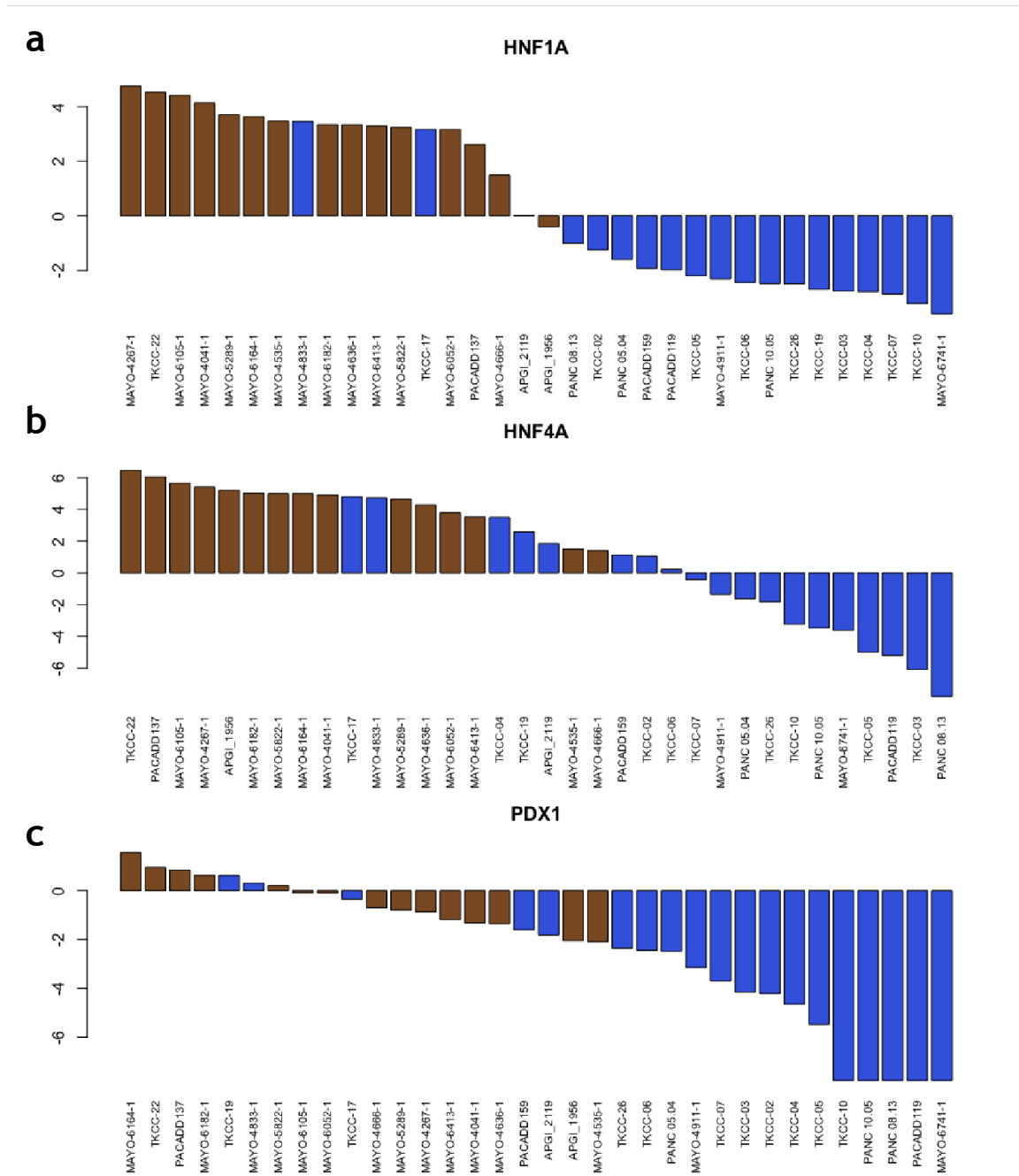


Figure 3.2| Genes associated with pancreatic identity are downregulated in squamous PDCLs. Bar-plots showing the expression of (a) *HNF1A*, (b) *HNF4A*, and (c) *PDX1* across PDCLs, coloured according to subtype and ordered from highest to lowest in terms of expression. As can be seen, expression is generally selectively found within classical (brown) rather than squamous (blue) PDCLs. The protein products of these three genes are all associated with pancreatic differentiation and identity, and the observation that their expression is lost in squamous PDCLs is in-line with observations within bulk tumour. All data are presented in LogCPM (log-transformed counts per million).

3.2.2 Subtype-associated metabolic signatures within PDCL transcriptomes

In order to identify pathways enriched for in subtype-associated gene modules and to quantify the collective expression of these functional biological pathways in PDCLs, the *dnet* R package (Fang and Gough, 2014) was implemented, allowing for enrichment analysis of pathways described in Gene Ontology (GO) (Ashburner *et al.*, 2000), KEGG (Kanehisa and Goto, 2000) and Reactome (Fabregat *et al.*, 2018)

databases, and Gene-Set Variation Analysis (GSVA) was employed (Hänzelmann, Castelo and Guinney, 2013). GSVA analysis revealed that differences in expression of genes associated with metabolism are a key feature that defines the two subtypes in PDCLs, with a range of molecular processes involving fatty acid and glucose biosynthesis/metabolism differentially co-ordinately regulated between subtypes (Figure 3.3a). Upregulation of fatty acid biosynthesis in classical PDCLs can be demonstrated through highlighting the expression of genes involved in lipid anabolism in the turquoise GP, the module described previously as being most closely associated with the classical subtype (Figure 3.3b). Of note is the conservation of this transcriptional upregulation between PDCLs and bulk tumour, as a similar enrichment of genes involved in lipid anabolism, such as Peroxisomal Trans-2-Enoyl-CoA Reductase (PECR), which acts to elongate FAs during the biosynthetic process, and Malonyl-CoA Decarboxylase (MLYCD), which regulates levels of malonyl-CoA, the key determinant in rates of biosynthesis, can be seen within the pancreatic progenitor subtype in patients. This serves to further validate this observation within the PDCL model.

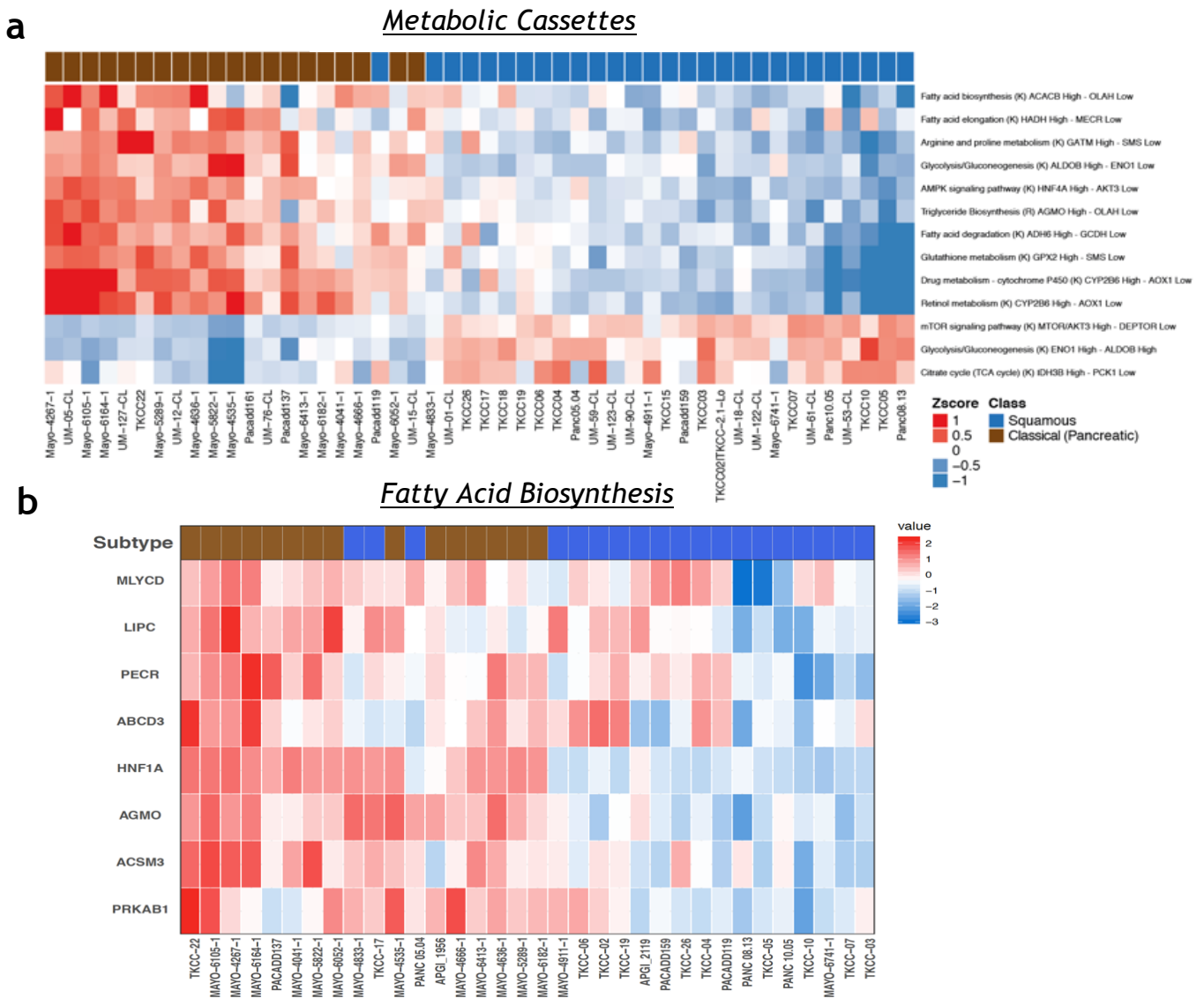


Figure 3.3 | Metabolic genes are dysregulated between subtypes. **a** Heatmap showing coordinated dysregulation of metabolic gene-sets highlighting the transcriptional distinction between PDAC subtypes. Analysis performed and data provided by Peter Bailey (unpublished). **b** Heatmap showing the expression of genes from the turquoise gene programme associated with the fatty acid biosynthetic process according to the GO database. Rows and columns were clustered according to Ward hierarchical clustering.

When assessing differences in expression of genes involved in glycolysis, isoform ratios are seen to inform subtype classification, with the aldolase family of enzymes best representing this phenomenon. The aldolases are essential enzymes for early glycolysis, catalysing the cleavage of fructose 1,6 bisphosphate into glyceraldehyde-3-phosphate. Early enzyme kinetic assays determined that Aldolase A (ALDOA) has the greatest cleavage efficiency for fructose 1,6 bisphosphate among the isoforms (Penhoet and Rutter, 1971), implicating it as the major aldolase driving glycolysis within cells (Chang *et al.*, 2018). Its expression is predominantly associated with energy-consuming muscle cells (Lebherz and Rutter, 1969), and loss of ALDOA has previously been linked to fatal rhabdomyolysis (Yao *et al.*, 2004). Additionally, increased levels of ALDOA have long been observed in patients with cancer (Asaka *et al.*, 1994; Li *et al.*, 2019). Within PDCLs, *ALDOA:ALDOB* expression ratios are found to be dysregulated across subtypes, with squamous cell-lines displaying greater levels of *ALDOA* transcript and classical cell-lines, *ALDOB* (Figure 3.4a-b). This association corresponds to a poorer prognosis in patients with a high *ALDOA:ALDOB* ratio (Figure 3.4c).

These observations work to collectively highlight the coordinated dysregulation of genes involved in metabolism between the subtypes and suggest a transcriptome-driven regulation of general metabolism in PDCLs. These findings were then validated at the proteomic level to ensure an association between abundance of metabolic enzymes and subtypes before confirming the effect on metabolic phenotypes.

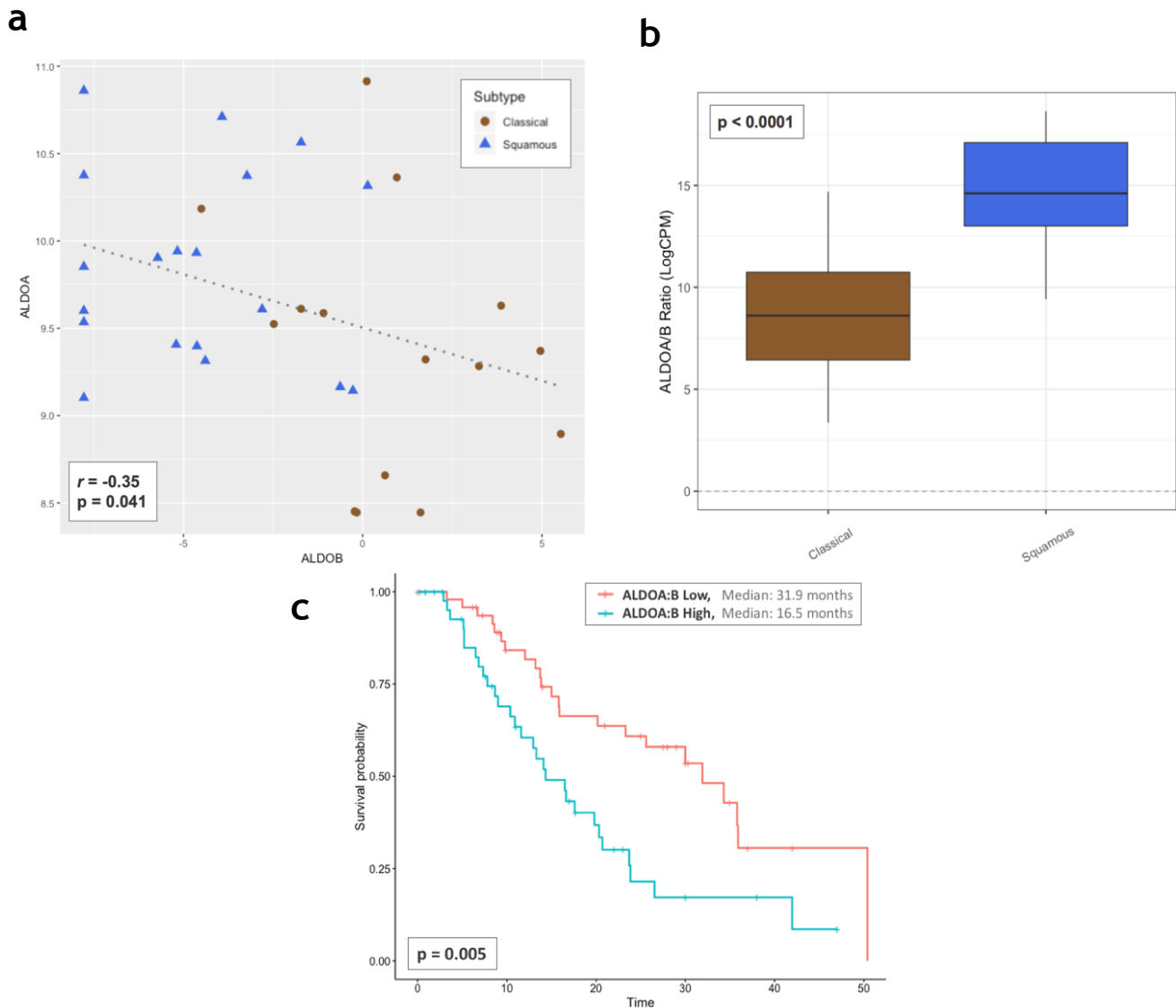


Figure 3.4 | Impact of metabolic isoform ratio on subtype and outcome. **a** Scatter-plot showing the expression of *ALDOA* plotted against expression of *ALDOB*, highlighting association between *ALDOA:ALDOB* ratio and subtype, as well as the significant negative correlation in expression between the two isoforms. High *ALDOA*/low *ALDOB* expression is associated with the squamous subtype (blue triangles) while the opposite is true for classical (brown circles). Test statistics correspond to the Pearson correlation coefficient, with linear regression (grey, dotted line) highlighting negative correlation. **b** Boxplot displaying the *ALDOA:ALDOB* ratios grouped according to subtype. As observed in (a), a high *ALDOA:ALDOB* ratio is highly significantly associated with the squamous subtype, as determined via Mann-Whitney U test. **c** Kaplan-Meier curve showing the significantly improved disease-specific survival prognosis in PDAC patients with low *ALDOA:ALDOB* ratio relative to those with high. Low/high patient classification was achieved by splitting the cohort in two across the median ratio and p-value calculated via logrank test.

3.3 Proteomic profiling validates and expands on transcriptomic analysis

In order to ensure that the observed dysregulation of genes involved in metabolism translated to differences in protein quantities between subtypes, PDCL proteomes were quantified via mass-spectrometry. This analysis was performed within a selection of cell-lines representative of the two distinct subtypes. This analysis firstly demonstrated that there was a strong correlation ($r = 0.78$; $p = 2.2 \times 10^{-16}$) between mRNA and protein abundances when considering genes/gene products involved in lipid biosynthesis and glycolysis, as defined by the canonical glycolysis and fatty acid biosynthetic processes specified in the GO database (Ashburner *et al.*, 2000) (Figure 3.5). These pathways consist of a variety of genes integral to both glycolysis and lipogenesis, including the aldolases, whose role in glycolysis is described in chapter 3.2.2, acetyl-CoA carboxylases and FASN, both catalysing intermediate reactions in FA biosynthesis, described in chapter 1.5.2, and AMPK subunits, which mediate the metabolic stress response described in 1.5.4, suggesting that transcriptomic analysis which demonstrates a dysregulation of metabolic cassettes (Figure 3.3a) should directly inform downstream proteomic data.

In order to investigate the extent to which pathways are affected by this dysregulation at the protein level, a subset of PDCLs most reflective of the subtype extremes were analysed, considering only proteins present in classical and absent in squamous. This validated the association between lipid biosynthesis and metabolism pathways and the classical subtype observed within the transcriptome (Figure 3.6). The findings that proteins involved in lipid biosynthesis and metabolism are more abundant in classical cell-lines, in conjunction with the previously described results obtained from RNA-seq analysis that corroborate the upregulation of genes associated with lipogenesis in classical PDCLs and suggest the more widespread dysregulation of metabolic cassettes between subtypes (Figure 3.3a), provide compelling evidence that different metabolic pathways are activated between the subtypes. These observations are consistent with the

research described in chapter 1.5.6 , which details the association of drivers of pancreatic cancer with upregulation of glycolysis, FA biosynthesis and FAO (Table 1.1). Before interrogating these pathways to identify potential susceptibilities, it was necessary to first validate these findings via functional assays.

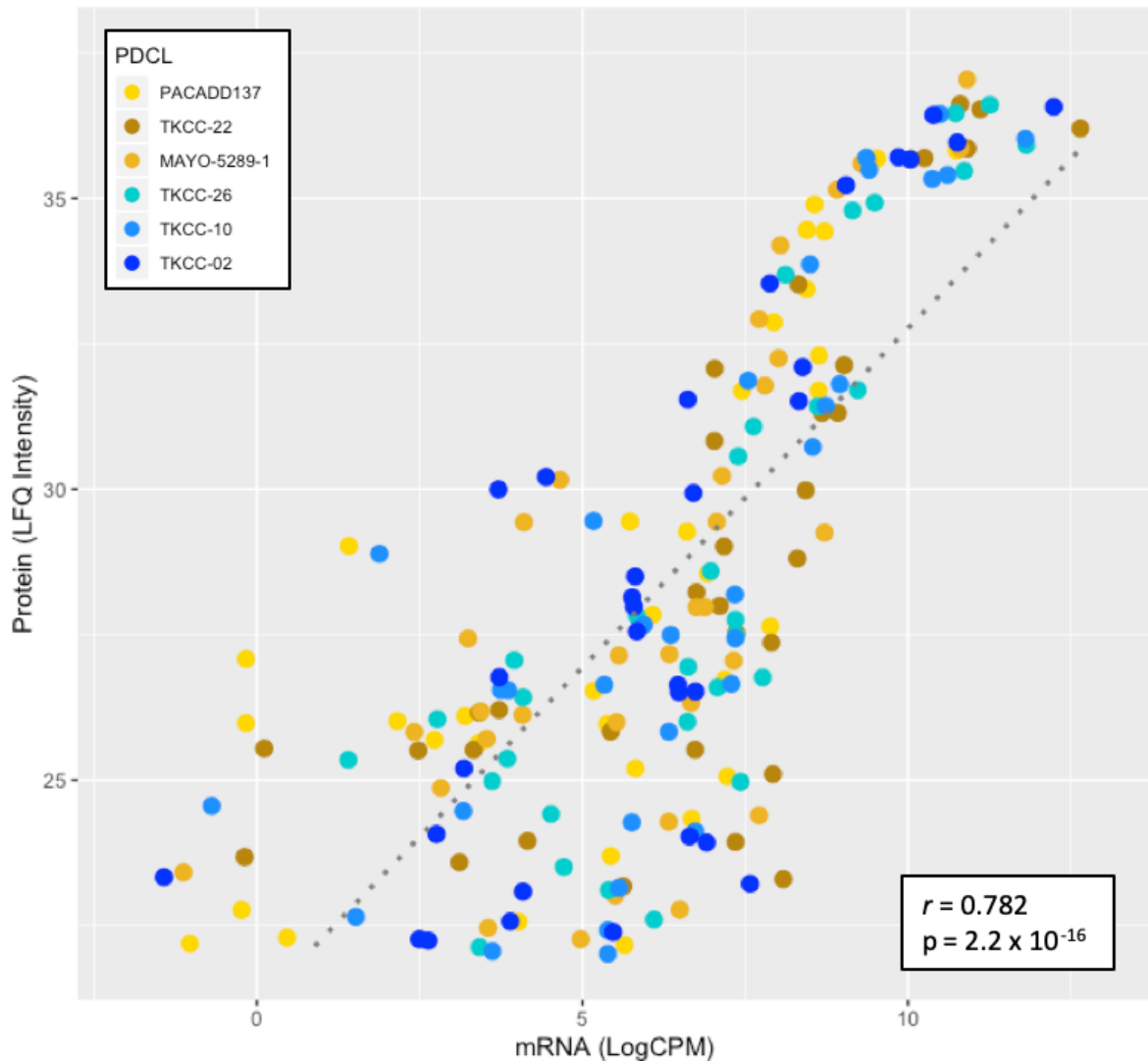


Figure 3.5 | Expression of metabolic genes correlates strongly to protein abundances in PDCLs. Scatter-plot showing correlation between the expression of genes as determined by RNA-seq in a selection of subtyped PDCLs (x-axis) and abundance of their corresponding gene product as determined by mass-spectrometry (y-axis). Genes were selected to display from the “canonical glycolysis” and “fatty acid biosynthetic process” pathways as defined by the GO database. Spearman’s rank correlation coefficient was calculated at 0.782, $p = 2.2 \times 10^{-16}$, with linear regression highlighting the positive correlation between transcript and protein abundances (dotted grey line).

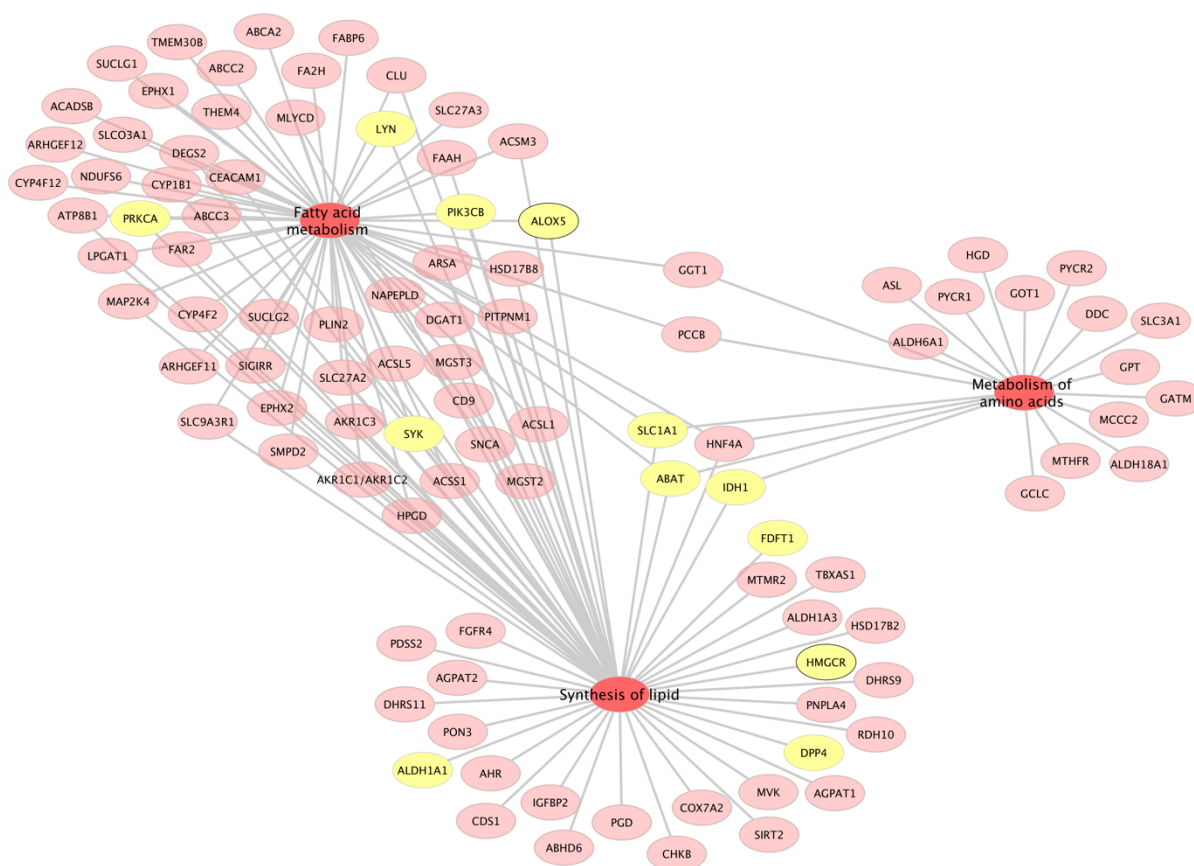


Figure 3.6 | Classical subtype PDCLs are defined by the presence of metabolic networks of proteins. Network plot displaying metabolic pathways enriched for proteins selectively found in classical cell-lines. Each red ellipse represents a protein associated with the classical subtype, associations between biological processes and proteins are highlighted in grey, and druggable targets are shown in yellow. Transcriptome analysis had previously highlighted upregulation of lipid biosynthesis within this subtype, with network analysis validating this phenomenon at the protein level. An association was also found between the classical subtype and metabolism of both lipids and amino acids. Analysis and data provided by Bryan Serrels (unpublished).

3.4 Metabolic characterisation reveals distinct metabolic phenotypic differences between subtypes

In order to characterise metabolism in PDCLs and validate results from RNA-seq and proteomics, the Seahorse XFe96 analyser was employed for quantification of

extracellular bioenergetics. This system functions through the quantification of oxygen consumption rates (OCR) and extracellular acidification rates (ECAR) within wells containing cells, as determined by shifts in oxygen and pH levels recorded by fluorescent biosensors (Wu *et al.*, 2006). OCR acts as a measure of oxidative phosphorylation as cellular oxygen consumption is coupled with the electron transport chain (ETC) and ATP production through the progression of the TCA cycle. ECAR is similarly linked to aerobic glycolysis due to the resultant lactate production and efflux of protons.

To generate a comprehensive profile in real-time, metabolic stress tests were performed. By measuring changes in extracellular flux in real-time upon the injection of various compounds into wells over the course of each assay, these protocols allow for basal and maximal read-outs for a range of metabolic functions.

3.4.1 Determining optimal conditions for bioenergetics assays

Before proceeding with extracellular flux assays, it was necessary to first determine the optimal seeding densities for each cell-line, as well as the minimum concentrations of injected compounds required to achieve maximal effects on metabolic pathways. These steps were required to avoid recording metabolic artefacts in response to over- or under-confluence, as well as to limit the possibility of off-target effects that might result from injecting high concentrations of compounds.

To ascertain the ideal plating conditions, cells were seeded at a range of densities, allowed 24 hours to attach, and viewed under a microscope. According to manufacturer's specifications, optimal confluency was determined to be 50-90% at the time of assay, with seeding densities selected to satisfy this criterion. Upon determining this, the optimal concentrations of oligomycin and FCCP were deduced in each cell-line by assaying shifts in ECAR and OCR respectively in response to increasing concentrations of each compound. As oligomycin/FCCP concentrations increase, ECAR/OCR rise until they reach a maximal level, with

final concentrations selected by determining the lowest concentration at which these maximal levels were recorded Table 3.1.

Table 3.1 | Cell-line optimisations determined for bioenergetic stress tests on Seahorse platform. Optimal overnight seeding densities and minimum oligomycin concentrations required to affect maximal metabolic response listed for each PDCL tested.

| PDCL | TKCC-22 | PaCaDD137 | Mayo-5289 | Mayo-4636 | TKCC-18 | TKCC-26 | TKCC-10 | TKCC-02 |
|---------------------------|-------------------|-------------------|-------------------|-------------------|-----------------|--------------------|--------------------|-------------------|
| Oligomycin Concentration | 1 μ M | 2.5 μ M | 2.5 μ M | 2.5 μ M | 1 μ M | 2.5 μ M | 1 μ M | 2.5 μ M |
| Cell Density (cells/well) | 2.2×10^4 | 2.5×10^4 | 3.5×10^4 | 1.5×10^4 | 2×10^4 | 1.85×10^4 | 1.75×10^4 | 1.3×10^4 |

3.4.2 Rates of glycolysis differ between subtypes in PDCLs

Rates of both basal and maximal glycolysis were recorded according to the glycolytic stress test (Figure 3.7). This experiment functions by first recording background levels of ECAR while cells are cultured in full media lacking glucose and serum (Table 2.4). This then acts as a measurement of non-glycolytic ECAR, and when glucose is subsequently injected into cell-plates followed by a rise in ECAR, this background level of acidification can be subtracted from recorded ECAR values to provide a quantification of basal glycolysis.

In order to measure glycolytic capacity, or maximal rates of glycolysis, oligomycin is subsequently injected into cells. This compound acts as an inhibitor of ATP Synthase (Symersky *et al.*, 2012), rapidly reducing levels of OXPHOS and leading to an increase in ADP/ATP ratios (Slater and Welle, 1969), which in turn drives anaerobic metabolism in the form of glycolysis. 2-DG, a glucose analogue that is taken up by glucose transporters in cells (Hansen *et al.*, 1995) but cannot be metabolised further, is lastly injected into cells, acting as an inhibitor of key glycolytic enzymes (Wick *et al.*, 1957). ECAR levels are then expected to drop, with this final measurement acting as a secondary measure of non-glycolytic ECAR.

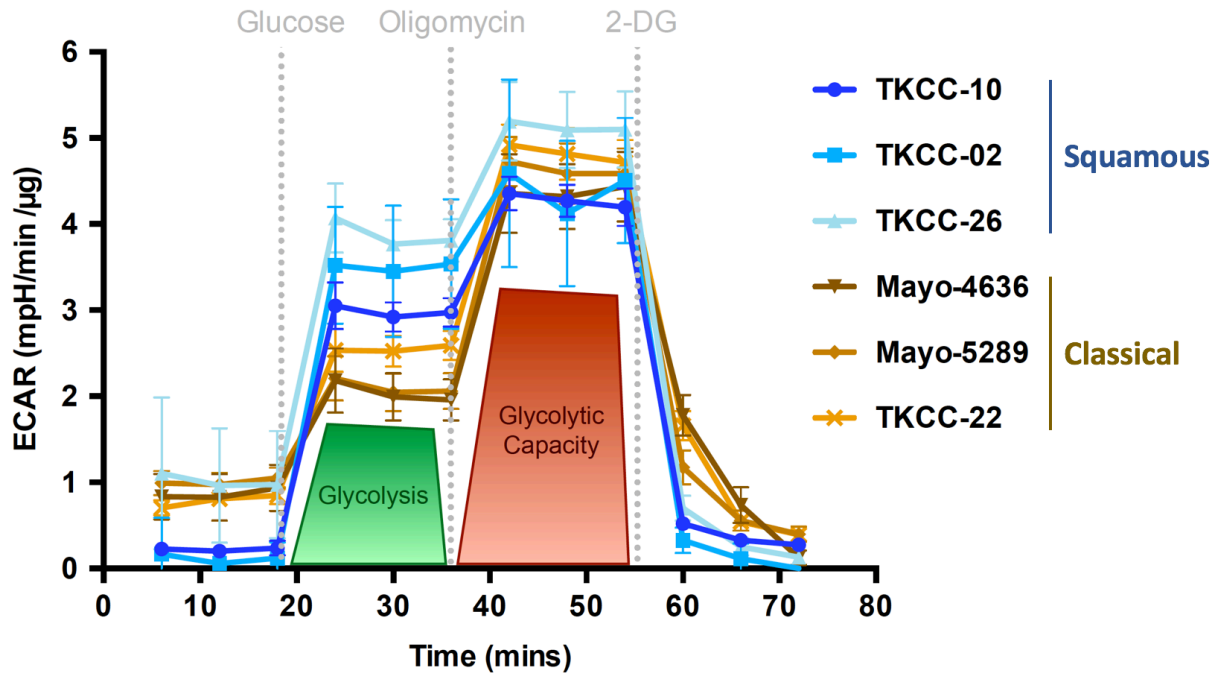


Figure 3.7 | Conducting glycolytic stress tests in PDCLs. Rates of basal and maximal glycolysis were determined in real-time via glycolytic stress test. Background, non-glycolytic acidification rates were measured in cells before addition of glucose. Basal rates of glycolysis (green) were subsequently obtained after injection of 10 mM glucose, with maximal rates, or glycolytic capacity, (red) next achieved via injection of a PDCL-dependent concentration of oligomycin. Finally, 50 mM 2-DG was injected in order to suppress glycolysis, providing a secondary measure of background acidification rates. Data presented as mean, with error bars representing SD, n=5.

The results of the glycolytic stress test determined that rates of basal glycolysis were significantly higher across all squamous PDCLs as compared to classical cells (Figure 3.8a) with a modest but significant, increase in maximal rates of glycolysis also observed in squamous PDCLs (Figure 3.8b). The greater increase in levels of basal glycolysis relative to maximal glycolysis in squamous PDCLs translated to lower rates of glycolytic reserve within this subtype (Figure 3.8c). This suggests that glycolysis within squamous PDCLs is, in general, operating at rates closer to maximum in the absence of a source of metabolic stress. These data collectively indicate a dependency on glycolysis and is suggestive of a potential sensitivity to therapeutic inhibition of this pathway (Issaq, Teicher and Monks, 2014).

3.4.3 Functional metabolic outputs validate subtype aligned-glycolytic phenotypes

In order to validate the findings determined via bioenergetic stress tests, additional colorimetric kits were implemented to directly quantify the consumption of glucose and production of lactate across PDCLs. Two assays were employed:

1. Abcam glucose uptake assay: this assay functions as outlined in (Saito *et al.*, 2011). Briefly, cells are exposed to the previously described glucose analogue 2-DG, which is taken up by cells at rates equivalent to glucose (Hansen, Gulve and Holloszy, 1994). Upon uptake, 2-DG is phosphorylated by hexokinases within cells, generating 2-DG-6-phosphate which cannot be metabolised further. The resultant 2-DG-6-phosphate is then exposed to high concentrations of glucose-6-phosphate dehydrogenase, leading to oxidation and the concurrent generation of NADPH. This NADPH is then harnessed via a recycling amplification reaction alongside glutathione and DTNB, allowing for colorimetric detection (Ellman, 1959). The production of NADPH, and hence signal, is directly proportionate to 2-DG uptake.
2. Abcam L-lactate assay: this assay functions similarly to the glucose uptake assay, with lactate dehydrogenase (LDH) utilised to convert L-lactate to pyruvate, producing NADH. NADH production is then quantified by exposure to tetrazolium salts, as in MTS/MTT assays, providing a colorimetric output which corresponds to starting quantities of lactate. As small quantities of LDH inherent to metabolically active cells are capable of influencing results, all samples were deproteinized using perchloric acid (Neuberg, Strauss and Lipkin, 1944) and subsequently neutralised using potassium hydroxide.

Results from colorimetric assays validated the previous Seahorse experiments, and found that squamous cells consistently consume more glucose (Figure 3.9a) and subsequently produce more lactate (Figure 3.9b) than compared to classical PDCLs. Furthermore, the results of the glucose uptake assay account for the

latency between addition of 2-DG and cessation of glycolysis observed in classical PDCLs during the glycolytic stress test (Figure 3.7), with squamous cell-lines taking up 2-DG at quicker rates, resulting in a more immediate inhibition of glycolytic enzymes.

Insulin has long been associated with stimulating the uptake of glucose (Park and Johnson, 1955; Levine and Goldstein, 1958). In order to quantify its possible influence as a supplement on the rate of glucose consumption, the glucose uptake assay was conducted in the presence and absence of insulin. Insulin was found to slightly increase glucose uptake, though not significantly, selectively in squamous cell-lines, but even in the absence of insulin, basal levels of glucose consumption were higher in all tested squamous PDCLs relative to classical. As such, insulin supplementation is not considered a likely contributor to described metabolic phenotypes. Though more data would be required to determine conclusively, the insulin-mediated increase in glycolysis associated with squamous PDCLs may be due to the secondary, noncatalytic function of the aldolase family of enzymes as modifiers of cell structure and endo/exocytosis (Volker and Knull, 1997; Merkulova *et al.*, 2011). In this role, aldolases have been shown to act as a scaffolding protein for the insulin-responsive glucose transporter, GLUT4 (SLC2A4), facilitating insulin-driven exocytosis of GLUT4 (Kao *et al.*, 1999). This interaction has been described as potential facilitator of a negative feedback system, wherein high levels of aldolase substrates, indicative of active glycolysis, inhibit the scaffolding function of aldolases and limit insulin-driven glucose transport. Within the context of the PDCLs, the more active aldolase isoform is associated with squamous PDCLs (Figure 3.4), which would allow this subtype to clear aldolase substrates quicker, liberating a greater proportion of aldolase to facilitate the translocation of GLUT4 to the cell membrane, enhancing insulin sensitivity.

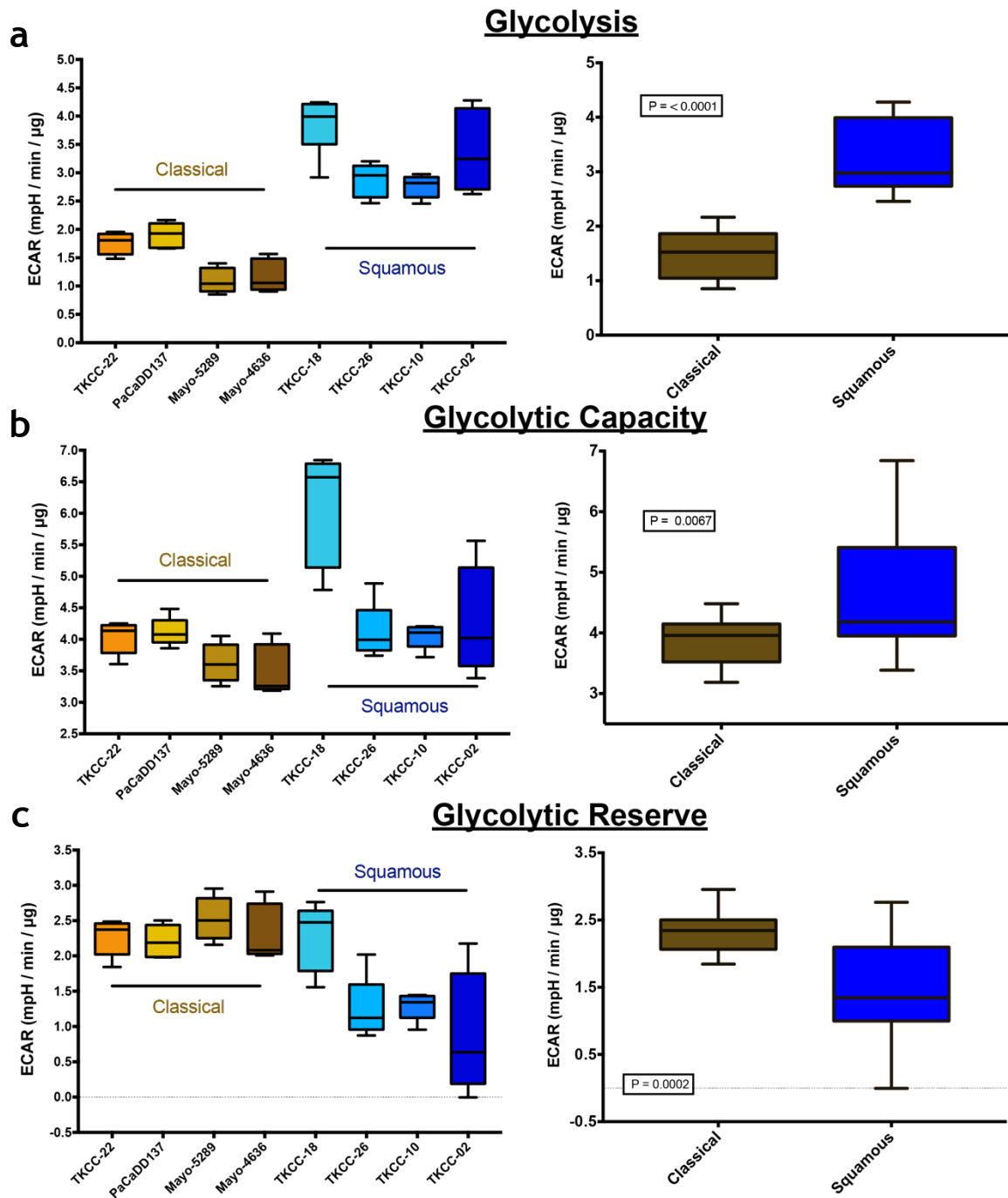


Figure 3.8 | Distinct glycolytic signatures define PDCL subtypes. **a** Boxplot displaying rates of basal glycolysis determined via glycolytic stress test across PDCLs. Data is presented as Individual cell-lines (left) and cell-lines grouped according to subtype (right). Subtypes are indicated by colouring, with squamous PDCLs (blue) displaying significantly higher rates of glycolysis than classical (brown). **b** Boxplot showing rates of glycolytic reserve, or the difference between basal and maximal observed rates of glycolysis, as in **(a)**. **c** Boxplots of glycolytic capacity, or rate of maximal glycolysis, as in **(a)**. Data presented with boxes indicating 25th to 75th percentiles, with lines representing median values and whiskers showing minima and maxima, $n=5$. P-values were determined according to a Mann-Whitney U test.

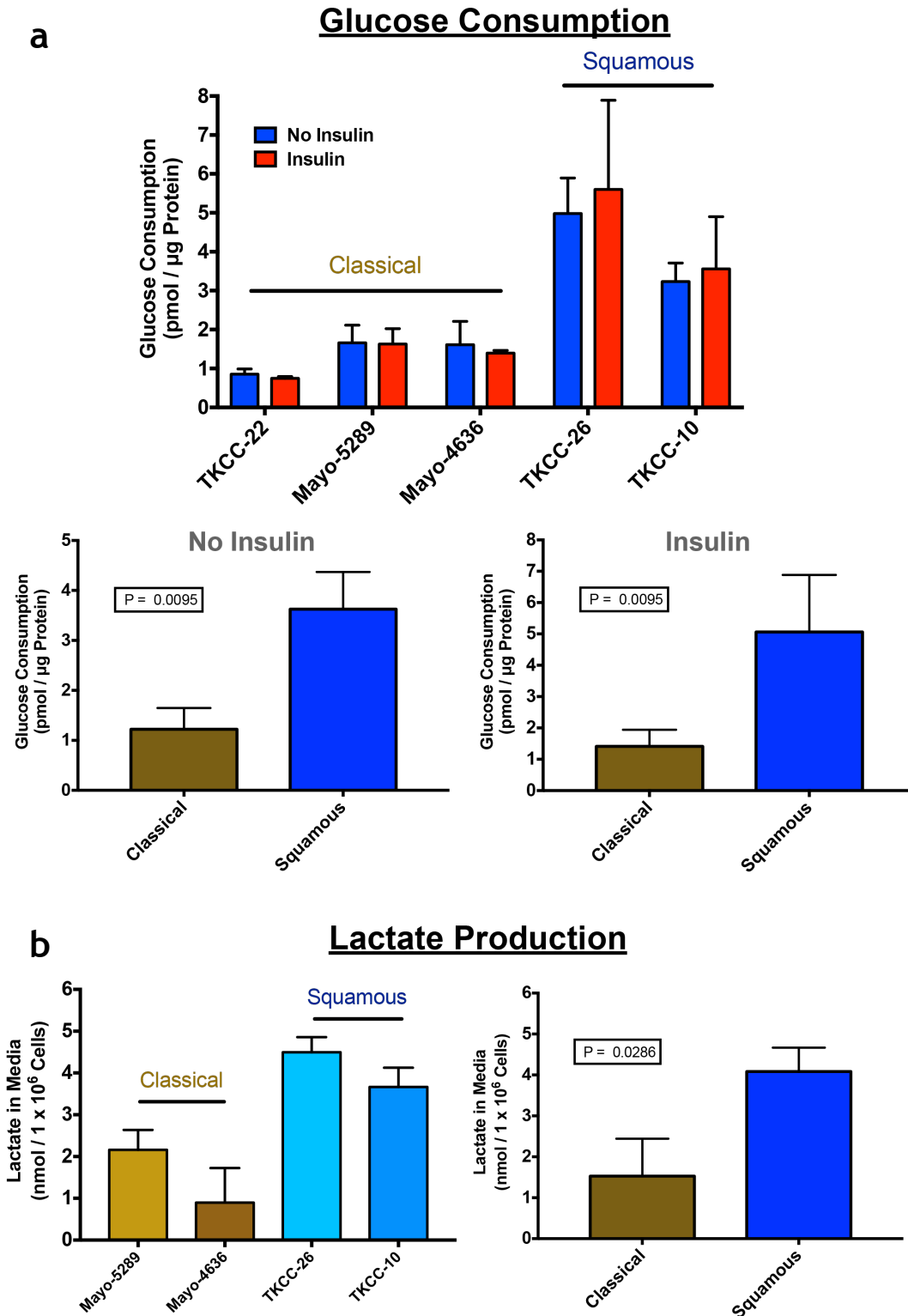


Figure 3.9 | Validating PDCL metabolic signature. a Bar-plot showing rates of glucose consumption in individual PDCLs ordered according to subtype. Measurements were recorded with cells cultured in medium without insulin (blue) and with insulin (red). b Bar-plots showing lactate production across PDCLs, with data presented according as in figure 3.7. All experiments were performed in duplicate mean and presented as mean with error bars representing SD. P-values were determined according to a Mann-Whitney U test.

3.4.4 Rates of Fatty Acid Oxidation co-segregate with PDCL subtypes

Basal and maximal Fatty acid oxidation (FAO) processes depend on the utilisation of both endogenous and exogenous fatty acids as fuel to drive the TCA cycle, and rates were determined in PDCLs using a modified version of the mitochondrial stress test (Figure 3.10), as described previously (Pike *et al.*, 2011).

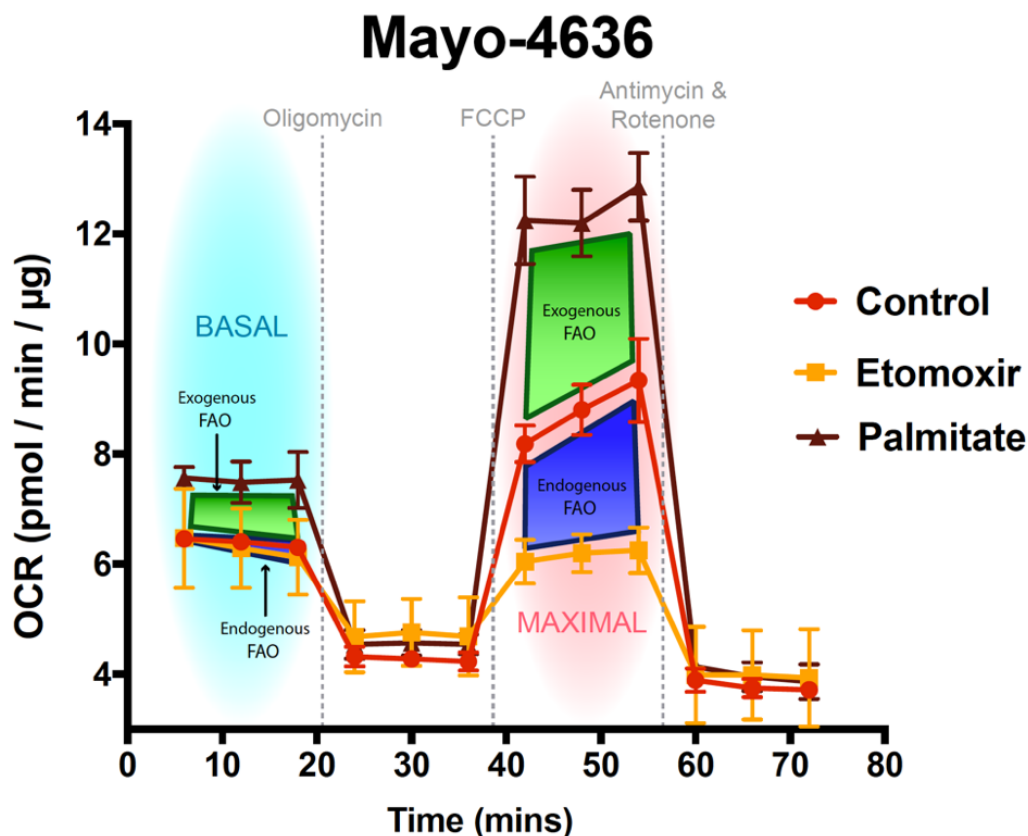


Figure 3.10 | Measuring rates of fatty acid oxidation in PDCLs. The FAO profile corresponding to the Mayo-4636 cell-line, representative of the classical subtype and selected for descriptive purposes. Basal exogenous FAO levels (time-point 6-18 mins, green box within cyan area) are measured by recording the natural rate of respiration in the absence of exogenous FAs (control, red curve) and then quantifying the increase in OCR recorded in the presence of the FA palmitate (dark red). Endogenous FAO (blue box) is similarly measured by quantifying the decrease in OCR induced by the drug Etomoxir (yellow curve), which prevents the metabolism of endogenous FAs. Maximal respiration (time-point 42-52 mins, red) is then calculated with the same conditions as basal rates after treating cells with the uncoupling agent FCCP, which drives oxidative respiration. Respiration is measured as the oxygen consumption rate (OCR) as normalised to total protein content of wells. Data presented as mean, with error bars representing SD, n=4.

Briefly, cells were cultured in glucose and glutamine-limited media (Table 2.4) for 4 hours in advance of the assay in order to promote the metabolism of surplus endogenous FAs and to encourage uptake of exogenous FAs during the course of the experiment. Cells were treated with either DMSO (control), an exogenous source of FA (palmitate), or an inhibitor of FA uptake across the mitochondria (etomoxir), which prevents FAO entirely. Oxygen consumption was then measured in real-time across a range of treatments affecting metabolism, with an initial injection of oligomycin, preventing TCA cycle driven ATP synthesis, and providing a measurement of ATP production (statistics not shown as ATP synthesis aligned closely with basal respiration, indicating no differential proton leak between PDCL subtypes). FCCP, an uncoupling agent which uncouples ETC from ATP synthesis, is subsequently added into wells, facilitating the efflux of protons across the mitochondrial membrane, disrupting the proton gradient and generating heat energy that is lost instead of cellular energy captured in ATP production. This results in an upregulation of ETC to offset the flooding of protons back into the inner mitochondrial matrix, leading to the oxidation of all substrates available to the cell to fuel the TCA cycle, and allowing a measurement of maximal rates of respiration. Finally, antimycin A and rotenone are injected, both acting as inhibitors of ETC complexes, preventing all oxygen consumption linked to respiration, allowing for the resolution of background OCR.

FAO assays revealed that the classical PDCLs use a significantly higher rate of exogenous FAs as a fuel source compared to squamous PDCLs (Figure 3.11a), though due to technical issues with their general growth properties and adherence, alongside additional washing steps necessary for this protocol, the squamous PDCL TKCC-02 were determined to be incompatible with this assay. In contrast, endogenous FAs are preferentially utilised to fuel basal respiration in a selection of classical PDCLs as compared to squamous, but no significant association exists between subtype and endogenous FA usage at maximal levels, when cells are placed under metabolic stress (Figure 3.11b). This observed increase in FAO in classical PDCLs thus validates the previously described findings at the transcriptomic and proteomic levels, which had collectively suggested an

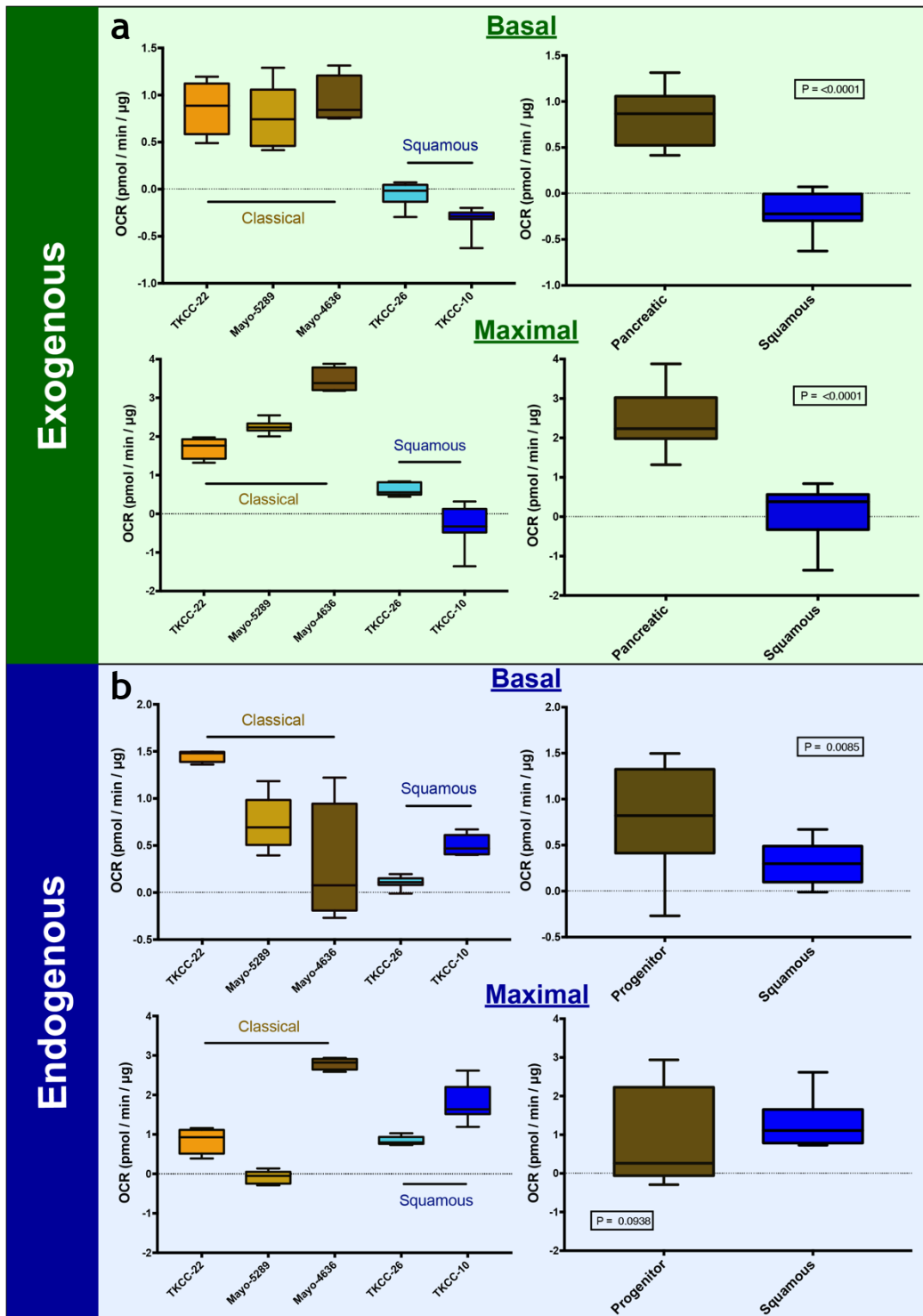


Figure 3.11 | Rates of FAO differ across PDCL subtypes. **a** Boxplots showing the rates of fatty acid oxidation fuelled by exogenous fatty acids. Data is presented as in figure 3.7. Classical PDCLs (brown) exhibit significantly higher rates of both basal (top) and maximal (bottom) exogenous FAO than squamous (blue). **b** Boxplots showing rates of FAO fuelled by endogenous fatty acids, as in (a). P-values were determined according to a Mann-Whitney U test. Data presented with boxes indicating 25th to 75th percentiles, with lines representing median values and whiskers showing minima and maxima, n=4.

upregulation of metabolic players involved in lipid and FA metabolism within this subtype. The increase in rates of exogenous FA supports the association between proteins involved in FA catabolism, such as acyl-CoA dehydrogenase short/branched chain (ACADSB), which oxidizes acyl-CoA derivatives as part of the FAO process (Rozen *et al.*, 1994), malonyl-CoA decarboxylase (MLYCD), which mediates the degradation of malonyl-CoA to acetyl-CoA, thus preventing the inhibition of FAO associated with malonyl-CoA described in chapter 1.5.4 , and SLC27A3, a fatty acid transporter associated with FA uptake into cells (Maekawa *et al.*, 2015), and the classical subtype. Additionally, the upregulation of genes involved in lipid biosynthesis in classical PDCLs may be linked to the increased rates of basal endogenous FAO in this subtype, as in the absence of metabolic stress, it is possible that a balance between catabolism and anabolism persists, as has been suggested in literature (Carracedo, Cantley and Pandolfi, 2013), described in greater detail in chapter 1.5.4 . As such, active FA synthesis within this subtype would produce FA stores which may be utilised to fuel FAO, reflected in increased rates of endogenous FAO.

3.4.5 Metabolic flexibility is associated with classical PDCLs

Emergence of resistance to therapeutic intervention is a common phenomenon in cancer (Holohan *et al.*, 2013) mediated by a variety of mechanisms including the emergence of drug-target mutations conferring resistance via tumour evolution (Gorre *et al.*, 2001; Pao *et al.*, 2005) or the activation of redundant, compensatory pathways (Wheeler *et al.*, 2008; Mao *et al.*, 2013), and therefore requires careful consideration in a preclinical setting. Flexibility in metabolism has previously been shown to mitigate sensitivity to otherwise effective therapies over time, with imatinib resistance in chronic myeloid leukaemia having been linked to enhanced glycolysis (F. Zhao *et al.*, 2010) and OXPHOS activation found to confer resistance to BRAF inhibition in melanoma (Haq *et al.*, 2013). In the context of pancreatic cancer, *in vitro* models have demonstrated that upregulation of glucose uptake and glycolysis (Shukla *et al.*, 2017; Zhao *et al.*, 2017), as well as lipid synthesis (Tadros *et al.*, 2017), may contribute to resistance to the standard of care therapeutic, gemcitabine.

Multiple research projects have also identified the potential of cancer cells to adapt to metabolic inhibition via various mechanisms, for example, inhibition of OXPHOS can be overcome across a range of cancer-types via upregulation of glycolysis (Zhong *et al.*, 2015; Nagana Gowda *et al.*, 2018). Similar phenomena have also been described within pancreatic cancer, with attempts to block glutamine dependency associated with PDAC (Son *et al.*, 2013) in cell-line models found to induce concerted compensatory changes, including a metabolic shift to FAO, which facilitates resistance to inhibition (Biancur *et al.*, 2017). Additionally, therapeutic inhibition of lactate dehydrogenase (LDH) in pancreatic cancer cells revealed an upregulation of OXPHOS via AMPK activation, conferring resistance to LDH inhibition (Boudreau *et al.*, 2016). Given these findings, as well as the close association between molecular drivers of pancreatic cancer and metabolic reprogramming (Table 1.1), there is a clear potential of therapeutic resistance emerging as a result of metabolic flexibility in PDAC which must therefore be addressed (Kimmelman, 2015).

In order to measure potential for metabolic flexibility within PDCLs, an assay designed according to the Mito Fuel Flex Test was conducted. This experiment allowed for the quantification of a cell-line's dependency on the three major metabolites responsible for driving mitochondrial respiration: glucose, glutamine, and fatty acids. Dependency scores were calculated for each of the three metabolites via treatment with inhibitors of key players in their respective metabolism, such as: UK5099, an inhibitor of the mitochondrial pyruvate carrier (Hildyard *et al.*, 2005) which prevents the utilisation of pyruvate, a primary product of glycolysis, to fuel OXPHOS; BPTES, a glutaminase inhibitor (Shukla *et al.*, 2012), prevents the hydrolysis of glutamine, disrupting its introduction to the TCA cycle; etomoxir, an inhibitor of CPT1A (Kruszynska, Stanley and Sherratt, 1987), as mentioned previously prevents the carnitine-dependent transfer of FAO intermediates into the mitochondria, inhibiting FAO. Capacity scores were subsequently calculated by employing combinations of these metabolic inhibitors, allowing a read-out of a cell's ability to compensate for the loss of various fuel sources with one of the three metabolites of interest. Flexibility was then

calculated by subtracting dependency scores from capacity scores. This analysis revealed that metabolic flexibility existed only within PDCLs classified as classical (Figure 3.12), with low dependencies and high flexibility seen particularly within Mayo-5289. Some negligible flexibility in glutamine metabolism was observed within TKCC-10 (squamous), but in general, squamous PDCLs displayed no flexibility and greater dependency than classical cell-lines.

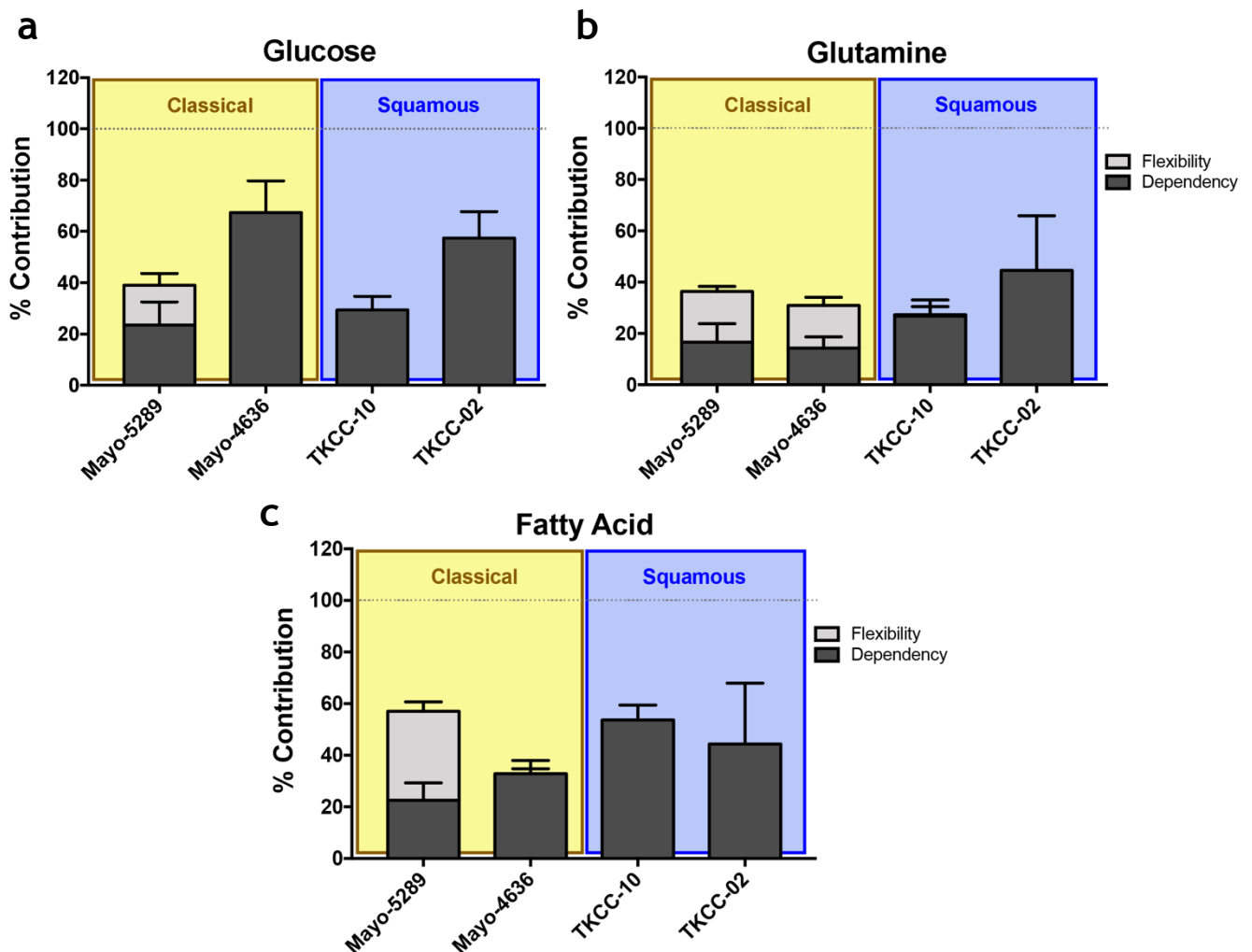
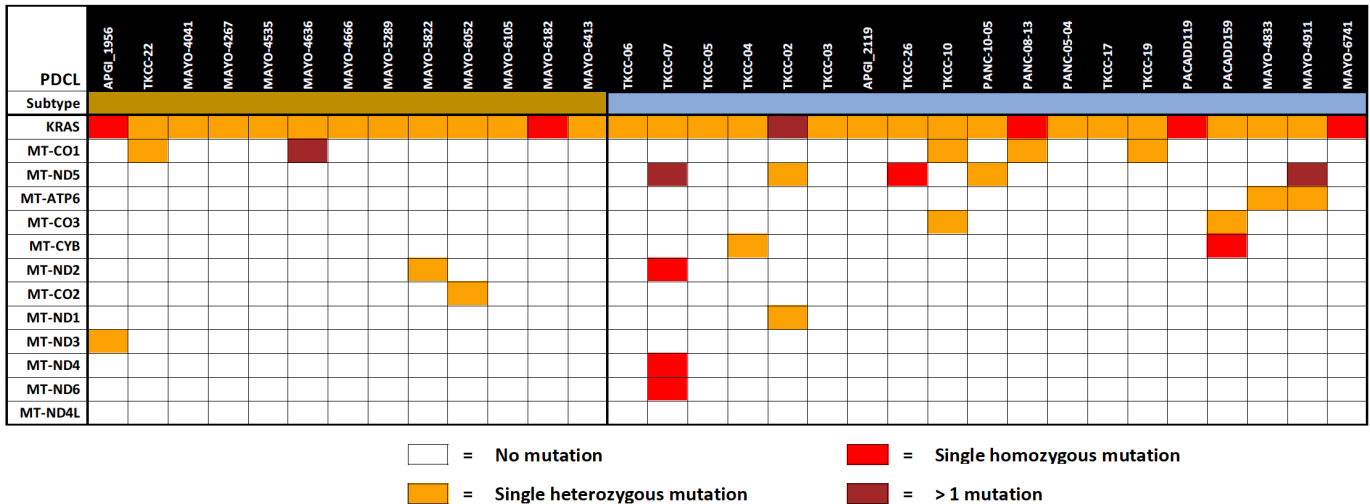


Figure 3.12 | Classical PDCLs display greater metabolic flexibility than squamous. Bar-plots showing metabolic dependency (dark grey) and flexibility (light grey) for glucose (a), glutamine (b) and fatty acids (c) across PDCLs representative of the squamous and classical subtypes. As can be seen, flexibility is observed only in classical cell-lines. Data are presented as mean, with error bars representing SD, n=5.

3.5 *KRAS* and mitochondrial gene mutation status do not account for subtype-associated metabolic dysregulation

As described in chapter 1.5.6 , *KRAS* mutation status has been implicated as a driver of glycolysis, with previous research additionally indicating an association exists between *KRAS* mutation copy number and metabolic reprogramming towards glycolytic activation (Kerr *et al.*, 2016). Similarly, the presence of mutations in mitochondrial DNA suggestive of mitochondrial dysfunction have been found to contribute to a more glycolytic, less oxidative phenotype in a collection of TKCC pancreatic cancer cell-lines (Hardie *et al.*, 2017). In order to assess this relationship within PDCLs, the mutation status of both *KRAS* and all genes expressed in PDCLs found within mitochondrial DNA, as determined by the Genome Reference Consortium Human (GRCh) genome, build 38 (Schneider *et al.*, 2017), was overlaid onto subtype. This revealed that, although there did appear to be a slightly higher frequency in both mitochondrial and homozygous *KRAS* mutations in squamous PDCLs (Table 3.2), neither association was significant according to a chi-squared test. These findings therefore suggest that neither mutant *KRAS* copy number, nor mitochondrial DNA mutation are major contributors to subtype-associated metabolism, thus justifying an approach that prioritises focus on those distinct biological processes associated with the two subtypes.

Table 3.2 | There is no apparent association between KRAS mutation copy number, mitochondrial mutations and PDCL subtype. Chart displaying mutation rates across *KRAS* and mitochondrial genes, with colouring to indicate nature of mutation. No significant association was found to exist between *KRAS* mutation status or mitochondrial mutation-load and subtype, according to chi-squared test.



3.1 Association of KRAS amino acid substitution and subtype specification

Though *KRAS* mutations most commonly affect codon 12 (Miglio *et al.*, 2014), previous research has shown that the exact amino acid substituted for the glycine residue at this position may act as a prognostic factor in PDAC (Bournet *et al.*, 2016), while mutations at codon 61 have been linked to a favourable outcome in patients (Witkiewicz *et al.*, 2015). As PDAC subtype is also a predictor of prognosis, it was decided to investigate any potential association between subtype and *KRAS* mutation type. As described in literature, most mutations within cell-lines were found in codon 12 (Table 3.3), however there was no correlation found between subtype and any specific *KRAS* mutation.

| | MAYO-6741-1 | TKCC-19 | TKCC-10 | APGI_2119 | TKCC-04 | TKCC-05 | TKCC-06 | TKCC-07 | MAYO-6413-1 | MAYO-5289-1 | MAYO-4666-1 | MAYO-4636-1 | MAYO-4267-1 | TKCC-22 | MAYO-4911-1 | MAYO-4833-1 | PANC 05.04 | PANC 08.13 | PANC 10.05 | TKCC-02 | TKCC-03 | MAYO-6182-1 | MAYO-6105-1 | MAYO-6052-1 | MAYO-4535-1 | MAYO-4041-1 | TKCC-26 | MAYO-5822-1 | APGI_1956 | PACADD159 | PACADD119 | TKCC-17 | PACADD137 | MAYO-6164-1 | | | |
|---------|-------------|---------|---------|-----------|---------|---------|---------|---------|-------------|-------------|-------------|-------------|-------------|---------|-------------|-------------|------------|------------|------------|---------|---------|-------------|-------------|-------------|-------------|-------------|---------|-------------|-----------|-----------|-----------|---------|-----------|-------------|--|--|--|
| Subtype | Blue | | | | | | | | Brown | | | | | | | Blue | | | | | | Brown | | Blue | | | Brown | | | | | | | | | | |
| G12V | Red | Red | Red | Red | Red | Red | Red | Red | Red | Red | Red | Red | Red | Red | | | | | | | | | | | | | | | | | | | | | | | |
| G12D | | | | | | | | | | | | | | | Red | Red | Red | Red | Red | Red | Red | Red | Red | Red | Red | Red | Red | | | | | | | | | | |
| G12R | | | | | | | | | | | | | | | | | | | | | | | | | | | Red | Red | Red | | | | | | | | |
| G12S | | | | | | | | | | | | | | | | | | | | | | | | | | | | | | | | Red | | | | | |
| G12A | | | | | | | | | | | | | | | | | | | | | | | | | | | | | | | | | Red | | | | |
| Q61H | | | | | | | | | | | | | | | | | | | | | | | | | | | | | | | | | | Red | | | |

Table 3.3 | Within PDCLs, mutations in *KRAS* do not show association between codon specificity or residue change and subtype. Chart displaying mutations within *KRAS* in PDCLs, with mutations (red shading) categorised according to codon affected and amino acid substitution. PDCL subtypes are indicated by colour, with blue representing the squamous and brown representing classical subtypes. As can be seen, there is no association between the various *KRAS* mutations and subtypes.

3.2 Discussion

This chapter aimed firstly to assess the relevance of PDCLs as an *in vitro* model of PDAC subtypes and secondly to identify vulnerabilities associated with subtypes via transcriptomic and proteomic analyses, with validation by functional assays. The first aim was achieved via analysis of RNA-seq data, which highlighted the conservation in co-ordinately expressed gene programmes between patients and cell-lines. Pathway analyses involving these gene programmes then revealed a dysregulation of genes involved in metabolism between the two identified *in vitro* subtypes, with both proteomics analysis and assays probing metabolic outputs pointing to an association between glycolysis and the squamous subtype, as well as FA synthesis and FAO with the classical subtype. This finding is particularly significant given that glycolysis, which is associated with the aggressive, squamous subtype, has been linked with a worse prognosis in PDAC (Baek *et al.*, 2014; Xiang *et al.*, 2018), echoed by previous findings that a poor prognosis glycolytic subtype exists in PDAC (Follia *et al.*, 2019) and that metabolic reprogramming has been long been described in PDAC, as described in chapter 1.5.6 .

The results outlined within this chapter collectively point to the existence of distinct metabolic subtypes in PDCLs which correlate with subtypes previously described in pancreatic cancer patients (Bailey *et al.*, 2016). This work therefore validates and expands on previous efforts to subtype pancreatic cancer via metabolite profiling, which demonstrated that cells subtyped into two divergent groups according to an alternative subtyping approach, as described in chapter 1.4.1 (Collisson *et al.*, 2011), exhibited distinct glycolytic and lipogenic dependencies (Daemen *et al.*, 2015). This study demonstrated that cell-lines classed as quasi-mesenchymal, analogous to the squamous subtype described within this work (Collisson *et al.*, 2019), displayed elevated levels of metabolites involved in glycolysis, such as glyceraldehyde-3-phosphate and lactate, while classical cell-lines exhibited upregulated long-chain FAs, such as oleic and palmitate. The findings described within this chapter therefore provide additional evidence for the existence of these subtypes, while suggesting the origins of such

are choreographed at the level of the transcriptome (Figure 3.1). Within PDCLs, initial analyses failed to narrow targets to a single driver accounting for the metabolic divergence observed between subtypes, although there is a clear and co-ordinately regulated shift in metabolic players at both the transcript and protein levels that aligns with subtype specification. Interrogating this metabolic dysregulation further therefore holds potential for identifying novel, subtype-associated vulnerabilities.

In order to facilitate the identification of novel therapeutic targets and maximise the possibility of identifying an effective treatment strategy, two separate approaches were taken at this point in the project (Figure 3.13). Firstly, transcriptome and proteome data were split by subtype and interrogated to highlight pathways that represent possible vulnerabilities, allowing for direct selection of key enzymes targetable through therapeutic modulation. This approach is supported by the previous successes of *in vitro* attempts to target both glycolysis (Maftouh *et al.*, 2014; Anderson *et al.*, 2017) and FA biosynthesis (Rajeshkumar *et al.*, 2015; Ventura *et al.*, 2015; Brandi *et al.*, 2017), while differences in subtype vulnerabilities may provide further explanation for instances whereby cells exhibited resistance to these therapeutic interventions (Kamphorst *et al.*, 2013; Boudreau *et al.*, 2016). Secondly, high-throughput screening was performed to select a broader set of compounds that can be subsequently narrowed according to stratifications described within this chapter. This strategy allows the potential to select for inhibitors that indirectly modulate metabolic pathways associated with the subtypes, while drug repurposing allows the possibility for expediting prospective clinical tests (Bertolini, Sukhatme and Bouche, 2015; Würth *et al.*, 2016).

The following chapter describes the identification of pathways found to functionally contribute to subtype-specific phenotypes in *in vitro* models, allowing the identification of key players within these pathways that can be inhibited via clinically relevant compounds. The additional observation that these subtype-associated pathways in cell-line models are reflective of dysregulation observed in patients reinforces the clinical potential of follow-up work to identify drug treatments following this approach.

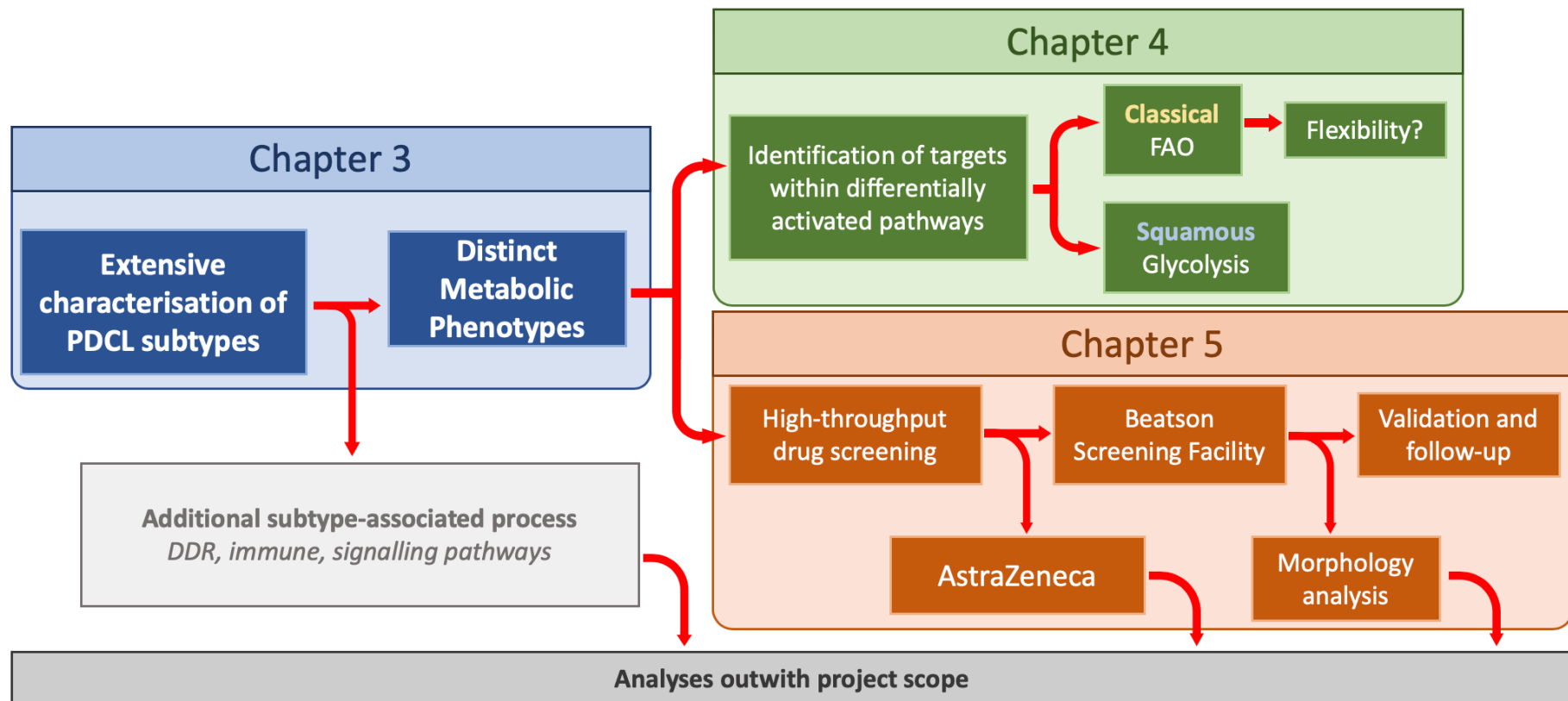


Figure 3.13| Two concurrent approaches taken to identify novel therapeutics. Flowchart outlining approaches described as part of project to dissect metabolic dysregulation and identification of therapeutics. Research described in chapter 3 (blue boxes) revealed metabolic distinctions between subtypes, with later chapters designated to discuss the two arms to achieve the end goal of identifying compounds effective in treating pancreatic cancer *in vitro*. The first, to be described in chapter 4 (green boxes), focused on key players within metabolic processes identified as being subtype-associated, while the second, to be described in chapter 5 (orange boxes), relied on high-throughput screening to identify novel therapeutics that may induce sensitivity in cells via metabolic inhibition.

Chapter 4 *Targeting Subtype- associated Metabolic Processes*

Targeting Subtype-associated Metabolic Processes

4.1 Introduction

Evidence points to the existence of a variety of potentially targetable metabolic alterations across a range of cancer-types (Martinez-Outschoorn *et al.*, 2017), as discussed in chapter 1.5 , with many pre-clinical research projects focused on exploiting these therapeutically, as described briefly in chapter 3.1 . In-line with these efforts, and guided by the distinct metabolic phenotypes identified within the PDCLs as described in the previous chapter, as defined by a dysregulation of metabolic players at the transcriptome and proteome levels, translating to differential activation of glycolysis and FA metabolism between subtypes, we sought to investigate potential individual targets within these pathways. As discussed in greater detail in chapter 1.5.1 , a major metabolic pathway long associated with oncogenesis is glycolysis, which is hyperactive in squamous PDCLs. Alongside this upregulation of glycolysis, aldolase isoform ratio is skewed towards expression of ALDOA (Figure 3.4), a highly active form of this enzyme which is involved in early-stage glycolysis. As such, this presented an ideal potential target to modulate therapeutically and it was decided to assess the ability of ALDOA inhibition in suppression of squamous-associated glycolysis, alongside any impact in cell viability.

Beyond inhibition of glycolysis, the potential of targeting fatty acid biosynthesis, another important metabolic process linked to cancer generation (Menendez and Lupu, 2007) and upregulated in classical PDCLs, was investigated. FA biosynthesis was targeted via inhibition of FASN, an enzyme necessary for lipogenesis and with previously described links to cancer progression, as discussed in chapter 1.5.2 .

Despite the potential of these approaches that target metabolism, as indicated by the dysregulation of various metabolic pathways between subtypes, it is expected that metabolic flexibility may prove a challenge when devising treatment strategies involving metabolic vulnerabilities. This is of particular concern as, beyond its identification in classical PDCLs (Figure 3.12), it has been described previously as a general feature of pancreatic cancer (Boudreau *et al.*, 2016; Biancur *et al.*, 2017). In order to account for any resistance to treatments potentially resulting from metabolic flexibility, compensatory activation of alternative metabolic pathways may be quantified on exposure to therapeutics. Should flexibility be identified within PDCLs, combinatorial approaches may be considered to suppress the upregulation of compensatory metabolism.

4.2 Inhibiting squamous-associated glycolysis limits viability in PDCLs

4.2.1 Identifying ALDOA as a potential target for inhibition of glycolysis in squamous subtype

As described in chapter 3.2.2, aldolase A (ALDOA) is the major functional isoform in a family of enzymes that catabolise one of the initial steps in glycolysis, and its expression is strongly associated with the squamous subtype. An siRNA screen conducted on a select number of PDCLs in the Institute of Cancer Research (ICR), London, showed that knockdown (KD) of *ALDOA* induced a significant loss of viability across 5 out of 9 cell-lines tested (Figure 4.1). The majority of the PDCLs included in this screen were classified as squamous, a subtype found to display high levels of glycolysis (Figure 3.8), with only one classical PDCL, TKCC-22, included in siRNA screening, which may be considered an outlier relative to other classical PDCLs, exhibiting the highest levels of *ALDOA* expression amongst all PDCLs. The observation that many squamous PDCLs are sensitive to *ALDOA* KD, alongside the expression pattern of aldolase isoforms within PDCLs, suggests that the squamous subtype utilises the highly active ALDOA isoform (Chang *et al.*, 2018)

to drive glycolysis and may be dependent on this for survival. This possibility was reinforced by previous research showing that the silencing of *ALDOA* inhibited glycolysis in two commercially available pancreatic cancer cell-lines and improved prognosis *in vivo* according to a xenograft model of breast cancer (Grandjean, de Jong, B. P. James, *et al.*, 2016). The same body of work that described this research employed a drug repurposing screen, which identified TDZD-8, an inhibitor of GSK-3 β (Martinez *et al.*, 2002), to act as a small-molecule inhibitor of *ALDOA*. This inhibition was resolved to be likely due to interaction between TDZD-8 and cysteine 289 of *ALDOA*, leading to conformational changes affecting the C-terminal tail of the protein, a site that has long been recognised as a regulator of *ALDOA* activity (Gamblin *et al.*, 1991), TDZD-8 was then found to mediate an anti-cancer effect in the same mouse model and, based on these collective findings, TDZD-8 was selected to test as an inhibitor of squamous-associated glycolysis.

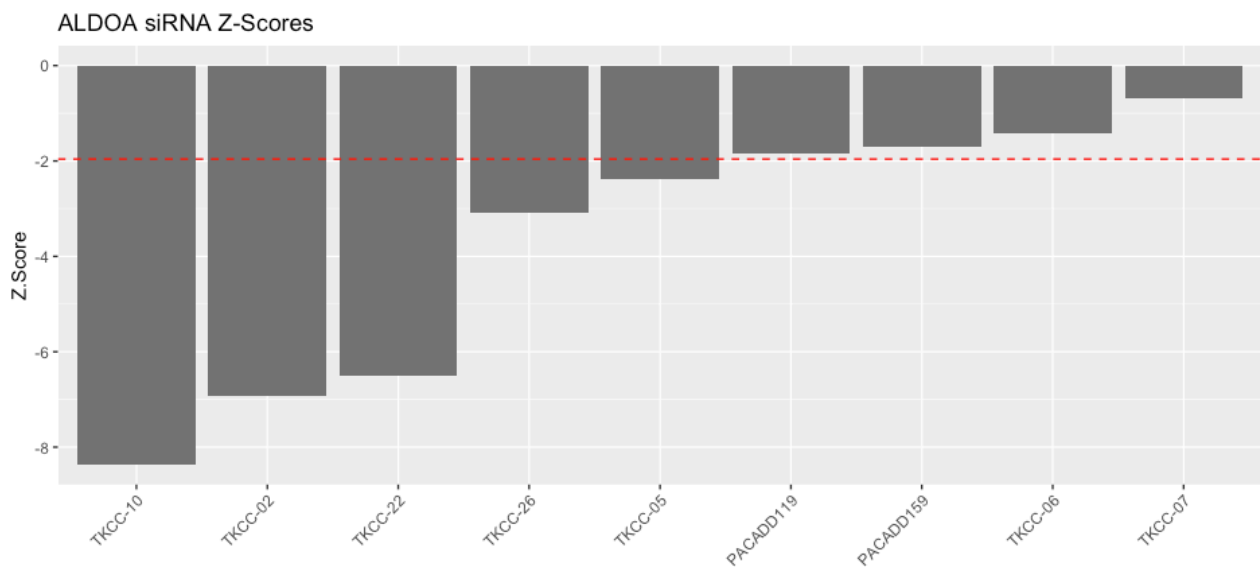


Figure 4.1 | *ALDOA* identified as possible target via siRNA-mediated KD. Barplot showing sensitivity of PDCLs to *ALDOA* KD, with cell-lines ordered according to sensitivity. As can be seen, a number of cell lines (5 out of 9) were found to be significantly sensitive. Significance was defined as a Z-score < -1.96, equivalent to $p < 0.05$, represented by the dashed, red line.

In order to first validate *ALDOA* as a driver of glycolysis in squamous cells, the effect of TDZD-8 on glycolytic rates were assessed across PDCLs at a 4 hour time-point, in line with previous publications (Grandjean, de Jong, B. P. James, *et al.*, 2016). This assay revealed that glycolysis was inhibited dramatically with TDZD-8

treatment, selectively in squamous PDCLs (Figure 4.2). This observation was dose-dependent, with rates of glycolysis tending to 0% at higher concentrations of TDZD-8, highlighting the importance of ALDOA in glucose metabolism.

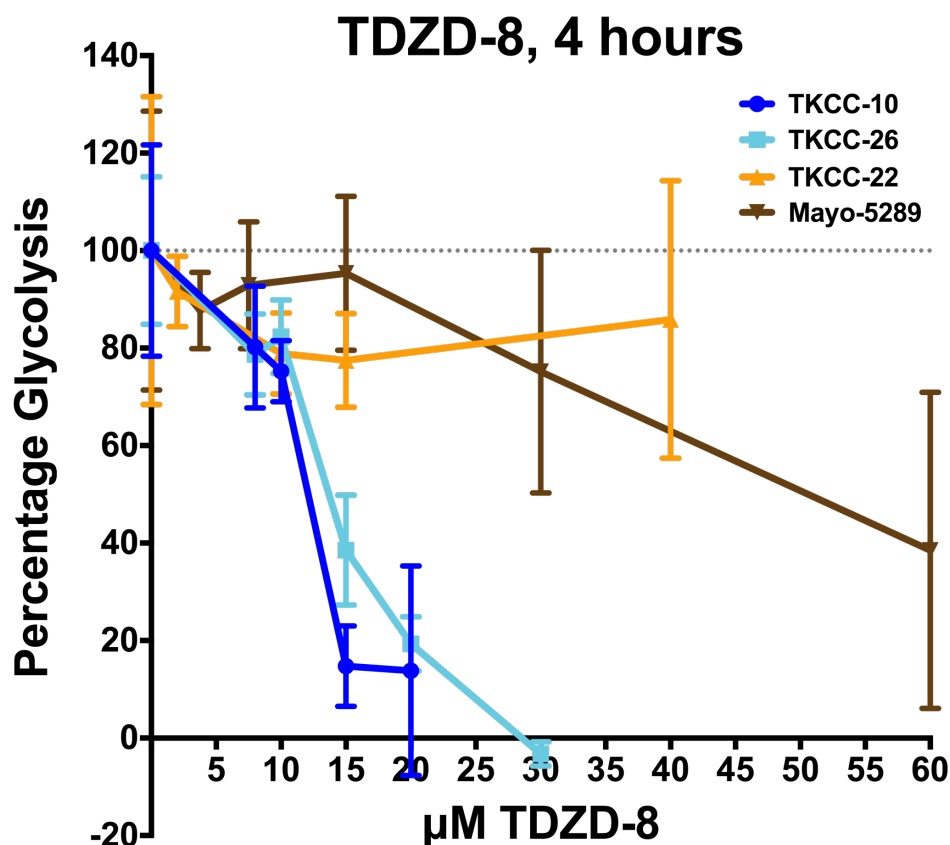


Figure 4.2 | ALDOA inhibition selectively reduces rates of glycolysis in Squamous PDCLs.

Scatter-plot showing inhibition of glycolysis, as determined via glycolytic stress test, in PDCLs after four hours treatment with TDZD-8, an inhibitor of ALDOA. As can be seen, inhibition of ALDOA leads to a reduction in glycolysis specifically in squamous cell-lines (blue), while classical PDCLs (brown) are largely unaffected. Glycolysis is presented as a percentage relative to glycolysis in DMSO-treated control cells. Data presented as mean, with error bars representing SD, $n=4$.

4.2.2 Inhibiting glycolysis via TDZD-8 treatment is effective in squamous PDCLs

Upon determining that TDZD-8 inhibited glycolysis specifically in squamous cell-lines, it was decided to assess the effect of the compound on cell viability. In

preparation for dose-response curve, it was first necessary to optimise concentrations and timeframes for testing. Firstly, it was found that TDZD-8 can maximally suppress glycolysis in a representative squamous cell-line within an hour after treatment, with high concentrations completely inhibiting glycolysis (Figure 4.3a). Subsequent assays showed that lower concentrations require a longer treatment time, up to 72-hours, before a response is seen (Figure 4.3b). The observation that TDZD-8 can induce a response within this short timeframe suggests a direct mechanism of inhibition, supporting the likelihood that TDZD-8 mediates its inhibition of glycolysis via on-target effects. Despite the rapid response, it was decided to allow 72 hours for dose-response curves, to maintain consistency with field standards.

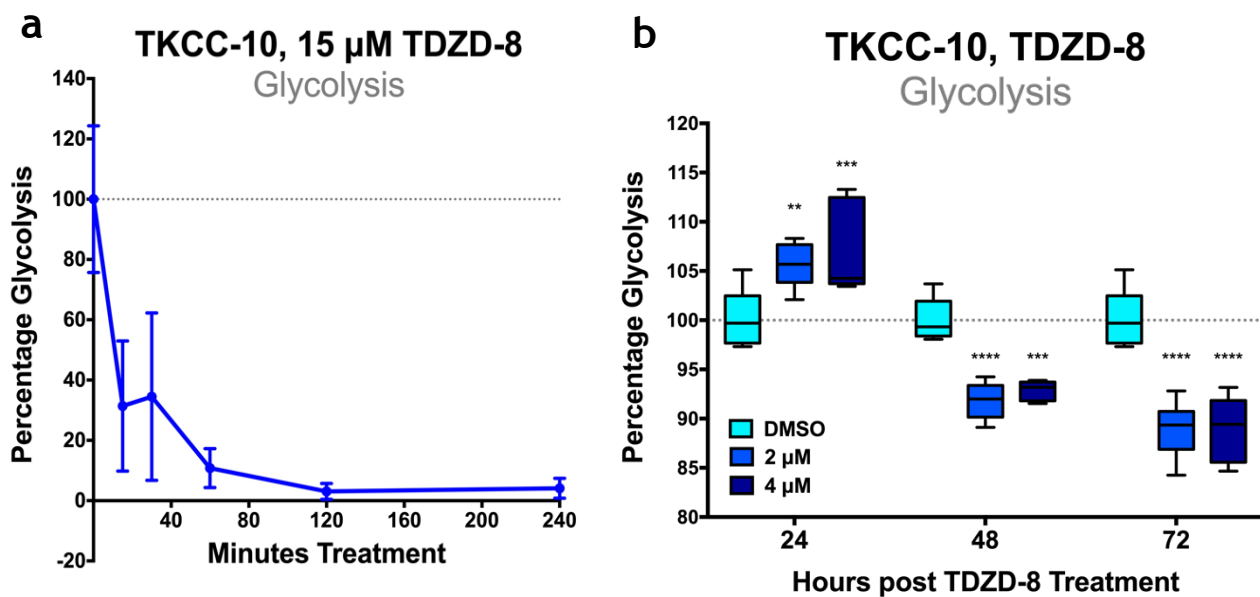


Figure 4.3 | Determining optimal conditions for TDZD-8 treatment. a Curve showing rapid response of a squamous cell-line, TKCC-10, to 15 μ M TDZD-8 treatment. Within an hour, glycolysis is almost completely inhibited. Data presented as mean, with error bars representing SD, n=8. b Box-plot showing changes in glycolysis after treatment with 2 μ M (blue) and 4 μ M (dark blue) relative to DMSO control (cyan). At 24-hours, no response in glycolysis is apparent, but at 48- and 72-hour time-points, a clear and significant decrease is observed. Data presented with boxes indicating 25th to 75th percentiles, with lines representing median values and whiskers showing minima and maxima, n=6.

Efforts to assess the sensitivities of six cell-lines, three representative of the each subtype, to TDZD-8 at a 72-hour time-point determined that squamous cell-lines were more sensitive to TDZD-8 (Figure 4.4) (Holly Brunton, unpublished data), with lower observed IC_{50} values obtained for all squamous PDCLs tested. Reduction in viability in squamous cells was found to correspond closely with decreased rates of glycolysis, suggesting that abrogation of ALDOA-driven glycolysis may be responsible for inhibition of growth in these cells. These results were not wholly consistent with siRNA screening (Figure 4.1), with PDCLs displaying different sensitivities to ALDOA KD as compared to TDZD-8 treatment. This may indicate a lack of specificity of TDZD-8, though it would be necessary to validate results from high-throughput siRNA screening before any conclusions could be made. However, due to time limitations, this was not possible within this project.

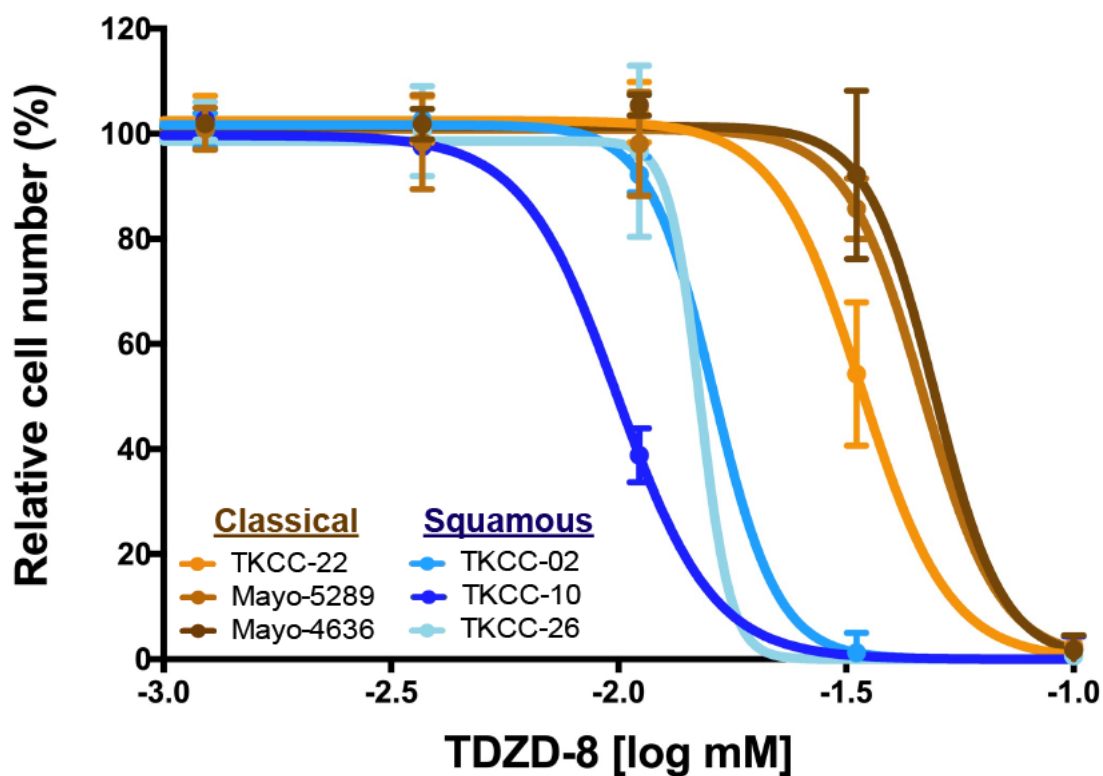


Figure 4.4 | Squamous PDCLs are selectively sensitive to ALDOA inhibition. Dose-response curve showing impact of 72 hours TDZD-8 treatment on cell viability. As can be seen, squamous PDCLs (blue) were found to be considerably more sensitive than classical (brown) PDCLs. Cell viability was determined via MTS assay, with values presented adjusted according to readings obtained from DMSO controls. Data provided by Dr Holly Brunton (unpublished) and are presented as the mean of three biological replicates, with error bars representing SD.

Despite squamous cell-lines having been previously found to display no metabolic flexibility to fuel mitochondrial respiration (Figure 3.12), it was necessary to assess whether inhibition of glycolysis was maintainable over time, with no escape mechanism to overcome sensitivity as previously described in chapter 3.4.5 and commonly seen when targeting other metabolic vulnerabilities in pancreatic cancer (Ying *et al.*, 2012; Son *et al.*, 2013; Boudreau *et al.*, 2016; Biancur *et al.*, 2017). As such resistance may arise in PDCLs upon ALDOA inhibition, glycolysis was recorded after 7 days of treatment with TDZD-8. Reduction in glycolysis was found to persist in the small population of cells still viable after a week of treatment without drug replenishment at IC₅₀ concentrations (15 µM) in TKCC-26 (Figure 4.5), thus demonstrating that inhibition of glycolysis is sustainable in squamous cell-lines.

4.1 Inhibition of fatty acid metabolism in classical subtype reveals metabolic flexibility

4.1.1 Inhibiting general oxidative phosphorylation in classical cells limits viability

As described in chapter 1.5.4 , AMPK is a key regulator of cellular metabolic stress and is activated when cellular energy is depleted (Jeon, Chandel and Hay, 2012). Upon activation, AMPK phosphorylates and inactivates key anabolic enzymes, such as acetyl-CoA carboxylases (Buzzai *et al.*, 2005), upregulates carnitine transporters (Zaugg *et al.*, 2011), and facilitates lipolysis (Gauthier *et al.*, 2008), leading to an initiation of FAO, while concurrently activating autophagy (Egan *et al.*, 2011; Kim *et al.*, 2011). Both processes allow for the recycling of a variety of cellular components and lipids, facilitating re-introduction into the TCA cycle, which in the context of cellular energetics would therefore promote OXPHOS. Within the PDCLs, it was demonstrated that phosphorylation of the functional, catalytic alpha subunit of AMPK is found to be associated PDCLs belonging to the classical subtype relative to squamous (Figure 4.6) (Holly Brunton, unpublished data). This observation,

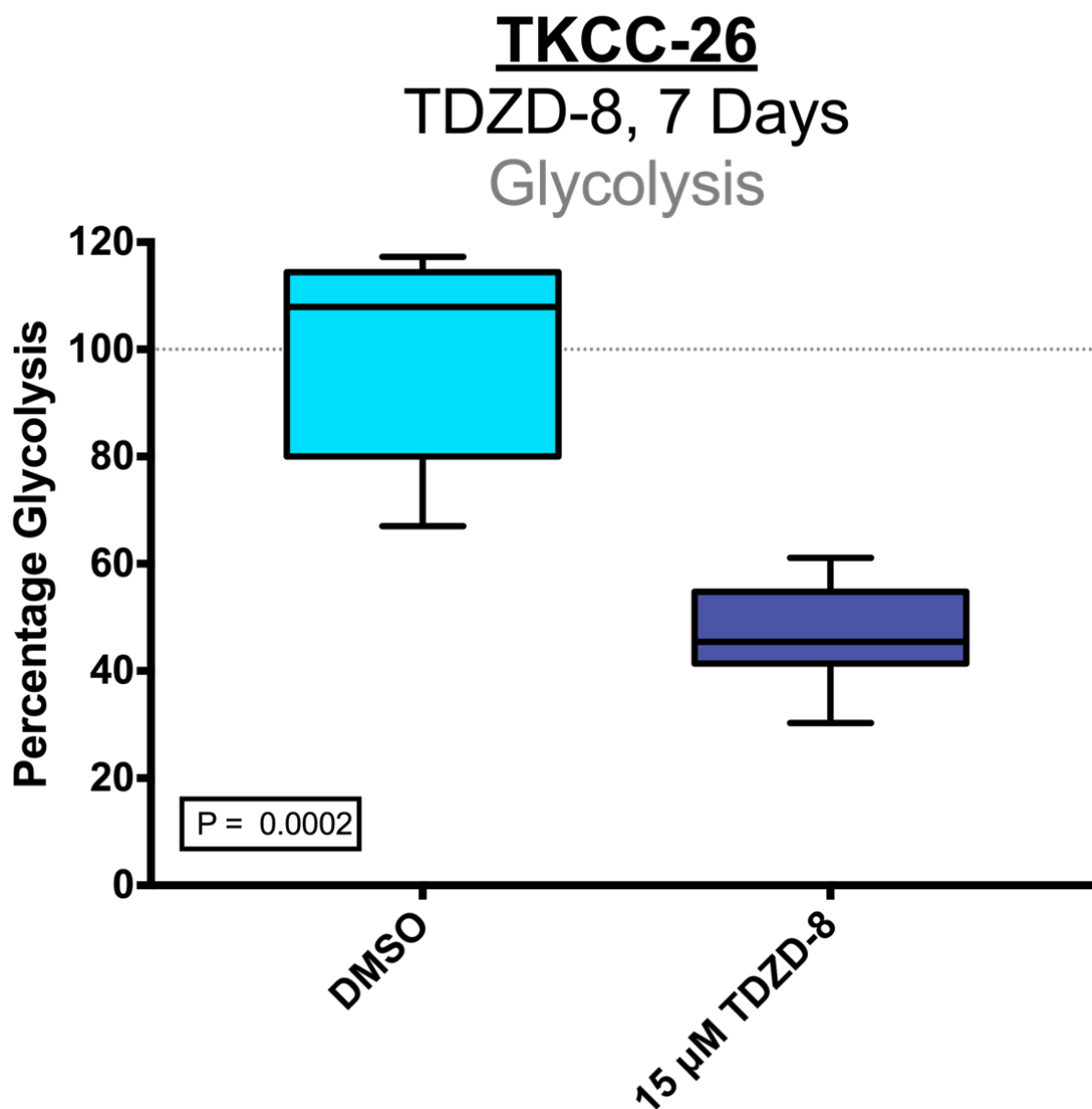


Figure 4.5| Inhibition of glycolysis by TDZD-8 is sustained at extended time-points. Box-plot showing glycolysis rates after 7 days treatment with 15 μM TDZD-8 in TKCC-26, a cell-line representative of the squamous subtype. As can be seen, rates of glycolysis are decreased on treatment with TDZD-8, relative to DMSO control. Glycolysis was recorded via glycolytic stress test, and results are shown as percentage basal glycolysis, adjusted according to cell number, as determined via glycolytic stress test. Data presented with boxes indicating 25th to 75th percentiles, with lines representing median values and whiskers showing minima and maxima, n=8.

when considered alongside the role of AMPK as an activator of FAO, may in part explain the increased rates of FAO in classical cell-lines, and points to AMPK as a potential target to suppress classical-associated metabolic pathways.

Compound C was selected to test as an inhibitor of AMPK in the PDCLs. This compound was initially identified by a high-throughput screen designed to identify AMPK inhibitors (Zhou *et al.*, 2001), which demonstrated its action as a reversible competitor of ATP capable of reversing the effects of the AMPK activator AICAR (Sun, Connors and Yang, 2007). Compound C has been widely used as an inhibitor of AMPK in cancer (Vucicevic *et al.*, 2011; Yang *et al.*, 2012; Garulli *et al.*, 2014).

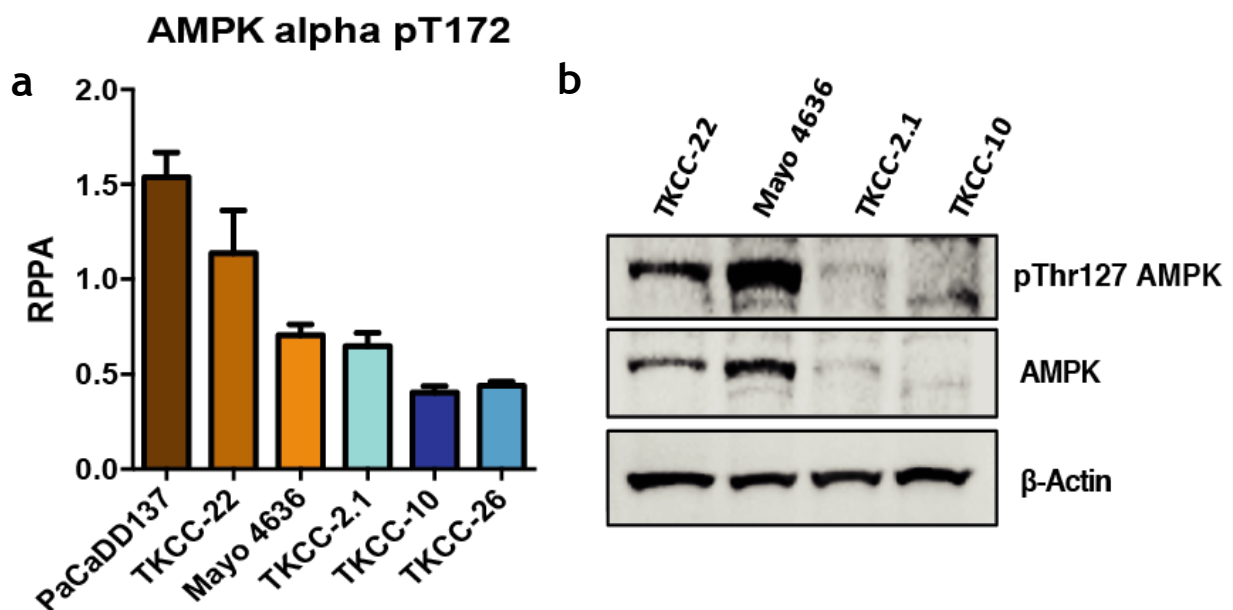


Figure 4.6 | AMPK is activated in classical PDCLs. **a** Reverse-phase protein array (RPPA) results, showing greater levels of phosphorylated AMPK α in classical cell-lines (brown), as compared to squamous (blue). **b** Results of western blot validating levels of phospho-AMPK α in PDCLs. Unphosphorylated AMPK α is also included, and levels of both active and inactive forms are seen to be higher in classical PDCLs. Data provided by Dr Holly Brunton (unpublished).

Dose-response curves demonstrated that classical PDCLs were more sensitive to treatment with compound C than squamous cell-lines (Figure 4.7) (Holly Brunton, unpublished data). Initial tests with compound C determined that rates of oxidative phosphorylation were decreased on treatment (Figure 4.8). This

observation was found only to be significant at maximal rates, under conditions of metabolic stress, which when taken into consideration alongside AMPK's role in regulating metabolic stress response as well as its inherent activation in classical PDCLs, implicates its involvement in driving the stress response, and hence OXPHOS, in classical PDCLs. This is in-line with previous research which demonstrated that compound C acts as an inhibitor of AMPK-associated respiratory capacity in cardiac myocytes (Pfleger, He and Abdellatif, 2015).

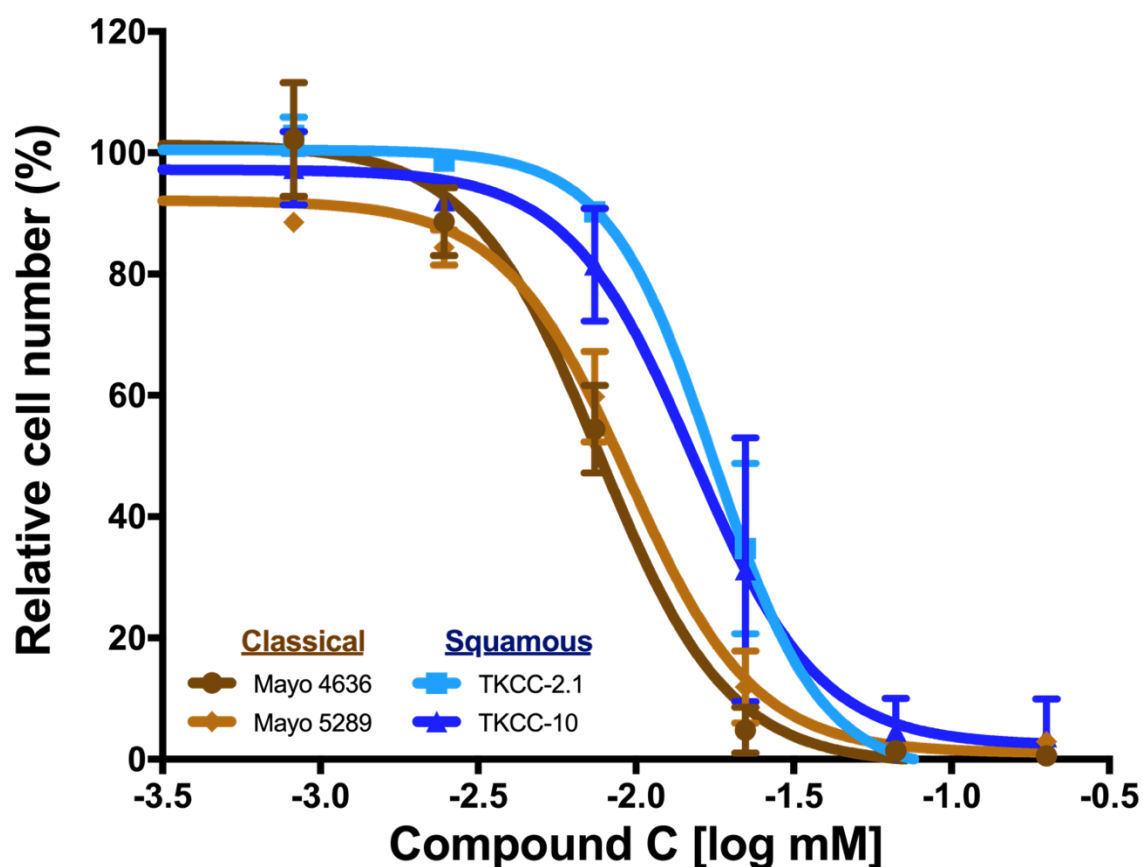


Figure 4.7| Classical cell-lines exhibit increased sensitivity to compound C. Dose-response curve showing response of PDCLs to 72 hours treatment of the AMPK inhibitor compound C. As can be seen, classical PDCLs (brown) were found to be more sensitive than squamous (blue). This result suggests that activated AMPK may be promoting the increased mitochondrial respiration associated with classical PDCLs, rendering this subtype sensitive to AMPK inhibition. Cell viability was determined via MTS assay, with values presented adjusted according to readings obtained from DMSO controls. Data provided by Dr Holly Brunton (unpublished) and are presented as the mean of three biological replicates, with error bars representing SD.

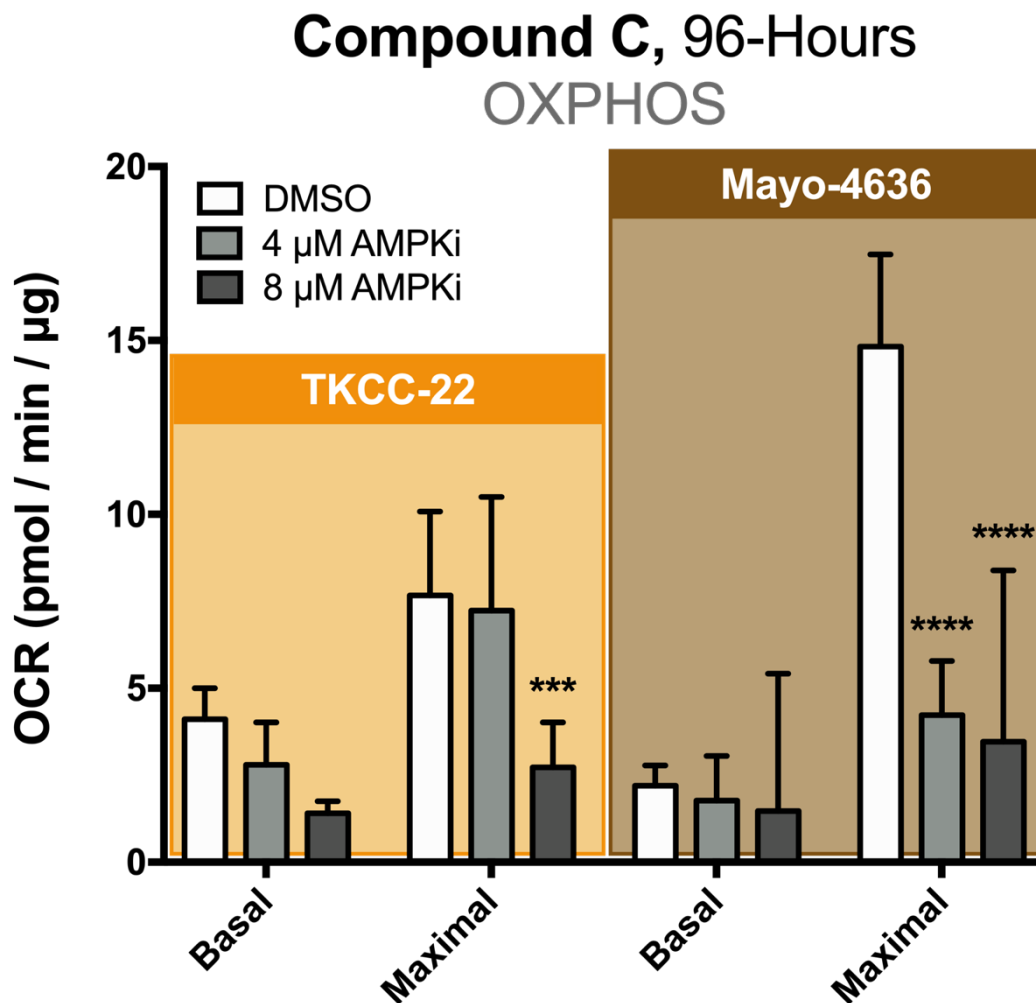


Figure 4.8 | AMPK inhibition decreases rates of stress-induced oxidative phosphorylation in classical PDCLs. Bar-plots showing rates of OXPHOS in two PDCLs representative of the classical subtype after 96 hours treatment with AMPK inhibitor compound C. As can be seen, compound C significantly reduces OXPHOS at maximal levels, which are induced by stimulators of mitochondrial stress. This highlights AMPK's role in activating metabolic stress in classical PDCLs. Both basal and maximal rates are shown. Data presented as mean, with error bars representing SD, n=8.

As metabolic flexibility was determined to be a feature associated with the classical subtype, it was necessary to ensure that alternative sources of cellular energy production were not activated in response to loss in OXPHOS observed with compound C treatment. To this end, glycolytic stress tests were performed, which found glycolytic rates to decrease upon treatment with compound C (Figure 4.9), with rates of glycolysis dropping by 54% and 46% in TKCC-22 and Mayo-5289 respectively. This result indicates that glycolysis is not activated as a response to OXPHOS suppression upon inhibition of AMPK.

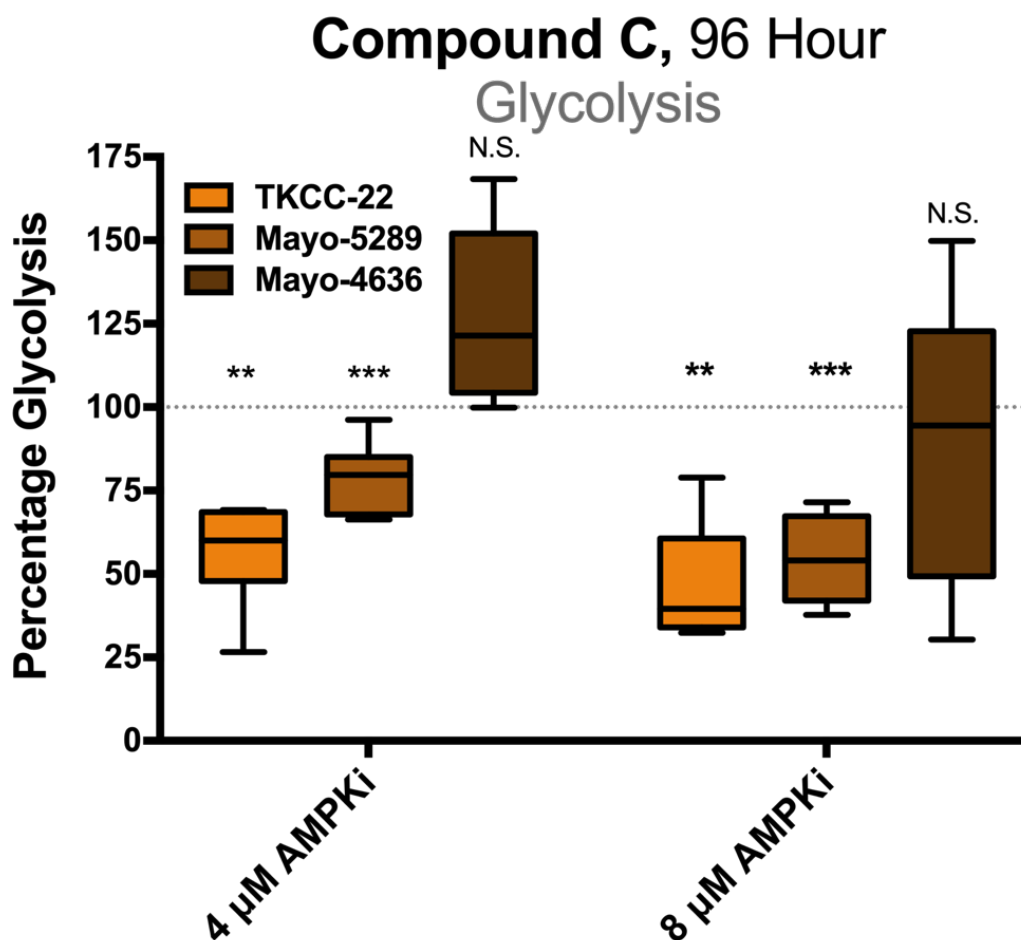


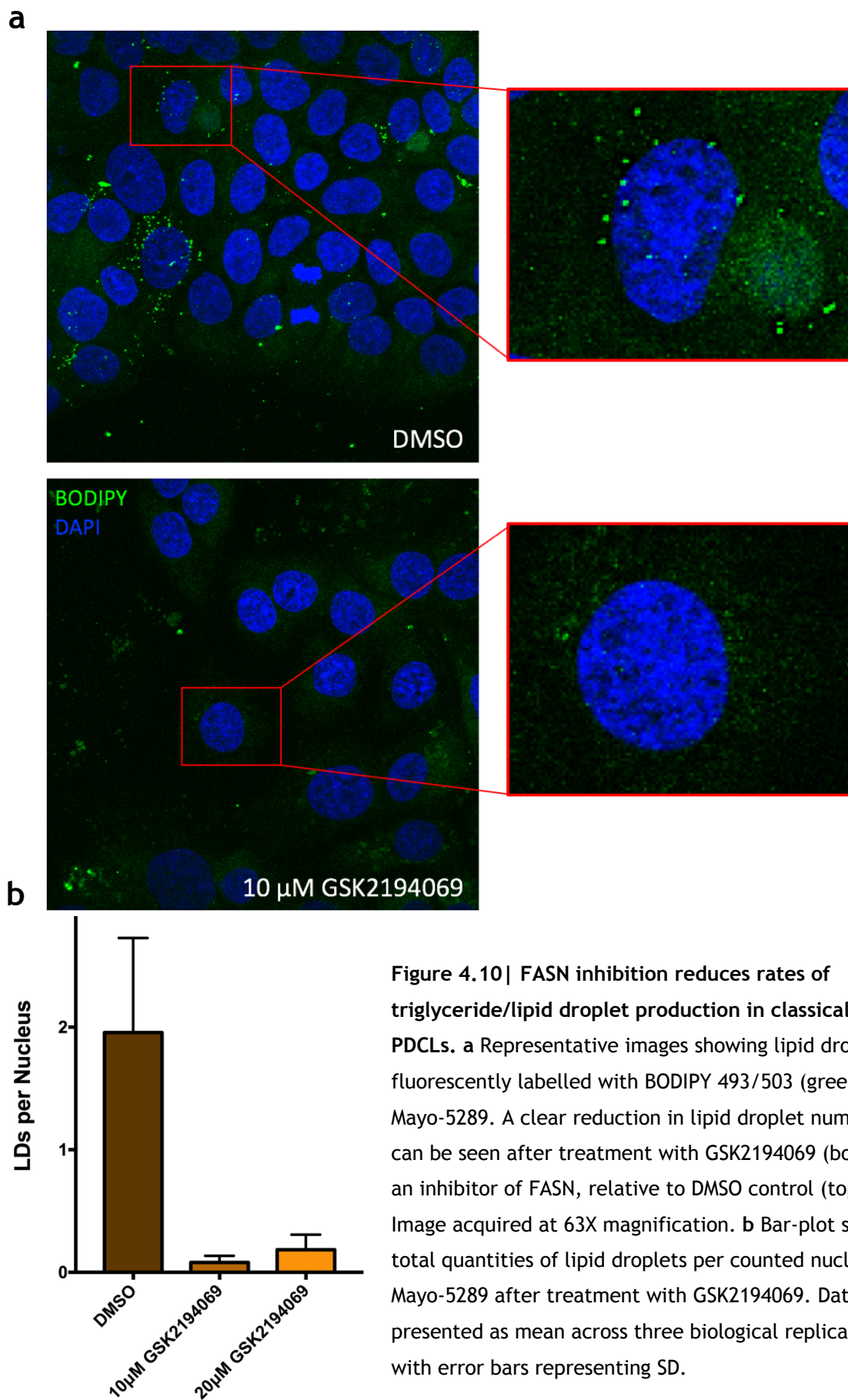
Figure 4.9 | AMPK inhibition decreases glycolysis in classical PDCLs. Box-plot showing rates of glycolysis in PDCLs representative of the classical subtype after 96 hours treatment with compound C. As can be seen, rates of glycolysis tend to decrease on treatment in a dose-dependent manner. This indicates that compensatory, glycolytic pathways are not activated upon inhibition of AMPK. Data presented with boxes indicating 25th to 75th percentiles, with lines representing median values and whiskers showing minima and maxima, n=6.

4.1.2 Inhibiting fatty acid biosynthesis in classical PDCLs induces increased glycolysis

FASN, a key enzyme in lipogenesis, has been implicated as a key driver of pathologic lipid biosynthesis in tumour cells in multiple cancer-types (Chajès *et al.*, 2006; Fiorentino *et al.*, 2008). Consequently, efforts have been made to formulate

inhibitors of FASN in the treatment of cancer (Menendez and Lupu, 2007), with GSK2194069 an example of a potent and selective inhibitor of FASN identified specifically to this end (Hardwicke *et al.*, 2014). Though FASN is involved in catalysing multiple reactions necessary in the generation of saturated FAs, GSK2194069 was found to act via inhibition of FASN's β -ketoacyl reductase activity, similar to other previously described inhibitors (Vázquez *et al.*, 2008). As an increase in genes and proteins involved in lipid biosynthesis, such as HMG-CoA reductase (HMGCR), a key enzyme in cholesterol biosynthesis, and acyl-CoA synthetase medium chain member 3 (ACSM3), a member of the acyl-CoA synthetases which regulate the balance between FA synthesis and FAO (Ellis, Bowman and Wolfgang, 2015), is associated with the classical subtype (Figure 3.3b and Figure 3.6) and previous work has indicated an increased dependence of classical PDCLs on FA biosynthesis (Daemen *et al.*, 2015), we assessed the differential efficacy of GSK2194069 between PDCL subtypes.

Firstly, it was necessary to validate that inhibition of FASN via GSK2194069 treatment induced a cessation of lipid biosynthesis. To this end, lipid droplets, which act as units of storage for the end product of lipid synthesis (TAGs), were quantified in cells treated with GSK2194069. Results showed that lipid droplet count was drastically reduced upon inhibition of FASN (Figure 4.10), suggesting that FASN is necessary for the synthesis of fatty acids required to produce TAGs, and hence lipid droplets. These results therefore justified the use of GSK2194069 as an inhibitor of lipid biosynthesis and provided evidence of on-target effects.



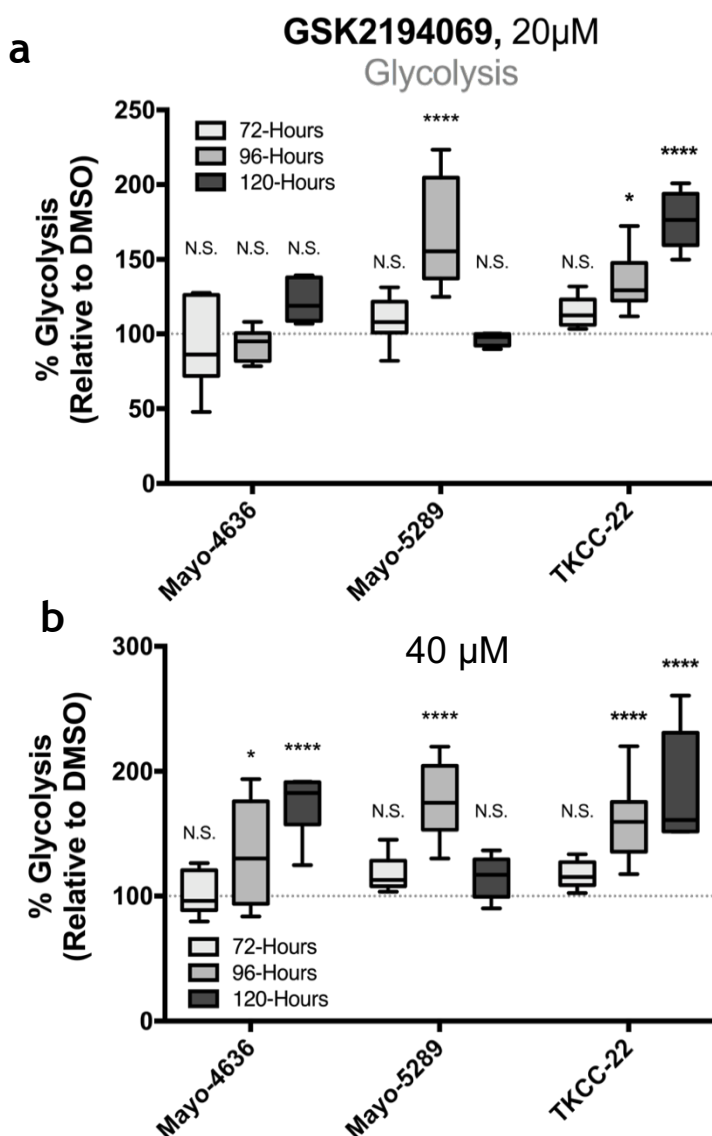


Figure 4.11 | GSK2194069-mediated FASN inhibition leads to increase in glycolysis in classical PDCLs. a Box-plot highlighting impact of 20 μ M GSK2194069 on glycolysis in classical cell-lines. As can be seen, 72-hour treatment was not sufficient to yield a significant response in any PDCL, while 96-hours elicited an increase in glycolysis in both Mayo-5289 and TKCC-22 cells. At 120-hours treatment, this response persists in TKCC-22, while it is lost in Mayo-5289. **b** Box-plot highlighting impact of 40 μ M GSK2194069 on glycolysis in classical cell-lines. As with 20 μ M, 72-hours was an insufficient time point to see a significant response, but at longer time-points, a response is seen across all PDCLs. At both concentrations, the effect on glycolysis within Mayo-5289 is alleviated at 120-hours, suggesting that this cell-line may break the drug down quicker than the others. This set of experiments revealed that the optimal treatment time/dose to yield the greatest response in glycolysis across all classical cell-lines was 40 μ M at 96-hours. Additionally, it was seen that inhibition of FASN induced a compensatory resistance mechanism in classical PDCLs. Data presented with boxes indicating 25th to 75th percentiles, with lines representing median values and whiskers showing minima and maxima, n=6.

Despite this impact on fatty acid biosynthesis, work performed by Holly Brunton showed no observable difference in impact on cell viability between subtypes upon GSK2194069 treatment. By quantifying rates in glycolysis after GSK2194069 treatment over concentrations of 20-40 μM between 72-120 hours, it was subsequently determined that FASN inhibition increased glycolysis in three PDCLs representative of the classical subtype (Figure 4.11). This finding suggests that classical cell-lines may utilise previously described metabolic flexibility as a mechanism to escape inhibition of FA biosynthesis; by targeting the stores of fatty acids required for FAO via inhibition of FASN, these cells can utilise glucose and glycolysis as an alternative source to generate required cellular energy.

4.2 Modulating metabolic flexibility in classical subtype PDAC

4.2.1 JQ1 treatment enhances subtype-associated metabolism in PDCLs

The bromodomain and extra terminal domain (BET) family of proteins coordinate gene expression through the binding of acetylated histones and recruit transcription factors and other regulators of transcription (Belkina and Denis, 2012). Due to their involvement in the regulation of genes involved in replication, including cyclin dependent kinases 6 and 9 (CDK6 and CDK9) (Dawson *et al.*, 2011), as well as the BET family protein BRD4's role in orchestrating mitotic transcription (Dey *et al.*, 2009), these epigenetic readers have presented as attractive targets in cancer research (Dawson, Kouzarides and Huntly, 2012). In order to target this family therapeutically, an inhibitor, JQ1, was designed to competitively bind to acetyl-lysine binding cavities within this family of BET proteins, thus preventing their pattern recognition and hence, function (Filippakopoulos *et al.*, 2010). JQ1 has previously demonstrated anti-cancer potential, with research showing JQ1 inhibits acinar-to-ductal metaplasia, which is an initial step in PDAC transformation, in explants from *KRAS* mutant mice (Mazur *et al.*, 2015), while it has also been proposed as one of very few therapeutic approaches available to

target c-Myc (Delmore *et al.*, 2011; Chen, Liu and Qing, 2018). Due to the role of c-Myc in metabolic reprogramming of pancreatic cancer discussed in chapter 1.5.6 JQ1's inhibition of c-Myc informs its potential as a modulator of metabolism, with previous research efforts demonstrating its ability to reverse c-Myc associated glycolysis in patient-derived xenograft models of pancreatic cancer (Sancho *et al.*, 2015). In addition to this, BRD4 has been shown to act as an inhibitor of autophagy, described in chapter 1.5.5, with JQ1 disrupting this function and facilitating the AMPK-mediated stress response (Sakamaki *et al.*, 2017), while JQ1 has also been shown to act more generally to inhibit mitochondrial activity, leading to a deficit in ATP production and activation of mitochondrial stress response via AMPK in leukemia and breast cancer cell-lines (Wang *et al.*, 2015). Beyond this, JQ1 mediated inhibition of BET-family proteins has also been shown to abrogate the transcription of a variety of genes associated with stroma-driven metabolism in pancreatic cancer cells, such as HMG-CoA reductase (HMGCR), a key driver of cholesterol biosynthesis, and glycine decarboxylase (GLDC) (Sherman *et al.*, 2017). This collection of findings highlights the diverse effects JQ1 has been demonstrated to mediate on cancer cell metabolism, and as these metabolic pathways align with those found to be associated with PDAC subtypes *in vitro*, encompassing aerobic glycolysis and AMPK stress-response, it was decided to investigate effects of JQ1 on metabolism within PDCLs.

Initial experiments were performed utilising the glycolytic stress test upon treatment of cells with JQ1, in order to assess the impact of BET inhibition on glycolytic profiles. Analysis revealed that JQ1 exposure enhanced the glycolytic characteristics indicative of subtype, with rates of glycolysis decreasing in classical PDCLs and increasing in squamous (Figure 4.12). These observed phenomena were particularly noticeable when considering basal rates of glycolysis in the classical subtype (Figure 4.12a), which when considered alongside current literature pointing to JQ1 as an activator of cellular stress response, suggests that JQ1 may promote AMPK activation in classical PDCLs, leading to a decrease in glycolysis and enhanced dependence on OXPHOS. This possibility is supported by the observation that phosphorylation of AMPK, as determined via western blotting, was selectively

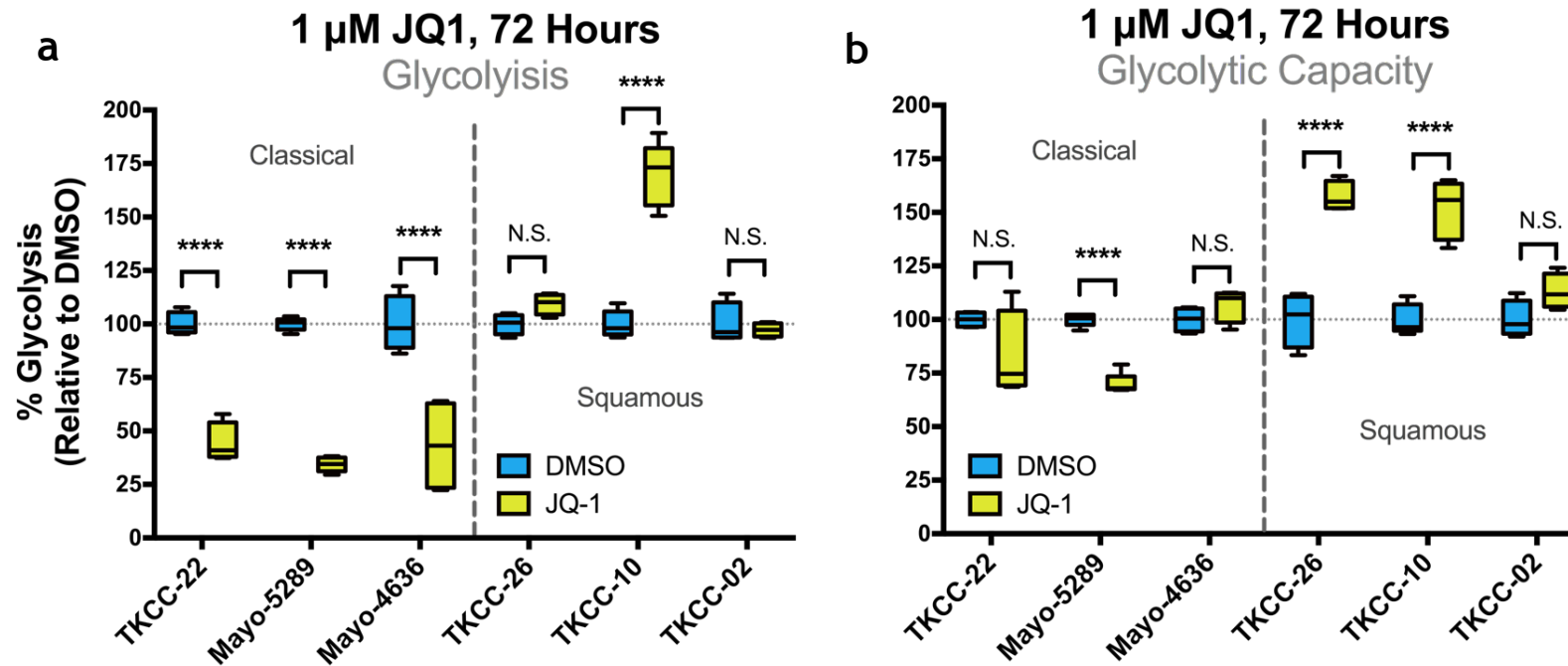


Figure 4.12 | JQ1 treatment differentially affects glycolysis across subtypes. **a** Box-plot highlighting changes in rates of basal glycolysis induced by treatment with JQ1. As can be seen, glycolysis is universally, significantly decreased across all classical PDCLs after 3 days exposure, while squamous cell-lines are largely unaffected. **b** Box-plot showing changes in maximal rates of glycolysis, with conditions as in **a**. Squamous cell-lines tend to exhibit an increase in glycolysis, in contrast to classical PDCLs. Taken together, these findings suggest that JQ1 drives cells towards a more extreme metabolic phenotype, reinforcing those traits in metabolism associated with subtype. Data presented with boxes indicating 25th to 75th percentiles, with lines representing median values and whiskers showing minima and maxima, n=4.

increased in classical PDCLs upon exposure to JQ1 (Figure 4.13). Western blotting in this instance showed inconsistencies with previous results, which indicated that Mayo-4636 has higher levels of phospho-AMPK than squamous PDCLs (Figure 4.6b). This may be due to passaging of Mayo-4636, a PDCL that has been demonstrated to incrementally shift from classical to squamous temporally, as determined via presence of HNF markers of the classical subtype (data not shown). As a higher passage of Mayo-4636 were used to generate Figure 4.13a, this PDCL may be more of an intermediate subtype than pure classical.

As additional evidence, JQ1 increased rates of exogenous FAO in a cell-line representative of the classical subtype (Figure 4.14). However, maximal rates of glycolysis are less impacted by JQ1 in classical PDCLs (Figure 4.12b), suggesting that BET inhibition does not reduce the metabolic flexibility associated with this subtype (Figure 3.12). In squamous PDCLs, the reverse is seen, with rates of glycolysis increased after treatment with JQ1 (Figure 4.12), which may demonstrate an inability to modulate a stress response via AMPK in this subtype (Figure 4.6).

4.2.2 JQ1's effect on metabolism is mediated by increased lipogenesis and associated stress response

As discussed in chapter 4.2.1 JQ1 acts as an inhibitor of BET proteins, which orchestrate transcriptional regulation via recruitment of transcription factors. Due to this role, it was decided to quantify the broad effect of JQ1 treatment on transcription in order to ascertain the mechanism by which BET inhibition mediates its effect on metabolism. To this end, RNA-seq was performed, with thanks, by Giuseppina Caligiuri and Peter Bailey on PDCLs representative of the subtypes after exposure to JQ1. Analysis of RNA-seq results revealed the upregulation of a number of genes whose protein products are involved in lipogenesis (Figure 4.15), including the acetyl-CoA carboxylases, described in chapter 1.5.2, lipins 1 and 2 (LPIN1/2), which catalyse one of the final steps in TAG synthesis. This upregulation of genes was particularly pronounced within the PDCL classified as classical. This was found to translate to a corresponding increase of protein abundances within

two of these gene targets that are integral to lipogenesis: FASN, described in chapters 1.5.2 and 4.1.2 , and ATP citrate lyase (ACLY), described briefly in 1.5.2 and a mediator of the initial step of lipid and FA biosynthesis, the degradation of cytosolic citrate (Figure 4.16).

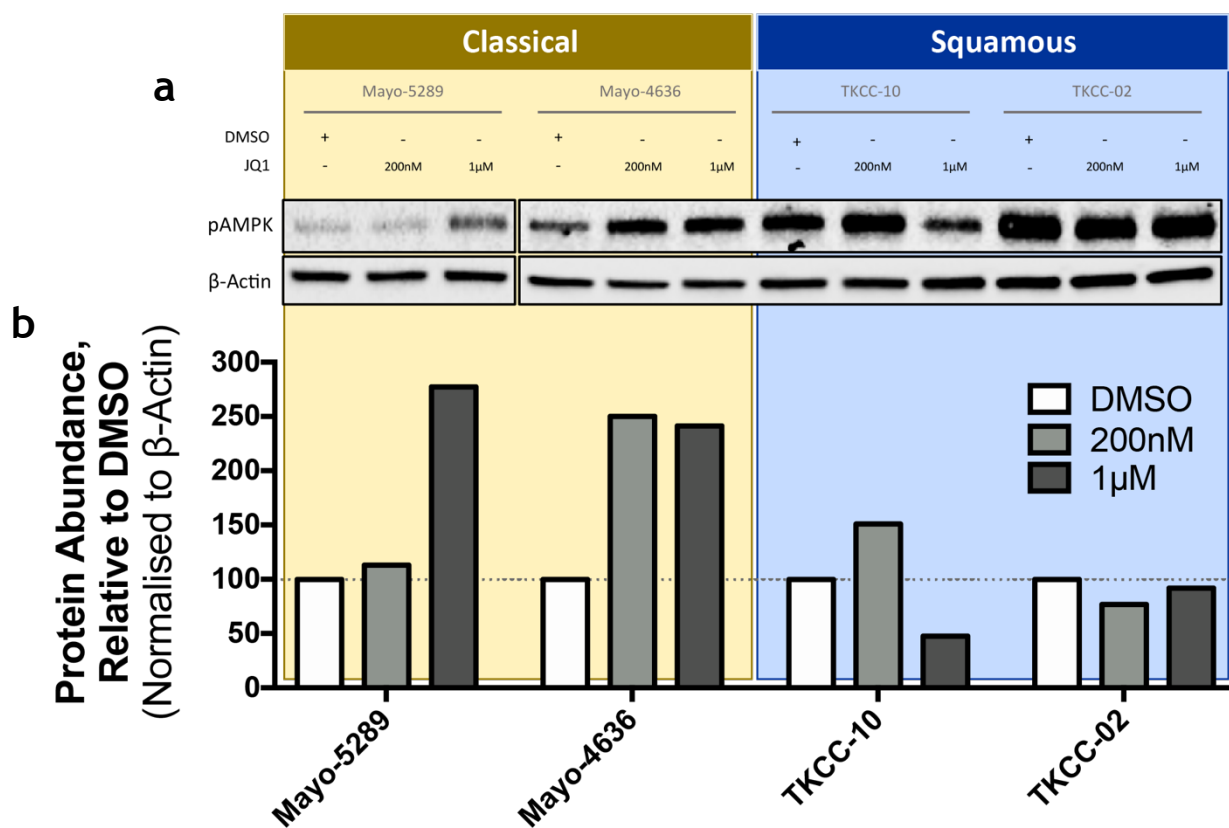


Figure 4.13 | JQ1 selectively activates mitochondrial stress in classical PDCLs. a Western blot showing levels of phospho-AMPK in PDCLs classed as classical (left, brown) as compared to squamous (right, blue). Mayo-5289 were run separately to the other PDCLs due to limitations in well number per gel. b Quantification of western blots shown in (a), normalised to DMSO control.

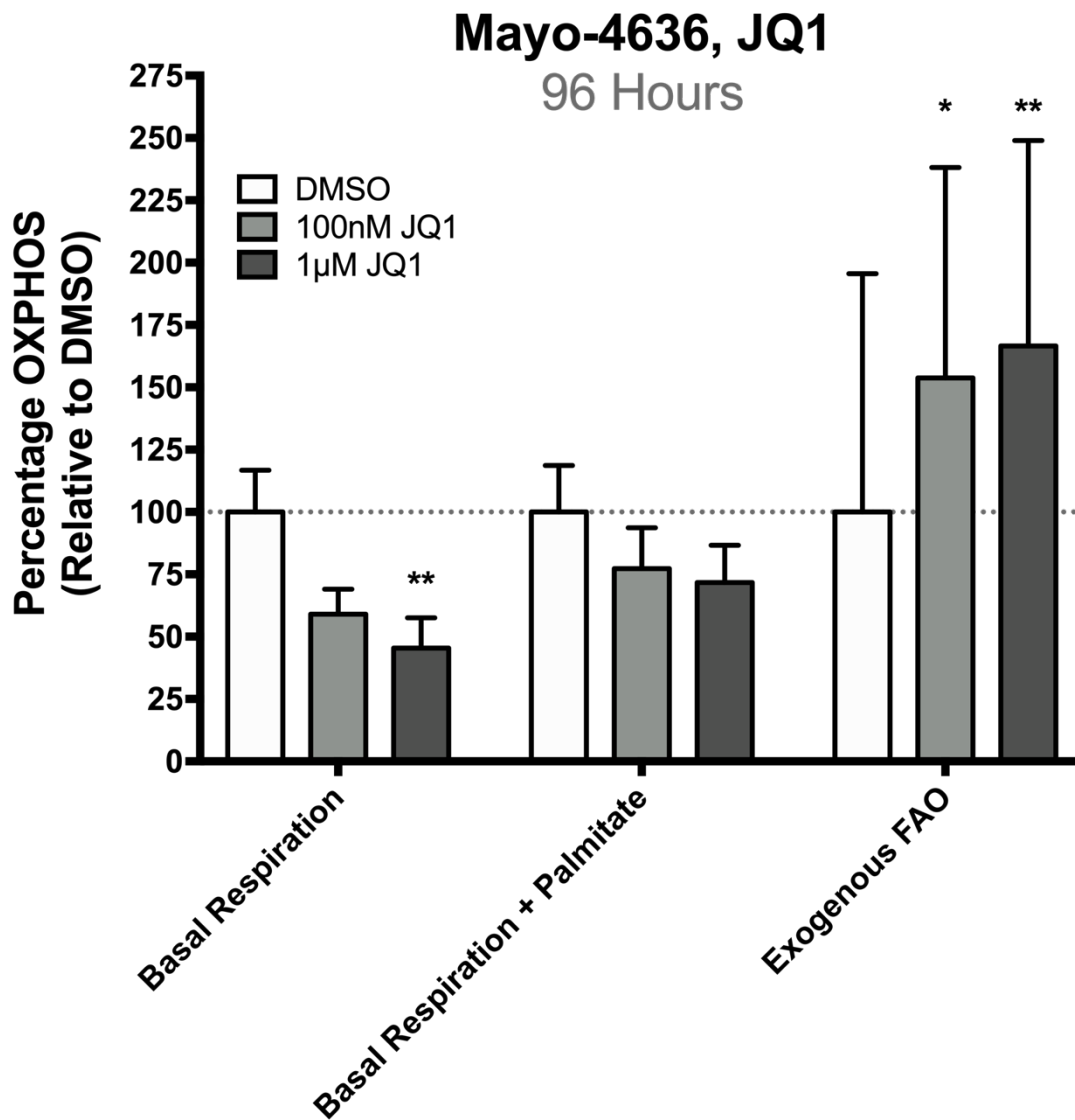


Figure 4.14 | JQ1 reduces overall levels of mitochondrial respiration in classical PDCL, while increasing FAO rates. Bar-plots showing levels of oxidative phosphorylation, as determined via mitochondrial stress-test, in Mayo-4636, a classical PDCL, upon JQ1 treatment. As can be seen, basal levels of respiration decrease on JQ1 treatment, with 1 μM sufficient to induce a significant response. This observation is abrogated upon addition of palmitate, an exogenous fatty acid, which is reflected by the significant increase in FAO observed after JQ1 treatment. These results suggest that FAO may be upregulated as a response to the observed decrease of overall mitochondrial respiration induced by JQ1 treatment. Data presented as mean, with error bars representing SD, n=8.

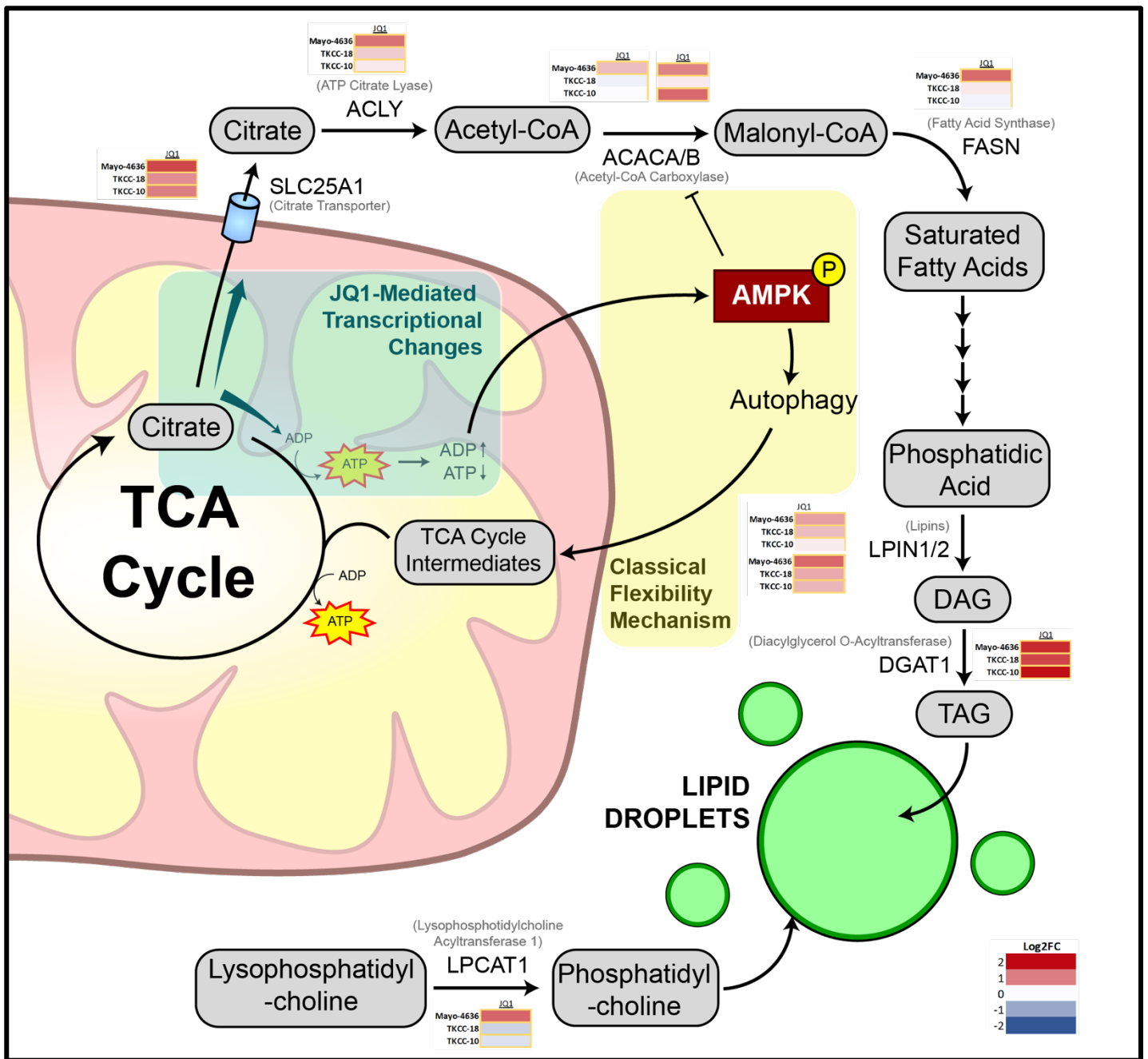


Figure 4.15 | JQ1 treatment increases transcription of genes involved in lipogenesis. Schematic showing lipogenesis pathway. Log fold-change of genes involved in the pathway, as determined via RNA-seq, is shown alongside the position of their respective protein products, with significant results highlighted by golden borders. As can be seen, JQ1 induces an upregulation of expression across a range of genes whose protein products contribute to lipid biosynthesis. This observation is particularly true within the more classical PDCL (Mayo-4636) relative to the more squamous (TKCC-10). These transcriptional changes are hypothesised to increase shuttling of citrate from mitochondria to fuel anabolism, resulting in a decrease in ATP generated via OXPHOS (blue-shaded rectangle). In classical cells, this is likely to activate the stress-response regulator, AMPK, allowing for an increase in compensatory metabolic pathways, including autophagy, which allows for recycling of metabolites through the TCA cycle (Guo *et al.*, 2016).

In order to verify that this dysregulation and downstream modulation of protein levels affected changes on a functional level, rates of lipid biosynthesis were inferred via staining and quantification of lipid droplets, an organelle whose production is associated with late-stage lipogenesis (Figure 4.15), by BODIPY 493/503 upon treatment with JQ1. This revealed an increase in lipid droplets in two PDCLs representative of the classical subtype (Mayo-5289 and Mayo-4636) and a squamous cell-line (TKCC-10) (Figure 4.17a). As it has previously been observed that induction of apoptosis often leads to an increase in lipid droplet abundance *in vitro* (Boren and Brindle, 2012), it was necessary to assess whether lipid droplet production associated with JQ1 treatment was due to increased lipogenesis resulting from transcriptional regulation, or apoptosis as a result of JQ1 exposure. Immunofluorescence of two markers of apoptosis, cleaved PARP and cleaved Caspase-3, indicated that apoptosis was not directly initiated by JQ1 treatment, with no significant induction of apoptosis observed in PDCLs representative of either classical or squamous subtypes (Figure 4.17b-c).

Collectively, these results show that JQ1 treatment leads to an upregulation of genes involved in lipogenesis, resulting in increased FA biosynthesis and generation of stores of lipid droplets. While the observation of increased LD count on exposure to JQ1 is consistent with previous research (Zirath *et al.*, 2013; Wang *et al.*, 2015), this has been proposed to be a result of FA uptake to offset mitochondrial dysfunction rather than biosynthesis. This hypothesis makes sense in light of the AMPK activation associated with JQ1 treatment (Sakamaki *et al.*, 2017), which would be expected to inhibit anabolic process such as lipogenesis (Hardie and Pan, 2002), and is corroborated by the finding that KD of c-Myc, which is a target of JQ1, leads to downregulation of genes central lipogenesis, including FASN, ACLY and ACACA, each described in chapter 1.5.2, in fibroblasts, alongside a concurrent increase in LD quantity (Edmunds *et al.*, 2014). The observation that these genes involved in lipid biosynthesis are upregulated in PDCLs after JQ1 treatment therefore represents a potentially novel mechanism by which lipogenesis is maintained in spite of the upregulated stress response, with increased FAO allowing for a recycling of cellular energy committed to lipid biosynthesis.

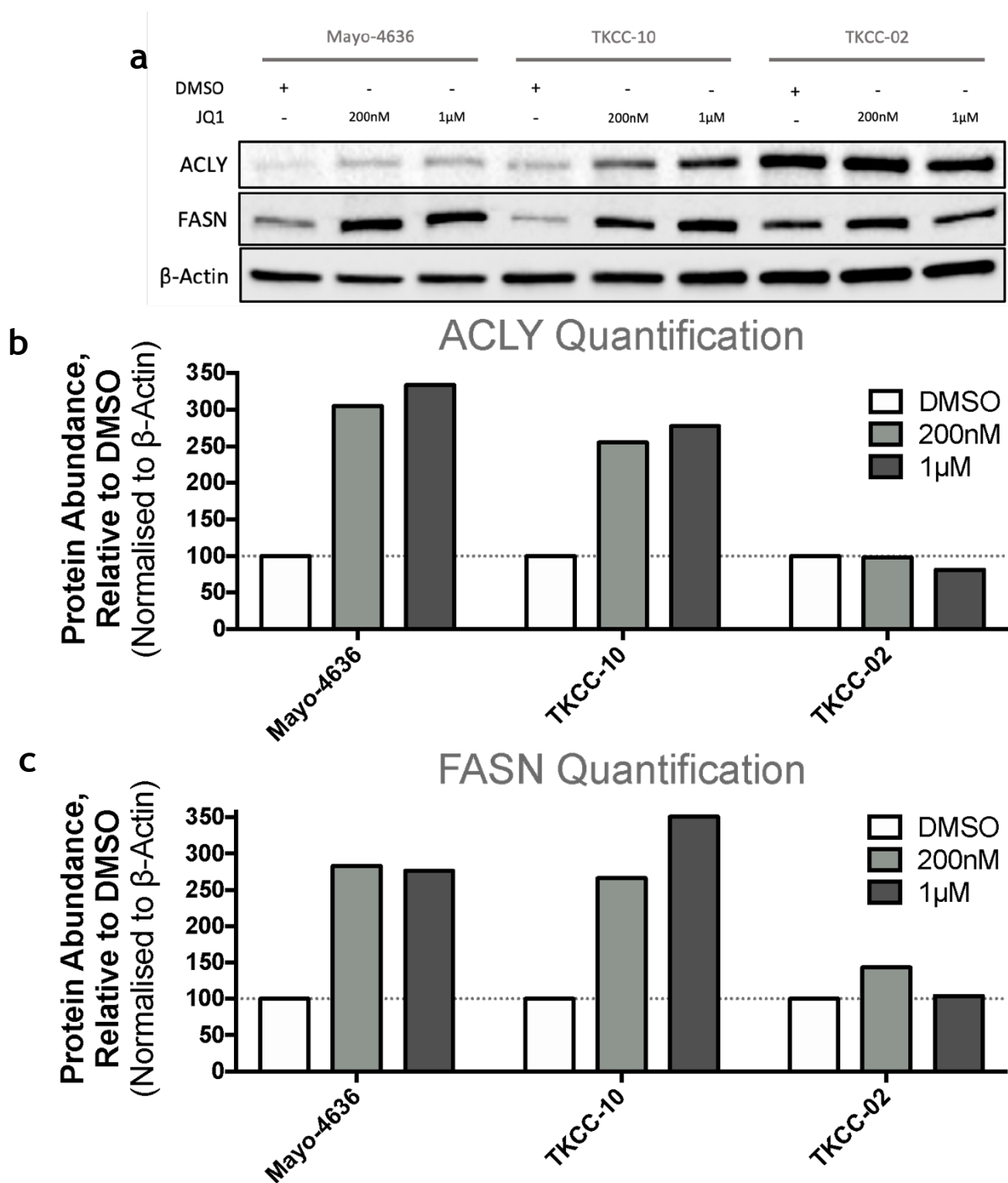


Figure 4.16 | JQ1 treatment leads to increased levels of proteins involved in lipogenesis. **a** Western blot showing levels of ACLY and FASN, two enzymes necessary for lipid biosynthesis. Upon treating PDCLs with JQ1 for 96 hours. Subsequent quantification of the bands corresponding to ACLY (**b**) and FASN (**c**) highlighted their upregulation upon treatment with JQ1. As both proteins are involved in the process of FAS, it is expected that JQ1 acts as a promotor of FA biosynthesis.

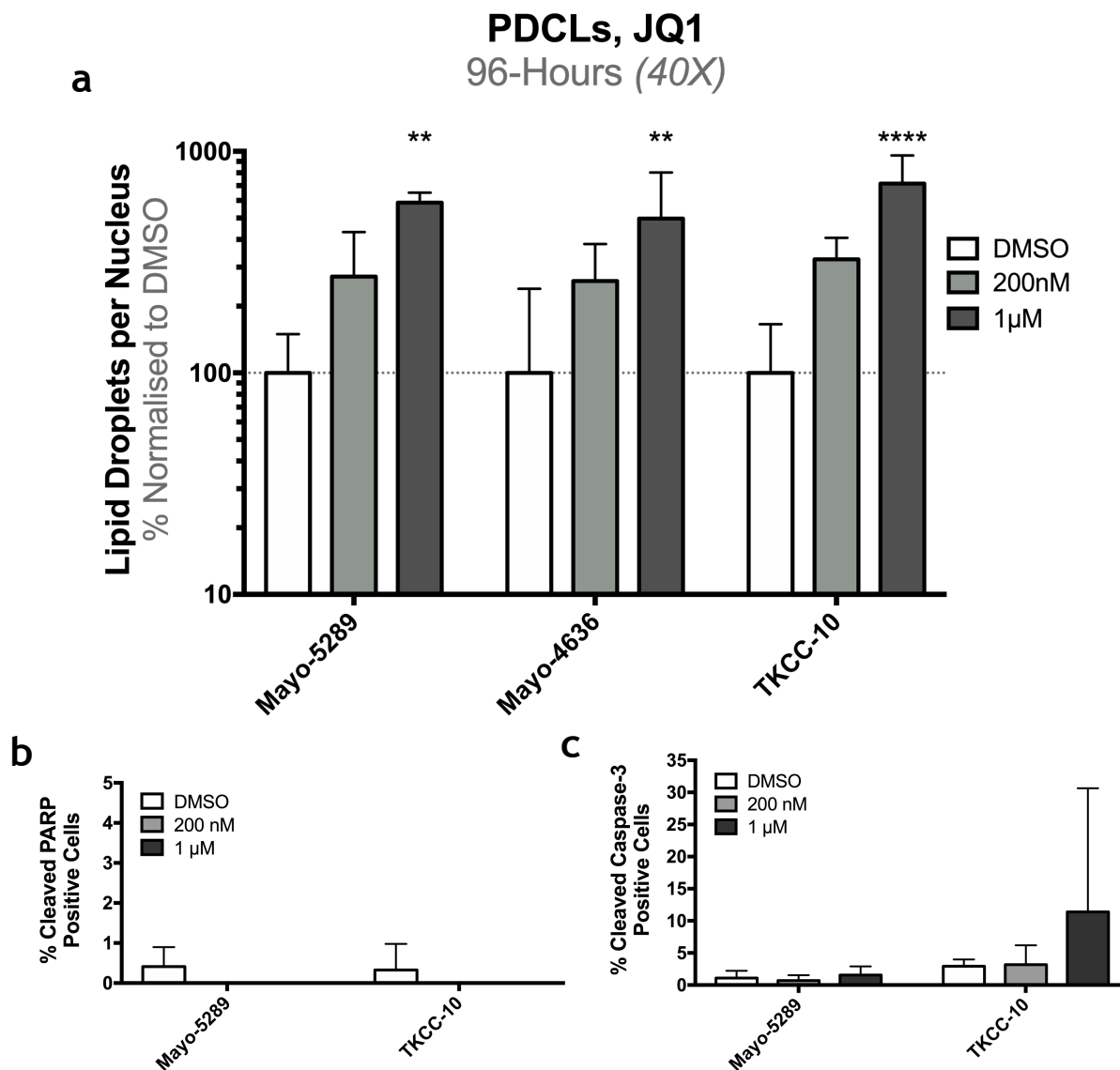


Figure 4.17 | JQ1 increases rates of lipid biosynthesis across both PDCL subtypes. **a** Bar-plot displaying the ratio of lipid droplets to nuclei across a selection of PDCLs representing both subtypes after 4 days treatment with JQ1, with DMSO representing a vehicle control. Results are shown as percentage relative to DMSO control, displayed on a log scale. As can be seen, increases lipid droplet production is associated with JQ1 treatment in a dose-dependent manner. **b** Bar-plot showing the percentage of cells determined to be positive for cleaved PARP via immunofluorescence upon JQ1 treatment. As can be seen, no increase in cleaved PARP was observed in either PDCL. **c** Bar-plot showing percentage cells positive for cleaved Caspase-3, as in (b). A slight increase in cleaved Caspase-3 was observed in TKCC-10 (squamous) at high concentrations of JQ1, however, this result was not found to be significant. This shows no significant correlation between apoptosis and lipid droplet formation. All data presented as mean across three biological replicates, with error bars representing SD.

4.2.3 JQ1 treatment enhances sensitivity to inhibitors of lipogenesis, highlighting potential as a combination treatment

As JQ1 acts to enhance both FAO and lipid biosynthesis in classical PDCLs, it was decided to assess the efficacy of combining JQ1 with the FA synthesis inhibitor, GSK2194069. By adding JQ1, it was possible to limit the increase in rates of glycolysis previously observed with FASN inhibition via GSK2194069 in classical PDCLs (Figure 4.11), with JQ1 exposure negating any observable increase in glycolysis (Figure 4.18a). This effect is thought to be due to the ability of JQ1 to activate the metabolic stress responder, AMPK, along with the associated downregulation of aerobic glycolysis (Faubert *et al.*, 2013) and upregulation of FAO (Hardie and Pan, 2002). Additionally, as JQ1 has been found to suppresses overall mitochondrial respiration (Zirath *et al.*, 2013), which in PDCLs results in an increased dependence on FAO (Figure 4.14), concurrent inhibition of FASN likely decreases the store of FAs available to fuel FAO. As such, this combination therapy is associated with decreased cell viability in classical PDCLs (Figure 4.18b) (Holly Brunton, unpublished data).

4.1 Discussion

By selecting potential targets within the metabolic pathways found to be functionally upregulated within the subtypes of PDAC, an inhibitor of squamous-associated glycolysis, TDZD-8, was identified with potential to induce selective sensitivity in PDCLs classed as squamous. These results therefore validated findings that demonstrated the role of ALDOA as an activator of glycolysis in pancreatic cancer cells (Grandjean, de Jong, B. James, *et al.*, 2016) and siRNA screening conducted within PDCLs (Figure 4.1), confirming ALDOA as a target for squamous-associated glycolysis. These findings also build on work that have demonstrated the efficacy of therapeutic interventions that target glycolysis in pancreatic cancer, such as LDH inhibition in pancreatic cancer cells cultured under hypoxia, and thus under conditions of induced anaerobic glycolysis (Le *et al.*, 2010; Maftouh

et al., 2014). It also supports observations that pancreatic cells exhibit differential sensitivities to LDH inhibition, with resistance dependent on AMPK-mediated activation of OXPHOS (Boudreau *et al.*, 2016) and wild-type TP53 (Rajeshkumar *et al.*, 2015), which is of relevance as the sensitive squamous subtype is associated with mutant TP53 in patients (Bailey *et al.*, 2016), although there is no significant association between subtype and TP53 mutation status in PDCLs.

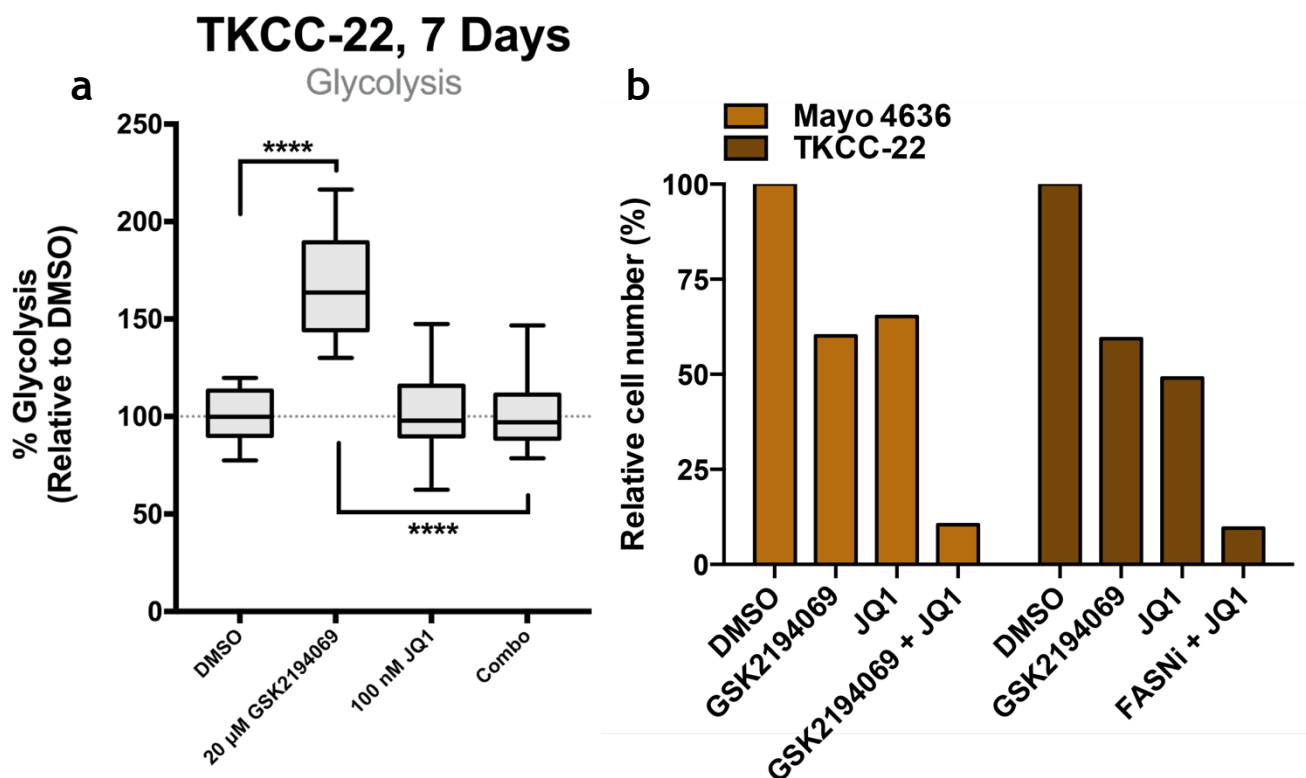


Figure 4.18 | JQ1 treatment suppresses induced metabolic plasticity in classical PDCL and increases sensitivity to FASN inhibition. a Box-plot showing basal rates of glycolysis in TKCC-22 after 7 days treatment with JQ1 and GSK2194069. As can be seen, in the absence of JQ1, FASN inhibition leads to increased glycolysis. This is suppressed upon addition of JQ1. Data presented with boxes indicating 25th to 75th percentiles, with lines representing median values and whiskers showing minima and maxima, n=8. b Bar-plot showing synergistic effects of GSK2194069 and JQ1 on cell viability, as determined via MTS, in PDCLs representative of the classical subtype at 30 μ M and 1 μ M respectively. Data for (b) provided by Dr Holly Brunton (unpublished).

One issue that would need to be addressed in future experiments involving TDZD-8 as a selective inhibitor of ALDOA is its lack of specificity: although TDZD-8 has been shown to potently inhibit ALDOA, it was initially described as an inhibitor of glycogen synthase kinase 3- β (GSK3 β) (Martinez *et al.*, 2002), which phosphorylates and inactivates glycogen synthase. GSK3 β is a known inhibitor of glucose homeostasis (Cline *et al.*, 2002; Patel *et al.*, 2008) and has been proposed as a therapeutic target in PC (Garcea *et al.*, 2007). For these reasons, it cannot be concluded with certainty from this work whether the anti-cancer and anti-glycolytic effects mediated by TDZD-8 in PDCLs are dependent on ALDOA or GSK3 β inhibition, with the possibility of both targets contributing to loss in viability observed on treatment. In order to validate which therapeutic target of TDZD-8 mediates its anti-glycolytic effects in squamous PDCLs, additional assays would be required. This could involve knock-down experiments, assessing the effects of KD of both targets on cell viability and glycolysis in comparison to TDZD-8 exposure; unfortunately, due to time constraints, this was not possible to complete as part of this project.

However, the same approach was met with less success when attempting to inhibit FAO in the pure classical progenitor subtype, with the targeting of stores of FAs via inhibition of FASN insufficient to induce a similar subtype-selective sensitivity. It was thought that metabolic flexibility inherent to this subtype (Figure 3.12) may have contributed to this observed resistance, a hypothesis supported by the observation that oncogenic KRAS can facilitate metabolic reprogramming conferring resistance to inhibition of FA synthesis *in vitro* (Kamphorst *et al.*, 2013), as well as the sensitivity of pure classical progenitor PDCLs to inhibition of AMPK, a regulator of metabolic flexibility in many cell-types (Faubert *et al.*, 2015). Concurrent treatment with the metabolic modulator JQ1 allowed for a mitigation of this sensitivity. It's thought that JQ1 treatment enhances sensitivity to FASN inhibition via an upregulation of lipogenesis, which is offset by a simultaneous increase in FAO as cells recycle energy committed to anabolic processes via the degradation of newly synthesised FA. By targeting FASN therapeutically, it is possible to prevent lipid biosynthesis proceeding to generation of long-chain FAs such as palmitate (Ventura *et al.*, 2015), which are shuttled into the mitochondria

to fuel FAO (Qu *et al.*, 2016). As such, a combination of JQ1 and FASN inhibition may result in a build-up of intermediate metabolites, such as cytosolic acetyl-CoA and malonyl-CoA, acting as an energy sink that cells are unable to efficiently recycle. Excess malonyl-CoA synthesised in this fashion would additionally serve to further promote lipogenic processes and inhibit FAO (Abu-Elheiga *et al.*, 2001), thus exacerbating limitations in available energy. Further work may be performed to confirm this hypothesis; for example, experiments assessing histone acetylation after JQ1 treatment could be implemented to infer levels of cytoplasmic acetyl-CoA generated via ACLY, as the two have been found to be correlated (Wellen *et al.*, 2009; Lee *et al.*, 2014).

As is the case with TDZD-8 as an inhibitor of ALDOA, lack of specificity may affect the validity of some findings described within this chapter. Previous work has found compound C, like many general purpose kinase inhibitors, to be lacking in specificity (Bain *et al.*, 2007), with an independent screen identifying a structurally identical compound they named Dorsomorphin, as an inhibitor of bone morphogenetic protein signalling (Yu *et al.*, 2008). Due to this lack of specificity, compound C's impact in inhibiting stress induced OXPHOS cannot be entirely ascribed with certainty to inhibition of AMPK. In order to further validate this, future work could include either AMPK knock-down or the testing of a second inhibitor, with one candidate being SBI-0206965. This compound was initially discovered as an inhibitor of ULK1 (Egan *et al.*, 2015), but was subsequently found to have selective inhibitory activity against both AMPK and ULK1 (Dite *et al.*, 2018). However, this would not serve to completely address the issue of specificity, as this compound does target ULK1.

Chapter 5 *High-Throughput Drug
Screening Reveals potential of
Statins in PC Treatment*

5.1 Introduction

De novo drug development is an intensive scientific procedure, requiring significant commitments of money, time and expertise to yield a product that can be considered for clinical use. Due to the restrictive nature of this kind of approach, there have been many studies in recent years aimed at assessing the efficacy of previously designed and publicly available compounds in a range of different cancer types via drug repurposing (Pollak, 2014; Würth *et al.*, 2016). One example of such being the discovery that disulfiram, a therapeutic primarily and historically used to treat alcoholism (Chick *et al.*, 1992), is effective in selectively inducing cell death in glioma cell-lines resistant to other lines of chemotherapeutics, identified via a drug repurposing screen (Triscott *et al.*, 2012). This finding has been expanded on by multiple preclinical research projects (Liu *et al.*, 2012; Lun *et al.*, 2016), with phase II clinical trials initiated to test its efficacy in glioblastoma patients (Huang *et al.*, 2018, 2019).

Concurrent with work outlined in the previous chapter that sought to identify inhibitors of subtype-associated pathways, a high-throughput drug repurposing screen was conducted with selected PDCLs in collaboration with the Beatson Screening Facility. Cell viability was used as primary output from this project, though cell morphology data were also collected. This is of relevance as previous work has described the value in screening the impact of compounds on various adverse effects on cells beyond toxicity (Martin *et al.*, 2014). However, analysis of morphology data is planned for the future and will be outwith the scope of this PhD project.

Analysis of cell viability data resultant from drug repurposing screening determined that the statin family of therapeutics, originally designed to reduce cholesterol levels in patients, effectively reduced viability selectively in squamous PDCLs. This finding was in accordance with other preclinical research efforts that indicate that statins may exhibit anti-cancer potential. Efforts were then concentrated on elucidating the mechanism by which statin sensitivity was

mediated differentially between subtypes. This was performed with the end goal of identifying strategies allowing for enhancement of statin treatment by either overcoming mechanisms of resistance in classical PDCLs or synergising with mechanisms of sensitivity in squamous PDCLs.

5.2 Identifying candidate metabolic targets via high-throughput screening

High-throughput screening within the Beatson Screening Facility was performed in a 384-well format, with cells seeded and drugs added 24 hours after seeding. 72 hours after treating, cells were stained with DAPI and whole-cell stain and read on the Operetta (Figure 5.1a), with screening conducted to allow for two runs per week (Figure 5.1b). Screening in the Beatson Screening Facility consisted of a single round of primary screening involving multiple drug concentrations.

5.2.1 Optimising PDCLs for High-Throughput Screening

5.2.1.1 Selecting PDCLs for screening

PDCLs were selected to best represent the diversity of a variety of features found across cell-lines (Table 5.1). This led to the inclusion of a range of PDCLs that can be characterised according to subtype as classical or squamous, with some PDCLs included representative of a less well defined, borderline phenotype. Additional subtyping metrics were assessed allowing for cell-lines to be considered in terms of structural variant features (Waddell, Pajic, A.-M. Patch, *et al.*, 2015) and DNA-damage response elements (Alexandrov *et al.*, 2013), providing a quantification of nuclear stability. Metabolic profile was also considered, with a mixture of PDCLs displaying active glycolysis and oxidative phosphorylation, as described throughout chapter 3.4, included in screening, though this expectedly correlated closely with the subtype grouping.

Table 5.1 | Selecting PDCLs for inclusion in screening project. Table showing characterization of PDCLs included in high-throughput screening. Characteristics pertaining to subtype, DNA-repair defects, and metabolism quantified across PDCLs, with cell-lines selected to represent the full spectrum of the set of PDCLs. The classical metric shows the collective expression of the classical-associated, turquoise gene programme. As no single gene programme is representative of the squamous subtype, the squamous metric shows the collective expression of genes determined to be upregulated in patients categorised as squamous. Subtype shows a categorical labelling summarising the classical and squamous measurements. Stability shows PDCLs subtyped according to structural variants, as in (Waddell, Pajic, A.-M. Patch, *et al.*, 2015), while BRCA score describes the COSMIC BRCA mutational signature (signature 3), as in (Alexandrov *et al.*, 2013). The metabolic metric shows which descriptor best reflects metabolic phenotype, with PDCLs described as glycolytic, high levels of aerobic glycolysis, or oxidative, high levels of oxidative phosphorylation.

| Cell-Line | Classical | Squamous | Subtype | Stability | BRCA Score | Class | Metabolic Profile |
|-----------|-----------|----------|------------|-----------|------------|-----------|-------------------|
| TKCC-22 | 0.457 | -0.604 | Classical | unstable | 5.31 | Metabolic | Oxidative |
| PaCaDD137 | 0.187 | -0.586 | Classical | stable | 0.17 | Immune | Oxidative |
| TKCC-17 | 0.275 | 0.287 | Borderline | scattered | 1.66 | Metabolic | |
| TKCC-19 | -0.013 | 0.429 | Borderline | scattered | 1.69 | Metabolic | |
| TKCC-02 | -0.266 | 0.402 | Squamous | unstable | 11.27 | Metabolic | Glycolytic |
| TKCC-07 | -0.499 | 0.532 | Squamous | focal | 3.00 | Immune | |
| TKCC-10 | -0.597 | 0.366 | Squamous | unstable | 4.28 | Immune | Glycolytic |
| TKCC-09 | | | | unstable | 5.48 | Immune | |

5.2.1.2 DMSO and Staurosporine Concentration

The primary endpoint of screening was percentage inhibition as determined via nuclear count. A variety of approaches can be implemented to identify significant hits, depending on the design of the assay, with Z-scores often employed for hit selection in post-screening analyses. This method depends on assigning Z-scores as determined relative to the standard deviation across a plate and assumes that

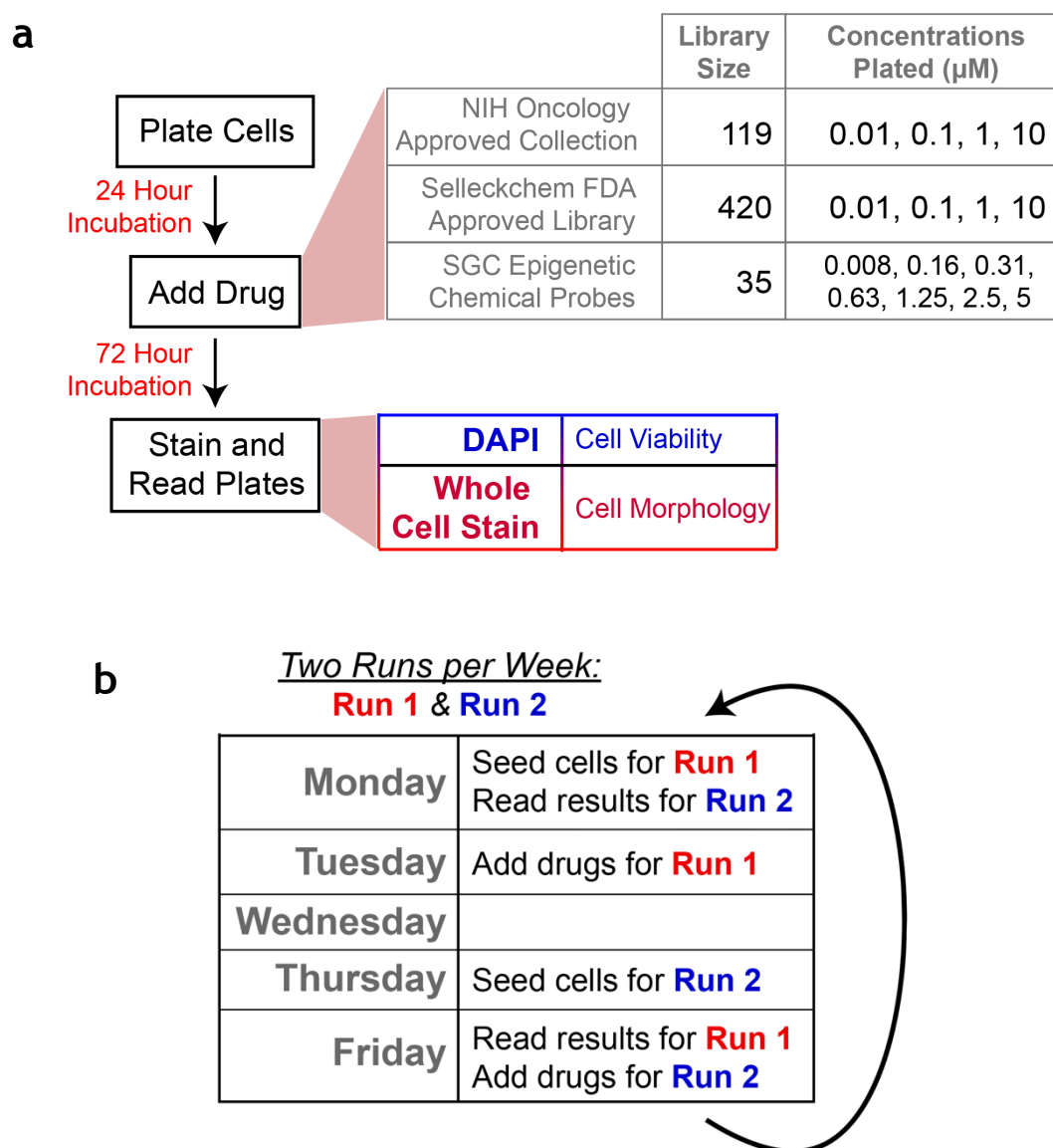


Figure 5.1 | Workflow of high-throughput screening with Beatson Screening Facility. a Schematic detailing high-throughput drug-screen, with details of drug libraries included and outputs of screen. b Scheduling of plates over the course of the screen, allowing for two runs per week.

most compounds will yield negative results (Malo *et al.*, 2006). As the libraries included in this screen contain a large number of potent active compounds with known anti-cancer properties, as will be discussed in chapter 5.2.2.1, this method was not applicable, and as such, precise neutral and inhibitor controls were required to ascertain percentage inhibition. To this end, DMSO was utilised as a neutral control, while staurosporine, commonly used to initiate apoptosis in cells (Frankfurt and Krishan, 2001; Herrmann *et al.*, 2007), acted as an inhibitor control.

5.2.2 High-Throughput Screening of PDCLs

5.2.2.1 Primary Screening

Primary screening was carried out with a variety of drug libraries, with in-house screening in collaboration with the Beatson Screening Facility including two libraries of clinically approved and well characterised compounds: one consisting of 119 approved oncology drugs assembled by the Developmental Therapeutics Program (Institute National Cancer), as well as a larger set of 420 more general purpose, FDA approved compounds, distributed by Selleckchem (Table 2.1). Both these libraries were screened at four concentrations, ranging from 10 nM to 10 μ M (Figure 5.1a). A smaller library of 35 epigenetic chemical probes, available from the structural genomics consortium (SGC) (Brown and Müller, 2015), was additionally included in this screen. Two rounds of screening were performed each week, allowing 24 hours for cells to attach and 72 hours for drug treatments (Figure 5.1b).

In anticipation of the in-house screening project, an extensive list of targets was generated for the compounds within the two large drug libraries. This was achieved by incorporating data downloaded in the XML format, with subsequent formatting, from the DrugBank database (Wishart *et al.*, 2018). This data provided annotations for targets alongside each drug, as well as associated gene targets, which informed later pathway analyses.

5.2.3 Analysis of Results from In-house Screening

Results were processed by the Beatson Screening Facility, with cell loss of viability (LOV) quantified via nuclear count acting as the primary output. Morphological data was also generated via whole-cell staining, although this was treated as a secondary output with results planned for more detailed analysis at a later time-point by the Beatson Screening Facility.

In order to first identify compounds acting selectively in one subtype relative to the other, compounds were scored according to mean LOV difference between PDCLs classed as extremely squamous (TKCC-02, TKCC-10) and extremely classical (TKCC-22, PaCaDD137) (Table 5.2). One primary observation made while analysing results from drug-screening was the subtype-selective response of PDCLs to treatment with a number of compounds that target elements within the DNA-damage response (DDR) and DNA replication, including irinotecan and etoposide, which inhibit topoisomerases and affect DNA structure through facilitating strand breaks in DNA (Champoux, 2001; Wood *et al.*, 2015), and fluorouracil, which inhibits thymidine synthesis, leading to an imbalance of deoxynucleotides and DNA damage (Yoshioka *et al.*, 1987; Longley, Harkin and Johnston, 2003). This squamous-associated effect was most apparent in the drug bleomycin, an inhibitor of DNA ligase, likely through DNA binding (Ono *et al.*, 1976), which is commonly used as part of the chemotherapeutic regimen to treat testicular cancer (Einhorn and Williams, 1980) and functions to kill cells via induction of single- and double-stranded breaks in DNA (Tounekti *et al.*, 2001). Though these responses were subtype selective, with squamous PDCLs exhibiting greater sensitivities than classical PDCLs, nuclear stability phenotypes (as specified in Table 5.1) were not predictive of sensitivities to these DDR modulating agents, with TKCC-10, TKCC-02 and TKCC-22 all classified as unstable (Waddell, Pajic, A. M. Patch, *et al.*, 2015), exhibiting high BRCA scores (Alexandrov *et al.*, 2013). As work involving DNA damage initiating agents was the research focus of others within the group, it was decided to investigate alternative hits.

Beyond compounds with known targets in the DDR pathway, two statins were found to induce loss of viability in a distinctly subtype selective fashion, specifically effecting a response in squamous PDCLs: pitavastatin and fluvastatin. This finding was of particular note as these two therapeutics have never been tested in clinical trials involving pancreatic cancer, according to the Aggregate Analysis of ClinicalTrials.gov (AACT) database (Clinical Trials Transformation Initiative), thus indicating the clinical novelty of such a therapeutic strategy in the context of PDAC. The statin family of therapeutics were originally designed to manage hypercholesterolemia via competitive inhibition of HMGCR and have historically been successfully employed to reduce LDL cholesterol in patients (Baigent *et al.*, 2005; LaRosa *et al.*, 2005). Within the context of cancer, multiple research projects have highlighted the statins family's ability to induce cell death across a range of

Table 5.2 | Identifying subtype-selective, metabolically active compounds. Table showing those compounds included in drug screening with significantly different responses between squamous and classical subtype PDCLs at 1 or 10 μ M. Compounds were ordered according to absolute mean difference in percentage loss of viability (LOV) between the two subtypes (red/green shading), taken as a mean of 1 and 10 μ M, with only compounds with mean LOV > 25% shown. Positive scores (red) indicate greater sensitivity in squamous cell-lines, while negative scores (green) indicate classical sensitivity. Selected gene product targets are shown to the right in blue, with genes grouped according to target proteins/pathways. As can be seen, two statins, pitavastatin and fluvastatin, were found to induce a highly subtype-selective response. The number of clinical trials relating to pancreatic cancer each compound was involved in is shown on the right.

| | Mean LOV Difference (%) | | DNA Ligases | | | DNA Topoisomerases | | | PC Clinical Trials |
|--------------------|-------------------------|------------|-------------|------|-------|--------------------|-------|------|--------------------|
| | 1 μ M | 10 μ M | LIG1 | LIG3 | HMGCR | TOP2A | TOP2B | TOP1 | |
| Bleomycin | 76.40 | 64.05 | | | | | | | |
| Pitavastatin | 54.08 | 75.20 | | | | | | | |
| Bleomycin | 61.75 | 55.60 | | | | | | | |
| Adefovir Dipivoxil | 28.20 | 52.60 | | | | | | | |
| Etoposide | 49.10 | 20.63 | | | | | | | |
| Irinotecan | 33.90 | 31.40 | | | | | | | |
| Fluorouracil | 24.12 | 37.47 | | | | | | | |
| Etoposide | 35.27 | 21.13 | | | | | | | |
| Disulfiram | -21.22 | -34.28 | | | | | | | |
| Fluvastatin | 8.25 | 47.05 | | | | | | | |

PC Clinical Trial Count



100
10
1
0

cancer-types *in vitro* (Dimitroulakos *et al.*, 1999, 2002; Mueck, Seeger and Wallwiener, 2003; Seeger, Wallwiener and Mueck, 2003), including in models of pancreatic cancer (Gbelcová *et al.*, 2008; Fendrich *et al.*, 2013), with the finding that PC cells are dependent on cholesterol uptake (Guillaumond *et al.*, 2015) providing additional rationale for targeting cholesterol synthesis in PDAC.

Despite these observations, clinical efforts to treat pancreatic cancer with statins has been met with mixed results: while some retrospective analyses of clinical trials have shown statin exposure to positively influence survival (Lee *et al.*, 2016; Moon *et al.*, 2016), randomised prospective trials indicate that addition of statin to standard of care treatment alone is not sufficient to benefit pancreatic cancer patients (Hong *et al.*, 2014). To further complicate statins' ability to treat pancreatic cancer, a meta-analysis found that cholesterol intake was correlated with an increased incidence of pancreatic cancer (Chen *et al.*, 2015), while more recent analysis has cast some doubt on this, indicating that patient LDL levels do not account for the relationship between statin exposure and survival (Huang *et al.*, 2017); however, there is insufficient clinical data to draw any firm conclusion from this study (Liu *et al.*, 2017). Recently, various preclinical research projects investigating the repurposing of statins for use in cancer management have focused on the observation that the anti-cancer effects associated with this family of therapeutics are observed in sub-populations of cell-lines (Clendening *et al.*, 2010; Goard *et al.*, 2014; Warita *et al.*, 2014). As these findings align with the results from screening, it was decided to pursue statins as a hit, with the potential to explore the mechanism of subtype-specific sensitivity.

5.2.4 Validating statins as major hit from screening

In order to ensure definitively that those statins identified via screening affected PDCLs in a subtype-selective manner, dose-response curves were generated to include supplementary PDCLs that best represent the two subtypes. As pitavastatin elicited a more potent response than fluvastatin (Table 5.2), this therapeutic was selected for further testing. Dose-response curves assessing pitavastatin's efficacy

validated the findings of high-throughput screening, highlighting the increased levels of sensitivity to statins within squamous PDCLs (Figure 5.2). As further validation, siRNA mediated KD of HMG-CoA Reductase (HMGCR), the primary target of pitavastatin, was shown to activate apoptosis, as determined via PARP cleavage, a commonly used marker of apoptosis (Boulares *et al.*, 1999; Soldani and Scovassi, 2002), as similarly observed on pitavastatin treatment in TKCC-02, the cell-line most sensitive to statin treatment (Figure 5.3).

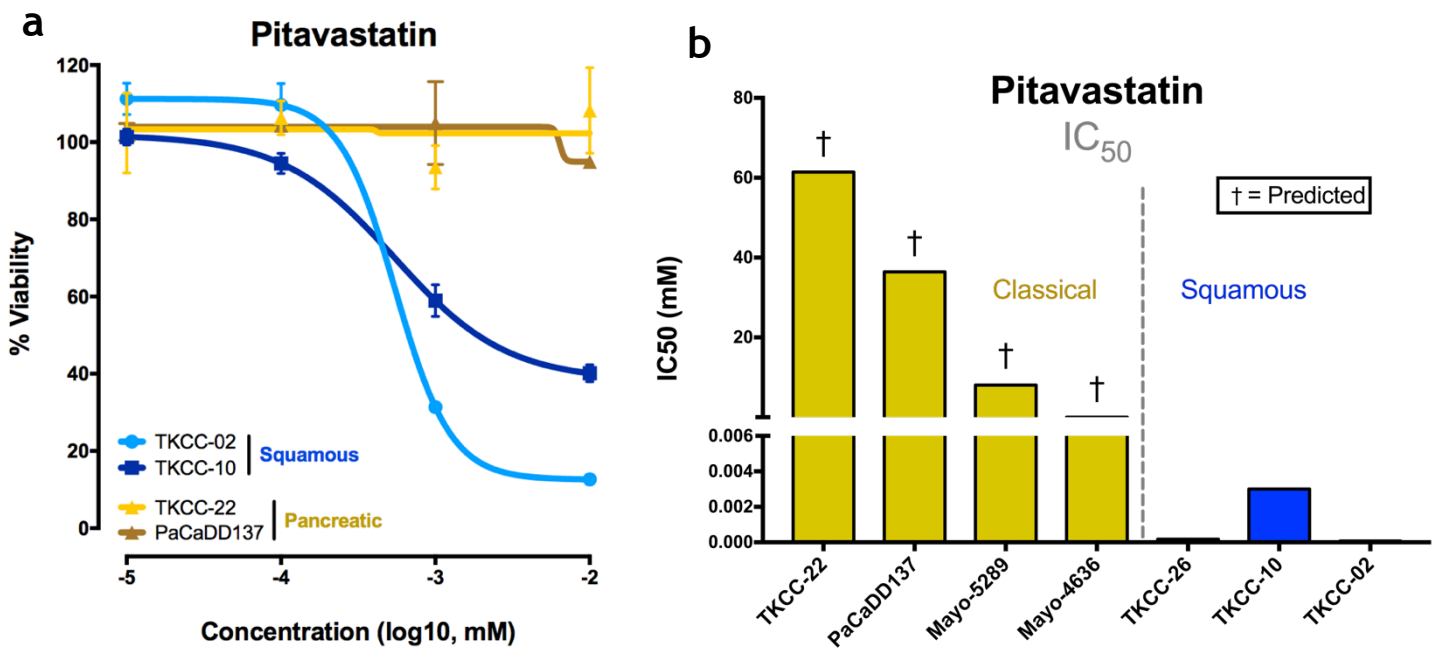


Figure 5.2 | Pitavastatin selectively inhibits squamous subtype PDCLs. **a** Dose-response curve showing effect of pitavastatin on PDCLs during high-throughput drug screening. Curves are coloured according to subtype, with squamous cell-lines (blue) displaying higher sensitivity than classical (yellow/brown). **b** Barplot showing the differences in IC₅₀ of pitavastatin between PDCLs of classical (yellow) vs squamous (blue) subtypes. Results were obtained for an extended set of cell-lines which validated results generated via high-throughput screening.

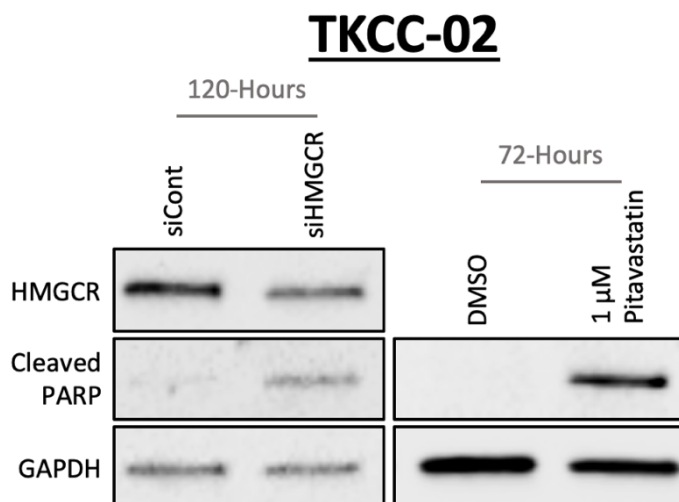


Figure 5.3 | Inhibition of HMGCR activity induces apoptosis in squamous PDCLs. Western blot showing induction of PARP cleavage on siRNA mediated silencing of HMGCR (left) and inhibition of HMGCR via pitavastatin treatment. As can be seen, HMGCR KD leads to a reduction in protein abundance, while both HMGCR KD and pitavastatin induce apoptosis, as denoted by PARP cleavage.

5.3 Cholesterol synthesis and HMGCR degradation potentially contribute to statin resistance in classical PDCLs

5.3.1 Quantifying anabolic processes reveals differences in cholesterol biosynthesis between subtypes

In order to assess whether rates of cholesterol biosynthesis align with differential sensitivities observed in statin sensitivity described above (Figure 5.2), cholesterol biosynthesis rates were quantified via isotope labelling. This process involves feeding cells with ^{13}C -labelled glucose and glutamine for 72 hours before metabolites are extracted and quantified via liquid or gas chromatography followed by mass-spectrophotometry. Both glucose and glutamine are taken up and catabolised to restore pools of cellular acetyl-CoA, an intermediate metabolite necessary for the synthesis of a range of biomolecules including fatty acids and sterols. By quantifying isotope ratios of metabolites downstream of acetyl-CoA in

this fashion, it's possible to quantitatively differentiate between newly synthesised and imported metabolites.

As suggested by previous RNA-seq data, classical cell-lines display higher rates of cholesterol biosynthesis (Figure 5.4a-b), with a greater proportion of cholesterol labelled with ^{13}C to unlabelled than squamous PDCLs. While the correlation between statin sensitivity and rates of cholesterol biosynthesis appears to be a novel finding in preclinical cancer research, work in breast cancer cells have shown that increased expression of genes involved in cholesterol synthesis corresponds to an enhanced resistance to treatment with atorvastatin (Kimbung *et al.*, 2016). These results align with findings that protein products involved in

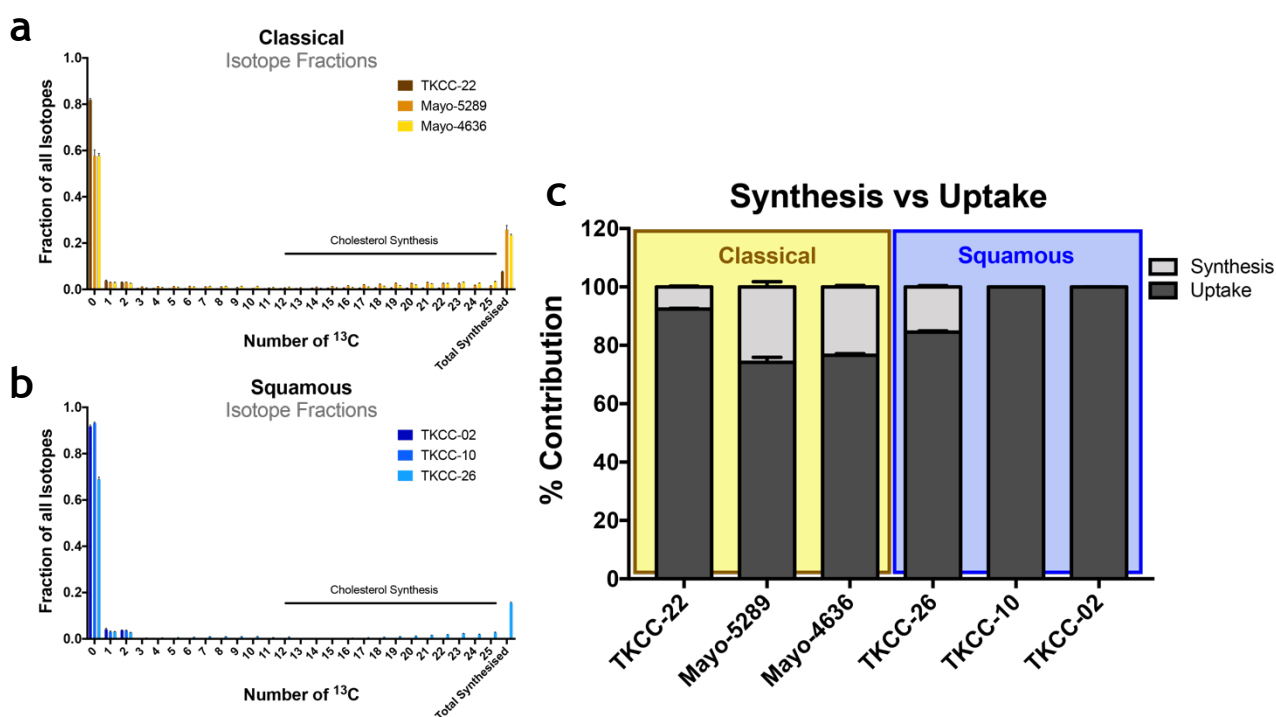


Figure 5.4 | Rates of cholesterol biosynthesis differ between subtypes. a Bar-plot showing distribution of cholesterol isotope labelling within PDCLs representative of the classical subtype. Up to 27 atoms of ^{13}C may be incorporated into a single molecule of cholesterol, with partially labelled molecules containing 12 or more ^{13}C atoms also resultant from *de novo* synthesis. b Bar-plots showing cholesterol synthesis in squamous PDCLs, as in (a). c Bar-plot showing ratios of synthesised cholesterol relative to unlabelled cholesterol taken-up by cells directly from media. As can be seen, rates of cholesterol synthesis are increased in classical PDCLs, with nearly no synthesis detected in the squamous TKCC-10 or TKCC-02 cell-lines.

cholesterol biosynthesis, including HMGCR, are upregulated in classical PDCLs (Figure 3.6). Sample preparation and mass-spectrometry was performed with thanks by Grace McGregor.

5.3.2 HMGCR degradation is found to be dysregulated between subtypes

In order to understand the difference in sensitivity to statins observed between subtypes, it was firstly necessary to consider the protein target of the statin family of therapeutics, HMGCR. HMGCR is an endoplasmic reticulum (ER)-bound enzyme integral to the biosynthesis of cholesterol (Stevenson, Huang and Olzmann, 2016), functioning to convert HMG-CoA to mevalonate, a precursor to synthesised sterols. Western blots were conducted initially to test for differences between protein abundances, however this revealed a putative cleavage band that appeared specifically within the resistant, classical PDCLs (Figure 5.5a). This observed band suggests upregulated degradation within this subpopulation of cell-lines, which is of particular interest due to previous work that identified cleavage of HMGCR in response to downstream products of the mevalonate pathway, suggestive of a negative feedback loop (Inoue *et al.*, 1991; Sever, Song, Yabe, Joseph L Goldstein, *et al.*, 2003; DeBose-Boyd, 2008). One paper in particular points to degradation induced by a cysteine-protease, resulting in cleavage along a membrane-spanning domain of the protein existing between residues 314-340 (Moriyama *et al.*, 1998). This sterol-dependent cleavage mirrors the ER-associated degradation of HMGCR, which is initiated via Insig-mediated ubiquitination of HMGCR's transmembrane region (Sever, Song, Yabe, Joseph L. Goldstein, *et al.*, 2003; Hartman *et al.*, 2010), though is induced independent of the proteasome and would likely mediate inactivation of HMGCR similarly via displacement from the ER. This event results in the generation of two cleavage products, one lighter (36 kDa) consisting of membrane-spanning domains, and another heavier (61 kDa) consisting of the catalytic domain. The observation of a putative cleavage product with the molecular weight of ~60 kDa is therefore in-line with these findings, as the

antibody used (ab174830, Abcam) was generated against an immunogen spanning 400-500 aa residues (Figure 5.5b).

Of additional note, no SNPs were found to occur within the HMGCR gene across all PDCLs included in analysis, ruling out the possibility of the band existing due to heterozygous mutation resulting in a truncated protein. This finding is of additional relevance as previous research has identified a genetic variation within the *HMGCR* gene that confers resistance to statins in colorectal cancer cells (Lipkin *et al.*, 2010) and has been confirmed within a range of *in vitro* systems (Medina *et al.*, 2008). This class of SNP is found within exon 13 in the catalytic region, encoding the statin-binding domain and is therefore distinct from the pattern of cleavage observed here.

5.3.1 Proteasomal inhibition partially inhibits HMGCR cleavage *in vitro*

To validate whether this observed band corresponds to HMGCR degradation, it was decided to assess the effect, if any, of protease inhibitors on band formation. ALLN, an inhibitor of cysteine-proteases including cathepsins and calpains (Sasaki *et al.*, 1990), which are associated with lysosomal and non-lysosomal protein degradation respectively (Chondrogianni, Fragoulis and Gonos, 2002), was first tested to assess whether inhibition of proteasomal protein degradation prevented the generation of this cleavage band (Figure 5.6a). Treatment with 25 μ M ALLN was seen to lead to an increase of overall HMGCR abundance, both intact protein and putative cleavage product (Figure 5.6b). This observation may be due to the inhibition of degradation of activated SREBP, an ER-localised transcriptomic activator of lipogenesis and promoter of *HMGCR* expression (Wang *et al.*, 1994), resulting in increased transcription and translation of HMGCR. Despite this general increase in protein levels of both bands, the shift in abundance of the putative cleavage band was observed to be slightly less relative to full-length HMGCR, suggesting that inhibition of cysteine-proteases may mitigate degradation as previously documented (Moriyama *et al.*, 1998), and that this band genuinely

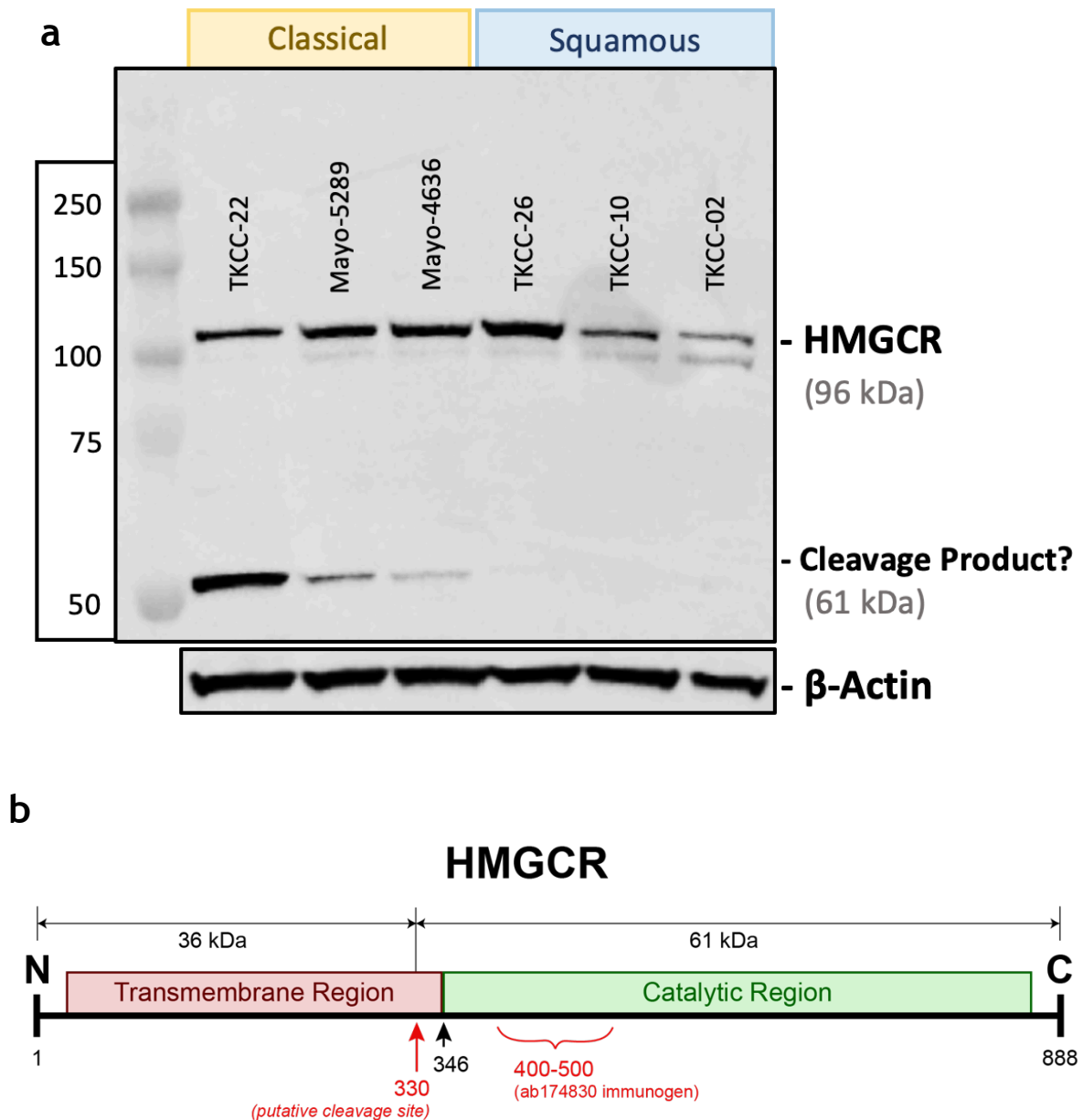


Figure 5.5 | HMGCR is potentially selectively cleaved in classical PDCLs. **a** Western blot showing the differential cleavage of HMGCR between PDCL subtypes. As can be seen, intact HMGCR was detected in all PDCLs tested, however, the putative cleavage product was found selectively in the three classical cell-lines (left, yellow) and was absent in squamous (right, blue). Labels for detected bands are shown to the right, alongside predicted molecular weights. Actin is shown as a loading control. **b** Schematic showing structure of the HMGCR protein. The cleavage site previously described (Moriyama *et al.*, 1998) is highlighted, along with the region against which the antibody used in (a) was manufactured.

corresponds to HMGCR degradation. The partial inhibitory effect observed may be due to additional proteasomal mechanisms also contributing to HMGCR degradation, which is supported by evidence that HMGCR is also ubiquitinated and targeted for proteasomal degradation (Sever, Song, Yabe, Joseph L Goldstein, *et al.*, 2003).

5.3.2 Mevalonate induces negligible levels of cleavage of HMGCR *in vitro*

As described in the previous section, it has been long established that downstream metabolites within the mevalonate pathway contribute to the degradation of HMGCR. Both sterol and non-sterol intermediates induce this degradation, including mevalonate itself (Roitelman and Simoni, 1992; Ravid *et al.*, 2000). In order to determine the effect, if any, mevalonate has on the cleavage product observed in a representative classical PDCL, Mayo-5289 were supplemented with mevalonate 5-phosphate at a range of concentrations for 24 hours. Western blotting was then performed in order to quantify changes in the abundance of intact HMGCR and the putative cleavage product (Figure 5.7a). This determined a slight, incremental increase in HMGCR degradation, with increased abundances observed in both full-length and cleaved HMGCR. While the increase in intact HMGCR is unexpected, though potentially accounted for by compensatory fluctuations in levels of downstream metabolites which may occur within the 24-hour time frame of the experiment, this increase is offset by the comparatively larger increase in abundance of the ~60 kDa cleavage band.

This observed increase in the putative cleavage band of HMGCR upon exposure to mevalonate, though slight, reinforces the likelihood of this being a true indicator of degradation. If so, this suggests that internal levels of the metabolites within the mevalonate pathway may be increased within classical PDCLs, thus inducing the increased levels of HMGCR cleavage associated with this subtype. Additionally, the higher rates of cholesterol synthesis found in this subtype (Figure 5.4) may be a contributor to this phenomenon. Though speculative, it's possible that increased

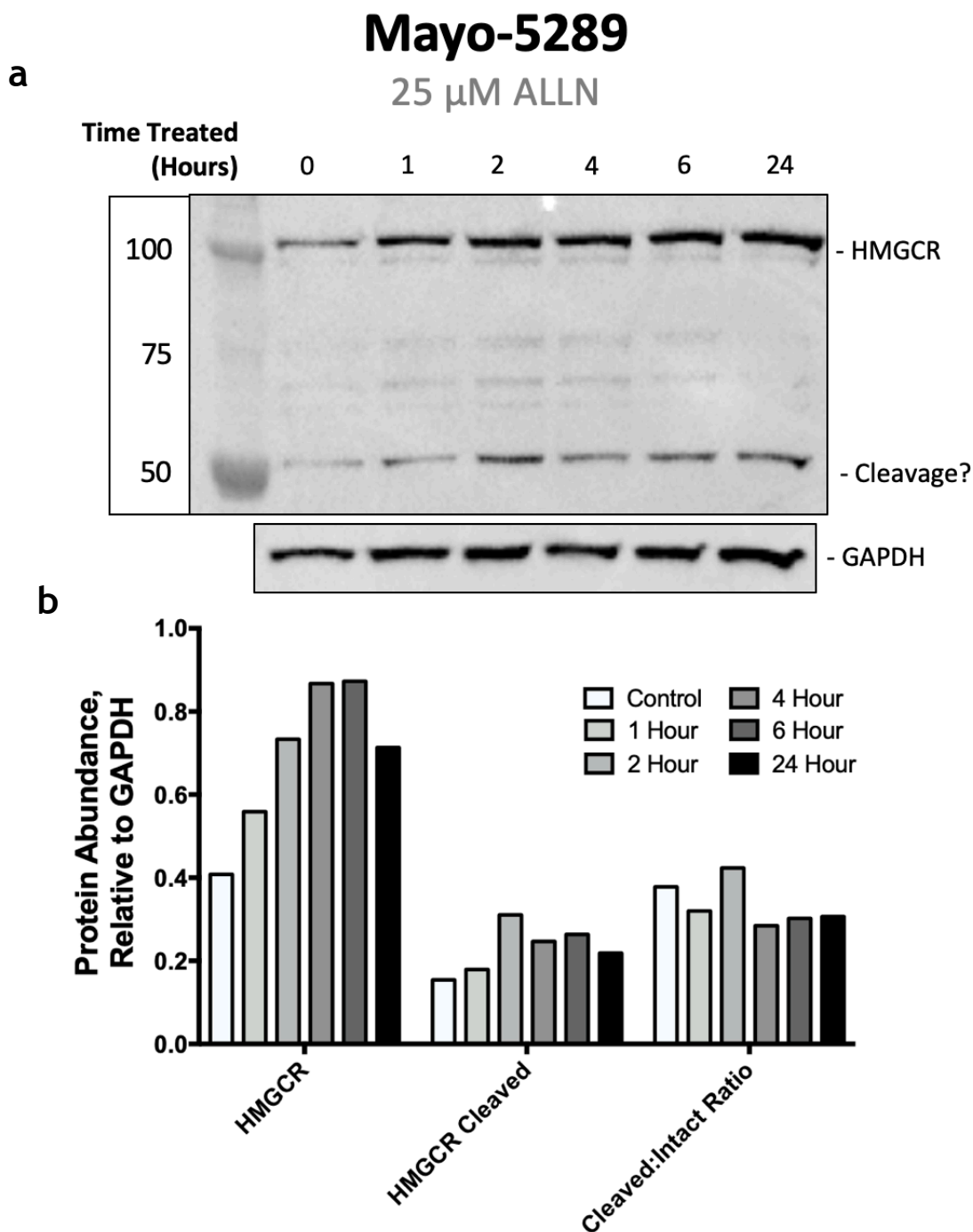


Figure 5.6 | Treatment with protease inhibitor ALLN moderately inhibits HMGCR cleavage *in vitro*. **a** Western blot showing HMGCR levels in response to 25 μ M ALLN treatment in Mayo-5289 across a range of time-points. As can be seen, ALLN treatment does appear to increase the presence of cleaved HMGCR, however this is observed alongside an increase of intact HMGCR, indicating that cleavage is not enhanced in the presence of mevalonate. **b** Quantification of western blot results shown in (a), normalised to loading control (GAPDH).

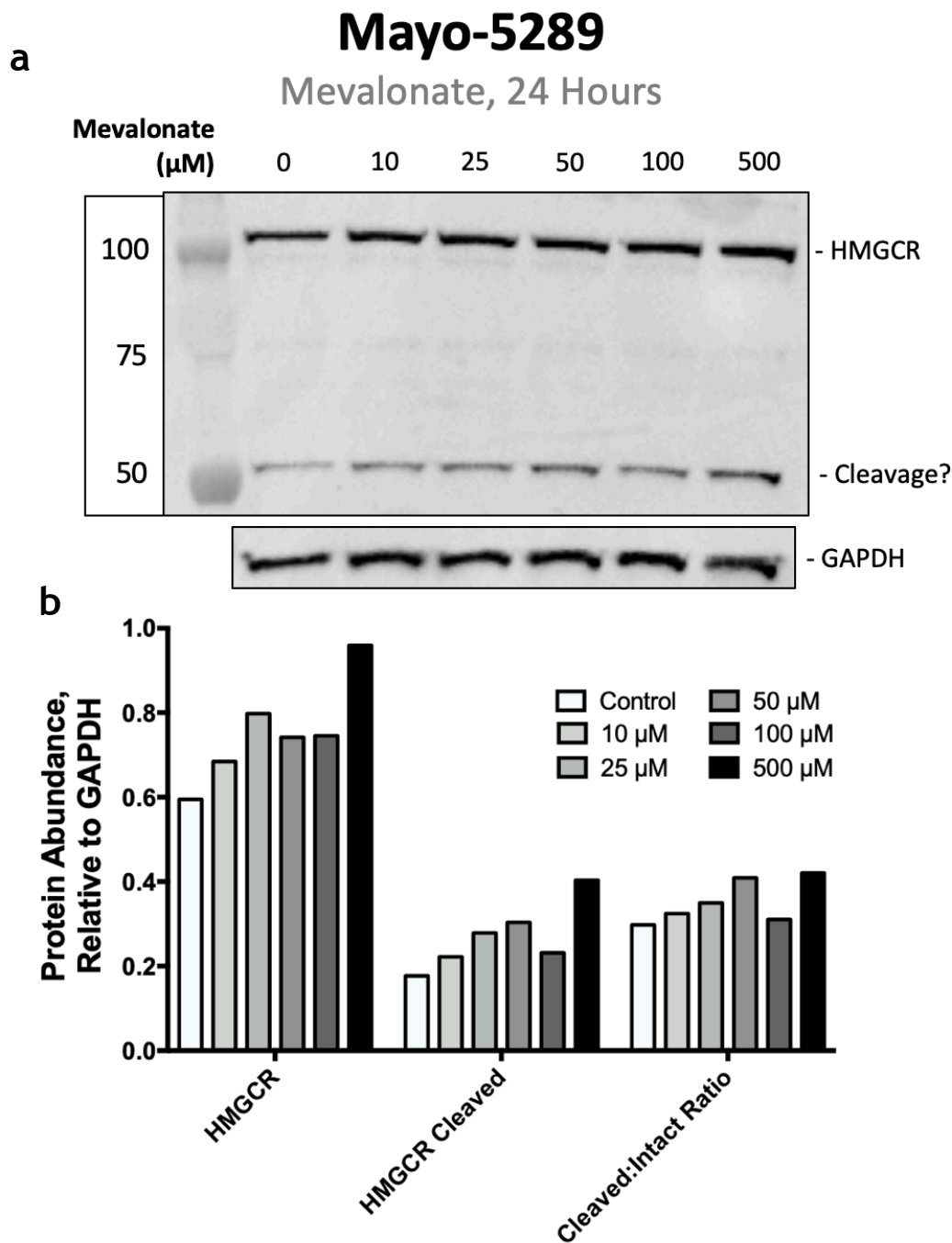


Figure 5.7 | Mevalonate exposure induces some HMGCR cleavage *in vitro*. **a** Western blot showing HMGCR levels in representative classical PDCL, Mayo-5289, exposed to increasing concentrations of mevalonate for 24 hours. As can be seen, exposure to high concentrations of mevalonate does appear to increase the presence of cleaved HMGCR, however this is observed alongside an increase of intact HMGCR. **b** Quantification of western blot results shown in (a), normalised to loading control (GAPDH). Results show that, although levels of both intact and cleaved forms of HMGCR increase upon mevalonate treatment, slightly more cleaved HMGCR is generated than whole, suggesting a slight increase in HMGCR degradation at higher mevalonate concentration.

levels of downstream metabolites in classical PDCLs induces cleavage of HMGCR, the effect of which is offset due to higher levels of HMGCR translation (as transcription is not significantly upregulated in either subtype), leading to roughly equivalent abundances of intact HMGCR across subtypes. This high level of turnover may allow classical PDCLs escape statin treatment, with pitavastatin unable to induce its inhibitory effect, allowing this subtype to overcome the sensitivity observed in squamous PDCLs. Due to time limitations, it was not possible to assess the impact of pitavastatin on rates of cholesterol synthesis via stable isotope tracing, which would be required to confirm this hypothesis.

5.4 Cholesterol localisation and lipid raft formation are indicators of statin sensitivity

5.4.1 Caveolin-1, a regulator of cholesterol homeostasis, is found selectively in squamous PDCLs

Beyond the potential of statin resistance being modulated by differential degradation of HMGCR, it was decided to investigate additional regulators of the mevalonate pathway to identify other possible contributors to subtype-associated statin sensitivity. By interrogating transcriptomic and proteomic data for proteins involved in the regulation of cellular cholesterol, it was determined that Caveolin-1 (CAV1) is selectively found in squamous PDCLs, which was validated by western blot (Figure 5.8). CAV1 is a cholesterol binding scaffolding protein (Murata *et al.*, 1995) and an integral constituent of caveolae (Rothberg *et al.*, 1992), specialised lipid rafts found within cell membranes and enriched for cholesterol. CAV1 is necessary for the formation of caveolae (Drab *et al.*, 2001) and its ectopic expression is also sufficient to lead to caveolae formation in CAV1 deficient cell-lines (Fra *et al.*, 1995).

The absence of CAV1 in classical PDCLs may provide an insight into the mechanism of resistance to pitavastatin associated with this subtype as research has described

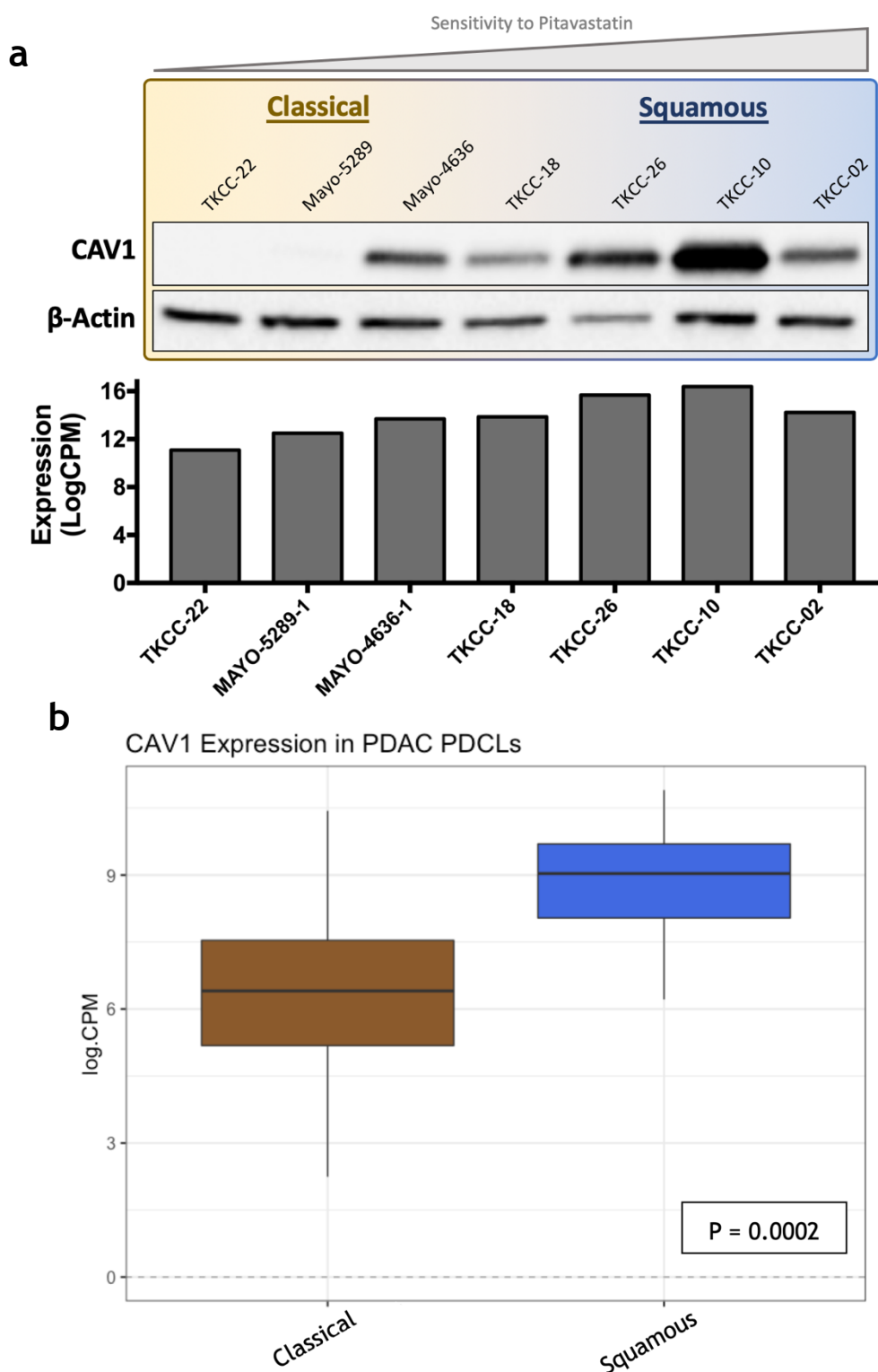


Figure 5.8 | CAV1 protein and mRNA is upregulated in the statin-sensitive, squamous subtype. **a** Western blot highlighting dysregulation of CAV1 at the protein level (top) in PDCLs ordered according to subtype and bar-plot showing similar expression of CAV1 according to RNA-seq (bottom). **b** Box-plot showing expression of CAV1 in PDCLs grouped according to subtype. P-values were determined according to a Mann-Whitney U test.

CAV1 as a regulator of cholesterol efflux (Frank *et al.*, 2001; Fu *et al.*, 2004) and cholesterol as an instigator of caveolin trafficking (Pol *et al.*, 2005). This complex interplay between localisation CAV1 and cholesterol homeostasis, though not completely elucidated, may modulate sensitivity due to the dependence of squamous PDCLs on caveolae and downstream signalling pathways (Anderson, 1998) or the inability of classical PDCLs to export and sequester cholesterol, driving the ER-localised HMGCR degradation previously described (Figure 5.6 and Figure 5.7). This possibility of CAV1 mediating sensitivity to pitavastatin is in-line with the finding that increased levels of caveolae are indicative of increased sensitivity to cholesterol depletion (Li *et al.*, 2006).

5.4.2 Cholesterol localisation differs between subtypes *in vitro*

To assess the possible correlation between the absence/presence of CAV1 within PDCLs on cholesterol localisation, filipin III was used to stain and visualise cholesterol in cells representative of both subtypes. Typical imaging via confocal microscopy requires a permeabilization step to allow the passage of fluorophores across the plasma membrane, allowing for internalisation of staining materials and visualisation. However, detergents commonly used to permeabilise mammalian cells, such as Triton X-100 and saponin, function via the disruption or removal of cholesterol at the cell membrane (Ingelmo-Torres *et al.*, 2009; Böttger and Melzig, 2013). In order to avoid this effect, it was decided to permeabilise cells with filipin III, which is known to permeabilise membranes (Knopik-Skrocka and Bielawski, 2002); it was first necessary to optimise the concentrations and time-points that would allow sufficient permeabilization for cholesterol visualisation (Figure 5.9). Recent publications describe using 50-100 µg/mL filipin III in combination with detergent-based permeabilization for cholesterol quantification (Hissa *et al.*, 2012; Warita *et al.*, 2014), while higher concentrations ranging from 150-1000 µg/mL were utilised in earlier studies which omitted additional permeabilization steps (Tillack and Kinsky, 1973; Milhaud, 1992). As such, it was decided to test concentrations between 100-500 µg.

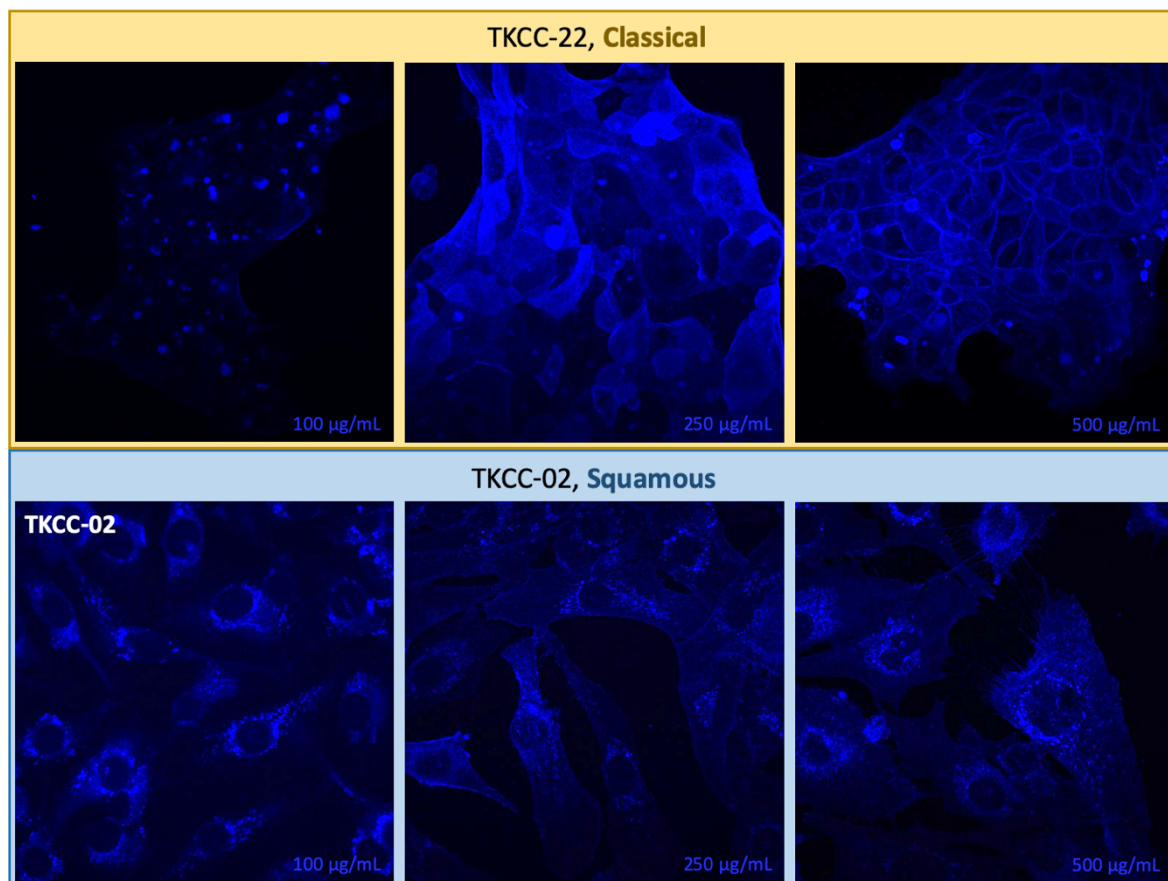


Figure 5.9 | Optimising filipin III concentrations in cholesterol visualisation reveals differential localisation between subtypes. Confocal images acquired at 40X magnification in TKCC-22 (top) and TKCC-02 PDCLs, representative of the classical and squamous subtypes respectively, treated for 30 mins with increasing concentrations of filipin III. As can be seen in TKCC-22, lower concentrations of filipin III induce minimal cholesterol staining, with a disparate staining pattern, while exposure to increased concentration leads to greater signal and the emergence of patterns consistent with cell membrane. This is contrast to TKCC-02 which seems largely unaffected by filipin III concentration, with a consistent staining across all doses.

It was observed that increasing concentrations of filipin III in PDCLs representative of the two subtypes had no visible effect on permeabilization within TKCC-02, a cell-line classed as squamous. This was found in contrast to the classical PDCL, TKCC-22, which required higher concentrations to effectively permeabilise cells, with staining patterns differing as filipin III concentrations increased. It was thought that this phenomenon may exist due to morphological distinctions between the two PDCLs, with TKCC-22 tending to grow in compact, epithelial-like layers, therefore requiring increased concentrations of filipin III to penetrate

clusters of cells, while TKCC-02 exhibit a more mesenchymal-like morphology, with individual cells growing disparately. Taking into account the stoichiometry of the binding of filipin with cholesterol and phospholipid to effect permeabilization (Milhaud, 1992), the more concentrated TKCC-22 cell-line would be expected to require greater concentrations of filipin to induce the same level of permeabilization as TKCC-02.

The results of filipin III staining optimisation indicate that cholesterol localisation differs between TKCC-22 and TKCC-02 (Figure 5.9). Though staining was carried out in the absence of additional cell markers, it appears that staining was localised to cell membranes in TKCC-22 at high concentrations of filipin III, with the boundaries of observable cell clusters visibly stained, along with what appears to well defined cell boundaries. However, in TKCC-02, staining appears centralised to perinuclear puncta, suggesting a localisation within the ER, where cholesterol biosynthesis is carried out, or within the Golgi network/transport vesicles. This suggests the upregulation of active flux of cholesterol in squamous PDCLs.

5.4.3 Lipid rafts are enriched in select squamous PDCLs, while CAV1 appears to colocalise with cholesterol

It was decided to assess the impact, if any, of pitavastatin treatment on caveolae formation, while simultaneously investigating CAV1 localisation within PDCLs. Caveolae imaging was achieved via exposure to cholera toxin subunit B (CT-B), a protein that binds to gangliosides GM1 found in lipid rafts, including caveolae (Holmgren *et al.*, 1975; Parton, 1994), conjugated to a fluorescent tag, allowing for the visualisation of lipid rafts as described in past publications (Calay *et al.*, 2010; Irwin *et al.*, 2011).

In the squamous PDCLs tested, CAV1 was found to form puncta in a very similar manner to cholesterol in TKCC-02, representative of the squamous subtype (Figure 5.10). This suggests a colocalization of the two and is consistent with the finding that CAV1 cycles between the ER, the Golgi network and caveolae at the plasma

membrane, leading to the hypothesis that this flux of CAV1 facilitates cholesterol transport (Dupree *et al.*, 1993; Conrad *et al.*, 1995). In contrast, very little staining was evident in Mayo-5289, suggesting absence or low levels of CAV1 and lipid rafts. The observation that CAV1 and cholesterol likely colocalise to

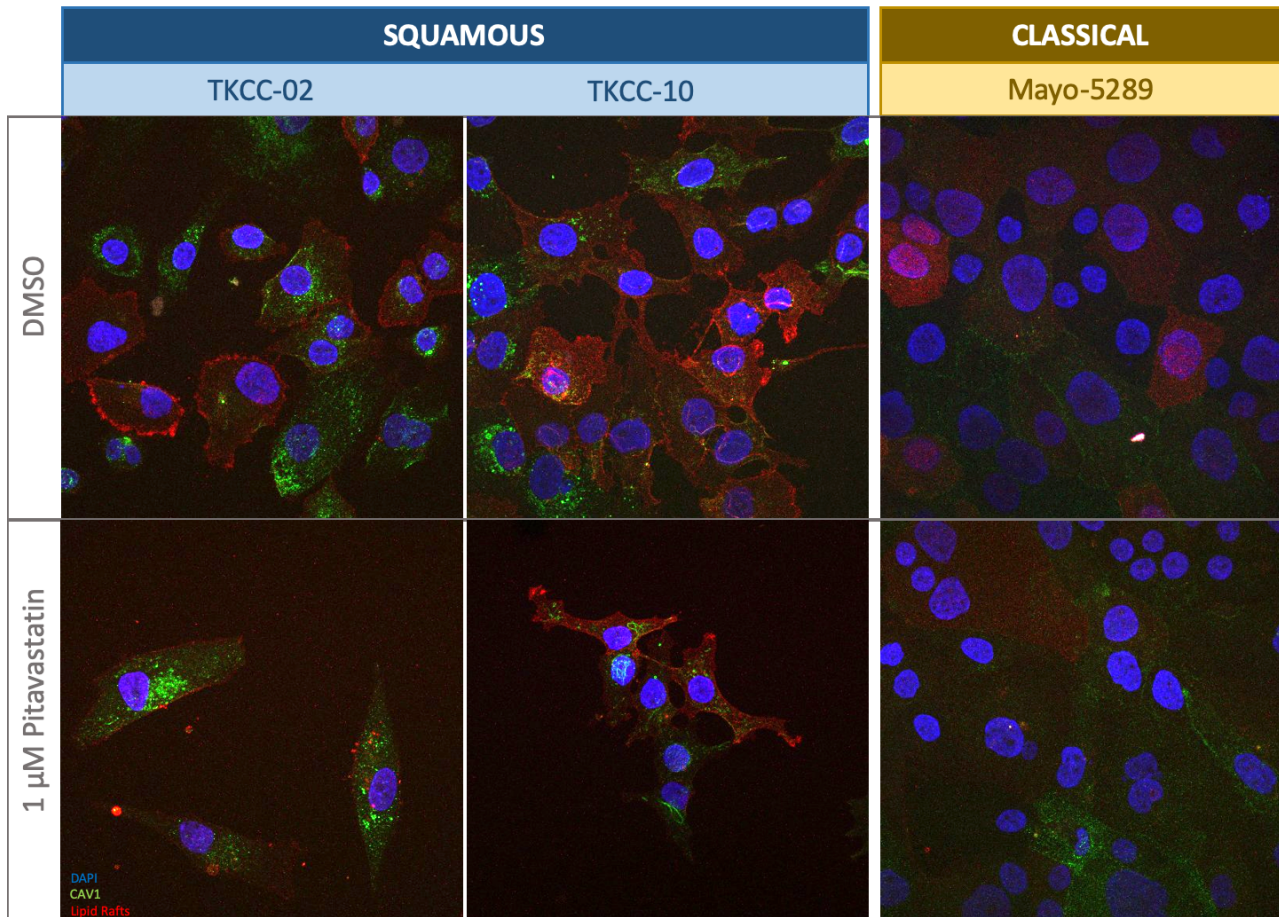


Figure 5.10 | Lipid rafts and CAV1 are visible only in squamous cell-lines, while pitavastatin has a minor effect on lipid raft formation. Confocal images at 40X magnification showing imaging of CAV1 protein localisation (green), as well as lipid rafts stained with fluorescently tagged cholera toxin B (red) and nuclei stained with DAPI (blue). Images were acquired in TKCC-02 (left), TKCC-10 (centre) and Mayo-5289 (right), with cells exposed to DMSO (top) or 1 μ M pitavastatin (bottom) for 72 hours. As can be seen, CAV1 and lipid rafts were most detectable within squamous PDCLs (blue), while the classical cell-line (brown), Mayo-5289, exhibited a lower intensity of staining with less discernible patterning, possibly reflecting noise rather than a true signal. This suggests a greater abundance of both CAV1 and lipid rafts in squamous PDCLs, with CAV1 accumulating in perinuclear puncta and lipid rafts detectable along cell membranes. Additionally, pitavastatin appears to have a minor impact on lipid raft formation, with a slight decrease in signal associated with treatment as compared to control, while no observable effect was seen on CAV1 localisation.

organelles associated with intracellular transport selectively in squamous PDCLs therefore supports the theory that interplay between the two molecules effects pitavastatin sensitivity. Though speculative, this may involve differential cholesterol efflux or sequestration, with the possibility that these phenomena influence HMGCR degradation via the negative feedback loop described in chapter 5.3 .

Secondarily, pitavastatin was found not to induce a major change in lipid raft formation or CAV1 localisation in either subtype, with patterns of staining remaining consistent between vehicle control (DMSO) and pitavastatin treatments (Figure 5.10). There did appear to be some slight decrease in signal of lipid raft staining along cell membranes upon pitavastatin treatment, however, it was not possible to quantify intensities. This suggests that pitavastatin has a minimal impact on lipid raft formation. In order to validate the subtype specificity of lipid rafts and CAV1 localisation, the analysis could be extended to additional PDCLs.

5.5 Interrogating downstream arms of mevalonate pathway implicates GGPP and cholesterol in mediating sensitivity to statins

5.5.1 Mevalonate pathway intermediates and cancer initiation and progression

A number of metabolites downstream within the mevalonate pathway have been associated with cancer development and progression, with mevalonate itself facilitating growth within various cancer models (Larson and Yachnin, 1984; Duncan, El-Sohemy and Archer, 2004), implicating this pathway in oncogenesis. This project focused on the involvement of two specific metabolites within the mevalonate pathway: cholesterol and geranylgeranyl pyrophosphate (GGPP). These

were selected due to their well-documented involvement in processes associated with pancreatic cancer.

Cholesterol's involvement in cancer development may be in part attributed to its role as a facilitator of a number of signalling pathways dependent on receptors associated with lipid rafts (Mollinedo and Gajate, 2015). This includes the PI3K/Akt pathway, which is often found activated in pancreatic cancers (Bondar *et al.*, 2002). GGPP, along with farnesyl pyrophosphate (FPP), are necessary for protein prenylation.

These targeted protein modifications have been demonstrated to be necessary for localisation of signalling proteins to cell membranes (Moore *et al.*, 1991; Hart and Donoghue, 1997), including KRAS (Chandra *et al.*, 2011), the mutated form of which is a common driver of pancreatic cancer. Due to the link between these metabolites and pancreatic cancer, as well as the widespread dietary availability of both (de Wolf *et al.*, 2017), it was decided to assess the impact of exposure to these molecules on pitavastatin sensitivity.

5.5.1 Dietary metabolites within mevalonate pathway induce pitavastatin resistance in squamous PDCLs

In order to assess the impact that these metabolites may have on pitavastatin sensitivity, dose-response curves were carried out in the absence or presence of mevalonate, cholesterol, and GGPP. As all media used to culture PDCLs were supplemented with FBS, which is highly rich in lipids, generally containing ~750 μM cholesterol (Whitford and Manwaring, 2004), it was necessary to delipidate FBS to accurately quantify cholesterol's influence on pitavastatin sensitivity.

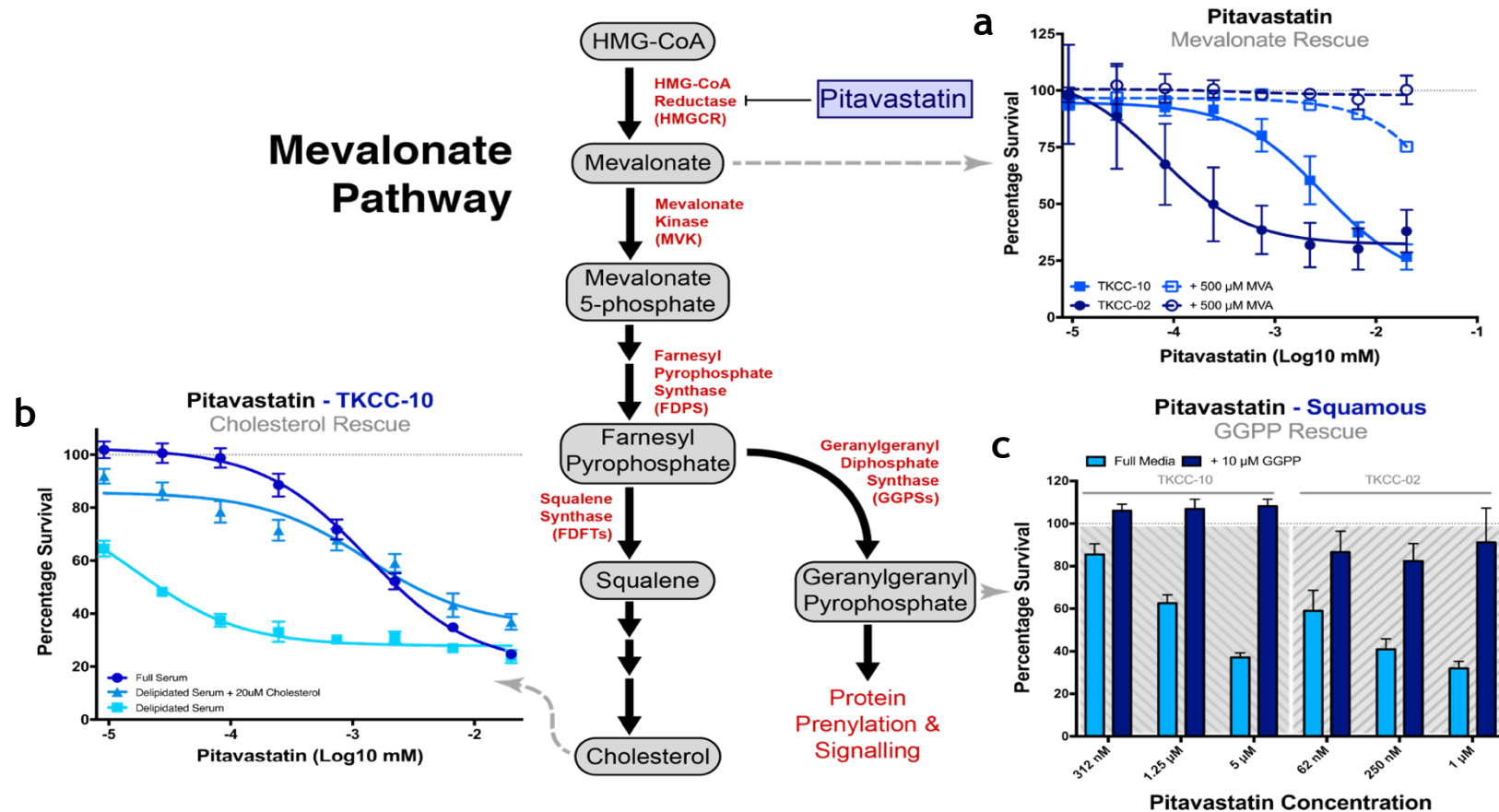


Figure 5.11 | Supplementing various metabolites in the mevalonate pathway rescues pitavastatin-induced apoptosis in vitro. Schematic outlining the key metabolites in the mevalonate pathway (grey ellipses), as well as the enzymes that mediate its progression (red). As can be seen, pitavastatin targets the HMGCR-induced conversion of HMG-CoA to mevalonate in the initial step of the pathway. **a** Dose-response curve showing the impact of 500 μM mevalonate on pitavastatin sensitivity in TKCC-02 and TKCC-10, two squamous PDCLs previously demonstrated to be highly sensitive to statins, after 72 hours treatment. As can be seen, mevalonate supplementation fully rescues the effect of pitavastatin in sensitive PDCLs. **b** Dose-response curve showing the effect of 20 μM cholesterol in delipidated medium on pitavastatin sensitivity in TKCC-10, relative to fully supplemented medium. As can be seen, cells are more sensitive to pitavastatin in delipidated medium relative to medium with full serum, an effect that is nearly fully mitigated on addition of cholesterol. **c** Bar-plots showing sensitivity of squamous PDCLs to three concentrations of pitavastatin, comparing with or without supplementation of 10 μM GGPP. As can be seen, addition of GGPP abrogates sensitivity to pitavastatin.

Primary findings showed that exposure to 500 μM mevalonate entirely mitigated sensitivity to pitavastatin in sensitive, squamous PDCLs (Figure 5.11a), thus fully implicating the mevalonate pathway and downstream components in mediating sensitivity to pitavastatin within this subtype. Further results showed that, while cells cultured in delipidated FBS exhibited enhanced sensitivity, cholesterol treatment also induced some resistance to pitavastatin in squamous PDCLs (Figure 5.11b). Exposure to GGPP in particular was seen to nullify the effects of pitavastatin on cell viability in those sensitive cell-lines (Figure 5.11c). These results are in accordance with previous findings that sensitivity to statin treatment can be abrogated with the addition of mevalonate and GGPP in *in vitro* models of various cancer types (Greenaway *et al.*, 2016; Ishikawa *et al.*, 2018; Sheikholeslami *et al.*, 2019), while the discovery that cholesterol supplementation can confer resistance to statin treatment is corroborated by observations that cholesterol can rescue statin mediated defects in myotube formation in myoblasts (Wei *et al.*, 2016).

These findings collectively highlight the potential of commonly found and widespread metabolites on mitigating the effects of pitavastatin, suggesting that additional precautions may be necessary when considering the clinical application of statins in treating pancreatic cancer. Before this family of therapeutics can represent a viable option in a clinical setting, efficacy will likely need to be enhanced through either diet limitation or potential combinatorial approaches.

5.6 Statin sensitivity is enhanced by concomitant EGFR inhibition

As clinical trials assessing the efficacy of statins in treating pancreatic cancer have yielded mixed results, as discussed in chapter 5.2.3, an observation possibly influenced by dietary intake, it was decided to interrogate downstream effectors of statin sensitivity in squamous PDCLs. This line of research was performed with the view of identifying therapeutics with potential to use in combination with

pitavastatin to enhance performance of the drug in both a preclinical and clinical setting.

5.6.1 Pitavastatin inhibits Akt activation in squamous PDCLs

Previous research efforts have demonstrated that statins inhibit AKT activity in a range of preclinical models of cancer via various potential mechanisms of action (Calay *et al.*, 2010; Wang *et al.*, 2016; Beckwitt, Shiraha and Wells, 2018). This observation is of importance due to the involvement of the PI3K/Akt pathway in pancreatic cancer oncogenesis (Bondar *et al.*, 2002). In order to confirm AKT as a downstream indicator of pitavastatin sensitivity in pancreatic cancer subtypes, the effect of pitavastatin treatment on AKT phosphorylation was assessed within PDCLs, with further on-target validation performed via HMGCR knockdown in TKCC-02, a sensitive cell-line classed as squamous (Figure 5.12). This revealed that both pitavastatin treatment and HMGCR KD were sufficient to reduce activation of AKT in the squamous PDCL, TKCC-02, while a resistant, classical cell-line, TKCC-22, exhibited a minimal decrease in levels of phospho-AKT upon pitavastatin treatment. These results therefore support previous work that has linked statin mediated HMGCR inhibition to disruption of AKT signalling, while demonstrating that this phenomenon is associated with sensitivity to statin treatment.

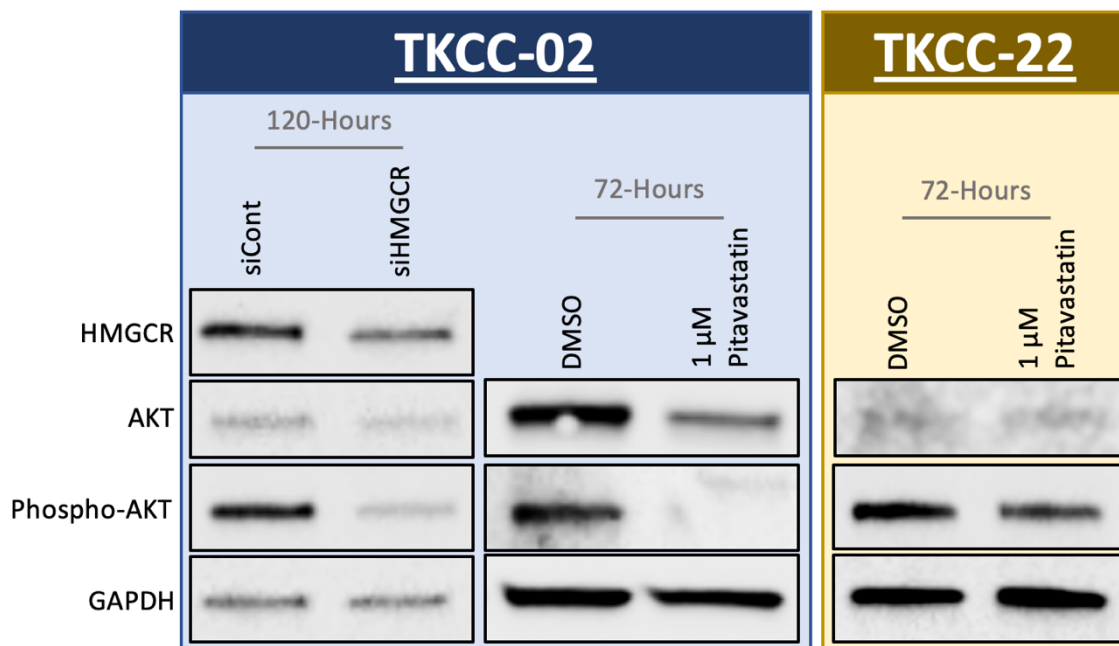


Figure 5.12 | Inhibition or loss of HMGCN leads to inactivation of AKT in sensitive PDCLs.

Western blot showing the decrease in AKT phosphorylation in response to both siRNA mediated knockdown of HMGCN (left) and inhibition of HMGCN via 1 μM pitavastatin treatment (right) in TKCC-02 (blue) and TKCC-22 (brown), representatives of the sensitive, squamous subtype and resistant, classical subtype respectively. Within TKCC-02, a slight decrease can be seen in total AKT levels after treatment with pitavastatin or HMGCN KD, while a more pronounced effect can be observed in levels of phospho-AKT after both treatments. In TKCC-22, there appears to be a slight decrease in phospho-AKT levels, though this effect is markedly less than that observed in TKCC-02.

5.6.2 Combinatorial gefitinib treatment induces cell-death at low pitavastatin concentration in squamous PDCLs

Multiple studies have linked statin-mediated inactivation of AKT to epidermal growth factor (EGFR) inhibition (Mantha *et al.*, 2005; Dimitroulakos, Lorimer and Goss, 2006), with EGFR being a well-established upstream activator of the PI3K-Akt pathway (Soltoff *et al.*, 1994; Mattoon *et al.*, 2004). Possible explanations for such a phenomenon suggest a displacement of EGFR from lipid rafts via cholesterol depletion (Irwin *et al.*, 2011) or a dissociation of upstream effectors, such as Rho-GTPases, from the cell membrane as a result in decreased prenylation, disrupting actin cytoskeleton organisation (T. T. Zhao *et al.*, 2010). Both mechanisms of

action would account for a loss of EGFR activity, with the involvement of EGFR in statin sensitivity reinforced by the finding that statin treatment improves survival in lung cancer patients receiving EGFR inhibitors (Hung *et al.*, 2017). With these findings in mind, it was decided to assess the efficacy of a combination of pitavastatin with erlotinib, a widely used EGFR inhibitor that has been shown to enhance gemcitabine sensitivity in pancreatic cancer (Moore *et al.*, 2007). The expectation is that this combinatorial approach, introducing an additional means of inhibiting EGFR, will enhance the on-target effect of statin treatment, further disrupting signalling pathways essential within squamous PDCLs.

Synergy between the two therapeutics was quantified via the SynergyFinder web application (Ianevski *et al.*, 2017), which allowed for the presentation of zero interaction potency (ZIP) scores (Yadav *et al.*, 2015) across all concentrations tested in both drugs. Combination treatments demonstrated that squamous PDCLs displayed high ZIP scores at low doses of both therapeutics, while classical cell-lines required treatment with highly concentrated doses before any synergy was observed (Figure 5.13). These results indicate a synergistic effect of the two therapeutics selectively in the squamous subtype, while highlighting the possibility that this combination may be effective in patients, with clinically viable doses likely to induce an effect.

5.1 Potential *in vivo* testing of statin efficacy

In order to assess the potential of testing a regimen of statin treatment in mouse models, as well as establish potential subgrouping, it was decided to test pitavastatin in a variety of cell-lines established from a genetically engineered mouse model (GEMM) induced by concurrent mutations of *Kras* and *Trp53* (Hingorani *et al.*, 2005). This model allows for the recapitulation of aggressive PDAC in mice that progresses in a similar fashion to the disease in human patients, bearing the hallmark genomic instability associated with human PDAC. Dose-response curves generated in three cell-lines derived from KPC tumours displayed

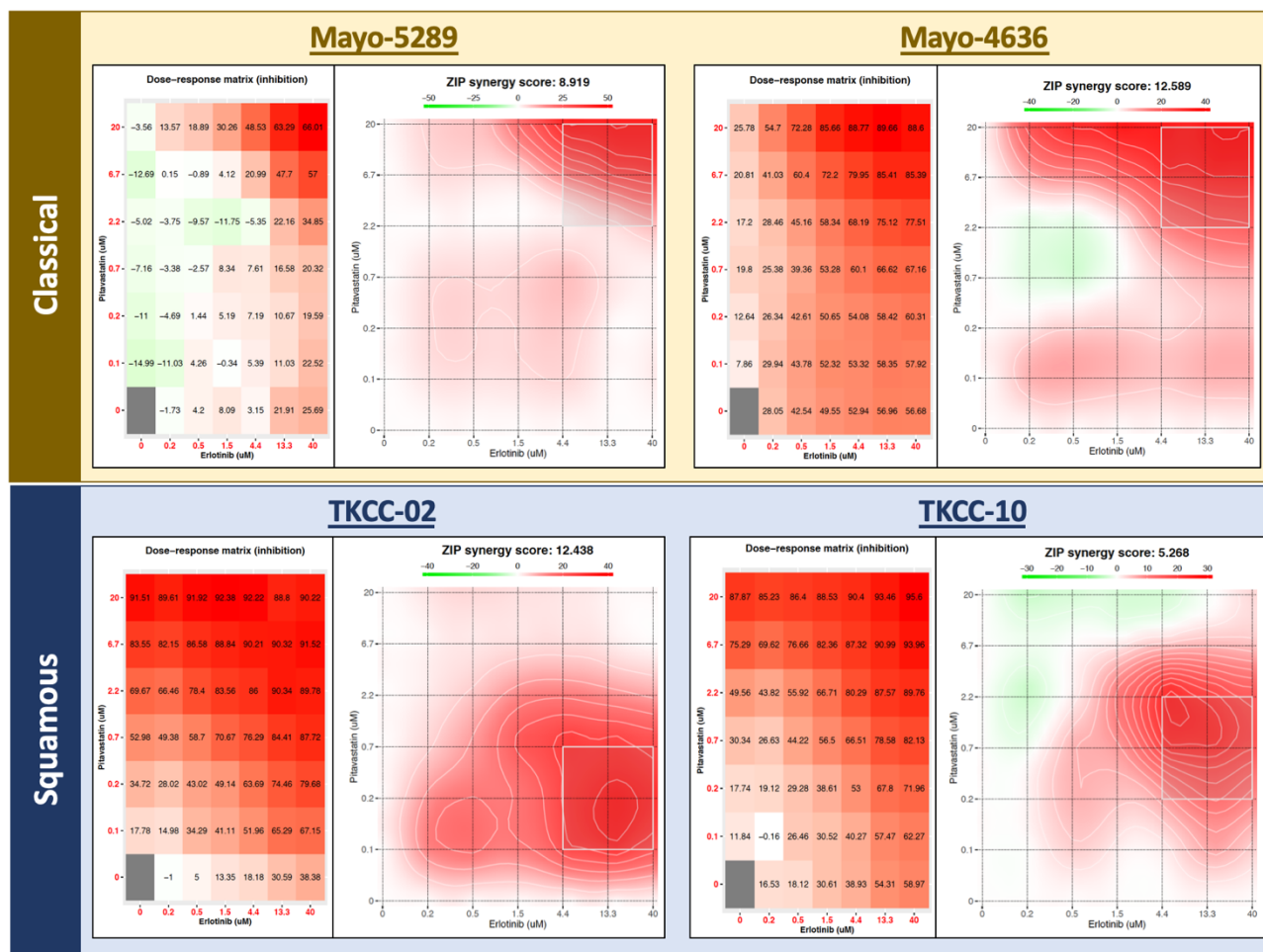


Figure 5.13 | Pitavastatin and erlotinib synergise at low concentrations in squamous PDCLs. Heatmaps showing synergies between erlotinib and pitavastatin in two PDCLs representative of each classical (top) and squamous (bottom) subtypes. For each PDCL, a heatmap representing the dose-response curves for each therapeutic is shown (left), as well as an equivalent heatmap displaying ZIP scores (right), with shading indicating areas of greatest synergy. Data corresponding to erlotinib is shown along the x-axis and pitavastatin along the y-axis. As can be seen, synergy in classical PDCLs is only seen at prohibitively high concentrations of both drugs, while in squamous cell-lines, synergy is observed at much lower concentrations (<5 μM pitavastatin, <10 μM Erlotinib).

differential sensitivities (Figure 5.14), with one cell-line in particular (Panc47) exhibiting a sensitivity approaching that observed in sensitive, squamous PDCLs ($\text{IC}_{50} = 2.6 \mu\text{M}$). This is suggestive of the existence of partial subtypes, a finding with particular relevance due to the clinical relevance of this *in vivo* model in *in vivo* research. In order to further validate this potential subgrouping, it was decided to assess the degradation status of HMGCR via western blot, as well as the

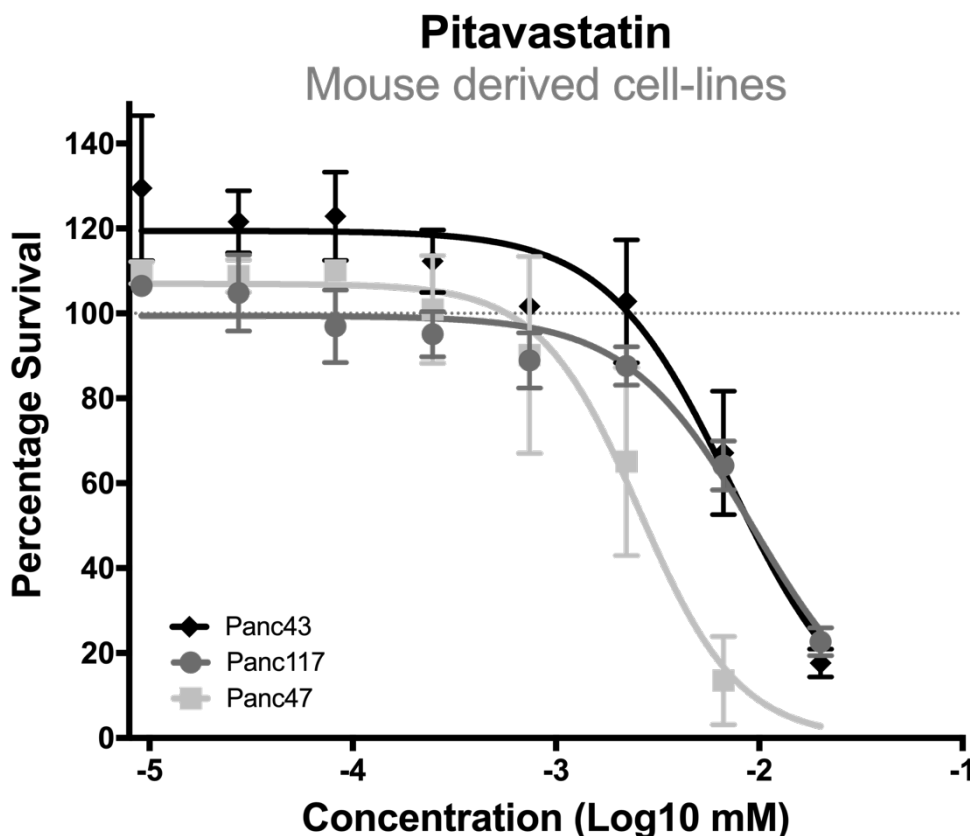


Figure 5.14 | Cell-lines derived from mouse models of pancreatic cancer exhibit differential sensitivity to pitavastatin treatment. Dose-response curve showing sensitivity of three KPC derived cell-lines after 72 hours exposure to pitavastatin. As can be seen, all cell-lines displayed some degree of sensitivity to treatment, with Panc47 in particular exhibiting loss of viability.

presence/absence of additional subtype-associated proteins; these were selected as putative markers of pitavastatin sensitivity.

Western blotting revealed the presence of the same ~60 kDa HMGCR degradation band as detected in PDCLs, with a complete absence this marker in Panc47, the cell-line most sensitive to pitavastatin treatment. In addition to this, there was a marked absence of HNF4A and slight decrease in HNF1A abundance, two transcription factors closely associated with the classical subtype in PDCLs (Figure 5.15). This finding, in contrast to what was seen in the more resistant mice cell-lines, further aligned Panc47 with the squamous subtype as presented in PDCLs. This close alignment suggests that the same mechanism of pitavastatin escape found in classical PDCLs may persist in the KPC model of pancreatic cancer,

therefore highlighting the potential of this *in vivo* system in modelling the complexities of subtype-associated responses to statin treatment and validating observations within PDCLs with the scope of greater clinical relevance.

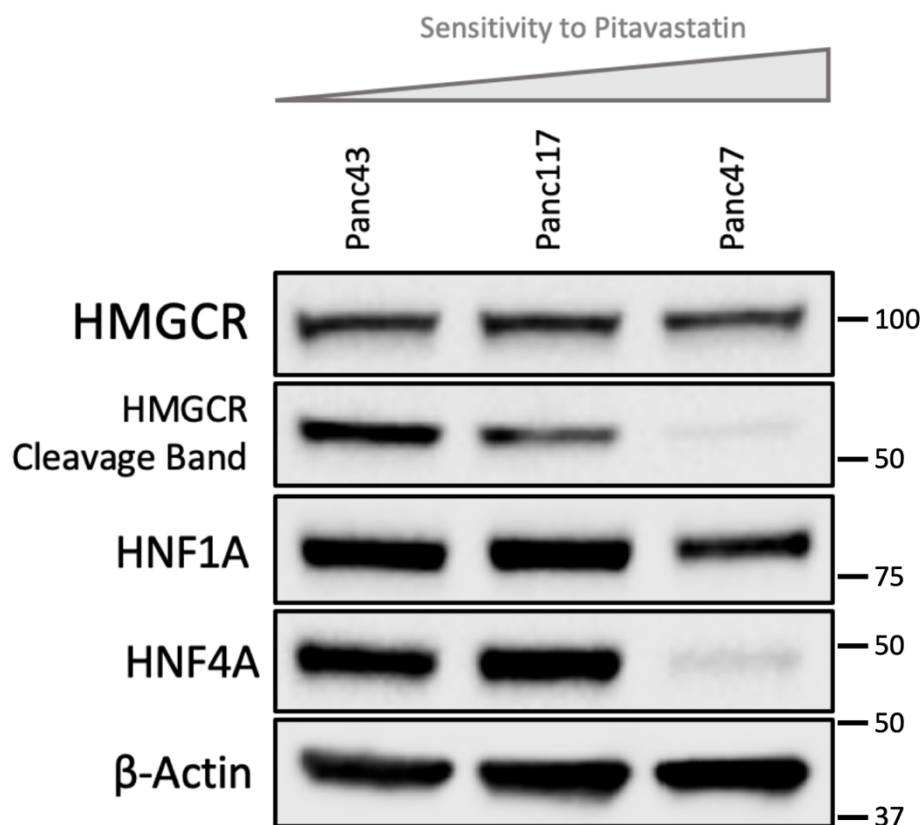


Figure 5.15 | Subtype-specific markers of pitavastatin sensitivity persist in mice models of pancreatic cancer. Western blot showing quantities of various protein products associated with pitavastatin resistance in PDCLs across three cell-lines derived from KPC mice, ordered according to increasing pitavastatin sensitivity. As previously seen in PDCLs, presence of HMGCR degradation corresponded to pitavastatin resistance, as did presence of protein markers indicative of the classical subtype. This mirrors what is found in human derived cell-lines, with cell-lines exhibiting a more squamous-like phenotype displaying greater sensitivities to pitavastatin.

5.2 Discussion

This chapter described the establishment of a collaborative high-throughput drug repurposing screen conducted in PDCLs in collaboration with the Beatson Screening Facility. This study identified a variety of compounds that elicit a subtype-

selective response, with a number of therapeutics implicated in DNA damage effecting sensitivity in squamous PDCLs (Table 5.2), including: bleomycin, which inhibits DNA ligase (Ono *et al.*, 1976), resulting in DNA breaks (Tounekti *et al.*, 2001); etoposide and irinotecan, which target topoisomerases 1 and 2 respectively (Pommier, 2013), enzymes that effect over- or underwinding of DNA via induction of strand breaks (Champoux, 2001); and fluorouracil, which induces DNA damage via dTTP depletion (Longley, Harkin and Johnston, 2003). These compounds are regularly used as part of clinical anti-cancer treatments, with proven efficacy against a range of cancer types (Einhorn and Williams, 1980; IMPACT, 1995; Hanna *et al.*, 2006), while irinotecan forms part of the FOLFIRINOX regimen which is used as standard of care in the treatment of PDAC (Conroy *et al.*, 2011). These results therefore suggest that the squamous subtype may be more sensitive to clinically relevant compounds that inhibit components of DDR, a finding that aligns with work that has demonstrated that enhanced replication stress is a signature of squamous PDCLs, conferring a dependency on DDR proteins (Dreyer *et al.*, 2019) including ATM and ATR serine/threonine kinases (ATM and ATR), which activate upon DNA damage (Durocher and Jackson, 2001; Bakkenist and Kastan, 2003), coordinating the cellular DDR response (Matsuoka *et al.*, 2007). As this work was the focus of a separate project within the group, it was decided to take alternative hits forward for follow-up analysis.

Beyond agents associated with DNA damage, screening results, supported by follow-up validation, identified the potential of statins to selectively induce cell-death in squamous cell-lines. This anti-cancer effect was most readily observed upon treatment with pitavastatin, a minimally metabolised statin (Kajinami, Takekoshi and Saito, 2003; Mukhtar, Reid and Reckless, 2005) whose efficacy as a therapeutic in an oncological context has been demonstrated in *in vitro* and *in vivo* models of a range of cancers (You *et al.*, 2016; Abdullah, Abed and Richardson, 2017), including PC (Villarino *et al.*, 2017).

Despite many preclinical efforts over the past decades, the mechanism by which statins effect their anti-cancer potential is still disputed (Sorrentino *et al.*, 2014; Wei *et al.*, 2016; Yu *et al.*, 2018). This chapter has attempted to determine these

mechanisms within pancreatic cancer cell-lines, taking an approach centred in comparisons between sensitive and resistant subtypes in PDCLs. This revealed a dysregulation of cholesterol homeostasis across subtypes, mediated by the absence or presence of caveolins. Those differences in cholesterol trafficking had apparent links to the activation of a negative feedback loop within the cholesterol biosynthesis pathway, potentially facilitating resistance to statin treatment. However, due to time constraints, it was not possible to assess the impact of CAV1 depletion on pitavastatin sensitivity, HMGCR degradation, cholesterol localisation, and lipid raft formation. This series of experiments would have been ideal to further investigate caveolin's involvement in cholesterol homeostasis and validate the relationship between intracellular trafficking and statin resistance, thus confirming the proposed mechanism of statin resistance. Despite this, it was determined that statins disrupted AKT signalling within sensitive cell-lines, with erlotinib selected as a therapeutic to partner with pitavastatin in order to take advantage of this downstream effect.

Although recent, prospective clinical trials involving statins have yielded mixed results, trial design choices that fail to fully take into account experimental data generated in preclinical research are likely to have negatively influenced results. One review argues that a range of crucial factors such as dietary intake of patients and dosing of therapeutics have not been optimised for the clinical success of statins in the context of oncology, while supporting the view that pitavastatin is the ideal choice of statin for cancer studies due to a favourable pharmacodynamic profile (Abdullah *et al.*, 2018). This importance of statin choice is reflected in a study that highlighted differential efficacy of a range of statins in *in vitro* and *in vivo* models of pancreatic cancer (Gbelcová *et al.*, 2008), although pitavastatin was not included in this set of experiments. Dietary factors, as explored in brief within this chapter, are also likely to confound sensitivity to pitavastatin in patients with PDAC. Recent research has supported this possibility, with indications that geranylgeraniol, a metabolite downstream of mevalonate and upstream of cholesterol in the mevalonate pathway, can interfere with anti-cancer properties of pitavastatin *in vivo* (de Wolf *et al.*, 2017), while demonstrating that this metabolite is present in a variety of widely consumed foodstuffs. This

highlights the need of clinical trial design to pay consideration to these concerns and echoes the findings that both cholesterol and GGPP mitigate pitavastatin sensitivity in PDCLs, as well as in a number of *in vitro* models of various cancer types (Greenaway *et al.*, 2016; Wei *et al.*, 2016; Sheikholeslami *et al.*, 2019).

Finally, findings described in this chapter have also highlighted the possibility of designing an effective therapeutic strategy in GEMMs in advance of clinical consideration, allowing for the *in vivo* assessment of pitavastatin efficacy. This would involve pitavastatin treatment with concurrent dietary limitation, ensuring a minimal intake of cholesterol and GGPP, with the additional possibility of treating with a combination of erlotinib. These *in vivo* experiments would be ideal for establishing a clinically viable regimen of therapeutic administration and dietary limitation, with the added benefit of facilitating dosage optimisation and allowing the assessment of efficacy of pitavastatin treatment in combination with erlotinib.

Chapter 6 *Concluding Remarks*

Concluding Remarks

6.1 Summary of project findings

In order to address the lack of therapeutics effective in treating pancreatic cancer, this body of work has outlined a subtype-focused approach. By harnessing an *in vitro* model of PDAC subtypes that reflects clinical subgrouping (Bailey *et al.*, 2016) and providing extensive characterisation of pathways associated with pancreatic cancer, it was intended to identify novel, stratified vulnerabilities likely to be represented in subgroups within a clinical setting. Interrogation of transcriptomic and proteomic data, in tandem with experiments quantifying rates of metabolic processes linked to PC (Ying *et al.*, 2012; Kamphorst *et al.*, 2013; Daemen *et al.*, 2015), led to the identification of highly divergent metabolic phenotypes which aligned closely to subtypes:

- Squamous; highly glycolytic phenotype, exhibiting increased aerobic glycolysis and decreased OXPHOS.
- Classical; highly oxidative with high levels of FAO, with an associated upregulation of lipid biosynthesis suggesting a balance between catabolism and anabolism.

This allowed for the generation of strategies to exploit potential vulnerabilities associated with these distinct metabolic dependencies, with two separate approaches developed in order to maximise the possibility of discovering effective therapeutics. This involved: (1) performing literature searches to identify novel drug targets corresponding to subtype-associated metabolic pathways, while incorporating all PDCL data available for review, including RNA-seq, proteomics, siRNA screening, and metabolic assays; (2) performing high-throughput drug repurposing screening, with libraries containing a variety of general purpose, metabolism-targeting compounds.

The first approach identified ALDOA, a highly active isoform of aldolase (Chang *et al.*, 2018), a glycolytic enzyme that catalyses early glycolysis, upregulated in the squamous subtype, as a potential target of squamous-associated glycolysis. Follow-up experiments involving a therapeutic inhibitor of ALDOA, TDZD-8 (Grandjean, de Jong, B. P. James, *et al.*, 2016), demonstrated its potential to successfully inhibit glycolysis selectively in PDCLs belonging to the squamous subtype. This effectively induced cell death *in vitro*, however, *in vivo* experiments would be required to validate its efficacy in treating pancreatic cancer. This strategy also allowed for the characterisation of metabolic flexibility within classical PDCLs, as inhibition of FA biosynthesis resulted in a compensatory activation of glycolysis within this subtype. This phenomenon bears clear clinical relevance due to its potential to facilitate emergence of resistance to metabolic inhibition (Boudreau *et al.*, 2016; Biancur *et al.*, 2017) and as a result of these observations, JQ1 was discovered to therapeutically mitigate this resistance mechanism. This inhibitor of epigenetic reader proteins was found to act to induce widespread changes at the transcriptomic level, effecting dysregulation of a range of metabolic genes, consistent with other research conducted within PC (Sakamaki *et al.*, 2017; Sherman *et al.*, 2017), allowing for the sensitisation of classical cell-lines to the targeting of lipid biosynthesis via FASN inhibitors.

The second approach of drug repurposing screening identified statins as a possible therapeutic effective selectively in squamous PDAC. In order to enhance clinical potential by finding optimal treatment strategies, the mechanism by which statin sensitivity is induced selectively in squamous PDCLs was investigated. This line of research identified the potential of pairing with the EGFR inhibitor erlotinib *in vitro*, alongside the possibility that dietary limitation may be necessary to induce a full response to statins in a clinical setting.

6.2 Conclusions and future work

Pancreatic cancer is highly aggressive, with the poor prognosis associated with the disease reflective of its refractory nature. Poor outcomes are in part accounted for

by the failure of standard of care therapeutics in effectively managing metastasised PDAC, with overall survivals of less than a year typically observed in patients receiving chemotherapeutic treatments (Kamisawa *et al.*, 2016). This shortcoming must be addressed and viable therapeutics found in order to improve PC prognoses, with one area of emerging interest of clinical potential being the targeting of cell metabolism in PDAC (Blum and Kloog, 2014; Cohen *et al.*, 2015; Garrido-Laguna and Hidalgo, 2015). This interest is driven by the degree of metabolic dysregulation observed in pancreatic cancer, with reprogramming in glycolysis (Zhou *et al.*, 2011; Ying *et al.*, 2012; Guillaumond *et al.*, 2013), glutamine metabolism (Son *et al.*, 2013; Biancur *et al.*, 2017), autophagy (Perera *et al.*, 2015; Yang *et al.*, 2018) and FAO (Khasawneh *et al.*, 2009; Kamphorst *et al.*, 2013) associated with cancer development, while preclinical efforts have demonstrated the efficacy of a range of therapeutics that target each of these pathways (Maftouh *et al.*, 2014; Ventura *et al.*, 2015; Brandi *et al.*, 2017).

Heterogeneity is a dominant feature of PC, which is defined by a high number of low prevalence mutations found in patient genomes (Biankin *et al.*, 2012; Waddell, Pajic, A.-M. Patch, *et al.*, 2015). This is most clearly apparent when considering the wide range of mutations that have been implicated in driving oncogenesis, with one study which harnessed a transposon-based insertional mutagenesis screen having identified >500 genes as candidate drivers, primarily acting as potential tumour suppressors whose loss promotes cancer progression in *in vivo* models (Mann *et al.*, 2012). In order to address this complex mutational landscape, recent efforts have focussed on subtyping patients into workable groups (Collisson *et al.*, 2011, 2019; Bailey *et al.*, 2016), allowing for the identification of shared vulnerabilities. These subtypes are of particular relevance to the field of clinical pancreatic cancer research as recent work has demonstrated the capacity to rapidly subtype PDAC patients upon diagnosis (Aguirre *et al.*, 2018). The work detailed as part of this thesis has described the definition of subtypes *in vitro*, which faithfully recapitulate those identified in patients. Due to this overlap, these cell-lines represent an ideal model to guide translational research efforts; as pathways dysregulated in patients are also perturbed in cell-lines, therapeutics

identified that act to inhibit these processes and which elicit a subtype-selective response are likely to be of clinical relevance.

This work has demonstrated the existence of distinct metabolic phenotypes, which are associated with PDAC subtypes and exhibit differential sensitivities to metabolic inhibition via therapeutics. This can be summarised as such: *in vitro*, the squamous subtype is defined by upregulated glycolysis, with an enhanced sensitivity to inhibition of glycolysis, while the classical subtype exhibits increased FA biosynthesis and metabolism. The discovery of these phenotypes and inherent vulnerabilities is supported by a similar project that identified two *in vitro* metabolic subtypes in pancreatic cancer, subsequently demonstrating that the upregulation of glycolysis and FA biosynthesis associated with these distinct groups predict sensitivity to targeting these processes (Daemen *et al.*, 2015). Efforts described in this thesis serve to expand on this, having identified a potential transcriptionally coordinated origin of metabolic reprogramming corresponding to gene dysregulation associated with subtypes (Bailey *et al.*, 2016). This is further evidenced by the finding that dysregulation of genes involved in glycolysis at the transcriptome level informs metabolic subtypes found in patient populations (Follia *et al.*, 2019). Work within has additionally identified metabolic flexibility associated with the classical subtype, a phenomenon described previously in pancreatic cancer (Kimmelman, 2015; Boudreau *et al.*, 2016; Biancur *et al.*, 2017), while JQ1, a therapeutic with clinically viable analogues (Alqahtani *et al.*, 2019), was found to abrogate this flexibility *in vitro*.

Expanding on the clinical utility of these described metabolic perturbations, the glycolytic phenotype associated with the squamous subtype has the potential for clinical detection via the diagnostic tool, FDG-PET. This imaging technique, described in chapter 1.5.1, allows for detection of transformed cells exhibiting the increased glucose uptake associated with the Warburg Effect (Adams *et al.*, 1998). Regarding the use of this tool in diagnosing PC, historic efforts have identified some factors that may confound efficacy of PDAC detection, including hyperglycaemia and diabetes status (Diederichs *et al.*, 1998, 2000), while recent meta-analyses have demonstrated that FDG-PET has limited utility in diagnosing PC

relative to alternative diagnostic tools (Wang *et al.*, 2013; Rijkers *et al.*, 2014). Despite these findings, FDG-PET has been shown demonstrate prognostic value, with a correlation found between FDG uptake and poor survival outcomes in patients with PC (Ahn *et al.*, 2014; Yamamoto *et al.*, 2015; Chen *et al.*, 2016). These observations are particularly striking given the poor prognosis associated with patients classified with squamous PDAC (Bailey *et al.*, 2016), along with the finding that glycolytic activation, as a result of the emergence of gemcitabine resistance in PDAC cell-lines, leads to enhanced FDG-PET detection upon implantation in *in vivo* models (Shukla *et al.*, 2017), and serve to collectively suggest that patients with squamous PDAC may be more readily detected via FDG-PET.

In addition to this, future work has been suggested within this thesis which would involve the probing of efficacy of statins in *in vivo* models of PDAC. Research was initially conducted in order to determine the mechanism of action by which statins exert their subtype-selective response, with squamous PDCLs exhibiting greater sensitivity than classical, as observed in drug repurposing screening and subsequently validated. This demonstrated the potential of commonly found foodstuffs to limit the anti-cancer efficacy of statin treatment *in vitro*, a finding in-line with other preclinical research efforts (Greenaway *et al.*, 2016; Wei *et al.*, 2016; Sheikholeslami *et al.*, 2019), suggesting that dietary limitation may be an effective strategy in a clinical setting (de Wolf *et al.*, 2017; Abdullah *et al.*, 2018). Additionally, combination therapies demonstrated the potential of pairing pitavastatin with erlotinib in squamous PDCLs, which supports previous observations that EGFR inhibition enhances statin's ability to inhibit cancer progression both *in vitro* (Mantha *et al.*, 2005; Dimitroulakos, Lorimer and Goss, 2006) and in patients with lung cancer (Hung *et al.*, 2017). As proof that these findings can be translated into clinically viable strategies, future work would be required to assess the efficacy of both treatment approaches in *in vivo* models of PDAC, which would ideally be conducted within mouse models of PDAC subtypes. Early subtyping efforts indicated that cell-lines derived from GEMMs of PDAC exhibited both classical and squamous subtypes (Collisson *et al.*, 2011), a finding supported by recent work that identified subtypes within the KPC model of PDAC

(Candido *et al.*, 2018). Research conducted as part of this thesis utilising cell-lines derived from KPC mice suggests that these cell-lines exhibit differential sensitivities to pitavastatin according to subtype, as determined by select biomarkers. Collectively, these findings therefore suggest the potential of assessing pitavastatin efficacy in KPC mouse models.

Finally, this work also describes the establishment of a collaborative high-throughput screening project with the Beatson Screening Facility. This project has the potential to be expanded on in future work, with morphological data resulting from the screen to be analysed in-house by the Screening Facility. Results obtained from these analyses may inform future projects, with the potential to identify novel therapeutics effective in treating PDAC subtypes *in vitro* necessitating follow-up studies including validation experiments and *in vivo* testing.

The work described within this thesis has outlined attempts to identify therapeutic strategies to effectively target metabolic processes in PDAC subtypes *in vitro*. This has revealed the potential of inhibiting both glycolysis and the mevalonate pathway within squamous cell-lines. It has also served to characterise metabolic flexibility associated with the classical subtype, which necessitates combinatorial strategies, targeting both flexibility and FA biosynthesis, to elicit a response. This work has therefore served to characterise associations between metabolic pathways and PDAC subtypes, facilitating the identification of a number of therapeutic targets, with screening projects initiated as part of this project poised to identify further clinically exploitable vulnerabilities.

References

Abdullah, M. I. *et al.* (2018) 'The poor design of clinical trials of statins in oncology may explain their failure - Lessons for drug repurposing.', *Cancer treatment reviews*, 69, pp. 84-89. doi: 10.1016/j.ctrv.2018.06.010.

Abdullah, M. I., Abed, M. N. and Richardson, A. (2017) 'Inhibition of the mevalonate pathway augments the activity of pitavastatin against ovarian cancer cells', *Scientific Reports*, 7(1), p. 8090. doi: 10.1038/s41598-017-08649-9.

Abu-Elheiga, L. *et al.* (2000) 'The subcellular localization of acetyl-CoA carboxylase 2.', *Proceedings of the National Academy of Sciences of the United States of America*, 97(4), pp. 1444-9. Available at: <http://www.ncbi.nlm.nih.gov/pubmed/10677481>.

Abu-Elheiga, L. *et al.* (2001) 'Continuous fatty acid oxidation and reduced fat storage in mice lacking acetyl-CoA carboxylase 2.', *Science (New York, N.Y.)*, 291(5513), pp. 2613-6. doi: 10.1126/science.1056843.

Adams, S. *et al.* (1998) 'Prospective comparison of 18 F-FDG PET with conventional imaging modalities (CT, MRI, US) in lymph node staging of head and neck cancer', *European Journal of Nuclear Medicine and Molecular Imaging*, 25(9), pp. 1255-1260. doi: 10.1007/s002590050293.

Agnese, S. T., Spierto, F. W. and Hannon, W. H. (1983) 'Evaluation of four reagents for delipidation of serum.', *Clinical biochemistry*, 16(2), pp. 98-100. Available at: <http://www.ncbi.nlm.nih.gov/pubmed/6192945>.

Aguirre, A. J. *et al.* (2018) 'Real-time Genomic Characterization of Advanced Pancreatic Cancer to Enable Precision Medicine', *Cancer Discovery*, 8(9), pp. 1096-1111. doi: 10.1158/2159-8290.CD-18-0275.

Ahlgren, U., Jonsson, J. and Edlund, H. (1996) 'The morphogenesis of the pancreatic mesenchyme is uncoupled from that of the pancreatic epithelium in IPF1/PDX1-deficient mice.', *Development (Cambridge, England)*, 122(5), pp. 1409-16. Available at: <http://www.ncbi.nlm.nih.gov/pubmed/8625829>.

Ahn, S. J. *et al.* (2014) 'Correlation between 18F-fluorodeoxyglucose positron emission tomography and pathologic differentiation in pancreatic cancer', *Annals*

- of *Nuclear Medicine*, 28(5), pp. 430-435. doi: 10.1007/s12149-014-0833-x.
- Alexakis, N. *et al.* (2004) 'Current standards of surgery for pancreatic cancer.', *The British journal of surgery*, 91(11), pp. 1410-27. doi: 10.1002/bjs.4794.
- Alexandrov, L. B. *et al.* (2013) 'Signatures of mutational processes in human cancer.', *Nature*, 500(7463), pp. 415-21. doi: 10.1038/nature12477.
- Ali, B. R. *et al.* (2010) 'A novel statin-mediated "prenylation block-and-release" assay provides insight into the membrane targeting mechanisms of small GTPases', *Biochemical and Biophysical Research Communications*, 397(1), pp. 34-41. doi: 10.1016/j.bbrc.2010.05.045.
- Alqahtani, A. *et al.* (2019) 'Bromodomain and extra-terminal motif inhibitors: a review of preclinical and clinical advances in cancer therapy.', *Future science OA*, 5(3), p. FSO372. doi: 10.4155/fsoa-2018-0115.
- Anderson, M. *et al.* (2017) 'Hexokinase 2 promotes tumor growth and metastasis by regulating lactate production in pancreatic cancer.', *Oncotarget*, 8(34), pp. 56081-56094. doi: 10.18632/oncotarget.9760.
- Anderson, R. G. (1998) 'The caveolae membrane system.', *Annual review of biochemistry*, 67, pp. 199-225. doi: 10.1146/annurev.biochem.67.1.199.
- Asaka, M. *et al.* (1994) 'Alteration of aldolase isozymes in serum and tissues of patients with cancer and other diseases.', *Journal of clinical laboratory analysis*, 8(3), pp. 144-8. Available at: <http://www.ncbi.nlm.nih.gov/pubmed/8046542>.
- Asano, T. *et al.* (2004) 'The PI 3-kinase/Akt signaling pathway is activated due to aberrant Pten expression and targets transcription factors NF- κ B and c-Myc in pancreatic cancer cells', *Oncogene*, 23(53), pp. 8571-8580. doi: 10.1038/sj.onc.1207902.
- Ashburner, M. *et al.* (2000) 'Gene ontology: tool for the unification of biology. The Gene Ontology Consortium.', *Nature genetics*, 25(1), pp. 25-9. doi: 10.1038/75556.
- Aune, D. *et al.* (2012) 'Body mass index, abdominal fatness and pancreatic cancer risk: a systematic review and non-linear dose-response meta-analysis of prospective studies.', *Annals of oncology : official journal of the European Society for Medical Oncology*, 23(4), pp. 843-52. doi: 10.1093/annonc/mdr398.
- Avan, A. *et al.* (2012) 'Molecular Mechanisms Involved in the Synergistic

- Interaction of the EZH2 Inhibitor 3-Deazaneplanocin A with Gemcitabine in Pancreatic Cancer Cells', *Molecular Cancer Therapeutics*, 11(8), pp. 1735-1746. doi: 10.1158/1535-7163.MCT-12-0037.
- Baek, G. *et al.* (2014) 'MCT4 defines a glycolytic subtype of pancreatic cancer with poor prognosis and unique metabolic dependencies.', *Cell reports*, 9(6), pp. 2233-49. doi: 10.1016/j.celrep.2014.11.025.
- Baigent, C. *et al.* (2005) 'Efficacy and safety of cholesterol-lowering treatment: prospective meta-analysis of data from 90,056 participants in 14 randomised trials of statins.', *Lancet (London, England)*, 366(9493), pp. 1267-78. doi: 10.1016/S0140-6736(05)67394-1.
- Bailey, P. *et al.* (2016) 'Genomic analyses identify molecular subtypes of pancreatic cancer', *Nature*, 531(7592), pp. 47-52. doi: 10.1038/nature16965.
- Bain, J. *et al.* (2007) 'The selectivity of protein kinase inhibitors: a further update.', *The Biochemical journal*, 408(3), pp. 297-315. doi: 10.1042/BJ20070797.
- Bakkenist, C. J. and Kastan, M. B. (2003) 'DNA damage activates ATM through intermolecular autophosphorylation and dimer dissociation', *Nature*, 421(6922), pp. 499-506. doi: 10.1038/nature01368.
- Bartz, R. *et al.* (2007) 'Lipidomics reveals that adiposomes store ether lipids and mediate phospholipid traffic.', *Journal of lipid research*, 48(4), pp. 837-47. doi: 10.1194/jlr.M600413-JLR200.
- Basturk, O. *et al.* (2015) 'A Revised Classification System and Recommendations From the Baltimore Consensus Meeting for Neoplastic Precursor Lesions in the Pancreas.', *The American journal of surgical pathology*, 39(12), pp. 1730-41. doi: 10.1097/PAS.0000000000000533.
- Beckwitt, C. H., Shiraha, K. and Wells, A. (2018) 'Lipophilic statins limit cancer cell growth and survival, via involvement of Akt signaling.', *PloS one*, 13(5), p. e0197422. doi: 10.1371/journal.pone.0197422.
- Beer, N. L. and Gloyn, A. L. (2016) 'Genome-edited human stem cell-derived beta cells: a powerful tool for drilling down on type 2 diabetes GWAS biology.', *F1000Research*, 5. doi: 10.12688/f1000research.8682.1.
- Belkina, A. C. and Denis, G. V. (2012) 'BET domain co-regulators in obesity, inflammation and cancer', *Nature Reviews Cancer*, 12(7), pp. 465-477. doi:

10.1038/nrc3256.

Bergmann, U. *et al.* (1995) 'Insulin-like growth factor I overexpression in human pancreatic cancer: evidence for autocrine and paracrine roles.', *Cancer research*, 55(10), pp. 2007-11. Available at:

<http://www.ncbi.nlm.nih.gov/pubmed/7743492>.

Bertolini, F., Sukhatme, V. P. and Bouche, G. (2015) 'Drug repurposing in oncology—patient and health systems opportunities', *Nature Reviews Clinical Oncology*, 12(12), pp. 732-742. doi: 10.1038/nrclinonc.2015.169.

Biancur, D. E. *et al.* (2017) 'Compensatory metabolic networks in pancreatic cancers upon perturbation of glutamine metabolism.', *Nature communications*, 8(May), p. 15965. doi: 10.1038/ncomms15965.

Biankin, A. V *et al.* (2012) 'Pancreatic cancer genomes reveal aberrations in axon guidance pathway genes.', *Nature*, 491(7424), pp. 399-405. doi: 10.1038/nature11547.

Blum, R. and Kloog, Y. (2014) 'Metabolism addiction in pancreatic cancer', *Cell Death and Disease*, 5(2), p. e1065. doi: 10.1038/cddis.2014.38.

Bondar, V. M. *et al.* (2002) 'Inhibition of the phosphatidylinositol 3'-kinase-AKT pathway induces apoptosis in pancreatic carcinoma cells in vitro and in vivo.', *Molecular cancer therapeutics*, 1(12), pp. 989-97. Available at: <http://www.ncbi.nlm.nih.gov/pubmed/12481421>.

Booth, L. *et al.* (2019) 'Prior exposure of pancreatic tumors to [sorafenib + vorinostat] enhances the efficacy of an anti-PD-1 antibody.', *Cancer biology & therapy*, 20(1), pp. 109-121. doi: 10.1080/15384047.2018.1507258.

Boren, J. and Brindle, K. M. (2012) 'Apoptosis-induced mitochondrial dysfunction causes cytoplasmic lipid droplet formation.', *Cell death and differentiation*, 19(9), pp. 1561-70. doi: 10.1038/cdd.2012.34.

Bosetti, C. *et al.* (2012) 'Pancreatic cancer: overview of descriptive epidemiology.', *Molecular carcinogenesis*, 51(1), pp. 3-13. doi: 10.1002/mc.20785.

Böttger, S. and Melzig, M. F. (2013) 'The influence of saponins on cell membrane cholesterol.', *Bioorganic & medicinal chemistry*, 21(22), pp. 7118-24. doi: 10.1016/j.bmc.2013.09.008.

Boudreau, A. *et al.* (2016) 'Metabolic plasticity underpins innate and acquired

resistance to LDHA inhibition', *Nature Chemical Biology*, 12(10), pp. 779-786. doi: 10.1038/nchembio.2143.

Boulares, A. H. *et al.* (1999) 'Role of Poly(ADP-ribose) Polymerase (PARP) Cleavage in Apoptosis', *Journal of Biological Chemistry*, 274(33), pp. 22932-22940. doi: 10.1074/jbc.274.33.22932.

Bournet, B. *et al.* (2016) 'KRAS G12D Mutation Subtype Is A Prognostic Factor for Advanced Pancreatic Adenocarcinoma.', *Clinical and translational gastroenterology*, 7, p. e157. doi: 10.1038/ctg.2016.18.

Brandi, J. *et al.* (2017) 'Proteomic analysis of pancreatic cancer stem cells: Functional role of fatty acid synthesis and mevalonate pathways', *Journal of Proteomics*, 150, pp. 310-322. doi: 10.1016/j.jprot.2016.10.002.

Brown, D. A. and London, E. (1998) 'FUNCTIONS OF LIPID RAFTS IN BIOLOGICAL MEMBRANES', *Annual Review of Cell and Developmental Biology*, 14(1), pp. 111-136. doi: 10.1146/annurev.cellbio.14.1.111.

Brown, D. A. and London, E. (2000) 'Structure and Function of Sphingolipid- and Cholesterol-rich Membrane Rafts', *Journal of Biological Chemistry*, 275(23), pp. 17221-17224. doi: 10.1074/jbc.R000005200.

Brown, P. J. and Müller, S. (2015) 'Open access chemical probes for epigenetic targets.', *Future medicinal chemistry*, 7(14), pp. 1901-17. doi: 10.4155/fmc.15.127.

Bryant, C., Voller, A. and Smith, M. J. (1964) 'The incorporation of radioactivity from (14C) Glucose into the Soluble metabolic intermediates of Malaria parasites.', *The American journal of tropical medicine and hygiene*, 13, pp. 515-9. doi: 10.4269/ajtmh.1964.13.515.

Burris, H. A. *et al.* (1997) 'Improvements in survival and clinical benefit with gemcitabine as first-line therapy for patients with advanced pancreas cancer: a randomized trial', *J Clin Oncol*, 15(6), pp. 2403-2413.

Burt, B. M. *et al.* (2001) 'Using positron emission tomography with [(18)F]FDG to predict tumor behavior in experimental colorectal cancer.', *Neoplasia (New York, N.Y.)*, 3(3), pp. 189-95. doi: 10.1038/sj.neo.7900147.

Buzzai, M. *et al.* (2005) 'The glucose dependence of Akt-transformed cells can be reversed by pharmacologic activation of fatty acid beta-oxidation.', *Oncogene*,

24(26), pp. 4165-73. doi: 10.1038/sj.onc.1208622.

Cai, Y. *et al.* (2017) 'Critical threshold levels of DNA methyltransferase 1 are required to maintain DNA methylation across the genome in human cancer cells', *Genome Research*, 27(4), pp. 533-544. doi: 10.1101/gr.208108.116.

Calay, D. *et al.* (2010) 'Inhibition of Akt signaling by exclusion from lipid rafts in normal and transformed epidermal keratinocytes.', *The Journal of investigative dermatology*, 130(4), pp. 1136-45. doi: 10.1038/jid.2009.415.

Cancer Genome Atlas Research Network. (2017) 'Integrated Genomic Characterization of Pancreatic Ductal Adenocarcinoma.', *Cancer cell*, 32(2), pp. 185-203.e13. doi: 10.1016/j.ccell.2017.07.007.

Candido, J. B. *et al.* (2018) 'CSF1R+ Macrophages Sustain Pancreatic Tumor Growth through T Cell Suppression and Maintenance of Key Gene Programs that Define the Squamous Subtype.', *Cell reports*, 23(5), pp. 1448-1460. doi: 10.1016/j.celrep.2018.03.131.

Carpenter, A. E. *et al.* (2006) 'CellProfiler: image analysis software for identifying and quantifying cell phenotypes.', *Genome biology*, 7(10), p. R100. doi: 10.1186/gb-2006-7-10-r100.

Carracedo, A., Cantley, L. C. and Pandolfi, P. P. (2013) 'Cancer metabolism: fatty acid oxidation in the limelight.', *Nature reviews. Cancer*, 13(4), pp. 227-32. doi: 10.1038/nrc3483.

Ceddia, R. B. (2013) 'The role of AMP-activated protein kinase in regulating white adipose tissue metabolism', *Molecular and Cellular Endocrinology*, 366(2), pp. 194-203. doi: 10.1016/j.mce.2012.06.014.

Chajès, V. *et al.* (2006) 'Acetyl-CoA carboxylase alpha is essential to breast cancer cell survival.', *Cancer research*, 66(10), pp. 5287-94. doi: 10.1158/0008-5472.CAN-05-1489.

Champoux, J. J. (2001) 'DNA topoisomerases: structure, function, and mechanism.', *Annual review of biochemistry*, 70, pp. 369-413. doi: 10.1146/annurev.biochem.70.1.369.

Chandra, A. *et al.* (2011) 'The GDI-like solubilizing factor PDE δ sustains the spatial organization and signalling of Ras family proteins.', *Nature cell biology*, 14(2), pp. 148-58. doi: 10.1038/ncb2394.

- Chang, Y.-C. *et al.* (2018) 'Roles of Aldolase Family Genes in Human Cancers and Diseases.', *Trends in endocrinology and metabolism: TEM*, 29(8), pp. 549-559. doi: 10.1016/j.tem.2018.05.003.
- Chapman, P. B. *et al.* (2011) 'Improved survival with vemurafenib in melanoma with BRAF V600E mutation.', *The New England journal of medicine*, 364(26), pp. 2507-16. doi: 10.1056/NEJMoa1103782.
- Chen, B.-B. *et al.* (2016) 'PET/MRI in pancreatic and periampullary cancer: correlating diffusion-weighted imaging, MR spectroscopy and glucose metabolic activity with clinical stage and prognosis', *European Journal of Nuclear Medicine and Molecular Imaging*, 43(10), pp. 1753-1764. doi: 10.1007/s00259-016-3356-y.
- Chen, H. *et al.* (2015) 'Association between cholesterol intake and pancreatic cancer risk: evidence from a meta-analysis.', *Scientific reports*, 5, p. 8243. doi: 10.1038/srep08243.
- Chen, H., Liu, H. and Qing, G. (2018) 'Targeting oncogenic Myc as a strategy for cancer treatment', *Signal Transduction and Targeted Therapy*, 3(1), p. 5. doi: 10.1038/s41392-018-0008-7.
- Chick, J. *et al.* (1992) 'Disulfiram Treatment of Alcoholism', *British Journal of Psychiatry*, 161(1), pp. 84-89. doi: 10.1192/bjp.161.1.84.
- Chondrogianni, N., Fragoulis, E. G. and Gonos, E. S. (2002) 'Protein degradation during aging: the lysosome-, the calpain- and the proteasome-dependent cellular proteolytic systems.', *Biogerontology*, 3(1-2), pp. 121-3. doi: <https://doi.org/10.1023/A:1015236203379>.
- Clarke, S. (1992) 'Protein Isoprenylation and Methylation at Carboxyl-Terminal Cysteine Residues', *Annual Review of Biochemistry*, 61(1), pp. 355-386. doi: 10.1146/annurev.bi.61.070192.002035.
- Clendening, J. W. *et al.* (2010) 'Exploiting the mevalonate pathway to distinguish statin-sensitive multiple myeloma.', *Blood*, 115(23), pp. 4787-97. doi: 10.1182/blood-2009-07-230508.
- Cline, G. W. *et al.* (2002) 'Effects of a novel glycogen synthase kinase-3 inhibitor on insulin-stimulated glucose metabolism in Zucker diabetic fatty (fa/fa) rats.', *Diabetes*, 51(10), pp. 2903-10. doi: 10.2337/diabetes.51.10.2903.
- Clinical Trials Transformation Initiative (no date) *Improving public access to*

aggregate content of *ClinicalTrials.gov*. Available at: <https://aact.ctti-clinicaltrials.org/> (Accessed: 5 May 2019).

Cohen, R. *et al.* (2015) 'Targeting cancer cell metabolism in pancreatic adenocarcinoma.', *Oncotarget*, 6(19), pp. 16832-47. doi: 10.18632/oncotarget.4160.

Collins, M. A. *et al.* (2012) 'Metastatic pancreatic cancer is dependent on oncogenic Kras in mice.', *PloS one*, 7(12), p. e49707. doi: 10.1371/journal.pone.0049707.

Collisson, E. A. *et al.* (2011) 'Subtypes of pancreatic ductal adenocarcinoma and their differing responses to therapy.', *Nature medicine*, 17(4), pp. 500-3. doi: 10.1038/nm.2344.

Collisson, E. A. *et al.* (2019) 'Molecular subtypes of pancreatic cancer.', *Nature reviews. Gastroenterology & hepatology*, 16(4), pp. 207-220. doi: 10.1038/s41575-019-0109-y.

Conrad, P. A. *et al.* (1995) 'Caveolin cycles between plasma membrane caveolae and the Golgi complex by microtubule-dependent and microtubule-independent steps.', *The Journal of cell biology*, 131(6 Pt 1), pp. 1421-33. doi: 10.1083/jcb.131.6.1421.

Conroy, T. *et al.* (2011) 'FOLFIRINOX versus gemcitabine for metastatic pancreatic cancer.', *The New England journal of medicine*, 364(19), pp. 1817-25. doi: 10.1056/NEJMoa1011923.

Cox, A. D. *et al.* (2014) 'Drugging the undruggable RAS: Mission possible?', *Nature reviews. Drug discovery*, 13(11), pp. 828-51. doi: 10.1038/nrd4389.

Csaki, L. S. and Reue, K. (2010) 'Lipins: multifunctional lipid metabolism proteins.', *Annual review of nutrition*, 30, pp. 257-72. doi: 10.1146/annurev.nutr.012809.104729.

Cubilla, A. L. and Fitzgerald, P. J. (1979) 'Classification of pancreatic cancer (nonendocrine).', *Mayo Clinic proceedings*, 54(7), pp. 449-58. Available at: <http://www.ncbi.nlm.nih.gov/pubmed/221755>.

Currie, E. *et al.* (2013) 'Cellular fatty acid metabolism and cancer.', *Cell metabolism*, 18(2), pp. 153-61. doi: 10.1016/j.cmet.2013.05.017.

Daemen, A. *et al.* (2015) 'Metabolite profiling stratifies pancreatic ductal

- adenocarcinomas into subtypes with distinct sensitivities to metabolic inhibitors', *Proceedings of the National Academy of Sciences*, 112(32), pp. E4410-E4417. doi: 10.1073/pnas.1501605112.
- Dang, C. V., Le, A. and Gao, P. (2009) 'MYC-Induced Cancer Cell Energy Metabolism and Therapeutic Opportunities', *Clinical Cancer Research*, 15(21), pp. 6479-6483. doi: 10.1158/1078-0432.CCR-09-0889.
- Daval, M. *et al.* (2005) 'Anti-lipolytic Action of AMP-activated Protein Kinase in Rodent Adipocytes', *Journal of Biological Chemistry*, 280(26), pp. 25250-25257. doi: 10.1074/jbc.M414222200.
- Davies, H. *et al.* (2002) 'Mutations of the BRAF gene in human cancer.', *Nature*, 417(6892), pp. 949-54. doi: 10.1038/nature00766.
- Dawson, M. A. *et al.* (2011) 'Inhibition of BET recruitment to chromatin as an effective treatment for MLL-fusion leukaemia', *Nature*, 478(7370), pp. 529-533. doi: 10.1038/nature10509.
- Dawson, M. A., Kouzarides, T. and Huntly, B. J. P. (2012) 'Targeting Epigenetic Readers in Cancer', *New England Journal of Medicine*, 367(7), pp. 647-657. doi: 10.1056/NEJMra1112635.
- DeBose-Boyd, R. A. (2008) 'Feedback regulation of cholesterol synthesis: sterol-accelerated ubiquitination and degradation of HMG CoA reductase', *Cell Research*, 18(6), pp. 609-621. doi: 10.1038/cr.2008.61.
- Decker, K. *et al.* (2006) 'Gata6 is an important regulator of mouse pancreas development.', *Developmental biology*, 298(2), pp. 415-29. doi: 10.1016/j.ydbio.2006.06.046.
- Degenhardt, K. *et al.* (2006) 'Autophagy promotes tumor cell survival and restricts necrosis, inflammation, and tumorigenesis.', *Cancer cell*, 10(1), pp. 51-64. doi: 10.1016/j.ccr.2006.06.001.
- Delmore, J. E. *et al.* (2011) 'BET bromodomain inhibition as a therapeutic strategy to target c-Myc.', *Cell*, 146(6), pp. 904-17. doi: 10.1016/j.cell.2011.08.017.
- Dey, A. *et al.* (2009) 'Brd4 marks select genes on mitotic chromatin and directs postmitotic transcription.', *Molecular biology of the cell*, 20(23), pp. 4899-909. doi: 10.1091/mbc.e09-05-0380.
- Diederichs, C. G. *et al.* (1998) 'FDG PET: elevated plasma glucose reduces both

- uptake and detection rate of pancreatic malignancies.’, *Journal of nuclear medicine : official publication, Society of Nuclear Medicine*, 39(6), pp. 1030-3. Available at: <http://www.ncbi.nlm.nih.gov/pubmed/9627339>.
- Diederichs, C. G. *et al.* (2000) ‘Values and limitations of 18F-fluorodeoxyglucose-positron-emission tomography with preoperative evaluation of patients with pancreatic masses.’, *Pancreas*, 20(2), pp. 109-16. doi: 10.1097/00006676-200003000-00001.
- Dimitroulakos, J. *et al.* (1999) ‘Increased sensitivity of acute myeloid leukemias to lovastatin-induced apoptosis: A potential therapeutic approach.’, *Blood*, 93(4), pp. 1308-18. Available at: <http://www.ncbi.nlm.nih.gov/pubmed/9949174>.
- Dimitroulakos, J. *et al.* (2002) ‘Microarray and biochemical analysis of lovastatin-induced apoptosis of squamous cell carcinomas.’, *Neoplasia (New York, N.Y.)*, 4(4), pp. 337-46. doi: 10.1038/sj.neo.7900247.
- Dimitroulakos, J., Lorimer, I. A. and Goss, G. (2006) ‘Strategies to enhance epidermal growth factor inhibition: targeting the mevalonate pathway.’, *Clinical cancer research : an official journal of the American Association for Cancer Research*, 12(14 Pt 2), pp. 4426s-4431s. doi: 10.1158/1078-0432.CCR-06-0089.
- Dite, T. A. *et al.* (2018) ‘AMP-activated protein kinase selectively inhibited by the type II inhibitor SBI-0206965.’, *The Journal of biological chemistry*, 293(23), pp. 8874-8885. doi: 10.1074/jbc.RA118.003547.
- Dobin, A. *et al.* (2013) ‘STAR: ultrafast universal RNA-seq aligner.’, *Bioinformatics (Oxford, England)*, 29(1), pp. 15-21. doi: 10.1093/bioinformatics/bts635.
- Drab, M. *et al.* (2001) ‘Loss of caveolae, vascular dysfunction, and pulmonary defects in caveolin-1 gene-disrupted mice.’, *Science (New York, N.Y.)*, 293(5539), pp. 2449-52. doi: 10.1126/science.1062688.
- Dreyer, S. B. *et al.* (2019) ‘Targeting DNA Damage Response and Replication Stress in Pancreatic Cancer’, *Australian Pancreatic Cancer Genome Initiative*, 16, p. 21. doi: 10.1101/713545.
- Druker, B. J. *et al.* (2006) ‘Five-year follow-up of patients receiving imatinib for chronic myeloid leukemia.’, *The New England journal of medicine*, 355(23), pp. 2408-2417. doi: 10.1056/NEJMoa062867.
- Duncan, R. E., El-Sohemy, A. and Archer, M. C. (2004) ‘Mevalonate promotes the

growth of tumors derived from human cancer cells in vivo and stimulates proliferation in vitro with enhanced cyclin-dependent kinase-2 activity.', *The Journal of biological chemistry*, 279(32), pp. 33079-84. doi: 10.1074/jbc.M400732200.

Dupree, P. *et al.* (1993) 'Caveolae and sorting in the trans-Golgi network of epithelial cells.', *The EMBO journal*, 12(4), pp. 1597-605. Available at: <http://www.ncbi.nlm.nih.gov/pubmed/8385608>.

Durocher, D. and Jackson, S. P. (2001) 'DNA-PK, ATM and ATR as sensors of DNA damage: variations on a theme?', *Current Opinion in Cell Biology*, 13(2), pp. 225-231. doi: 10.1016/S0955-0674(00)00201-5.

Edghill, E. L. *et al.* (2006) 'Hepatocyte nuclear factor-1 beta mutations cause neonatal diabetes and intrauterine growth retardation: support for a critical role of HNF-1beta in human pancreatic development.', *Diabetic medicine : a journal of the British Diabetic Association*, 23(12), pp. 1301-6. doi: 10.1111/j.1464-5491.2006.01999.x.

Edmunds, L. R. *et al.* (2014) 'c-Myc programs fatty acid metabolism and dictates acetyl-CoA abundance and fate.', *The Journal of biological chemistry*, 289(36), pp. 25382-92. doi: 10.1074/jbc.M114.580662.

Egan, D. F. *et al.* (2011) 'Phosphorylation of ULK1 (hATG1) by AMP-activated protein kinase connects energy sensing to mitophagy.', *Science (New York, N.Y.)*, 331(6016), pp. 456-61. doi: 10.1126/science.1196371.

Egan, D. F. *et al.* (2015) 'Small Molecule Inhibition of the Autophagy Kinase ULK1 and Identification of ULK1 Substrates.', *Molecular cell*, 59(2), pp. 285-97. doi: 10.1016/j.molcel.2015.05.031.

Einhorn, L. H. and Williams, S. D. (1980) 'Chemotherapy of disseminated testicular cancer. A random prospective study.', *Cancer*, 46(6), pp. 1339-44. Available at: <http://www.ncbi.nlm.nih.gov/pubmed/6158370>.

Ellis, J. M., Bowman, C. E. and Wolfgang, M. J. (2015) 'Metabolic and Tissue-Specific Regulation of Acyl-CoA Metabolism', *PLOS ONE*. Edited by Z. Andrews, 10(3), p. e0116587. doi: 10.1371/journal.pone.0116587.

Ellman, G. L. (1959) 'Tissue sulfhydryl groups.', *Archives of biochemistry and biophysics*, 82(1), pp. 70-7. doi: 10.1016/0003-9861(59)90090-6.

- Fabregat, A. *et al.* (2018) 'The Reactome Pathway Knowledgebase.', *Nucleic acids research*, 46(D1), pp. D649-D655. doi: 10.1093/nar/gkx1132.
- Fajans, S. S., Bell, G. I. and Polonsky, K. S. (2001) 'Molecular mechanisms and clinical pathophysiology of maturity-onset diabetes of the young.', *The New England journal of medicine*, 345(13), pp. 971-80. doi: 10.1056/NEJMra002168.
- Fang, H. and Gough, J. (2014) 'The "dnet" approach promotes emerging research on cancer patient survival.', *Genome medicine*, 6(8), p. 64. doi: 10.1186/s13073-014-0064-8.
- Faubert, B. *et al.* (2013) 'AMPK is a negative regulator of the Warburg effect and suppresses tumor growth in vivo.', *Cell metabolism*, 17(1), pp. 113-24. doi: 10.1016/j.cmet.2012.12.001.
- Faubert, B. *et al.* (2015) 'The AMP-activated protein kinase (AMPK) and cancer: many faces of a metabolic regulator.', *Cancer letters*, 356(2 Pt A), pp. 165-70. doi: 10.1016/j.canlet.2014.01.018.
- Fendrich, V. *et al.* (2013) 'Simvastatin delay progression of pancreatic intraepithelial neoplasia and cancer formation in a genetically engineered mouse model of pancreatic cancer', *Pancreatology*, 13(5), pp. 502-507. doi: 10.1016/j.pan.2013.08.002.
- Ferraz, T. P. L. *et al.* (2004) 'Comparison of six methods for the extraction of lipids from serum in terms of effectiveness and protein preservation.', *Journal of biochemical and biophysical methods*, 58(3), pp. 187-93. doi: 10.1016/j.jbbm.2003.10.008.
- Filippakopoulos, P. *et al.* (2010) 'Selective inhibition of BET bromodomains.', *Nature*, 468(7327), pp. 1067-73. doi: 10.1038/nature09504.
- Fiorentino, M. *et al.* (2008) 'Overexpression of fatty acid synthase is associated with palmitoylation of Wnt1 and cytoplasmic stabilization of beta-catenin in prostate cancer.', *Laboratory investigation; a journal of technical methods and pathology*, 88(12), pp. 1340-8. doi: 10.1038/labinvest.2008.97.
- Flier, J. S. *et al.* (1987) 'Elevated levels of glucose transport and transporter messenger RNA are induced by ras or src oncogenes.', *Science (New York, N.Y.)*, 235(4795), pp. 1492-5. doi: 10.1126/science.3103217.
- Follia, L. *et al.* (2019) 'Integrative Analysis of Novel Metabolic Subtypes in

Pancreatic Cancer Fosters New Prognostic Biomarkers.’, *Frontiers in oncology*, 9, p. 115. doi: 10.3389/fonc.2019.00115.

Folmes, C. D. L. *et al.* (2011) ‘Somatic oxidative bioenergetics transitions into pluripotency-dependent glycolysis to facilitate nuclear reprogramming.’, *Cell metabolism*, 14(2), pp. 264-71. doi: 10.1016/j.cmet.2011.06.011.

Fra, A. M. *et al.* (1995) ‘De novo formation of caveolae in lymphocytes by expression of VIP21-caveolin.’, *Proceedings of the National Academy of Sciences of the United States of America*, 92(19), pp. 8655-9. doi: 10.1073/pnas.92.19.8655.

Frank, P. G. *et al.* (2001) ‘Influence of caveolin-1 on cellular cholesterol efflux mediated by high-density lipoproteins.’, *American journal of physiology. Cell physiology*, 280(5), pp. C1204-14. doi: 10.1152/ajpcell.2001.280.5.C1204.

Frankfurt, O. S. and Krishan, A. (2001) ‘Enzyme-linked immunosorbent assay (ELISA) for the specific detection of apoptotic cells and its application to rapid drug screening.’, *Journal of Immunological Methods*, 253(1-2), pp. 133-144. doi: 10.1016/S0022-1759(01)00387-8.

Fritz, I. B. and Yue, K. T. (1963) ‘Long-chain Carnitine Acyltransferase and the role of Acylcarnitine derivatives in the catalytic increase of fatty acid oxidation induced by carnitine.’, *Journal of lipid research*, 4, pp. 279-88. Available at: <http://www.ncbi.nlm.nih.gov/pubmed/14168165>.

Fu, Y. *et al.* (2004) ‘Expression of caveolin-1 enhances cholesterol efflux in hepatic cells.’, *The Journal of biological chemistry*, 279(14), pp. 14140-6. doi: 10.1074/jbc.M311061200.

Gallego-Ortega, D. *et al.* (2009) ‘Differential role of human choline kinase alpha and beta enzymes in lipid metabolism: implications in cancer onset and treatment.’, *PloS one*, 4(11), p. e7819. doi: 10.1371/journal.pone.0007819.

Gamblin, S. J. *et al.* (1991) ‘Activity and specificity of human aldolases’, *Journal of Molecular Biology*, 219(4), pp. 573-576. doi: 10.1016/0022-2836(91)90650-U.

Garcea, G. *et al.* (2007) ‘Glycogen synthase kinase-3 beta; a new target in pancreatic cancer?’, *Current cancer drug targets*, 7(3), pp. 209-15. Available at: <http://www.ncbi.nlm.nih.gov/pubmed/17504118>.

Garrido-Laguna, I. and Hidalgo, M. (2015) ‘Pancreatic cancer: from state-of-the-art treatments to promising novel therapies.’, *Nature reviews. Clinical oncology*,

12(6), pp. 319-34. doi: 10.1038/nrclinonc.2015.53.

Garulli, C. *et al.* (2014) 'Dorsomorphin reverses the mesenchymal phenotype of breast cancer initiating cells by inhibition of bone morphogenetic protein signaling.', *Cellular signalling*, 26(2), pp. 352-62. doi: 10.1016/j.cellsig.2013.11.022.

Gatenby, R. A. and Gillies, R. J. (2004) 'Why do cancers have high aerobic glycolysis?', *Nature reviews. Cancer*, 4(11), pp. 891-9. doi: 10.1038/nrc1478.

Gauthier, M.-S. *et al.* (2008) 'AMP-activated Protein Kinase Is Activated as a Consequence of Lipolysis in the Adipocyte', *Journal of Biological Chemistry*, 283(24), pp. 16514-16524. doi: 10.1074/jbc.M708177200.

Gbelcová, H. *et al.* (2008) 'Differences in antitumor effects of various statins on human pancreatic cancer.', *International journal of cancer*, 122(6), pp. 1214-21. doi: 10.1002/ijc.23242.

Gillen, S. *et al.* (2010) 'Preoperative/neoadjuvant therapy in pancreatic cancer: a systematic review and meta-analysis of response and resection percentages.', *PLoS medicine*, 7(4), p. e1000267. doi: 10.1371/journal.pmed.1000267.

Goard, C. A. *et al.* (2014) 'Identifying molecular features that distinguish fluvastatin-sensitive breast tumor cells.', *Breast cancer research and treatment*, 143(2), pp. 301-12. doi: 10.1007/s10549-013-2800-y.

Goodall, C. R. (1993) '13 Computation using the QR decomposition', in, pp. 467-508. doi: 10.1016/S0169-7161(05)80137-3.

Gorre, M. E. *et al.* (2001) 'Clinical resistance to STI-571 cancer therapy caused by BCR-ABL gene mutation or amplification', *Science*, 293(5531), pp. 876-880. doi: 10.1126/science.1062538.

Grandjean, G., de Jong, P. R., James, B. P., *et al.* (2016) 'Definition of a Novel Feed-Forward Mechanism for Glycolysis-HIF1 α Signaling in Hypoxic Tumors Highlights Aldolase A as a Therapeutic Target.', *Cancer research*, 76(14), pp. 4259-69. doi: 10.1158/0008-5472.CAN-16-0401.

Grandjean, G., de Jong, P. R., James, B., *et al.* (2016) 'Definition of a Novel Feed-Forward Mechanism for Glycolysis-HIF1 α Signaling in Hypoxic Tumors Highlights Aldolase A as a Therapeutic Target.', *Cancer research*, 76(14), pp. 4259-4269. doi: 10.1158/0008-5472.CAN-16-0401.

- Greenaway, J. B. *et al.* (2016) 'Ovarian tumour growth is characterized by mevalonate pathway gene signature in an orthotopic, syngeneic model of epithelial ovarian cancer.', *Oncotarget*, 7(30), pp. 47343-47365. doi: 10.18632/oncotarget.10121.
- Guillaumond, F. *et al.* (2013) 'Strengthened glycolysis under hypoxia supports tumor symbiosis and hexosamine biosynthesis in pancreatic adenocarcinoma.', *Proceedings of the National Academy of Sciences of the United States of America*, 110(10), pp. 3919-24. doi: 10.1073/pnas.1219555110.
- Guillaumond, F. *et al.* (2015) 'Cholesterol uptake disruption, in association with chemotherapy, is a promising combined metabolic therapy for pancreatic adenocarcinoma.', *Proceedings of the National Academy of Sciences of the United States of America*, 112(8), pp. 2473-8. doi: 10.1073/pnas.1421601112.
- Guo, J. Y. *et al.* (2016) 'Autophagy provides metabolic substrates to maintain energy charge and nucleotide pools in Ras-driven lung cancer cells.', *Genes & development*, 30(15), pp. 1704-17. doi: 10.1101/gad.283416.116.
- Gysin, S. *et al.* (2011) 'Therapeutic strategies for targeting ras proteins.', *Genes & cancer*, 2(3), pp. 359-72. doi: 10.1177/1947601911412376.
- Hale, M. A. *et al.* (2005) 'The homeodomain protein PDX1 is required at mid-pancreatic development for the formation of the exocrine pancreas.', *Developmental biology*, 286(1), pp. 225-37. doi: 10.1016/j.ydbio.2005.07.026.
- Hancock, J. F. *et al.* (1989) 'All ras proteins are polyisoprenylated but only some are palmitoylated.', *Cell*, 57(7), pp. 1167-77. doi: 10.1016/0092-8674(89)90054-8.
- Hanna, N. *et al.* (2006) 'Randomized Phase III Trial Comparing Irinotecan/Cisplatin With Etoposide/Cisplatin in Patients With Previously Untreated Extensive-Stage Disease Small-Cell Lung Cancer', *Journal of Clinical Oncology*, 24(13), pp. 2038-2043. doi: 10.1200/JCO.2005.04.8595.
- Hansen, P. A. *et al.* (1995) 'Skeletal muscle glucose transport and metabolism are enhanced in transgenic mice overexpressing the Glut4 glucose transporter.', *The Journal of biological chemistry*, 270(4), pp. 1679-84. doi: 10.1074/jbc.270.5.1679.
- Hansen, P. A., Gulve, E. A. and Holloszy, J. O. (1994) 'Suitability of 2-deoxyglucose for in vitro measurement of glucose transport activity in skeletal muscle.', *Journal of applied physiology (Bethesda, Md. : 1985)*, 76(2), pp. 979-85.

doi: 10.1152/jappl.1994.76.2.979.

Hänzelmann, S., Castelo, R. and Guinney, J. (2013) 'GSVA: gene set variation analysis for microarray and RNA-seq data.', *BMC bioinformatics*, 14, p. 7. doi: 10.1186/1471-2105-14-7.

Hao, X. *et al.* (2017) 'DNA methylation markers for diagnosis and prognosis of common cancers', *Proceedings of the National Academy of Sciences*, 114(28), pp. 7414-7419. doi: 10.1073/pnas.1703577114.

Haq, R. *et al.* (2013) 'Oncogenic BRAF regulates oxidative metabolism via PGC1 α and MITF.', *Cancer cell*, 23(3), pp. 302-15. doi: 10.1016/j.ccr.2013.02.003.

Hardie, D. G. and Pan, D. A. (2002) 'Regulation of fatty acid synthesis and oxidation by the AMP-activated protein kinase.', *Biochemical Society transactions*, 30(Pt 6), pp. 1064-70. doi: 10.1042/.

Hardie, R.-A. *et al.* (2017) 'Mitochondrial mutations and metabolic adaptation in pancreatic cancer.', *Cancer & metabolism*, 5, p. 2. doi: 10.1186/s40170-017-0164-1.

Hardwicke, M. A. *et al.* (2014) 'A human fatty acid synthase inhibitor binds β -ketoacyl reductase in the keto-substrate site.', *Nature chemical biology*, 10(9), pp. 774-9. doi: 10.1038/nchembio.1603.

Hart, K. C. and Donoghue, D. J. (1997) 'Derivatives of activated H-ras lacking C-terminal lipid modifications retain transforming ability if targeted to the correct subcellular location.', *Oncogene*, 14(8), pp. 945-53. doi: 10.1038/sj.onc.1200908.

Hartman, I. Z. *et al.* (2010) 'Sterol-induced Dislocation of 3-Hydroxy-3-methylglutaryl Coenzyme A Reductase from Endoplasmic Reticulum Membranes into the Cytosol through a Subcellular Compartment Resembling Lipid Droplets', *Journal of Biological Chemistry*, 285(25), pp. 19288-19298. doi: 10.1074/jbc.M110.134213.

Hayhurst, G. P. *et al.* (2001) 'Hepatocyte Nuclear Factor 4 (Nuclear Receptor 2A1) Is Essential for Maintenance of Hepatic Gene Expression and Lipid Homeostasis', *Molecular and Cellular Biology*, 21(4), pp. 1393-1403. doi: 10.1128/MCB.21.4.1393-1403.2001.

Vander Heiden, M. G. (2011) 'Targeting cancer metabolism: a therapeutic window opens.', *Nature reviews. Drug discovery*, 10(9), pp. 671-84. doi: 10.1038/nrd3504.

- Herrmann, R. *et al.* (2007) 'Screening for Compounds That Induce Apoptosis of Cancer Cells Grown as Multicellular Spheroids', *Journal of Biomolecular Screening*, 13(1), pp. 1-8. doi: 10.1177/1087057107310442.
- Hessmann, E. *et al.* (2016) 'MYC in pancreatic cancer: novel mechanistic insights and their translation into therapeutic strategies', *Oncogene*, 35(13), pp. 1609-1618. doi: 10.1038/onc.2015.216.
- Hildyard, J. C. W. *et al.* (2005) 'Identification and characterisation of a new class of highly specific and potent inhibitors of the mitochondrial pyruvate carrier', *Biochimica et Biophysica Acta (BBA) - Bioenergetics*, 1707(2-3), pp. 221-230. doi: 10.1016/j.bbabi.2004.12.005.
- Hingorani, S. R. *et al.* (2005) 'Trp53R172H and KrasG12D cooperate to promote chromosomal instability and widely metastatic pancreatic ductal adenocarcinoma in mice.', *Cancer cell*, 7(5), pp. 469-83. doi: 10.1016/j.ccr.2005.04.023.
- Hissa, B. *et al.* (2012) 'Membrane cholesterol regulates lysosome-plasma membrane fusion events and modulates Trypanosoma cruzi invasion of host cells.', *PLoS neglected tropical diseases*, 6(3), p. e1583. doi: 10.1371/journal.pntd.0001583.
- Hoadley, K. A. *et al.* (2014) 'Multiplatform analysis of 12 cancer types reveals molecular classification within and across tissues of origin.', *Cell*, 158(4), pp. 929-944. doi: 10.1016/j.cell.2014.06.049.
- Von Hoff, D. D. *et al.* (2013) 'Increased survival in pancreatic cancer with nab-paclitaxel plus gemcitabine.', *The New England journal of medicine*, 369(18), pp. 1691-703. doi: 10.1056/NEJMoa1304369.
- Holliday, R. (2006) 'Epigenetics: A Historical Overview', *Epigenetics*, 1(2), pp. 76-80. doi: 10.4161/epi.1.2.2762.
- Holmgren, J. *et al.* (1975) 'Interaction of cholera toxin and membrane GM1 ganglioside of small intestine.', *Proceedings of the National Academy of Sciences of the United States of America*, 72(7), pp. 2520-4. doi: 10.1073/pnas.72.7.2520.
- Holohan, C. *et al.* (2013) 'Cancer drug resistance: an evolving paradigm', *Nature Reviews Cancer*, 13(10), pp. 714-726. doi: 10.1038/nrc3599.
- Hong, J. Y. *et al.* (2014) 'Randomized double-blinded, placebo-controlled phase II trial of simvastatin and gemcitabine in advanced pancreatic cancer patients.',

- Cancer chemotherapy and pharmacology*, 73(1), pp. 125-30. doi: 10.1007/s00280-013-2328-1.
- Hoskins, J. W. *et al.* (2014) 'Transcriptome analysis of pancreatic cancer reveals a tumor suppressor function for HNF1A.', *Carcinogenesis*, 35(12), pp. 2670-8. doi: 10.1093/carcin/bgu193.
- Hruban, R. H. *et al.* (2006) 'Pathology of genetically engineered mouse models of pancreatic exocrine cancer: consensus report and recommendations.', *Cancer research*, 66(1), pp. 95-106. doi: 10.1158/0008-5472.CAN-05-2168.
- Huang, B. Z. *et al.* (2017) 'Influence of Statins and Cholesterol on Mortality Among Patients With Pancreatic Cancer.', *Journal of the National Cancer Institute*, 109(5). doi: 10.1093/jnci/djw275.
- Huang, J. *et al.* (2018) 'Final results of a phase I dose-escalation, dose-expansion study of adding disulfiram with or without copper to adjuvant temozolomide for newly diagnosed glioblastoma', *Journal of Neuro-Oncology*, 138(1), pp. 105-111. doi: 10.1007/s11060-018-2775-y.
- Huang, J. *et al.* (2019) 'A multicenter phase II study of temozolomide plus disulfiram and copper for recurrent temozolomide-resistant glioblastoma', *Journal of Neuro-Oncology*, 142(3), pp. 537-544. doi: 10.1007/s11060-019-03125-y.
- Hung, M.-S. *et al.* (2017) 'Statin improves survival in patients with EGFR-TKI lung cancer: A nationwide population-based study.', *PloS one*, 12(2), p. e0171137. doi: 10.1371/journal.pone.0171137.
- Huo, H. *et al.* (2003) 'Lipid Rafts/Caveolae Are Essential for Insulin-like Growth Factor-1 Receptor Signaling during 3T3-L1 Preadipocyte Differentiation Induction', *Journal of Biological Chemistry*, 278(13), pp. 11561-11569. doi: 10.1074/jbc.M211785200.
- Hwang, R. F. *et al.* (2008) 'Cancer-Associated Stromal Fibroblasts Promote Pancreatic Tumor Progression', *Cancer Research*, 68(3), pp. 918-926. doi: 10.1158/0008-5472.CAN-07-5714.
- lanevski, A. *et al.* (2017) 'SynergyFinder: a web application for analyzing drug combination dose-response matrix data.', *Bioinformatics (Oxford, England)*, 33(15), pp. 2413-2415. doi: 10.1093/bioinformatics/btx162.
- IMPACT (1995) 'Efficacy of adjuvant fluorouracil and folinic acid in colon cancer.

- International Multicentre Pooled Analysis of Colon Cancer Trials (IMPACT) investigators.', *Lancet (London, England)*, 345(8955), pp. 939-44. doi: 7715291.
- Ingelmo-Torres, M. *et al.* (2009) 'Triton X-100 promotes a cholesterol-dependent condensation of the plasma membrane.', *The Biochemical journal*, 420(3), pp. 373-81. doi: 10.1042/BJ20090051.
- Inoue, S. *et al.* (1991) 'Inhibition of degradation of 3-hydroxy-3-methylglutaryl-coenzyme A reductase in vivo by cysteine protease inhibitors.', *The Journal of biological chemistry*, 266(20), pp. 13311-7. Available at: <http://www.ncbi.nlm.nih.gov/pubmed/1906466>.
- Irwin, M. E. *et al.* (2011) 'Lipid raft localization of EGFR alters the response of cancer cells to the EGFR tyrosine kinase inhibitor gefitinib.', *Journal of cellular physiology*, 226(9), pp. 2316-28. doi: 10.1002/jcp.22570.
- Ishikawa, T. *et al.* (2018) 'Concomitant attenuation of HMG-CoA reductase expression potentiates the cancer cell growth-inhibitory effect of statins and expands their efficacy in tumor cells with epithelial characteristics.', *Oncotarget*, 9(50), pp. 29304-29315. doi: 10.18632/oncotarget.25448.
- Issaq, S. H., Teicher, B. A. and Monks, A. (2014) 'Bioenergetic properties of human sarcoma cells help define sensitivity to metabolic inhibitors.', *Cell cycle (Georgetown, Tex.)*, 13(7), pp. 1152-61. doi: 10.4161/cc.28010.
- Jacobs, E. J. *et al.* (2010) 'Family history of cancer and risk of pancreatic cancer: a pooled analysis from the Pancreatic Cancer Cohort Consortium (PanScan).', *International journal of cancer*, 127(6), pp. 1421-8. doi: 10.1002/ijc.25148.
- Jansen, J. M. *et al.* (2017) 'Inhibition of prenylated KRAS in a lipid environment.', *PloS one*, 12(4), p. e0174706. doi: 10.1371/journal.pone.0174706.
- Jeon, S.-M., Chandel, N. S. and Hay, N. (2012) 'AMPK regulates NADPH homeostasis to promote tumour cell survival during energy stress.', *Nature*, 485(7400), pp. 661-5. doi: 10.1038/nature11066.
- Jones, S. *et al.* (2008) 'Core signaling pathways in human pancreatic cancers revealed by global genomic analyses.', *Science (New York, N.Y.)*, 321(5897), pp. 1801-6. doi: 10.1126/science.1164368.
- Kajinami, K., Takekoshi, N. and Saito, Y. (2003) 'Pitavastatin: efficacy and safety profiles of a novel synthetic HMG-CoA reductase inhibitor.', *Cardiovascular drug*

reviews, 21(3), pp. 199-215. Available at:

<http://www.ncbi.nlm.nih.gov/pubmed/12931254>.

Kamerkar, S. *et al.* (2017) 'Exosomes facilitate therapeutic targeting of oncogenic KRAS in pancreatic cancer.', *Nature*, 546(7659), pp. 498-503. doi: 10.1038/nature22341.

Kamisawa, T. *et al.* (2016) 'Pancreatic cancer.', *Lancet (London, England)*. Elsevier Ltd, 388(10039), pp. 73-85. doi: 10.1016/S0140-6736(16)00141-0.

Kamphorst, J. J. *et al.* (2013) 'Hypoxic and Ras-transformed cells support growth by scavenging unsaturated fatty acids from lysophospholipids.', *Proceedings of the National Academy of Sciences of the United States of America*, 110(22), pp. 8882-7. doi: 10.1073/pnas.1307237110.

Kanehisa, M. and Goto, S. (2000) 'KEGG: kyoto encyclopedia of genes and genomes.', *Nucleic acids research*, 28(1), pp. 27-30. doi: 10.1093/nar/28.1.27.

Kao, A. W. *et al.* (1999) 'Aldolase Mediates the Association of F-actin with the Insulin-responsive Glucose Transporter GLUT4', *Journal of Biological Chemistry*, 274(25), pp. 17742-17747. doi: 10.1074/jbc.274.25.17742.

Karantza-Wadsworth, V. *et al.* (2007) 'Autophagy mitigates metabolic stress and genome damage in mammary tumorigenesis.', *Genes & development*, 21(13), pp. 1621-35. doi: 10.1101/gad.1565707.

Kerr, E. M. *et al.* (2016) 'Mutant Kras copy number defines metabolic reprogramming and therapeutic susceptibilities.', *Nature*, 531(7592), pp. 110-3. doi: 10.1038/nature16967.

Khasawneh, J. *et al.* (2009) 'Inflammation and mitochondrial fatty acid beta-oxidation link obesity to early tumor promotion.', *Proceedings of the National Academy of Sciences of the United States of America*, 106(9), pp. 3354-9. doi: 10.1073/pnas.0802864106.

Kim, J. *et al.* (2011) 'AMPK and mTOR regulate autophagy through direct phosphorylation of Ulk1.', *Nature cell biology*, 13(2), pp. 132-41. doi: 10.1038/ncb2152.

Kim, J., Lee, J. and Iyer, V. R. (2008) 'Global identification of Myc target genes reveals its direct role in mitochondrial biogenesis and its E-box usage in vivo.', *PLoS one*, 3(3), p. e1798. doi: 10.1371/journal.pone.0001798.

- Kimbung, S. *et al.* (2016) 'High expression of cholesterol biosynthesis genes is associated with resistance to statin treatment and inferior survival in breast cancer.', *Oncotarget*, 7(37), pp. 59640-59651. doi: 10.18632/oncotarget.10746.
- Kimmelman, A. C. (2015) 'Metabolic Dependencies in RAS-Driven Cancers', *Clinical Cancer Research*, 21(8), pp. 1828-1834. doi: 10.1158/1078-0432.CCR-14-2425.
- Kleeff, J. *et al.* (2007) 'Pancreatic cancer microenvironment.', *International journal of cancer*, 121(4), pp. 699-705. doi: 10.1002/ijc.22871.
- Knopik-Skrocka, A. and Bielawski, J. (2002) 'The mechanism of the hemolytic activity of polyene antibiotics.', *Cellular & molecular biology letters*, 7(1), pp. 31-48. Available at: <http://www.ncbi.nlm.nih.gov/pubmed/11944048>.
- Kong, B. *et al.* (2016) 'A subset of metastatic pancreatic ductal adenocarcinomas depends quantitatively on oncogenic Kras/Mek/Erk-induced hyperactive mTOR signalling', *Gut*, 65(4), pp. 647-657. doi: 10.1136/gutjnl-2014-307616.
- Kosti, I. *et al.* (2016) 'Cross-tissue Analysis of Gene and Protein Expression in Normal and Cancer Tissues.', *Scientific reports*, 6, p. 24799. doi: 10.1038/srep24799.
- Kruszynska, Y. T., Stanley, H. and Sherratt, A. (1987) 'Glucose kinetics during acute and chronic treatment of rats with 2[6(4-chloro-phenoxy) hexyl]oxirane-2-carboxylate, etomoxir', *Biochemical Pharmacology*, 36(22), pp. 3917-3921. doi: 10.1016/0006-2952(87)90458-8.
- Kuhajda, F. P. *et al.* (1994) 'Fatty acid synthesis: a potential selective target for antineoplastic therapy.', *Proceedings of the National Academy of Sciences of the United States of America*, 91(14), pp. 6379-83. Available at: <http://www.ncbi.nlm.nih.gov/pubmed/8022791>.
- Lai, E. C. (2002) 'Micro RNAs are complementary to 3' UTR sequence motifs that mediate negative post-transcriptional regulation', *Nature Genetics*, 30(4), pp. 363-364. doi: 10.1038/ng865.
- Lal, G. *et al.* (2000) 'Inherited predisposition to pancreatic adenocarcinoma: role of family history and germ-line p16, BRCA1, and BRCA2 mutations.', *Cancer research*, 60(2), pp. 409-16. Available at: <http://www.ncbi.nlm.nih.gov/pubmed/10667595>.
- Langfelder, P. *et al.* (2011) 'Is my network module preserved and reproducible?',

- PLoS computational biology*, 7(1), p. e1001057. doi: 10.1371/journal.pcbi.1001057.
- Langfelder, P. and Horvath, S. (2007) 'Eigengene networks for studying the relationships between co-expression modules', *BMC Systems Biology*, 1(1), p. 54. doi: 10.1186/1752-0509-1-54.
- Langfelder, P. and Horvath, S. (2008) 'WGCNA: an R package for weighted correlation network analysis.', *BMC bioinformatics*, 9, p. 559. doi: 10.1186/1471-2105-9-559.
- Laplante, M. and Sabatini, D. M. (2009) 'mTOR signaling at a glance', *Journal of Cell Science*, 122(20), pp. 3589-3594. doi: 10.1242/jcs.051011.
- LaRosa, J. C. *et al.* (2005) 'Intensive lipid lowering with atorvastatin in patients with stable coronary disease.', *The New England journal of medicine*, 352(14), pp. 1425-35. doi: 10.1056/NEJMoa050461.
- Larson, R. A. and Yachnin, S. (1984) 'Mevalonic acid induces DNA synthesis in chronic lymphocytic leukemia cells.', *Blood*, 64(1), pp. 257-62. Available at: <http://www.ncbi.nlm.nih.gov/pubmed/6610447>.
- Law, C. W. *et al.* (2014) 'Voom: precision weights unlock linear model analysis tools for RNA-seq read counts.', *Genome biology*, 15(2), p. R29. doi: 10.1186/gb-2014-15-2-r29.
- Le, A. *et al.* (2010) 'Inhibition of lactate dehydrogenase A induces oxidative stress and inhibits tumor progression', *Proceedings of the National Academy of Sciences*, 107(5), pp. 2037-2042. doi: 10.1073/pnas.0914433107.
- Lebherz, H. G. and Rutter, W. J. (1969) 'Distribution of fructose diphosphate aldolase variants in biological systems.', *Biochemistry*, 8(1), pp. 109-21. Available at: <http://www.ncbi.nlm.nih.gov/pubmed/5777313>.
- Lee, H. S. *et al.* (2016) 'Statin Use and Its Impact on Survival in Pancreatic Cancer Patients.', *Medicine*, 95(19), p. e3607. doi: 10.1097/MD.0000000000003607.
- Lee, H. S. *et al.* (2017) 'A novel HDAC inhibitor, CG200745, inhibits pancreatic cancer cell growth and overcomes gemcitabine resistance', *Scientific Reports*, 7(1), p. 41615. doi: 10.1038/srep41615.
- Lee, J. V *et al.* (2014) 'Akt-dependent metabolic reprogramming regulates tumor cell histone acetylation.', *Cell metabolism*, 20(2), pp. 306-319. doi:

10.1016/j.cmet.2014.06.004.

Levine, R. and Goldstein, M. S. (1958) 'On the mechanism of action of insulin.', *Hormoner*, 11(2), pp. 2-22. Available at:

<http://www.ncbi.nlm.nih.gov/pubmed/13548924>.

Li, D. *et al.* (2007) 'Dietary mutagen exposure and risk of pancreatic cancer.', *Cancer epidemiology, biomarkers & prevention : a publication of the American Association for Cancer Research, cosponsored by the American Society of Preventive Oncology*, 16(4), pp. 655-61. doi: 10.1158/1055-9965.EPI-06-0993.

Li, F. *et al.* (2005) 'Myc Stimulates Nuclearly Encoded Mitochondrial Genes and Mitochondrial Biogenesis', *Molecular and Cellular Biology*, 25(14), pp. 6225-6234. doi: 10.1128/MCB.25.14.6225-6234.2005.

Li, X. *et al.* (2019) 'Fructose-Bisphosphate Aldolase A Regulates Hypoxic Adaptation in Hepatocellular Carcinoma and Involved with Tumor Malignancy.', *Digestive diseases and sciences*. doi: 10.1007/s10620-019-05642-2.

Li, Y. C. *et al.* (2006) 'Elevated levels of cholesterol-rich lipid rafts in cancer cells are correlated with apoptosis sensitivity induced by cholesterol-depleting agents.', *The American journal of pathology*, 168(4), pp. 1107-18; quiz 1404-5. doi: 10.2353/ajpath.2006.050959.

Liao, Y., Smyth, G. K. and Shi, W. (2014) 'featureCounts: an efficient general purpose program for assigning sequence reads to genomic features.', *Bioinformatics (Oxford, England)*, 30(7), pp. 923-30. doi: 10.1093/bioinformatics/btt656.

Lipkin, S. M. *et al.* (2010) 'Genetic Variation in 3-Hydroxy-3-Methylglutaryl CoA Reductase Modifies the Chemopreventive Activity of Statins for Colorectal Cancer', *Cancer Prevention Research*, 3(5), pp. 597-603. doi: 10.1158/1940-6207.CAPR-10-0007.

Liu, M. *et al.* (2017) 'RE: Influence of Statins and Cholesterol on Mortality Among Patients With Pancreatic Cancer.', *Journal of the National Cancer Institute*, 109(12). doi: 10.1093/jnci/djx102.

Liu, P. *et al.* (2012) 'Cytotoxic effect of disulfiram/copper on human glioblastoma cell lines and ALDH-positive cancer-stem-like cells', *British Journal of Cancer*, 107(9), pp. 1488-1497. doi: 10.1038/bjc.2012.442.

- Lomakin, I. B., Xiong, Y. and Steitz, T. A. (2007) 'The Crystal Structure of Yeast Fatty Acid Synthase, a Cellular Machine with Eight Active Sites Working Together', *Cell*, 129(2), pp. 319-332. doi: 10.1016/j.cell.2007.03.013.
- Lomberk, G. *et al.* (2018) 'Distinct epigenetic landscapes underlie the pathobiology of pancreatic cancer subtypes', *Nature Communications*, 9(1), p. 1978. doi: 10.1038/s41467-018-04383-6.
- Longley, D. B., Harkin, D. P. and Johnston, P. G. (2003) '5-Fluorouracil: mechanisms of action and clinical strategies', *Nature Reviews Cancer*, 3(5), pp. 330-338. doi: 10.1038/nrc1074.
- Love, M. I., Huber, W. and Anders, S. (2014) 'Moderated estimation of fold change and dispersion for RNA-seq data with DESeq2.', *Genome biology*, 15(12), p. 550. doi: 10.1186/s13059-014-0550-8.
- Lun, X. *et al.* (2016) 'Disulfiram when Combined with Copper Enhances the Therapeutic Effects of Temozolomide for the Treatment of Glioblastoma', *Clinical Cancer Research*, 22(15), pp. 3860-3875. doi: 10.1158/1078-0432.CCR-15-1798.
- Lunt, S. Y. and Vander Heiden, M. G. (2011) 'Aerobic glycolysis: meeting the metabolic requirements of cell proliferation.', *Annual review of cell and developmental biology*, 27, pp. 441-64. doi: 10.1146/annurev-cellbio-092910-154237.
- Luo, Z. *et al.* (2015) 'Hepatocyte nuclear factor 1A (HNF1A) as a possible tumor suppressor in pancreatic cancer.', *PLoS one*, 10(3), p. e0121082. doi: 10.1371/journal.pone.0121082.
- Lynch, T. J. *et al.* (2004) 'Activating mutations in the epidermal growth factor receptor underlying responsiveness of non-small-cell lung cancer to gefitinib.', *The New England journal of medicine*, 350(21), pp. 2129-39. doi: 10.1056/NEJMoa040938.
- Maekawa, M. *et al.* (2015) 'Investigation of the fatty acid transporter-encoding genes SLC27A3 and SLC27A4 in autism', *Scientific Reports*, 5(1), p. 16239. doi: 10.1038/srep16239.
- Maftouh, M. *et al.* (2014) 'Synergistic interaction of novel lactate dehydrogenase inhibitors with gemcitabine against pancreatic cancer cells in hypoxia', *British Journal of Cancer*, 110(1), pp. 172-182. doi: 10.1038/bjc.2013.681.

- Malo, N. *et al.* (2006) 'Statistical practice in high-throughput screening data analysis', *Nature Biotechnology*, 24(2), pp. 167-175. doi: 10.1038/nbt1186.
- Mann, K. M. *et al.* (2012) 'Sleeping Beauty mutagenesis reveals cooperating mutations and pathways in pancreatic adenocarcinoma', *Proceedings of the National Academy of Sciences of the United States of America*, 109(16), pp. 5934-5941. doi: 10.1073/pnas.1202490109.
- Mantha, A. J. *et al.* (2005) 'Targeting the mevalonate pathway inhibits the function of the epidermal growth factor receptor.', *Clinical cancer research : an official journal of the American Association for Cancer Research*, 11(6), pp. 2398-407. doi: 10.1158/1078-0432.CCR-04-1951.
- Mao, M. *et al.* (2013) 'Resistance to BRAF inhibition in BRAF-mutant colon cancer can be overcome with PI3K inhibition or demethylating agents.', *Clinical cancer research : an official journal of the American Association for Cancer Research*, 19(3), pp. 657-67. doi: 10.1158/1078-0432.CCR-11-1446.
- Mao, Y. *et al.* (2017) 'RNA sequencing analyses reveal novel differentially expressed genes and pathways in pancreatic cancer.', *Oncotarget*, 8(26), pp. 42537-42547. doi: 10.18632/oncotarget.16451.
- Margueron, R., Trojer, P. and Reinberg, D. (2005) 'The key to development: interpreting the histone code?', *Current opinion in genetics & development*, 15(2), pp. 163-76. doi: 10.1016/j.gde.2005.01.005.
- Martin, H. L. *et al.* (2014) 'High-content, high-throughput screening for the identification of cytotoxic compounds based on cell morphology and cell proliferation markers.', *PloS one*, 9(2), p. e88338. doi: 10.1371/journal.pone.0088338.
- Martinez-Garcia, E. *et al.* (2011) 'The MMSET histone methyl transferase switches global histone methylation and alters gene expression in t(4;14) multiple myeloma cells.', *Blood*, 117(1), pp. 211-20. doi: 10.1182/blood-2010-07-298349.
- Martinez-Outschoorn, U. E. *et al.* (2017) 'Cancer metabolism: a therapeutic perspective', *Nature Reviews Clinical Oncology*, 14(1), pp. 11-31. doi: 10.1038/nrclinonc.2016.60.
- Martinez, A. *et al.* (2002) 'First non-ATP competitive glycogen synthase kinase 3 beta (GSK-3beta) inhibitors: thiadiazolidinones (TDZD) as potential drugs for the

- treatment of Alzheimer's disease.', *Journal of medicinal chemistry*, 45(6), pp. 1292-9. Available at: <http://www.ncbi.nlm.nih.gov/pubmed/11881998>.
- Matsuoka, S. *et al.* (2007) 'ATM and ATR Substrate Analysis Reveals Extensive Protein Networks Responsive to DNA Damage', *Science*, 316(5828), pp. 1160-1166. doi: 10.1126/science.1140321.
- Mattoon, D. R. *et al.* (2004) 'The docking protein Gab1 is the primary mediator of EGF-stimulated activation of the PI-3K/Akt cell survival pathway.', *BMC biology*, 2, p. 24. doi: 10.1186/1741-7007-2-24.
- Mazur, P. K. *et al.* (2015) 'Combined inhibition of BET family proteins and histone deacetylases as a potential epigenetics-based therapy for pancreatic ductal adenocarcinoma', *Nature Medicine*, 21(10), pp. 1163-1171. doi: 10.1038/nm.3952.
- McCabe, M. T. *et al.* (2012) 'EZH2 inhibition as a therapeutic strategy for lymphoma with EZH2-activating mutations', *Nature*, 492(7427), pp. 108-112. doi: 10.1038/nature11606.
- McDonald, O. G. *et al.* (2017) 'Epigenomic reprogramming during pancreatic cancer progression links anabolic glucose metabolism to distant metastasis', *Nature Genetics*, 49(3), pp. 367-376. doi: 10.1038/ng.3753.
- Medina, M. W. *et al.* (2008) 'Alternative splicing of 3-hydroxy-3-methylglutaryl coenzyme A reductase is associated with plasma low-density lipoprotein cholesterol response to simvastatin.', *Circulation*, 118(4), pp. 355-62. doi: 10.1161/CIRCULATIONAHA.108.773267.
- Menendez, J. A. and Lupu, R. (2007) 'Fatty acid synthase and the lipogenic phenotype in cancer pathogenesis.', *Nature reviews. Cancer*, 7(10), pp. 763-77. doi: 10.1038/nrc2222.
- Merkulova, M. *et al.* (2011) 'Aldolase directly interacts with ARNO and modulates cell morphology and acidic vesicle distribution', *American Journal of Physiology-Cell Physiology*, 300(6), pp. C1442-C1455. doi: 10.1152/ajpcell.00076.2010.
- Miglio, U. *et al.* (2014) 'KRAS mutational analysis in ductal adenocarcinoma of the pancreas and its clinical significance', *Pathology - Research and Practice*, 210(5), pp. 307-311. doi: 10.1016/j.prp.2014.01.011.
- Milhaud, J. (1992) 'Permeabilizing action of filipin III on model membranes through a filipin-phospholipid binding.', *Biochimica et biophysica acta*, 1105(2), pp. 307-

18. doi: 10.1016/0005-2736(92)90209-5.

Moessinger, C. *et al.* (2011) 'Human lysophosphatidylcholine acyltransferases 1 and 2 are located in lipid droplets where they catalyze the formation of phosphatidylcholine.', *The Journal of biological chemistry*, 286(24), pp. 21330-9. doi: 10.1074/jbc.M110.202424.

Moffitt, R. A. *et al.* (2015) 'Virtual microdissection identifies distinct tumor- and stroma-specific subtypes of pancreatic ductal adenocarcinoma.', *Nature genetics*, 47(10), pp. 1168-78. doi: 10.1038/ng.3398.

Mollinedo, F. and Gajate, C. (2015) 'Lipid rafts as major platforms for signaling regulation in cancer.', *Advances in biological regulation*, 57, pp. 130-46. doi: 10.1016/j.jbior.2014.10.003.

Monaghan, A. P. *et al.* (1993) 'Postimplantation expression patterns indicate a role for the mouse forkhead/HNF-3 alpha, beta and gamma genes in determination of the definitive endoderm, chordamesoderm and neuroectoderm.', *Development (Cambridge, England)*, 119(3), pp. 567-78. Available at: <http://www.ncbi.nlm.nih.gov/pubmed/8187630>.

Moon, D. C. *et al.* (2016) 'Concomitant Statin Use Has a Favorable Effect on Gemcitabine-Erlotinib Combination Chemotherapy for Advanced Pancreatic Cancer.', *Yonsei medical journal*, 57(5), pp. 1124-30. doi: 10.3349/ymj.2016.57.5.1124.

Moore, M. J. *et al.* (2007) 'Erlotinib plus gemcitabine compared with gemcitabine alone in patients with advanced pancreatic cancer: a phase III trial of the National Cancer Institute of Canada Clinical Trials Group.', *Journal of clinical oncology : official journal of the American Society of Clinical Oncology*, 25(15), pp. 1960-6. doi: 10.1200/JCO.2006.07.9525.

Moores, S. L. *et al.* (1991) 'Sequence dependence of protein isoprenylation.', *The Journal of biological chemistry*, 266(22), pp. 14603-10. Available at: <http://www.ncbi.nlm.nih.gov/pubmed/1860864>.

Moriyama, T. *et al.* (1998) 'Degradation of HMG-CoA reductase in vitro. Cleavage in the membrane domain by a membrane-bound cysteine protease.', *The Journal of biological chemistry*, 273(34), pp. 22037-43. Available at: <http://www.ncbi.nlm.nih.gov/pubmed/9705346>.

- Moser, C. *et al.* (2008) 'Inhibition of insulin-like growth factor-I receptor (IGF-IR) using NVP-AEW541, a small molecule kinase inhibitor, reduces orthotopic pancreatic cancer growth and angiogenesis', *European Journal of Cancer*, 44(11), pp. 1577-1586. doi: 10.1016/j.ejca.2008.04.003.
- Moskaluk, C. A., Hruban, R. H. and Kern, S. E. (1997) 'p16 and K-ras gene mutations in the intraductal precursors of human pancreatic adenocarcinoma.', *Cancer research*, 57(11), pp. 2140-3. Available at: <http://www.ncbi.nlm.nih.gov/pubmed/9187111>.
- Mosmann, T. (1983) 'Rapid colorimetric assay for cellular growth and survival: application to proliferation and cytotoxicity assays.', *Journal of immunological methods*, 65(1-2), pp. 55-63. doi: 10.1016/0022-1759(83)90303-4.
- Mueck, A. O., Seeger, H. and Wallwiener, D. (2003) 'Effect of statins combined with estradiol on the proliferation of human receptor-positive and receptor-negative breast cancer cells.', *Menopause (New York, N.Y.)*, 10(4), pp. 332-6. doi: 10.1097/01.GME.0000055485.06076.00.
- Mukhtar, R. Y. A., Reid, J. and Reckless, J. P. D. (2005) 'Pitavastatin.', *International journal of clinical practice*, 59(2), pp. 239-52. doi: 10.1111/j.1742-1241.2005.00461.x.
- Munyon, W. H. and Merchant, D. J. (1959) 'The relation between glucose utilization, lactic acid production and utilization and the growth cycle of L strain fibroblasts.', *Experimental cell research*, 17(3), pp. 490-8. Available at: <http://www.ncbi.nlm.nih.gov/pubmed/13672205>.
- Murata, M. *et al.* (1995) 'VIP21/caveolin is a cholesterol-binding protein.', *Proceedings of the National Academy of Sciences of the United States of America*, 92(22), pp. 10339-43. doi: 10.1073/pnas.92.22.10339.
- Muzumdar, M. D. *et al.* (2017) 'Survival of pancreatic cancer cells lacking KRAS function.', *Nature communications*, 8(1), p. 1090. doi: 10.1038/s41467-017-00942-5.
- Nagana Gowda, G. A. *et al.* (2018) 'A Metabolomics Study of BPTES Altered Metabolism in Human Breast Cancer Cell Lines.', *Frontiers in molecular biosciences*, 5, p. 49. doi: 10.3389/fmolb.2018.00049.
- National Cancer Institute (no date) *Developmental Therapeutics Program*. Available

at: <http://dtp.cancer.gov> (Accessed: 20 May 2019).

Nebbioso, A. *et al.* (2018) 'Cancer epigenetics: Moving forward.', *PLoS genetics*, 14(6), p. e1007362. doi: 10.1371/journal.pgen.1007362.

Neuberg, C., Strauss, E. and Lipkin, L. E. (1944) 'Convenient method for deproteinization.', *Arch. Biochem.*, 4, pp. 101-104.

Ng SSW *et al.* (2000) 'Inhibition of phosphatidylinositide 3-kinase enhances gemcitabine-induced apoptosis in human pancreatic cancer cells.', *Cancer research*, 60(19), pp. 5451-5. doi: 11034087.

Notta, F. *et al.* (2016) 'A renewed model of pancreatic cancer evolution based on genomic rearrangement patterns.', *Nature*, 538(7625), pp. 378-382. doi: 10.1038/nature19823.

Odom, D. T. *et al.* (2004) 'Control of pancreas and liver gene expression by HNF transcription factors.', *Science (New York, N.Y.)*, 303(5662), pp. 1378-81. doi: 10.1126/science.1089769.

Ono, H., Basson, M. D. and Ito, H. (2016) 'P300 inhibition enhances gemcitabine-induced apoptosis of pancreatic cancer.', *Oncotarget*, 7(32), pp. 51301-51310. doi: 10.18632/oncotarget.10117.

Ono, T. *et al.* (1976) 'Actions of bleomycin on DNA ligase and polymerases.', *Progress in biochemical pharmacology*, 11, pp. 48-58. Available at: <http://www.ncbi.nlm.nih.gov/pubmed/63970>.

Ostrem, J. M. *et al.* (2013) 'K-Ras(G12C) inhibitors allosterically control GTP affinity and effector interactions.', *Nature*, 503(7477), pp. 548-51. doi: 10.1038/nature12796.

Pal, K. *et al.* (2014) 'Inhibition of endoglin-GIPC interaction inhibits pancreatic cancer cell growth.', *Molecular cancer therapeutics*, 13(10), pp. 2264-75. doi: 10.1158/1535-7163.MCT-14-0291.

Pao, W. *et al.* (2005) 'Acquired Resistance of Lung Adenocarcinomas to Gefitinib or Erlotinib Is Associated with a Second Mutation in the EGFR Kinase Domain', *PLoS Medicine*. Edited by E. T. Liu, 2(3), p. e73. doi: 10.1371/journal.pmed.0020073.

Park, C. R. and Johnson, L. H. (1955) 'Effect of insulin on transport of glucose and galactose into cells of rat muscle and brain.', *The American journal of physiology*, 182(1), pp. 17-23. doi: 10.1152/ajplegacy.1955.182.1.17.

- Parton, R. G. (1994) 'Ultrastructural localization of gangliosides; GM1 is concentrated in caveolae.', *The journal of histochemistry and cytochemistry : official journal of the Histochemistry Society*, 42(2), pp. 155-66. doi: 10.1177/42.2.8288861.
- Patel, S. *et al.* (2008) 'Tissue-specific role of glycogen synthase kinase 3beta in glucose homeostasis and insulin action.', *Molecular and cellular biology*, 28(20), pp. 6314-28. doi: 10.1128/MCB.00763-08.
- Penhoet, E. E. and Rutter, W. J. (1971) 'Catalytic and immunochemical properties of homomeric and heteromeric combinations of aldolase subunits.', *The Journal of biological chemistry*, 246(2), pp. 318-23. Available at: <http://www.ncbi.nlm.nih.gov/pubmed/5542002>.
- Perera, R. M. *et al.* (2015) 'Transcriptional control of autophagy-lysosome function drives pancreatic cancer metabolism', *Nature*, 524(7565), pp. 361-365. doi: 10.1038/nature14587.
- Perugini, R. A. *et al.* (2000) 'Pancreatic Cancer Cell Proliferation Is Phosphatidylinositol 3-Kinase Dependent', *Journal of Surgical Research*, 90(1), pp. 39-44. doi: 10.1006/jsre.2000.5833.
- Pfleger, J., He, M. and Abdellatif, M. (2015) 'Mitochondrial complex II is a source of the reserve respiratory capacity that is regulated by metabolic sensors and promotes cell survival', *Cell Death & Disease*, 6(7), pp. e1835-e1835. doi: 10.1038/cddis.2015.202.
- Pike, L. S. *et al.* (2011) 'Inhibition of fatty acid oxidation by etomoxir impairs NADPH production and increases reactive oxygen species resulting in ATP depletion and cell death in human glioblastoma cells.', *Biochimica et biophysica acta*. Elsevier B.V., 1807(6), pp. 726-34. doi: 10.1016/j.bbabbio.2010.10.022.
- Pike Winer, L. S. and Wu, M. (2014) 'Rapid analysis of glycolytic and oxidative substrate flux of cancer cells in a microplate.', *PloS one*, 9(10), p. e109916. doi: 10.1371/journal.pone.0109916.
- Pol, A. *et al.* (2005) 'Cholesterol and fatty acids regulate dynamic caveolin trafficking through the Golgi complex and between the cell surface and lipid bodies.', *Molecular biology of the cell*, 16(4), pp. 2091-105. doi: 10.1091/mbc.e04-08-0737.

- Pollak, M. (2014) 'Overcoming Drug Development Bottlenecks With Repurposing: Repurposing biguanides to target energy metabolism for cancer treatment.', *Nature medicine*, 20(6), pp. 591-3. doi: 10.1038/nm.3596.
- Pommier, Y. (2013) 'Drugging topoisomerases: lessons and challenges.', *ACS chemical biology*, 8(1), pp. 82-95. doi: 10.1021/cb300648v.
- Prasad, V. V. and Gopalan, R. O. (2015) 'Continued use of MDA-MB-435, a melanoma cell line, as a model for human breast cancer, even in year, 2014', *npj Breast Cancer*, 1(1), p. 15002. doi: 10.1038/npjbcancer.2015.2.
- Qu, Q. *et al.* (2016) 'Fatty acid oxidation and carnitine palmitoyltransferase I: emerging therapeutic targets in cancer', *Cell Death & Disease*, 7(5), pp. e2226-e2226. doi: 10.1038/cddis.2016.132.
- Racker, E., Resnick, R. J. and Feldman, R. (1985) 'Glycolysis and methylaminoisobutyrate uptake in rat-1 cells transfected with ras or myc oncogenes.', *Proceedings of the National Academy of Sciences of the United States of America*, 82(11), pp. 3535-8. doi: 10.1073/pnas.82.11.3535.
- Raimondi, S. *et al.* (2007) 'Early onset pancreatic cancer: evidence of a major role for smoking and genetic factors.', *Cancer epidemiology, biomarkers & prevention: a publication of the American Association for Cancer Research, cosponsored by the American Society of Preventive Oncology*, 16(9), pp. 1894-7. doi: 10.1158/1055-9965.EPI-07-0341.
- Rajeshkumar, N. V. *et al.* (2015) 'Therapeutic Targeting of the Warburg Effect in Pancreatic Cancer Relies on an Absence of p53 Function', *Cancer Research*, 75(16), pp. 3355-3364. doi: 10.1158/0008-5472.CAN-15-0108.
- Ravid, T. *et al.* (2000) 'The ubiquitin-proteasome pathway mediates the regulated degradation of mammalian 3-hydroxy-3-methylglutaryl-coenzyme A reductase.', *The Journal of biological chemistry*, 275(46), pp. 35840-7. doi: 10.1074/jbc.M004793200.
- Rijkers, A. P. *et al.* (2014) 'Usefulness of F-18-fluorodeoxyglucose positron emission tomography to confirm suspected pancreatic cancer: A meta-analysis', *European Journal of Surgical Oncology (EJSO)*, 40(7), pp. 794-804. doi: 10.1016/j.ejso.2014.03.016.
- Roitelman, J. and Simoni, R. D. (1992) 'Distinct sterol and nonsterol signals for the

regulated degradation of 3-hydroxy-3-methylglutaryl-CoA reductase.', *The Journal of biological chemistry*, 267(35), pp. 25264-73. Available at:

<http://www.ncbi.nlm.nih.gov/pubmed/1460026>.

Rolland, F., Winderickx, J. and Thevelein, J. M. (2002) 'Glucose-sensing and -signalling mechanisms in yeast.', *FEMS yeast research*, 2(2), pp. 183-201. doi: 10.1111/j.1567-1364.2002.tb00084.x.

Rothberg, K. G. *et al.* (1992) 'Caveolin, a protein component of caveolae membrane coats.', *Cell*, 68(4), pp. 673-82. doi: 10.1016/0092-8674(92)90143-z.

Rozen, R. *et al.* (1994) 'Isolation and Expression of a cDNA Encoding the Precursor for a Novel Member (ACADSB) of the Acyl-CoA Dehydrogenase Gene Family', *Genomics*, 24(2), pp. 280-287. doi: 10.1006/geno.1994.1617.

Rückert, F. *et al.* (2012) 'Five primary human pancreatic adenocarcinoma cell lines established by the outgrowth method.', *The Journal of surgical research*, 172(1), pp. 29-39. doi: 10.1016/j.jss.2011.04.021.

Saito, K. *et al.* (2011) 'An enzymatic photometric assay for 2-deoxyglucose uptake in insulin-responsive tissues and 3T3-L1 adipocytes.', *Analytical biochemistry*, 412(1), pp. 9-17. doi: 10.1016/j.ab.2011.01.022.

Sakamaki, J.-I. *et al.* (2017) 'Bromodomain Protein BRD4 Is a Transcriptional Repressor of Autophagy and Lysosomal Function.', *Molecular cell*, 66(4), pp. 517-532.e9. doi: 10.1016/j.molcel.2017.04.027.

Sancho, P. *et al.* (2015) 'MYC/PGC-1 α Balance Determines the Metabolic Phenotype and Plasticity of Pancreatic Cancer Stem Cells', *Cell Metabolism*, 22(4), pp. 590-605. doi: 10.1016/j.cmet.2015.08.015.

Sasaki, T. *et al.* (1990) 'Inhibitory effect of di- and tripeptidyl aldehydes on calpains and cathepsins.', *Journal of enzyme inhibition*, 3(3), pp. 195-201. Available at: <http://www.ncbi.nlm.nih.gov/pubmed/2079636>.

Schindelin, J. *et al.* (2012) 'Fiji: an open-source platform for biological-image analysis.', *Nature methods*, 9(7), pp. 676-82. doi: 10.1038/nmeth.2019.

Schneider, V. A. *et al.* (2017) 'Evaluation of GRCh38 and de novo haploid genome assemblies demonstrates the enduring quality of the reference assembly.', *Genome research*, 27(5), pp. 849-864. doi: 10.1101/gr.213611.116.

Seeger, H., Wallwiener, D. and Mueck, A. O. (2003) 'Statins can inhibit

proliferation of human breast cancer cells in vitro.’, *Experimental and clinical endocrinology & diabetes : official journal, German Society of Endocrinology [and] German Diabetes Association*, 111(1), pp. 47-8. doi: 10.1055/s-2003-37501.

Semenza, G. L. *et al.* (1994) ‘Transcriptional regulation of genes encoding glycolytic enzymes by hypoxia-inducible factor 1.’, *The Journal of biological chemistry*, 269(38), pp. 23757-63. Available at:
<http://www.ncbi.nlm.nih.gov/pubmed/8089148>.

Sever, N., Song, B.-L., Yabe, D., Goldstein, Joseph L, *et al.* (2003) ‘Insig-dependent ubiquitination and degradation of mammalian 3-hydroxy-3-methylglutaryl-CoA reductase stimulated by sterols and geranylgeraniol.’, *The Journal of biological chemistry*, 278(52), pp. 52479-90. doi: 10.1074/jbc.M310053200.

Sever, N., Song, B.-L., Yabe, D., Goldstein, Joseph L., *et al.* (2003) ‘Insig-dependent Ubiquitination and Degradation of Mammalian 3-Hydroxy-3-methylglutaryl-CoA Reductase Stimulated by Sterols and Geranylgeraniol’, *Journal of Biological Chemistry*, 278(52), pp. 52479-52490. doi: 10.1074/jbc.M310053200.

Sharma, S. V *et al.* (2010) ‘A chromatin-mediated reversible drug-tolerant state in cancer cell subpopulations.’, *Cell*, 141(1), pp. 69-80. doi: 10.1016/j.cell.2010.02.027.

Sheikholeslami, K. *et al.* (2019) ‘Simvastatin Induces Apoptosis in Medulloblastoma Brain Tumor Cells via Mevalonate Cascade Prenylation Substrates’, *Cancers*, 11(7), p. 994. doi: 10.3390/cancers11070994.

Sherman, M. H. *et al.* (2017) ‘Stromal cues regulate the pancreatic cancer epigenome and metabolome.’, *Proceedings of the National Academy of Sciences of the United States of America*, 114(5), pp. 1129-1134. doi: 10.1073/pnas.1620164114.

Shih, D. Q. *et al.* (2001) ‘Loss of HNF-1 α function in mice leads to abnormal expression of genes involved in pancreatic islet development and metabolism.’, *Diabetes*, 50(11), pp. 2472-80. Available at:
<http://www.ncbi.nlm.nih.gov/pubmed/11679424>.

Shim, H. *et al.* (1997) ‘c-Myc transactivation of LDH-A: Implications for tumor metabolism and growth’, *Proceedings of the National Academy of Sciences*, 94(13),

pp. 6658-6663. doi: 10.1073/pnas.94.13.6658.

Shukla, K. *et al.* (2012) 'Design, synthesis, and pharmacological evaluation of bis-2-(5-phenylacetamido-1,2,4-thiadiazol-2-yl)ethyl sulfide 3 (BPTES) analogs as glutaminase inhibitors.', *Journal of medicinal chemistry*, 55(23), pp. 10551-63. doi: 10.1021/jm301191p.

Shukla, S. K. *et al.* (2017) 'MUC1 and HIF-1alpha Signaling Crosstalk Induces Anabolic Glucose Metabolism to Impart Gemcitabine Resistance to Pancreatic Cancer', *Cancer Cell*, 32(1), pp. 71-87.e7. doi: 10.1016/j.ccell.2017.06.004.

Siegel, R. L., Miller, K. D. and Jemal, A. (2017) 'Cancer Statistics, 2017.', *CA: a cancer journal for clinicians*, 67(1), pp. 7-30. doi: 10.3322/caac.21387.

Singh, A. *et al.* (2009) 'A gene expression signature associated with "K-Ras addiction" reveals regulators of EMT and tumor cell survival.', *Cancer cell*, 15(6), pp. 489-500. doi: 10.1016/j.ccr.2009.03.022.

Slamon, D. J. *et al.* (2001) 'Use of chemotherapy plus a monoclonal antibody against HER2 for metastatic breast cancer that overexpresses HER2.', *The New England journal of medicine*, 344(11), pp. 783-92. doi: 10.1056/NEJM200103153441101.

Slater, E. C. and Welle, H. F. (1969) 'Applications of Oligomycin and Related Inhibitors in Bioenergetics', in *Inhibitors Tools in Cell Research*. Berlin, Heidelberg: Springer Berlin Heidelberg, pp. 258-278. doi: 10.1007/978-3-642-46158-3_22.

Smith, P. K. *et al.* (1985) 'Measurement of protein using bicinchoninic acid.', *Analytical biochemistry*, 150(1), pp. 76-85. Available at: <http://www.ncbi.nlm.nih.gov/pubmed/3843705>.

Soldani, C. and Scovassi, A. I. (2002) 'Poly(ADP-ribose) polymerase-1 cleavage during apoptosis: an update.', *Apoptosis: an international journal on programmed cell death*, 7(4), pp. 321-8. doi: 12101391.

Soltoff, S. P. *et al.* (1994) 'ErbB3 is involved in activation of phosphatidylinositol 3-kinase by epidermal growth factor.', *Molecular and cellular biology*, 14(6), pp. 3550-8. doi: 10.1128/mcb.14.6.3550.

Son, J. *et al.* (2013) 'Glutamine supports pancreatic cancer growth through a KRAS-regulated metabolic pathway.', *Nature*, 496(7443), pp. 101-5. doi:

10.1038/nature12040.

Sorrentino, G. *et al.* (2014) 'Metabolic control of YAP and TAZ by the mevalonate pathway.', *Nature cell biology*, 16(4), pp. 357-66. doi: 10.1038/ncb2936.

Staubach, S. and Hanisch, F.-G. (2011) 'Lipid rafts: signaling and sorting platforms of cells and their roles in cancer', *Expert Review of Proteomics*, 8(2), pp. 263-277. doi: 10.1586/epr.11.2.

Stevenson, J., Huang, E. Y. and Olzmann, J. A. (2016) 'Endoplasmic Reticulum-Associated Degradation and Lipid Homeostasis', *Annual Review of Nutrition*, 36(1), pp. 511-542. doi: 10.1146/annurev-nutr-071715-051030.

Sun, Y., Connors, K. E. and Yang, D.-Q. (2007) 'AICAR induces phosphorylation of AMPK in an ATM-dependent, LKB1-independent manner', *Molecular and Cellular Biochemistry*, 306(1-2), pp. 239-245. doi: 10.1007/s11010-007-9575-6.

Symersky, J. *et al.* (2012) 'Oligomycin frames a common drug-binding site in the ATP synthase.', *Proceedings of the National Academy of Sciences of the United States of America*, 109(35), pp. 13961-5. doi: 10.1073/pnas.1207912109.

Tadros, S. *et al.* (2017) 'De Novo Lipid Synthesis Facilitates Gemcitabine Resistance through Endoplasmic Reticulum Stress in Pancreatic Cancer', *Cancer Research*, 77(20), pp. 5503-5517. doi: 10.1158/0008-5472.CAN-16-3062.

Takahashi, Y. *et al.* (2007) 'Bif-1 interacts with Beclin 1 through UVRAG and regulates autophagy and tumorigenesis.', *Nature cell biology*, 9(10), pp. 1142-51. doi: 10.1038/ncb1634.

Thomson, J. M. *et al.* (2006) 'Extensive post-transcriptional regulation of microRNAs and its implications for cancer.', *Genes & development*, 20(16), pp. 2202-7. doi: 10.1101/gad.1444406.

Tillack, T. W. and Kinsky, S. C. (1973) 'A freeze-etch study of the effects of filipin on liposomes and human erythrocyte membranes.', *Biochimica et biophysica acta*, 323(1), pp. 43-54. doi: 10.1016/0005-2736(73)90430-6.

van Tinteren, H. *et al.* (2002) 'Effectiveness of positron emission tomography in the preoperative assessment of patients with suspected non-small-cell lung cancer: the PLUS multicentre randomised trial', *The Lancet*, 359(9315), pp. 1388-1392. doi: 10.1016/S0140-6736(02)08352-6.

Tounekti, O. *et al.* (2001) 'The ratio of single- to double-strand DNA breaks and

their absolute values determine cell death pathway.’, *British journal of cancer*, 84(9), pp. 1272-9. doi: 10.1054/bjoc.2001.1786.

Triscott, J. *et al.* (2012) ‘Disulfiram, a drug widely used to control alcoholism, suppresses the self-renewal of glioblastoma and over-rides resistance to temozolomide’, *Oncotarget*, 3(10). doi: 10.18632/oncotarget.604.

Vázquez, M. J. *et al.* (2008) ‘Discovery of GSK837149A, an inhibitor of human fatty acid synthase targeting the β -ketoacyl reductase reaction’, *FEBS Journal*, 275(7), pp. 1556-1567. doi: 10.1111/j.1742-4658.2008.06314.x.

Ventura, R. *et al.* (2015) ‘Inhibition of de novo Palmitate Synthesis by Fatty Acid Synthase Induces Apoptosis in Tumor Cells by Remodeling Cell Membranes, Inhibiting Signaling Pathways, and Reprogramming Gene Expression’, *EBioMedicine*, 2(8), pp. 808-824. doi: 10.1016/j.ebiom.2015.06.020.

Viale, A. *et al.* (2014) ‘Oncogene ablation-resistant pancreatic cancer cells depend on mitochondrial function.’, *Nature*, 514(7524), pp. 628-32. doi: 10.1038/nature13611.

Vigil, D. *et al.* (2010) ‘Ras superfamily GEFs and GAPs: validated and tractable targets for cancer therapy?’, *Nature reviews. Cancer*, 10(12), pp. 842-57. doi: 10.1038/nrc2960.

Villarino, N. *et al.* (2017) ‘A screen for inducers of bHLH activity identifies pitavastatin as a regulator of p21, Rb phosphorylation and E2F target gene expression in pancreatic cancer.’, *Oncotarget*, 8(32), pp. 53154-53167. doi: 10.18632/oncotarget.18587.

Volker, K. W. and Knull, H. R. (1997) ‘A Glycolytic Enzyme Binding Domain on Tubulin’, *Archives of Biochemistry and Biophysics*, 338(2), pp. 237-243. doi: 10.1006/abbi.1996.9819.

Vrieling, A. *et al.* (2010) ‘Cigarette smoking, environmental tobacco smoke exposure and pancreatic cancer risk in the European Prospective Investigation into Cancer and Nutrition.’, *International journal of cancer*, 126(10), pp. 2394-403. doi: 10.1002/ijc.24907.

Vucicevic, L. *et al.* (2011) ‘Compound C induces protective autophagy in cancer cells through AMPK inhibition-independent blockade of Akt/mTOR pathway.’, *Autophagy*, 7(1), pp. 40-50. doi: 10.4161/auto.7.1.13883.

- Waddell, N., Pajic, M., Patch, A.-M., *et al.* (2015) 'Whole genomes redefine the mutational landscape of pancreatic cancer.', *Nature*. Nature Publishing Group, a division of Macmillan Publishers Limited. All Rights Reserved., 518(7540), pp. 495-501. doi: 10.1038/nature14169.
- Waddell, N., Pajic, M., Patch, A. M., *et al.* (2015) 'Whole genomes redefine the mutational landscape of pancreatic cancer', *Nature*, 518(7540), pp. 495-501. doi: 10.1038/nature14169.
- Walther, T. C. and Farese, R. V (2009) 'The life of lipid droplets.', *Biochimica et biophysica acta*, 1791(6), pp. 459-66. doi: 10.1016/j.bbaliip.2008.10.009.
- Wang, H. *et al.* (2015) 'Structurally diverse c-Myc inhibitors share a common mechanism of action involving ATP depletion.', *Oncotarget*, 6(18), pp. 15857-70. doi: 10.18632/oncotarget.4327.
- Wang, P. *et al.* (2020) 'Mu-KRAS attenuates Hippo signaling pathway through PKC α to sustain the growth of pancreatic cancer', *Journal of Cellular Physiology*, 235(1), pp. 408-420. doi: 10.1002/jcp.28981.
- Wang, T. *et al.* (2016) 'Simvastatin-induced breast cancer cell death and deactivation of PI3K/Akt and MAPK/ERK signalling are reversed by metabolic products of the mevalonate pathway.', *Oncotarget*, 7(3), pp. 2532-44. doi: 10.18632/oncotarget.6304.
- Wang, X. *et al.* (1994) 'SREBP-1, a membrane-bound transcription factor released by sterol-regulated proteolysis.', *Cell*, 77(1), pp. 53-62. doi: 10.1016/0092-8674(94)90234-8.
- Wang, Z. *et al.* (2013) 'FDG-PET in diagnosis, staging and prognosis of pancreatic carcinoma: A meta-analysis', *World Journal of Gastroenterology*, 19(29), pp. 4808-4817. doi: 10.3748/wjg.v19.i29.4808.
- Warburg, O. (1956) 'On respiratory impairment in cancer cells.', *Science (New York, N.Y.)*, 124(3215), pp. 269-70. Available at: <http://www.ncbi.nlm.nih.gov/pubmed/13351639>.
- Warita, K. *et al.* (2014) 'Statin-induced mevalonate pathway inhibition attenuates the growth of mesenchymal-like cancer cells that lack functional E-cadherin mediated cell cohesion.', *Scientific reports*, 4, p. 7593. doi: 10.1038/srep07593.
- Wei, W. *et al.* (2016) 'Ligand Activation of ERR α by Cholesterol Mediates Statin and

- Bisphosphonate Effects', *Cell Metabolism*, 23(3), pp. 479-491. doi: 10.1016/j.cmet.2015.12.010.
- Weinhouse, S. (1956) 'On respiratory impairment in cancer cells.', *Science (New York, N.Y.)*, 124(3215), pp. 267-9. doi: 10.1126/science.124.3215.267.
- Wellen, K. E. *et al.* (2009) 'ATP-Citrate Lyase Links Cellular Metabolism to Histone Acetylation', *Science*, 324(5930), pp. 1076-1080. doi: 10.1126/science.1164097.
- Wheeler, D. L. *et al.* (2008) 'Mechanisms of acquired resistance to cetuximab: role of HER (ErbB) family members.', *Oncogene*, 27(28), pp. 3944-56. doi: 10.1038/onc.2008.19.
- Whitford, W. and Manwaring, J. (2004) 'Lipids in Cell Culture Media', *Fish. Appl. Notes*, pp. 152-154.
- Wick, A. N. *et al.* (1957) 'Localization of the primary metabolic block produced by 2-deoxyglucose.', *The Journal of biological chemistry*, 224(2), pp. 963-9. Available at: <http://www.ncbi.nlm.nih.gov/pubmed/13405925>.
- Wilding, L. and Gannon, M. (no date) 'The role of pdx1 and HNF6 in proliferation and differentiation of endocrine precursors.', *Diabetes/metabolism research and reviews*, 20(2), pp. 114-23. doi: 10.1002/dmrr.429.
- Wise, D. R. *et al.* (2008) 'Myc regulates a transcriptional program that stimulates mitochondrial glutaminolysis and leads to glutamine addiction', *Proceedings of the National Academy of Sciences*, 105(48), pp. 18782-18787. doi: 10.1073/pnas.0810199105.
- Wishart, D. S. *et al.* (2018) 'DrugBank 5.0: a major update to the DrugBank database for 2018.', *Nucleic acids research*, 46(D1), pp. D1074-D1082. doi: 10.1093/nar/gkx1037.
- Witkiewicz, A. K. *et al.* (2015) 'Whole-exome sequencing of pancreatic cancer defines genetic diversity and therapeutic targets.', *Nature communications*, 6, p. 6744. doi: 10.1038/ncomms7744.
- de Wolf, E. *et al.* (2017) 'Dietary geranylgeraniol can limit the activity of pitavastatin as a potential treatment for drug-resistant ovarian cancer.', *Scientific reports*, 7(1), p. 5410. doi: 10.1038/s41598-017-05595-4.
- Wood, J. P. *et al.* (2015) 'Comet assay measures of DNA damage as biomarkers of irinotecan response in colorectal cancer in vitro and in vivo.', *Cancer medicine*,

4(9), pp. 1309-21. doi: 10.1002/cam4.477.

Wu, M. *et al.* (2006) 'Multiparameter metabolic analysis reveals a close link between attenuated mitochondrial bioenergetic function and enhanced glycolysis dependency in human tumor cells', *AJP: Cell Physiology*, 292(1), pp. C125-C136. doi: 10.1152/ajpcell.00247.2006.

Würth, R. *et al.* (2016) 'Drug-repositioning opportunities for cancer therapy: novel molecular targets for known compounds', *Drug Discovery Today*, 21(1), pp. 190-199. doi: 10.1016/j.drudis.2015.09.017.

Xiang, J. *et al.* (2018) 'TCF7L2 positively regulates aerobic glycolysis via the EGLN2/HIF-1 α axis and indicates prognosis in pancreatic cancer', *Cell Death & Disease*, 9(3), p. 321. doi: 10.1038/s41419-018-0367-6.

Yadav, B. *et al.* (2015) 'Searching for Drug Synergy in Complex Dose-Response Landscapes Using an Interaction Potency Model.', *Computational and structural biotechnology journal*, 13, pp. 504-13. doi: 10.1016/j.csbj.2015.09.001.

Yamamoto, T. *et al.* (2015) 'Preoperative FDG-PET Predicts Early Recurrence and a Poor Prognosis After Resection of Pancreatic Adenocarcinoma', *Annals of Surgical Oncology*, 22(2), pp. 677-684. doi: 10.1245/s10434-014-4046-2.

Yang, A. *et al.* (2018) 'Autophagy Sustains Pancreatic Cancer Growth through Both Cell-Autonomous and Nonautonomous Mechanisms', *Cancer Discovery*, 8(3), pp. 276-287. doi: 10.1158/2159-8290.CD-17-0952.

Yang, S. *et al.* (2011) 'Pancreatic cancers require autophagy for tumor growth.', *Genes & development*, 25(7), pp. 717-29. doi: 10.1101/gad.2016111.

Yang, W.-L. *et al.* (2012) 'AMPK inhibitor compound C suppresses cell proliferation by induction of apoptosis and autophagy in human colorectal cancer cells.', *Journal of surgical oncology*, 106(6), pp. 680-8. doi: 10.1002/jso.23184.

Yao, D. C. *et al.* (2004) 'Hemolytic anemia and severe rhabdomyolysis caused by compound heterozygous mutations of the gene for erythrocyte/muscle isozyme of aldolase, ALDOA(Arg303X/Cys338Tyr).', *Blood*, 103(6), pp. 2401-3. doi: 10.1182/blood-2003-09-3160.

Yin, W., Mu, J. and Birnbaum, M. J. (2003) 'Role of AMP-activated Protein Kinase in Cyclic AMP-dependent Lipolysis In 3T3-L1 Adipocytes', *Journal of Biological Chemistry*, 278(44), pp. 43074-43080. doi: 10.1074/jbc.M308484200.

- Ying, H. *et al.* (2012) 'Oncogenic Kras maintains pancreatic tumors through regulation of anabolic glucose metabolism.', *Cell*, 149(3), pp. 656-70. doi: 10.1016/j.cell.2012.01.058.
- Yonezawa, S. *et al.* (2008) 'Precursor lesions of pancreatic cancer.', *Gut and liver*, 2(3), pp. 137-54. doi: 10.5009/gnl.2008.2.3.137.
- Yoshioka, A. *et al.* (1987) 'Deoxyribonucleoside triphosphate imbalance. 5-Fluorodeoxyuridine-induced DNA double strand breaks in mouse FM3A cells and the mechanism of cell death.', *The Journal of biological chemistry*, 262(17), pp. 8235-41. Available at: <http://www.ncbi.nlm.nih.gov/pubmed/2954951>.
- You, H.-Y. *et al.* (2016) 'Pitavastatin suppressed liver cancer cells in vitro and in vivo.', *OncoTargets and therapy*, 9, pp. 5383-8. doi: 10.2147/OTT.S106906.
- Yu, F.-X. *et al.* (2012) 'Regulation of the Hippo-YAP Pathway by G-Protein-Coupled Receptor Signaling', *Cell*, 150(4), pp. 780-791. doi: 10.1016/j.cell.2012.06.037.
- Yu, P. B. *et al.* (2008) 'Dorsomorphin inhibits BMP signals required for embryogenesis and iron metabolism.', *Nature chemical biology*, 4(1), pp. 33-41. doi: 10.1038/nchembio.2007.54.
- Yu, R. *et al.* (2018) 'Statin-Induced Cancer Cell Death Can Be Mechanistically Uncoupled from Prenylation of RAS Family Proteins.', *Cancer research*, 78(5), pp. 1347-1357. doi: 10.1158/0008-5472.CAN-17-1231.
- Yue, Z. *et al.* (2003) 'Beclin 1, an autophagy gene essential for early embryonic development, is a haploinsufficient tumor suppressor.', *Proceedings of the National Academy of Sciences of the United States of America*, 100(25), pp. 15077-82. doi: 10.1073/pnas.2436255100.
- Zaugg, K. *et al.* (2011) 'Carnitine palmitoyltransferase 1C promotes cell survival and tumor growth under conditions of metabolic stress.', *Genes & development*, 25(10), pp. 1041-51. doi: 10.1101/gad.1987211.
- Zeitouni, D. *et al.* (2016) 'KRAS Mutant Pancreatic Cancer: No Lone Path to an Effective Treatment', *Cancers*, 8(4), p. 45. doi: 10.3390/cancers8040045.
- Zhang, W. *et al.* (2014) 'Downstream of Mutant KRAS, the Transcription Regulator YAP Is Essential for Neoplastic Progression to Pancreatic Ductal Adenocarcinoma', *Science Signaling*, 7(324), pp. ra42-ra42. doi: 10.1126/scisignal.2005049.
- Zhao, F. *et al.* (2010) 'Imatinib resistance associated with BCR-ABL upregulation is

dependent on HIF-1 α -induced metabolic reprogramming.’, *Oncogene*, 29(20), pp. 2962-72. doi: 10.1038/onc.2010.67.

Zhao, H. *et al.* (2017) ‘Up-regulation of glycolysis promotes the stemness and EMT phenotypes in gemcitabine-resistant pancreatic cancer cells’, *Journal of Cellular and Molecular Medicine*, 21(9), pp. 2055-2067. doi: 10.1111/jcmm.13126.

Zhao, Q.-Y. *et al.* (2016) ‘Global histone modification profiling reveals the epigenomic dynamics during malignant transformation in a four-stage breast cancer model.’, *Clinical epigenetics*, 8, p. 34. doi: 10.1186/s13148-016-0201-x.

Zhao, T. T. *et al.* (2010) ‘Lovastatin inhibits EGFR dimerization and AKT activation in squamous cell carcinoma cells: potential regulation by targeting rho proteins.’, *Oncogene*, 29(33), pp. 4682-92. doi: 10.1038/onc.2010.219.

Zhong, Y. *et al.* (2015) ‘Application of mitochondrial pyruvate carrier blocker UK5099 creates metabolic reprogram and greater stem-like properties in LnCap prostate cancer cells in vitro.’, *Oncotarget*, 6(35), pp. 37758-69. doi: 10.18632/oncotarget.5386.

Zhou, G. *et al.* (2001) ‘Role of AMP-activated protein kinase in mechanism of metformin action.’, *The Journal of clinical investigation*, 108(8), pp. 1167-74. doi: 10.1172/JCI13505.

Zhou, W. *et al.* (2011) ‘Proteomic analysis of pancreatic ductal adenocarcinoma cells reveals metabolic alterations.’, *Journal of proteome research*, 10(4), pp. 1944-52. doi: 10.1021/pr101179t.

Zimmermann, G. *et al.* (2013) ‘Small molecule inhibition of the KRAS-PDE δ interaction impairs oncogenic KRAS signalling’, *Nature*, 497(7451), pp. 638-642. doi: 10.1038/nature12205.

Zirath, H. *et al.* (2013) ‘MYC inhibition induces metabolic changes leading to accumulation of lipid droplets in tumor cells’, *Proceedings of the National Academy of Sciences*, 110(25), pp. 10258-10263. doi: 10.1073/pnas.1222404110.

Zu, X. L. and Guppy, M. (2004) ‘Cancer metabolism: facts, fantasy, and fiction.’, *Biochemical and biophysical research communications*, 313(3), pp. 459-65. doi: 10.1016/j.bbrc.2003.11.136.